CHAPTER 4: REACTOR

This chapter was prepared using the latest approved version of the licensing topical report "General Electric Standard Application for Reactor Fuel" (GESTAR II) NEDE-24011-P-A including the "United States Supplement," NEDE-24011-P-A-US (Reference 1). Applicable sections of this report are referenced as noted in Sections 4.1 through 4.4. Reference is made to standardized information contained in the topical report, consistent with the NRC overall standardization philosophy. Additional cycle-specific reload information is in the cycle-specific supplemental reload licensing report.

4.1 REACTOR SUMMARY DESCRIPTION

The reactor assembly consists of the reactor pressure vessel (RPV) and its internal components, including the core, shroud, steam separator and dryer assemblies, and jet pumps. Also included in the reactor assembly are the control rods, control rod drive (CRD) housings, and the CRDs. The RPV cutaway, Figure 4.1-1, shows the arrangement of reactor assembly components. A summary of the important design and performance characteristics is given in Section 1.3. Loading conditions for reactor assembly components are specified in Table 3.9-14. Summary tables of the pertinent reactor data are presented at the end of Sections 4.2, 4.3, and 4.4.

4.1.1 Reactor Pressure Vessel

The RPV design and description are covered in Section 5.4.

4.1.2 Reactor Internal Components

The major reactor internal components are the core (fuel, channels, control rods, and instrumentation), the core support structure (including the core shroud, shroud head separators, top guide, and core support plate), the steam dryer assembly, and the jet pumps. Except for the zircaloy in the reactor core, these reactor internals are stainless steel or other corrosion- resistant alloys. All major internal components of the RPV can be removed except the jet pump diffusers, the core shroud, the core spray spargers, and the jet pump inlet piping. The removal of the steam dryers, shroud head separators, fuel assemblies, incore assemblies, control rods, and control rod guide tubes can be accomplished on a routine basis.

4.1.2.1 Reactor Core

4.1.2.1.1 General

The design of the Fermi 2 BWR core and fuel is based on the proper combination of many design variables and operating experience. These factors contribute to the achievement of high reliability.

A number of important features of the BWR core design are summarized in the following:

a. The BWR core mechanical design is based on conservative application of stress limits, operating experience, and experimental test results. The pressure levels

(approximately 1000 psia) result in moderate cladding temperatures and stress levels.

b. The low coolant saturation temperature, high heat transfer coefficients, and neutral water chemistry of the BWR are significant, advantageous factors in minimizing zircaloy temperature and associated temperature-dependent corrosion and hydride buildup. The relatively uniform fuel cladding temperatures throughout the core minimize migration of the hydrides to cold cladding zones and reduce thermal stresses.

c. The basic thermal and mechanical criteria applied in the design have been proven by irradiation of statistically significant quantities of fuel. The design heat fluxes and linear heat generation rates are similar to values proven in fuel assembly irradiation.

d. The design power distribution used in sizing the core represents a worst-expected state of operation.

e. The GE thermal analysis basis, GETAB, is applied to ensure that more than 99.9 percent of the fuel rods in the core are expected to avoid boiling transition for the most severe abnormal operational transient described in Chapter 15 and the cycle-specific supplemental reload licensing report. The possibility of boiling transition occurring during normal reactor operation is insignificant.

f. Because of the large negative moderator density coefficient of reactivity, the BWR has a number of inherent advantages. These are the use of recirculation coolant flow for load following, the inherent self-flattening of the radial power distribution, the ease of control, the spatial xenon stability, and the ability to override xenon in order to follow load.

Boiling water reactors do not have instability problems due to xenon. This has been demonstrated by special tests which have been conducted on operating BWRs in an attempt to force the reactor into xenon instability, and by calculations. No xenon instabilities have ever been observed in the test results. All of these indicators have proven that xenon transients are highly damped in a BWR due to the large negative power coefficient of reactivity (Reference 1).

Important features of the reactor core arrangement are as follows:

a. The bottom-entry cruciform control rods consist of: (1) boron carbide (B_4C) in stainless steel tubes or (2) boron carbide (B_4C) in stainless steel tubes and hafnium metal. Original, Duralife-140, and Duralife-215 control rods are surrounded by a stainless steel sheath. Marathon C and Ultra-HD control rods have absorber tubes that are edge welded to form the cruciform shape.

b. The fixed in-core ion chambers provide continuous-power-range neutron flux monitoring. A probe tube in each in-core assembly provides for a traversing ion chamber for calibration and axial detail. Source range monitors (SRM) and intermediate range monitors (IRM) are located in-core and are axially retractable. The in-core location of the startup and IRM instruments provides coverage of the large reactor core and provides an acceptable signal-to-noise ratio and neutron-to-gamma ratio. All in-core instrument leads enter from the

bottom and the instruments are in service during refueling. In-core instrumentation is further discussed in Chapter 7.

c. As shown by experience obtained at Dresden 1 and other plants, the operator, utilizing the in-core flux monitor system, can maintain the desired power distribution within a large core by proper control rod scheduling.

d. The zircaloy reusable channels provide a fixed flow path for the boiling coolant, serve as a guiding surface for the control rods, and protect the fuel during handling operations.

e. The mechanical reactivity control permits criticality checks during refueling. The core is designed to be subcritical at any time in its operating history with any one control rod fully withdrawn.

f. The selected control rod pitch represents a practical value of individual control rod reactivity worth and allows ample clearance below the RPV between CRD mechanisms for ease of maintenance and removal.

4.1.2.1.2 Core Configuration

The reactor core is arranged as an upright circular cylinder containing a large number of fuel cells and is located within the RPV. The coolant flows upward through the core. The core arrangement (plan view) and the lattice configuration are shown in Figure 4.1-2.

4.1.2.1.3 Fuel Assembly Description

As can be seen from Figure 4.1-2, the BWR core is essentially composed of only two components: fuel assemblies and control rods. The fuel assembly and control rod mechanical designs (See Subsection 4.5.2.2) are basically the same as those used in Dresden 1 and in all subsequent GE BWRs. A description of the fuel assembly including fuel rods, water rods, other fuel assembly components, and channels is given in Section 4.2. A brief description of the fuel rods and bundle is given below.

4.1.2.1.3.1 Fuel Rod

A fuel rod consists of uranium oxide (UO_2) pellets and a zircaloy cladding tube. Barrier fuel bundles consist of fuel rods with a thin, high purity zirconium liner, i.e. barrier, mechanically bonded to the cladding tube. A fuel rod is made by stacking pellets into a zircaloy cladding tube that is evacuated, backfilled with helium, and sealed by welding zircaloy end plugs in each end of the tube.

The BWR fuel rod is designed as a pressure vessel. The ASME Boiler and Pressure Vessel (B&PV) Code, Section III, is used as a guide in the mechanical design and stress analysis of the fuel rod.

The rod is designed to withstand the applied loads, both external and internal. The fuel pellet is sized to provide sufficient clearance within the fuel tube to accommodate axial and radial differential expansion between fuel and cladding. Overall fuel rod design is conservative in its accommodation of the mechanisms affecting fuel in a BWR environment. Fuel rod design bases are discussed in more detail in Subsection 4.2.1.

4.1.2.1.3.2 Fuel Bundle

Each fuel bundle contains fuel rods and water rods that are spaced and supported in a square array by spacers and a lower and upper tie plate. The fuel bundle has two important design features:

a. The bundle design places minimum external forces on a fuel rod; each fuel rod is free to expand in the axial direction.

b. The unique structural design permits the removal and replacement, if required, of individual fuel rods.

Before fuel is inserted into the reactor, a zirconium fuel channel is placed around the fuel bundle, forming a fuel assembly.

The fuel assemblies of which the core is comprised are designed to meet all the criteria for core performance and to provide ease of handling. Selected fuel rods in each assembly differ from the others in uranium enrichment. This arrangement produces more uniform power production across the fuel assembly.

4.1.2.1.4 Assembly Support and Control Rod Location

A few peripheral fuel assemblies (24) and their individual fuel support pieces are supported by the core support plate. Otherwise, individual fuel assemblies in the core rest on fuel support pieces mounted on top of the control rod guide tubes. Each guide tube, with its fuel support piece, bears the weight of four assemblies and is supported by a control rod drive penetration nozzle in the bottom head of the RPV. The core support plate provides lateral support and guidance at the top of each control rod guide tube. For a discussion of fuel channel wear from flow-induced instrument tube vibrations caused by flow through the bypass holes in the core support plate, see Subsection 4.5.1.2.3.

The top guide, mounted inside the core shroud, provides lateral support and guidance for each fuel assembly. The reactivity of the core is controlled by cruciform control rods containing boron carbide or a combination of boron carbide and hafnium metal and by the associated mechanical hydraulic drive system. The control rods occupy alternate spaces between fuel assemblies. Each independent CRD enters the core from the bottom and can accurately position its associated control rod during normal operation and yet exert approximately 10 times the force of gravity to insert the control rod during the scram mode of operation. Bottom entry allows optimum power shaping in the core, ease of refueling, and convenient CRD maintenance.

4.1.2.2 Shroud

The shroud is a cylindrical, stainless steel structure that surrounds the core and provides a barrier to separate the upward flow through the core from the downward flow in the annulus. The shroud also provides a floodable volume in the unlikely event of an incident that tends to drain the RPV. A flange at the top of the shroud cylinder mates with a flange on the shroud head to form the core discharge plenum. The shroud support is welded to the RPV wall and is designed to support and locate the jet pumps and core support structure. The 20 jet pump discharge diffusers penetrate the shroud support below the core elevation to introduce the coolant to the lower inlet plenum.

Mounted inside the shroud in the space between the top of the core and the flange at the top of the shroud are the two core spray spargers with spray nozzles for injection of cooling water. The core spray spargers and nozzles do not interfere with the installation or removal of fuel from the core. A pipe for the injection of neutron absorber (sodium pentaborate) solution is mounted below the core to ensure mixing with the cooling water rising through the core.

4.1.2.3 Shroud Head and Separators

The shroud head and separators consist of a flange and dome onto which is welded an array of standpipes (225), with a steam separator located at the top of each standpipe. The shroud head mounts on the flange at the top of the shroud top cylinder and forms the cover (shroud head) of the core discharge plenum region. The joint between the shroud head and shroud top cylinder does not require a gasket or other replacement sealing techniques. The fixed axial flow-type steam separators have no moving parts and are made of stainless steel.

In each separator, the steam/water mixture rising from the standpipe impinges on vanes that give the mixture a spin to establish a vortex wherein the centrifugal forces separate the steam from the water. Steam leaves the separator at the top and passes into the wet steam plenum below the dryer. The separated water exits from the lower end of the separator and enters the pool that surrounds the standpipes to enter the downcomer annulus. An internal steam separator schematic is shown in Figure 4.1-3.

For ease of removal, the shroud head and separators are bolted to the top cylinder by long shroud head bolts that extend above the separators for easy access during refueling. The shroud head and separators are guided into position on the shroud and flange with guide rods and locating pins. The objective of the longbolt design is to provide direct access to the bolts during reactor refueling operations with minimum-depth underwater tool manipulation during the removal and installation of the assemblies.

4.1.2.4 Steam Dryer Assembly

The steam dryer assembly is mounted in the RPV above the shroud head and separators and forms the top and sides of the wet steam plenum. Vertical guide rods on the inside of the RPV provide alignment for the dryer assembly during installation. The dryer assembly is supported by pads extending from the RPV wall and is locked into position during operation by the RPV top head. Steam from the separators flows upward into the dryer assembly. The steam leaving the top of the dryer assembly flows into four RPV steam outlet nozzles that are located alongside the steam dryer assembly. Moisture is removed by the dryer vanes and flows first through a system of troughs and pipes to the pool surrounding the separators and then into the downcomer annulus between the shroud and RPV wall. A schematic of a typical steam dryer panel is shown in Figure 4.1-4.

4.1.3 Reactivity Control Systems

4.1.3.1 Operation

The control rods perform dual functions of power distribution shaping and reactivity control. Power distribution in the core is controlled during operation of the reactor by manipulation of

selected patterns of rods. The rods, which enter from the bottom of the near-cylindrical reactor core, are positioned in a manner such as to counterbalance steam voids in the top of the core and effect significant power flattening.

The reactivity control function requires that all rods be available for both reactor scram and reactivity regulation. Because of this, the control elements are mechanically designed to withstand the dynamic forces resulting from a scram. They are connected to bottom-mounted, hydraulically actuated drive mechanisms that allow either axial positioning for reactivity regulation or rapid scram insertion. The design of the rod-to-drive connection permits each blade to be attached or detached from its CRD without disturbing the remainder of the control system. The bottom-mounted CRDs permit the entire control system to be left intact and operable for tests with the RPV open. See also Subsection 4.5.2.2.2.4.

4.1.3.2 Description of Rods

The cruciform-shaped control rods consist of (1) boron carbide (B_4C) in stainless steel tubes or (2) boron carbide (B_4C) in stainless steel tubes and hafnium metal. Original, Duralife-140, and Duralife-215 control rods are surrounded by a stainless steel sheath. Marathon C and Ultra-HD control rods have absorber tubes that are edge welded to form the cruciform shape. Hafnium metal (another neutron absorber) is used in the newer control rod designs to extend service life. Refer to Subsection 4.5.2.1.2 for a description of the control rods.

Control rods are cooled by the core bypass flow that is made up of leakage through various flow paths of the fuel support and lower core plate structure.

4.1.3.3 Supplementary Reactivity Control

The control requirements of the initial core are considerably in excess of the equilibrium core requirements because all the fuel is fresh. The initial core control requirements are met by use of the combined effects of the movable control rods and a supplementary burnable poison. The supplementary burnable poison is gadolinia (Gd_2O_3) mixed with UO_2 in several fuel rods in each fuel bundle.

4.1.4 Analysis Techniques

4.1.4.1 Reactor Internal Components

Computer codes used for the analysis of the internal components are listed below:

a. MASS (Mechanical Analysis of Space Structure)

b. SNAP and MULTISHELL

c. GASP

d. NOHEAT

e. FINITE

f. SAMIS (Structural Analysis and Matrix Interpretive System)

g. GEMOP (General Matrix Manipulation Program)

h. SHELL 5 and SHELL 9

i. HEATER

j. FAP-71 (Fatigue Analysis Program)

k. DYSEA (Dynamic and Seismic Analysis).

Detailed descriptions of these programs are given in the subsections that follow.

4.1.4.1.1 MASS (Mechanical Analysis of Space Structure)

4.1.4.1.1.1 Program Description

The program, proprietary of GE, is an outgrowth of the plate and panel analysis program originally developed by L. Beitch in the early 1960s. The program is based on the principle of the finite element method. Governing matrix equations are formed in terms of joint displacements using a "stiffness-influence-coefficient" concept originally proposed by L. Beitch (Reference 1a). The program offers curved beam, plate, and shell elements. It can handle mechanical and thermal loads in a static analysis and predict natural frequencies and mode shapes in a dynamic analysis.

4.1.4.1.1.2 Program Version

The Nuclear Energy Division of GE is using a past revision of MASS. This revision is identified as revision "0" in the computer production library.

4.1.4.1.1.3 History of Use

Since its development in the early 1960s, the program has been successfully applied to a wide variety of jet-engine structural problems, many of which involve extremely complex geometries. The use of the program in the GE Nuclear Energy Division also started shortly after its development.

4.1.4.1.1.4 Extent of Application

In addition to the GE Jet Engine Division, the Nuclear Energy Division, and the Missile and Space Division, the Appliance Division and the Turbine Division have also applied the program to a wide range of engineering problems. The Nuclear Energy Division used it mainly for piping and reactor internals analysis.

4.1.4.1.2 SNAP (MULTISHELL)

4.1.4.1.2.1 Program Description

The SNAP program, which is also called MULTISHELL, is a code that determines the loads, deformations, and stresses of axisymmetric shells of revolution (cylinders, cones, disks, toroids, and rings) for axisymmetric thermal boundary and surface load conditions. Thin shell theory is inherent in the solution of E. Reissner's differential equations for each shell's influence coefficients. Surface loading capability includes pressure, average temperature, and linear through-wall gradients; the latter two may be linearly varied over the shell meridian. The theoretical limitations of this program are the same as those of classical theory.

4.1.4.1.2.2 Program Version

The current version maintained by the GE Jet Engine Division at Evandale, Ohio.

4.1.4.1.2.3 History of Use

The initial version of the Shell Analysis Program was completed by the Jet Engine Division in l96l. Since then, a considerable amount of modification and addition has been made to accommodate its broadening area of application. Its application in the Nuclear Energy Division had a history of over 10 years when used for the Fermi 2 analysis.

4.1.4.1.2.4 Extent of Application

The program has been used to analyze jet engine, space vehicle, and nuclear reactor components. Because of its efficiency and economy, in addition to reliability, it has been one of the main shell analysis programs in GE's Nuclear Energy Division.

4.1.4.1.2.5 Test Problems

The program has been used to analyze the pressure vessel specified in Article I-7 of ASME Section III. The program results are compared with those from other shell programs under three loadings: internal pressure, axial temperature gradient, and linear radial temperature gradient. It was found that the thin-shell theory programs (OMP, SOR, and MULTISHELL) were within 4 percent of thin-shell theoretical results for the pressure loading and within 1 percent of each other for the other two loadings. The thick-shell theory program (SEAL-SHELL-2) was within 7 percent of theory for the pressure loading and within 9 percent of the thin-shell codes on the other two loadings. Detailed results are presented in Figures 4.l-5 through 4.1-13.

4.1.4.1.3 GASP

4.1.4.1.3.1 Program Description

GASP is a finite element program for the stress analysis of axisymmetric or plane two-dimensional geometries. The element representations can be either quadrilateral or triangular. Axisymmetric or plane structural loads can be input at nodal points. Displacements, temperatures, pressure loads, and axial inertia can be accommodated. Effective plastic stress and strain distributions can be calculated using a bilinear stress-strain relationship by means of an iterative convergence procedure.

4.1.4.1.3.2 Program Version and Computer

The GE version, originally obtained from the developer, Professor E. L. Wilson, operates on the Honeywell 6000 computer.

4.1.4.1.3.3 History of Use

The program was developed by E. L. Wilson in l965 (Reference 2). The present version in GE's Nuclear Energy Division has been in operation since l967.

4.1.4.1.3.4 Extent of Application

The application of GASP in the GE Nuclear Energy Division is mainly for elastic analysis of axisymmetric and plane structures under thermal and pressure loads. The GE version has been extensively tested and used by engineers in the company.

4.1.4.1.3.5 Test Problems

The ASME computer-program-verification problem l9 (Reference 3) was solved using the triangular elements of GASP and ANSYS (Figure 4.1-14). The results of both solutions are very close to each other and they agree with a closed-form solution given in Reference 3 (Figure 4.1-15).

4.1.4.1.4 NOHEAT

4.1.4.1.4.1 Program Description

The NOHEAT program (Reference 4) is a two-dimensional and axisymmetric transient nonlinear temperature analysis program. An unconditionally stable numerical integration scheme is combined with iteration procedure to compute temperature distribution within the body subjected to arbitrary time- and temperature-dependent boundary conditions.

This program utilizes the finite element method. Included in the analysis are the three basic forms of heat transfer, conduction, radiation, and convection, as well as internal heat generation. In addition, cooling pipe boundary conditions are also treated. The output includes temperature of all the nodal points for the time instants required by the user. The program can handle multitransient temperature input.

4.1.4.1.4.2 Program Version

The current version of the program is an improvement of the program NOHEAT originally developed by I. Farhoomand and Professor E. L. Wilson of the University of California at Berkeley.

4.1.4.1.4.3 History of Use

The program was developed in l97l and installed in the Honeywell computer by one of its original developers, I. Farhoomand, in 1972. A number of heat transfer problems related to the reactor pedestal have been satisfactorily solved using the program.

4.1.4.1.4.4 Extent of Application

The program using finite element formulation is compatible with the finite element stress-analysis computer program GASP. Such compatibility simplified the connection of the two analyses and minimized human error.

4.1.4.1.4.5 Test Problems

Problem 1

Problem 1 involves one-dimensional temperature response of a plate with insulated back face after sudden change in external front surface temperature.

The prescribed heat-input boundary condition is useful in problems of aerodynamics, nuclear reactor power plants, and similar problems. The temperature response of a plate caused by a sudden change in external front surface temperature has been solved by direct integration technique (Reference 5). Figure 4.1-16 shows the response in a nondimensional form. The following variables are used in the description of the figure:

a. T_o = Initial temperature of figure

b. T_e = Boundary temperature

c. α = Thermal diffusivity of body material = $k/\rho c$

d. k = Conductance

e. ρ = Density

f. c = Specific heat

g. t = Time

h. L = Plate thickness

i. T = Temperature of the body at time t.

A linear finite element analysis was conducted using T = 0, T_e = 100, k = 0.0006, ρ = 0.3, c = 0.1, L = 100. The finite element mesh is shown in Figure 4.1-17. The result of the finite element analysis (dark circles in Figure 4.1-16) indicates excellent agreement with the result of the analytical solution.

Problem 2

Problem 2 involves temperature response of the front face of a plate with insulated back face after sudden exposure to constant-temperature radiation.

This example demonstrates the accuracy of the finite element as compared with an analytical solution of a radiation heat transfer problem. Consider a plate of thickness L, with finite conductivity k, specific heat c, and density ρ. The back face of the plate is insulated and the front face is subjected to a constant radiation heat flow with sink temperature, T_s = 0°R. The time variation of the temperature of the front surface was computed in a nondimensional form by the application of an approximate analytical technique (Reference 5). Figure 4.1-18 presents the temperature response for a particular value of parameter M. The variables used to construct Figure 4.l-18 are

a. σ = 17.3×10^{-10} Btu/hr ft^4/°R

b. F_e = Shape factor for plate surface

c. F_A = Shape factor for sink

d. T_o = Initial temperature of plate (°R)

e. T_e = Surface temperature of plate (°R).

Several finite element analyses with the same time increment but different numbers of iterations within each cycle were conducted. The finite element mesh layout is shown in Figure 4.1-19. In the analyses F_A = F_e = 1., T_o = 500, M = l, α = k/c = 0.02 and T_x = 0°R.

Comparison of the finite element solutions with the analytical solution indicates that the incremental approach without iteration does not converge to the "true" solution. However, if one iteration is made in each time increment, the finite element result becomes nearly identical to the analytical result.

4.1.4.1.5 FINITE

4.1.4.1.5.1 Program Description

FINITE is a general-purpose finite element computer program for elastic stress analyses of two-dimensional structural problems including plane stress, plane strain, and axisymmetric structures. It has provision for thermal, mechanical, and body force loads. The materials of the structure may be homogeneous or nonhomogeneous and isotropic or orthotropic. The development of the FINITE program is based on the GASP program, described in Subsection 4.1.4.1.3.

4.1.4.1.5.2 Program Version

The present version of the program at the GE Nuclear Energy Division was obtained from the developer, J. E. McConoclee of the GE Gas Turbine Department in 1969 (Reference 6).

4.1.4.1.5.3 History of Use

Since its completion in 1969, the program has been widely used in the GE Gas Turbine and Jet Engine Divisions for the analysis of turbine components.

4.1.4.1.5.4 Extent of Application

The program is used at GE's Nuclear Energy Division in the analysis of axisymmetric or nearly axisymmetric BWR internals.

4.1.4.1.5.5 Test Problems

Two simple examples are described herein with a comparison of the stresses calculated by FINITE with theoretical solutions.

The two cases considered are

a. A tube with internal pressure

b. A spinning disk of elliptical cross section.

The analytical models for these cases are shown in Figures 4.1-20 and 4.1-21, and comparisons of the calculated stresses with theoretical solutions are shown in Figures 4.1-22 and 4.1-23.

Figure 4.1-22 shows a comparison of the radial and tangential stresses at the midlength of the tube with those calculated using the Lamé solution.

Figure 4.1-23 shows a comparison of the radial and tangential stresses calculated by FINITE using the plane stress (with variable thickness) option with those obtained using the analysis of Goldberg and Sadowsky (Reference 7). This problem could have been done more exactly using the axisymmetric option which would have given the variation of the stresses through the thickness of the disk. However, the purpose in this case was explicitly to check out the

use of the variable thickness plane stress case and a comparison of these results with an exact solution. Another purpose of this case was to check out the use of the skew boundary condition.

4.1.4.1.6 SAMIS (Structural Analysis and Matrix Interpretive System)

4.1.4.1.6.1 Program Description

The SAMIS program (References 8 through 10) is well designed to solve problems involving matrix algebra with particular emphasis on structural applications. The user has control over the flow of the calculations through the use of "pseudo instructions." Execution of the program is performed in two phases: the generation phase and the manipulative phase. Input data defining the idealization of a structure is read and stiffness, stress, and load coefficient matrices are generated for elements available to the user. The program has two fundamental and widely used finite elements incorporated. A triangular flat plate element, called a facet, is available for idealization of plate and shell structures, and a straight beam element is available for idealization of frames and trusses and plate/shell structure stiffener representation.

The element formulation and analyses are based on the finite element matrix displacement method. The triangular plate and beam elements are capable of resisting stretching, shearing, bending, and twisting stresses. In the second phase of execution, the generated or input matrices are manipulated according to the rules of matrix algebra as directed by the user.

The program is written in modular form, making it easy to add new modules without major reprogramming of subroutines. This facilitates adding to the structural element library other elements to extend idealization capability. Those structural problems consisting of elements that cannot be adequately idealized by triangular plate or beam elements may have their stiffness coefficients submitted directly as input matrices.

4.1.4.1.6.2 Program Version

The SAMIS version was obtained from the developer, Philco Corporation, Western Development Laboratory, via the Space Division. A considerable amount of modification was made on the input and output of the original version to suit the analysis need of this division of GE. Both spectrum and time-history analyses can be performed using the GE Nuclear Energy Division version.

4.1.4.1.6.3 History of Use

The SAMIS program was developed by the Philco Corporation, Western Development Laboratories, under contract to and in association with the Jet Propulsion Laboratory in 1966. The program was first used by GE in 1967 and in the Nuclear Energy Division of GE in 1970.

4.1.4.1.6.4 Extent of Application

The current GE version of SAMIS has been extensively used since 1970 in the analysis of reactor components' response to seismic loadings. Results of test problems were found to agree closely with theoretical results of the same problem.

4.1.4.1.6.5 Test Problem

The clamped square plate frequency study considers a square plate having all four of its edges clamped. Figure 4.1-24 shows a quarter panel of the plate.

The particular plate dimensions and material properties used in the analysis were as follows:

a. $a = 10$ in.

b. $t = 0.05$ in.

c. $E = 30 \times 10^6$ lb/in.^{2}

d. $\nu = 0.03$

e. $\rho = 7.26 \times 10^{-4}$ lb-sec^2/in.^{4}.

For all grids used in the study, the triangular elements in any one grid were all uniform size except as noted.

A total of four grid models were analyzed for the clamped plate, each based on selected value of a/c = a/d or c = d for the square plate models. Each case will be referred to by number. In the table below are listed four cases and the grid size function for each case.

Case No.	a/c, a/d
1	4
2	5
3	6
4	7

For each case, three sets of modes were computed: symmetric modes, antisymmetric modes, and mixed modes (symmetric about X and antisymmetric about Y). The fourth set of modes was not required since the plate is square and the remaining mixed mode set (symmetric about Y and antisymmetric about X) would only be duplicate frequencies of the first mixed mode set.

Table 4.1-1 is a list of computed frequencies for the clamped square plate models. The first six frequencies are listed for each case along with the percent variation from the theoretical frequencies. The table shows, as would be expected, successive improvement in computed frequencies as the grid is refined. The results for Case Number 4 show rather good agreement for all six frequency values, the largest difference being in the third and sixth frequency values which differ from the exact frequency by 12.6 percent and 13.3 percent, respectively. A number of other models could be analyzed using larger grid size functions; however, it is doubtful that the improvement in accuracy would be as marked as in the initial four models for the six frequencies.

4.1.4.1.7 GEMOP (General Matrix Manipulation Program)

4.1.4.1.7.1 Program Description

GEMOP is a general matrix manipulation program capable of performing the majority of standard matrix operations. There presently are 41 operation commands in the program. A

maximum of nine full 60 by 60 matrices and six 60-element vectors may be stored in core at any one time. Also available for search and storage are up to a maximum of three tapes. This latest version of the program includes subroutines for calculating earthquake, or other forcing functions, and response of a lumped-mass structure, either by time-history or spectral response methods. The most used features are in the eigenvalue, eigenvector subroutine and response subroutine. The response is calculated for a system subjected to any piecewise linear forcing function.

4.1.4.1.7.2 Program Version

The current version of the program being used in GE was obtained from the originator, the Knolls Atomic Power Laboratory, in June 1969. It was converted from Control Data Corporation to GE computers.

4.1.4.1.7.3 History of Use

The program was originally written in the GE Knolls Atomic Power Laboratory for the solution of vibration problems.

4.1.4.1.7.4 Extent of Application

Since its installation in the Nuclear Energy Division in 1969, the general matrix manipulation program has been constantly used to solve seismic problems involving small lumped-mass systems of less than 80 degrees of freedom. Because of its limitation on problem size, the program is being replaced by SAMIS.

4.1.4.1.7.5 Test Problems

To evaluate its capability, the computer program has been used to solve the following sample problem. The satisfactory agreement between the lumped-mass numerical solution and the continuous system theoretical solution indicates the reliability of the general matrix manipulation program.

Consider a simply supported beam with a suddenly applied load at its center as the problem.

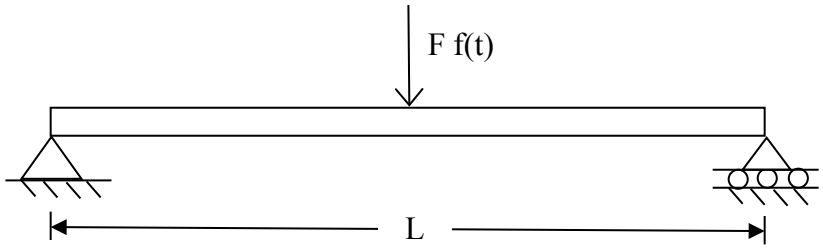

L = l00 in.

E = 30 x $l0^6$ psi

I = 2.5907 $in.^4$

A = 9.8696 $in.^2$

$\rho = 0.3$ lb/in.^{3}

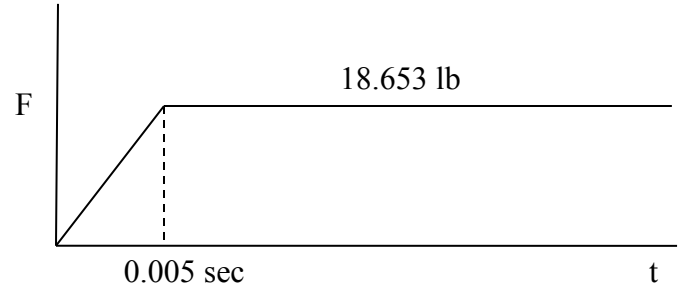

For this problem the beam is modeled as a five-lump mass system, or

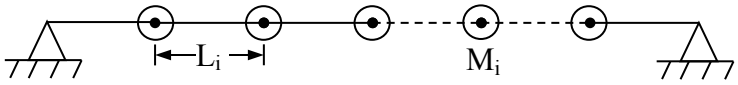

all lengths are equal

$L_i = L/6$

all masses are equal

$$M_i = \frac{M}{5} = \frac{AL\rho}{5g} \qquad (4.1\text{-}1)$$

A comparison of the calculated natural frequencies of the lumped-mass system compared with the continuous system shows very good agreement.

Beam Natural Frequencies

Mode	GEMOP Lumped-Mass Frequency (Hz)	Continuous System Frequency (Hz)	GEMOP Error (percent)
1	5.00	5.00	0.0
2	19.98	20.00	0.1
3	44.66	45.00	0.8
4	77.33	80.00	3.3
5	110.59	125.00	11.5

The maximum displacement response of the beam is calculated considering zero damping and a cutoff frequency of 45 Hz. With this cutoff frequency, the calculated response included the effect of Modes 1, 2, and 3. The calculated maximum response for this second case was 0.997 in., compared with the theoretical value of 1.00 in. This indicates an error of only 0.32 percent.

4.1.4.1.8 SHELL 5 and SHELL 9

4.1.4.1.8.1 Program Description

SHELL 5 and SHELL 9 are two finite-shell element programs used to analyze smoothly curved thin-shell structures with any distribution of elastic material properties, boundary constraints, and mechanical thermal and displacement loading conditions. The basic element is triangular. Its membrane displacement fields are linear polynomial functions and its bending displacement field is a cubic polynomial function (Reference 11). Five degrees of freedom (three displacements and two bending rotations) are obtained at each nodal point. SHELL 9 is an improvement of SHELL 5. It includes a more accurate shell element with nine degrees of freedom at each node. Output displacements and stresses are in a local (tangent) surface coordinate system.

Due to the approximation of element membrane displacements by linear functions, the in-plane rotation about the surface normal is neglected. Therefore, the only rotations considered are those caused by bending of the shell cross section. Application of the method is not recommended for shell intersection (or discontinuous surface) problems where in-plane rotation can be significant.

4.1.4.1.8.2 Program Version

A copy of the source deck of SHELL 5 is maintained in the GE Nuclear Energy Division. SHELL 9 is a proprietary computer program of Gulf Atomic Incorporated.

4.1.4.1.8.3 History of Use

SHELL 5 and SHELL 9 are programs developed by Gulf General Atomic Incorporated (Reference 12) in 1969. The programs have been in production status at Gulf General Atomic and other major computer operating systems since 1970.

4.1.4.1.8.4 Extent of Application

SHELL 5 has been used at GE to analyze the reactor shroud support and torus.

4.1.4.1.8.5 Test Problems

Two examples showing comparisons of solutions obtained by the present method with a solution based on a simpler model, an exact solution, and experimental data are presented in Figures 4.1-25 through 4.1-29. Figure 4.1-26 shows the radial displacement for the line-loaded cylinder shown in Figure 4.1-25 compared with the exact solution (Reference 13) and a solution obtained for the element model of Reference 11 with linear membrane and cubic bending displacement approximations. Symmetry permitted the analysis of one slice. In order to show the dependence of the solution on the mesh density, the circumferential angle of the slice was varied, which is equivalent to varying the number of elements. It should be pointed out that this comparison does not constitute a complete study, and other examples may show different convergence behavior. The differences between the two models shown by this example warrant further study.

Figure 4.1-27 shows the finite element idealization of a nozzle-to-cylinder intersection problem that is under experimental investigation at the Oak Ridge National Laboratory.

Because of symmetry about the longitudinal plane, only half of the structure is analyzed for internal pressure. The idealization consisted of 640 modal points and 1168 elements. Comparisons of the analysis with the experimental data in the vicinity of the right-angle intersection for the longitudinal plane are shown in Figures 4.1-28 and 4.1-29. Figure 4.1-28 shows the axial and circumferential outside surface stresses for the cylinder. Figure 4.1-29 shows the axial and circumferential outside surface stresses for the nozzle. The analytical results compare favorably with the distribution and magnitude of experimental stresses (obtained from strain gage results).

4.1.4.1.9 HEATER

4.1.4.1.9.1 Program Description

HEATER is a computer program (Reference 14) used in the hydraulic design of feedwater spargers and their associated delivery heads and piping. The program utilizes test data obtained by GE using full-scale mockups of a feedwater sparger combined with a series of models that represent the complex mixing processes obtained in the upper plenum, downcomer, and lower plenum. Mass and energy balances throughout the nuclear steam supply system (NSSS) are modeled in detail.

4.1.4.1.9.2 Program Version

This program was developed at GE's Nuclear Energy Division.

4.1.4.1.9.3 History of Use

The program was developed by various individuals beginning in 1970. The present version of the program has been in operation since January 1972.

4.1.4.1.9.4 Extent of Application

The program is used in the hydraulic design of the feedwater spargers for each BWR plant in the evaluation of design modifications and the evaluation of unusual operational conditions.

4.1.4.1.9.5 Test Problems

Various critical parts of the program have been verified by hand calculation. The program has also been used to predict test results.

4.1.4.1.10 FAP-71 (Fatigue Analysis Program)

4.1.4.1.10.1 Program Description

The FAP-71 computer code, or Fatigue Analysis Program, is a stress-analysis tool used as an aid in performing ASME B&PV Code Section III structural design calculations. Specifically, FAP-71 is used in determining the primary plus secondary stress range and number of allowable fatigue cycles at points of interest. For structural locations at which the $3S_m$ (P+Q) ASME Code limit is exceeded, the program can perform either (or both) of two elastic-plastic fatigue life evaluations: (a) the method reported in ASME Paper 68-PVP-3; and (b) the present method documented in Paragraph NB-3228.3 of the 1971 Edition of the ASME B&PV Section III Code.

The program can accommodate up to 25 transient stress states of as many as 20 structural locations.

4.1.4.1.10.2 Program Version

The present version of FAP-71 was completed by L. Young of GE's Nuclear Energy Division in 1971 (Reference 15).

4.1.4.1.10.3 History of Use

Since its completion in 1971, the program has been applied to several design analyses of GE BWR vessels.

4.1.4.1.10.4 Extent of Application

The program is used in conjunction with several shell analysis programs in determining the fatigue life of BWR mechanical components subject to thermal transients.

4.1.4.1.10.5 Test Problems

The program has been verified using hand calculations.

4.1.4.1.11 DYSEA

4.1.4.1.11.1 Program Description

The DYSEA (Dynamic and Seismic Analysis) program is a GE proprietary program developed specifically for seismic and dynamic analyses of the reactor building coupled to the RPV and internals. It calculates the dynamic response of linear structural systems by either temporal modal superposition or response spectrum method. Fluid-structure interaction effect in the RPV is taken into account by way of hydrodynamic mass.

The DYSEA program was based on the SAP IV program with added capability to handle the hydrodynamic mass effect. Structural stiffness and mass matrices similar to SAP IV are formulated. Solution is obtained in time domain by calculating the dynamic response mode by mode. Time integration is performed by using Newmark's β-method. Response spectrum solution is also available as an option.

4.1.4.1.11.2 Program Version

The DYSEA version was developed at GE by modifying the SAP IV program. Capability was added to handle the hydrodynamic mass effect due to fluid-structure interaction in the reactor. It can handle three-dimensional dynamic problems with beams, trusses, and springs. Both acceleration time-histories and response spectra may be used as input.

4.1.4.1.11.3 History of Use

The DYSEA program was developed in the summer of 1976. It has been adopted as a standard production program since 1977 and has been used extensively in all dynamic and seismic analyses of the reactor building coupled to the RPV and internals.

4.1.4.1.11.4 Extent of Application

The current version of DYSEA has been used in all dynamic and seismic analyses since its development. Results from test problems were found to be in close agreement with those obtained from either verified programs or analytic solutions.

4.1.4.1.11.5 Test Problems

Problem 1

The first test problem involves finding the eigenvalues and eigenvectors from the following characteristic equation:

$$(\omega^2[\mathrm{M}] - [\mathrm{K}])\{\chi\} = 0$$

where ω is the circular frequency and χ is the eigenvector. The stiffness and the mass matrices are represented by [K] and [M], respectively, and are given by

$$[\mathrm{M}] = \begin{bmatrix} 1-\frac{4}{\pi^2} & \frac{4}{\pi^2} & -\frac{4}{9\pi^2} \\ & 1-\frac{4}{9\pi^2} & \frac{4}{\pi^2} \\ Symmetric & & 1-\frac{4}{25\pi^2} \end{bmatrix}$$

$$[\mathrm{K}] = \begin{bmatrix} 1+\frac{4}{\pi^2} & 3 & \frac{5}{9} \\ & 1+\frac{9\pi^2}{4} & 15 \\ Symmetric & & 1+\frac{25\pi^2}{4} \end{bmatrix}$$

The analytic solutions and the solutions from DYSEA are

Eigenvalues ω_i

i	DYSEA Solution	Analytic Solution
1	5.7835	5.7837
2	30.4889	30.4878
3	75.0493	75.0751

Eigenvector χ

DYSEA Solution

$$\begin{bmatrix} 1.000 & 1.000 & 1.000 \\ -0.0319 & -1.5536 & -1.2105 \\ -0.0072 & -0.066 & 2.0271 \end{bmatrix}$$

Analytic Solution

$$\begin{bmatrix} 1.000 & 1.000 & 1.000 \\ -0.0319 & -1.554 & -1.211 \\ -0.0072 & 0.0666 & 2.027 \end{bmatrix}$$

Problem 2

The second test problem compares the dynamic responses of the reactor building coupled to the RPV and internals when subjected to earthquake ground motion.

The mathematical model of the reactor building coupled to the RPV and internals is given in Figure 4.1-30. The input in the form of ground spectra is applied at the basemat level. Response spectrum analysis was used in the analysis.

Natural frequencies of the system and the maximum responses at key locations have been calculated by both DYSEA and SAMIS. Comparisons of results are given in Tables 4.1-2 and 4.1-3. The results calculated by DYSEA agree closely with those obtained by SAMIS.

4.1.4.2 Fuel Rod Thermal Analysis

Fuel thermal design analysis techniques are described in Subsection 4.2.3.

4.1.4.3 Reactor Systems Dynamics

The analysis techniques and computer codes used in reactor systems dynamics are described in Reference 16.

4.1.4.4 Nuclear Analysis

The analysis techniques and nuclear data used to determine the neutronic characteristics of the assembly and the core are generally similar to those used in the industry for light-water reactors. The methods are described fully in Subsection 4.3.3.

4.1.4.5 Neutron Fluence Calculations

The neutron fluence calculational technique is described in Subsection 4.3.2.8.

4.1.4.6 Thermal-Hydraulic Calculations

The thermal-hydraulic calculational techniques are described in Subsection 4.4.4.5.

4.1 REACTOR SUMMARY DESCRIPTION

REFERENCES

1. General Electric Co. "General Electric Standard Application for Reactor Fuel, GESTAR-II," NEDE-24011-P-A, (Latest Approved Revision as identified in the COLR).

1a. L. Beitch, "Shell Structures Solved Numerically by Using a Network of Partial Panels," AIAA J., Vol. 5, No. 3, March 1967.

2. E. L. Wilson, A Digital Computer Program for the Finite Element Analysis of Solids With Non-linear Material Properties, Aerojet General Technical Memo No. 23, July 1965.

3. I. S. Tuba and W. B. Wright (Editors), Pressure Vessel and Piping - 1972 Computer Program Verification, ASME, New York, 1972.

4. I. Farhoomand and E. L. Wilson, Non-Linear Heat Transfer Analysis of Axisymmetric Solids, SESM Report SESM71-6, University of California, Berkeley, California 1971.

5. P. J. Schneider, Temperature Response Charts, John Wiley & Sons, Inc., New York, 1963.

6. J. E. McConoclee, FINITE-Users Manual, General Electric TIS Report DF 69SL206, March 1969.

7. M. A. Goldberg and M. Sadowsky, "Stress in an Ellipsoidal Rotor in a Centrifugal Force Field," Journal of Applied Mechanics, Vol. 26, No. 4, p. 549, December 1959.

8. R. J. Melosh et al., Structural Analysis and Matrix Interpretive System (SAMIS) Program Report, Revision 1, Jet Propulsion Laboratory, Pasadena, California, Technical Memorandum 33-307, December 15, 1966.

9. R. J. Melosh and H. N. Christiansen, Structural Analysis and Matrix Interpretive System (SAMIS) Program: Technical Report, Jet Propulsion Laboratory, Pasadena, California, Technical Memorandum 33-311, November 1, 1966.

10. T. E. Lang, Structural Analysis and Matrix Interpretive System (SAMIS) User Report, Jet Propulsion Laboratory, Pasadena, California, Technical Memorandum 33-305, March 1, 1967.

11. R. W. Clough and C. P. Johnson, "A Finite Element Approximation for the Analysis of Thin Shells," Intl. J. Solid Structures, Vol. 4, 1968.

12. A Computer Program for the Structural Analysis of Arbitrary Three-Dimensional Thin Shells, Gulf General Atomic Inc., Report No. GA-9952.

13. S. Timoshenko and S. Woinowsky-Krieger, Theory of Plates and Shells, McGraw-Hill Book Company, New York, 1959.

14. A. B. Burgess, User Guide and Engineering Description of HEATER Computer Program, March 1974.

REFERENCES

15. L. J. Young, FAP-71 (Fatigue Analysis Program) Computer Code, GE/NED, Design Analysis Unit, R. A. Report No. 409, January 1972.

16. L. A. Carmichael and G. J. Scatena, Stability and Dynamic Performance of the General Electric Boiling Water Reactor, APED-5652, April 1969.

TABLE 4.1-1 CLAMPED SQUARE PLATE THEORETICAL AND COMPUTED FREQUENCY COMPARISON

Case No:	f_1[a]	% Diff.	f_2	% Diff.	f_3	% Diff.	f_4	% Diff.	f_5	% Diff.	f_6	% Diff.
Theory	176.5		359.9		530.9		645.5		648.6		810.0	
1	205.6	16.5	438.0	21.7	817.4	54.0	727.7	12.7	769.3	18.6	1476.0	82.2
2	190.7	8.0	409.1	13.8	696.5	31.2	672.7	4.2	702.3	8.3	1076.1	32.9
3	183.8	4.1	391.2	8.7	600.2	13.5	705.1	9.2	719.2	10.9	999.0	23.3
4	183.3	3.8	380.7	5.8	597.9	12.6	657.3	1.8	670.4	3.4	917.4	13.3

[a] Frequency values f_1 to f_6 are in cps

TABLE 4.1-2 COMPARISON OF NATURAL FREQUENCIES

	X-Direction Frequency		Y-Direction Frequency	
Mode	Old Analysis	DYSEA	Old Analysis	DYSEA
1	2.810	2.727	2.678	2.649
2	3.040	2.999	2.810	2.728
3	3.764	3.763	3.762	3.758
4	3.791	3.781	3.771	3.769
5	4.588	4.576	4.578	4.531
6	5.041	5.044	5.040	5.039
7	5.776	5.791	5.486	5.431
8	6.071	6.047	6.069	6.025
9	8.731	8.625	8.598	8.524
10	10.950	11.270	9.614	9.824
11	12.796	12.800	12.563	12.760

TABLE 4.1-3 COMPARISON OF MAXIMUM LOADS

Structural Component	DYSEA Solution	SAMIS Solution
I. RPV and internals		
Fuel moment	17.11 (in-K)[a]	18.64 (in-K)
Top guide shear	188 (K)	204 (K)
Shroud head shear	198 (K)	213 (K)
Shroud head moment	16,783 (in-K)	18,150 (in-K)
Shroud support shear	479.3 (K)	503.3 (K)
Shroud support moment	119,020 (in-K)	126,600 (in-K)
II. Building		
RPV pedestal		
- Shear	602 (K)	575.9 (K)
- Moment	94,200 (in-K)	91,500 (in-K)
Containment		
- Shear	2,902 (K)	2,908 (K)
- Moment	1,413,000 (in-K)	1,434,000 (in-K)
Shield building		
- Shear	34,037 (K)	38,060 (K)
- Moment	38,494,000 (in-K)	37,270,000 (in-K)

[a] K = kips, 1 kip = 100 lb.

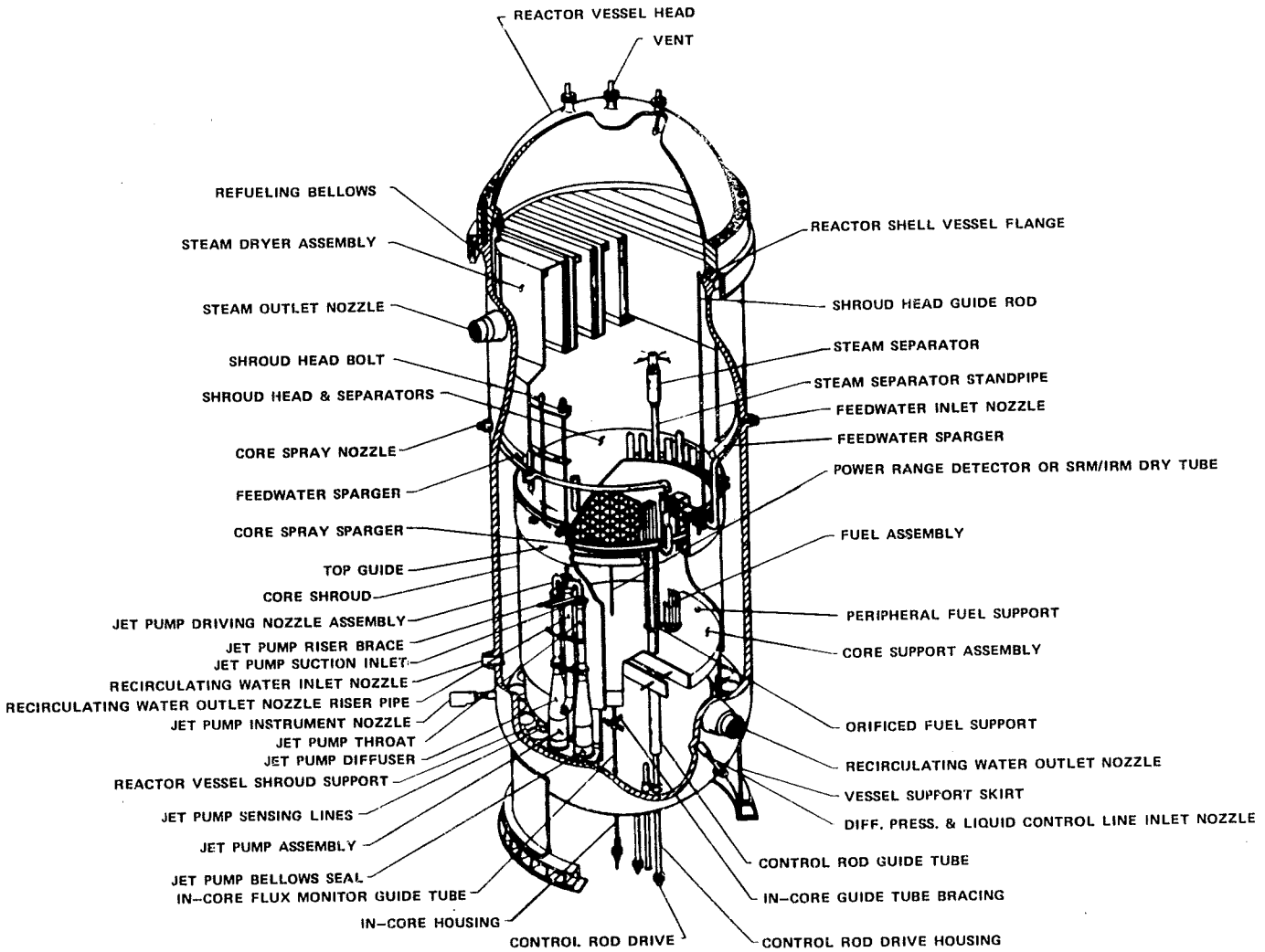

Fermi 2
UPDATED FINAL SAFETY ANALYSIS REPORT

FIGURE 4.1-1

REACTOR VESSEL CUTAWAY

GENERAL ELECTRIC CO. DRAWING

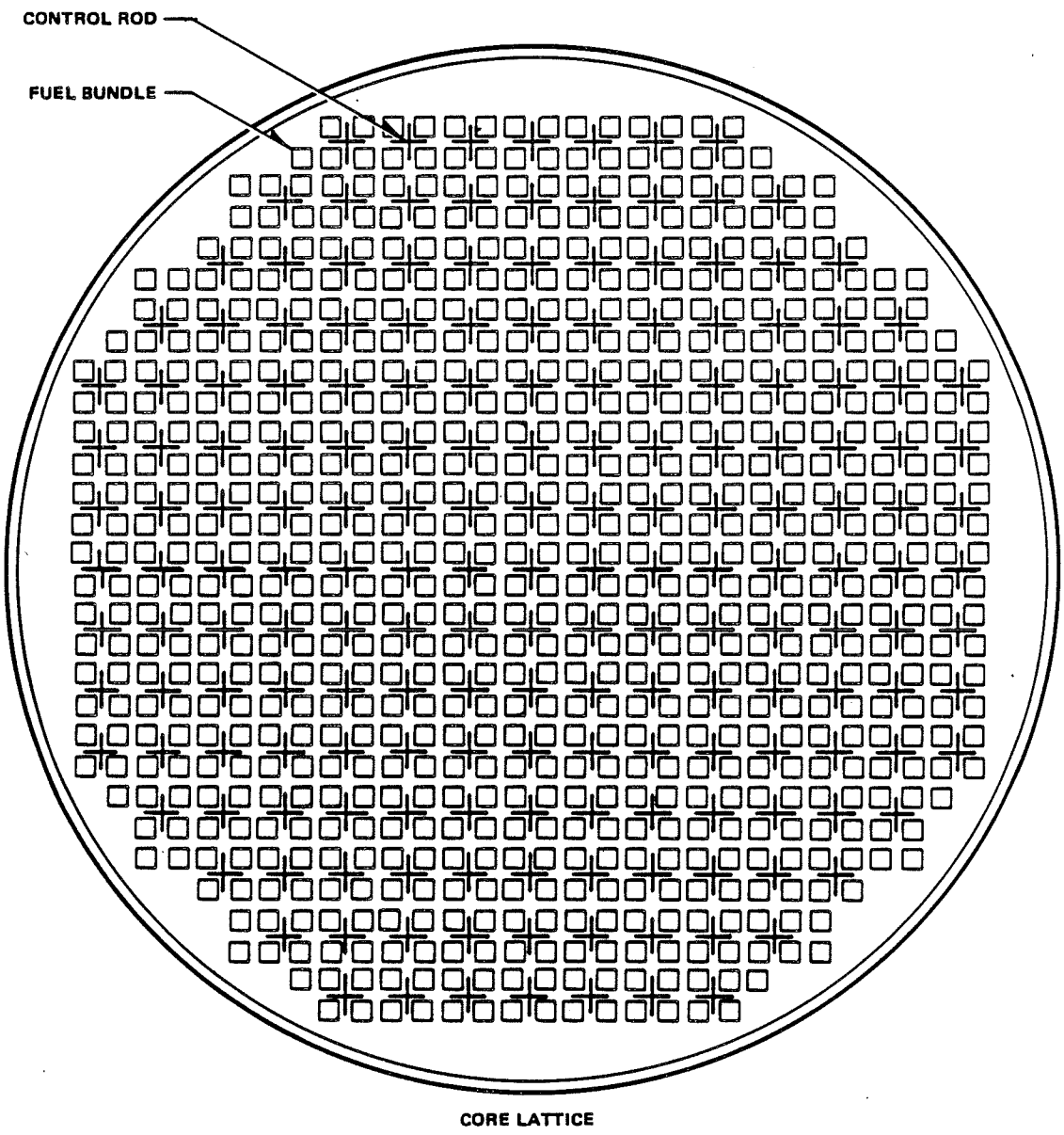

Fermi 2
UPDATED FINAL SAFETY ANALYSIS REPORT

FIGURE 4.1-2

TYPICAL CORE ARRANGEMENT

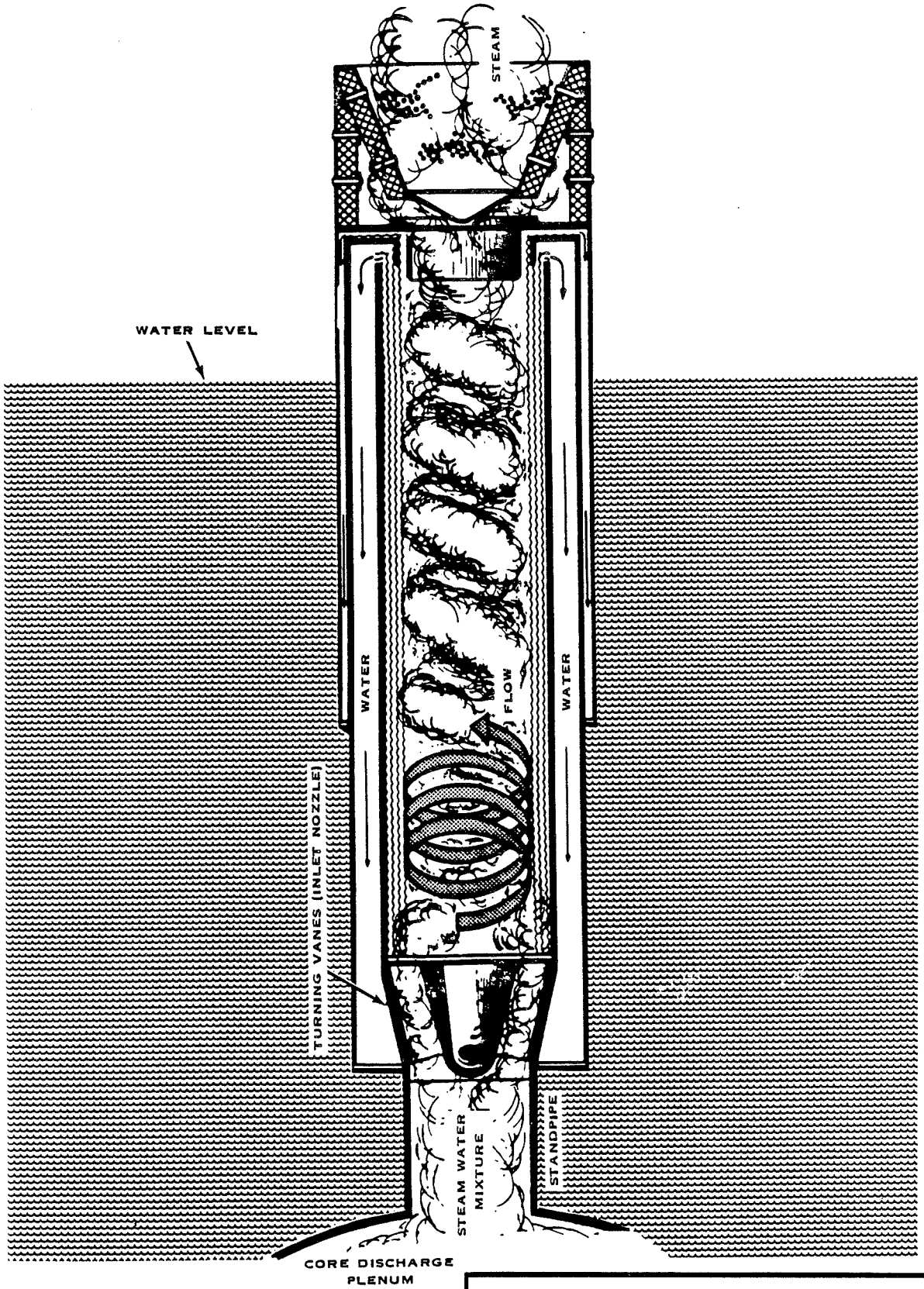

Fermi 2
UPDATED FINAL SAFETY ANALYSIS REPORT

FIGURE 4.1-3

STEAM SEPARATOR

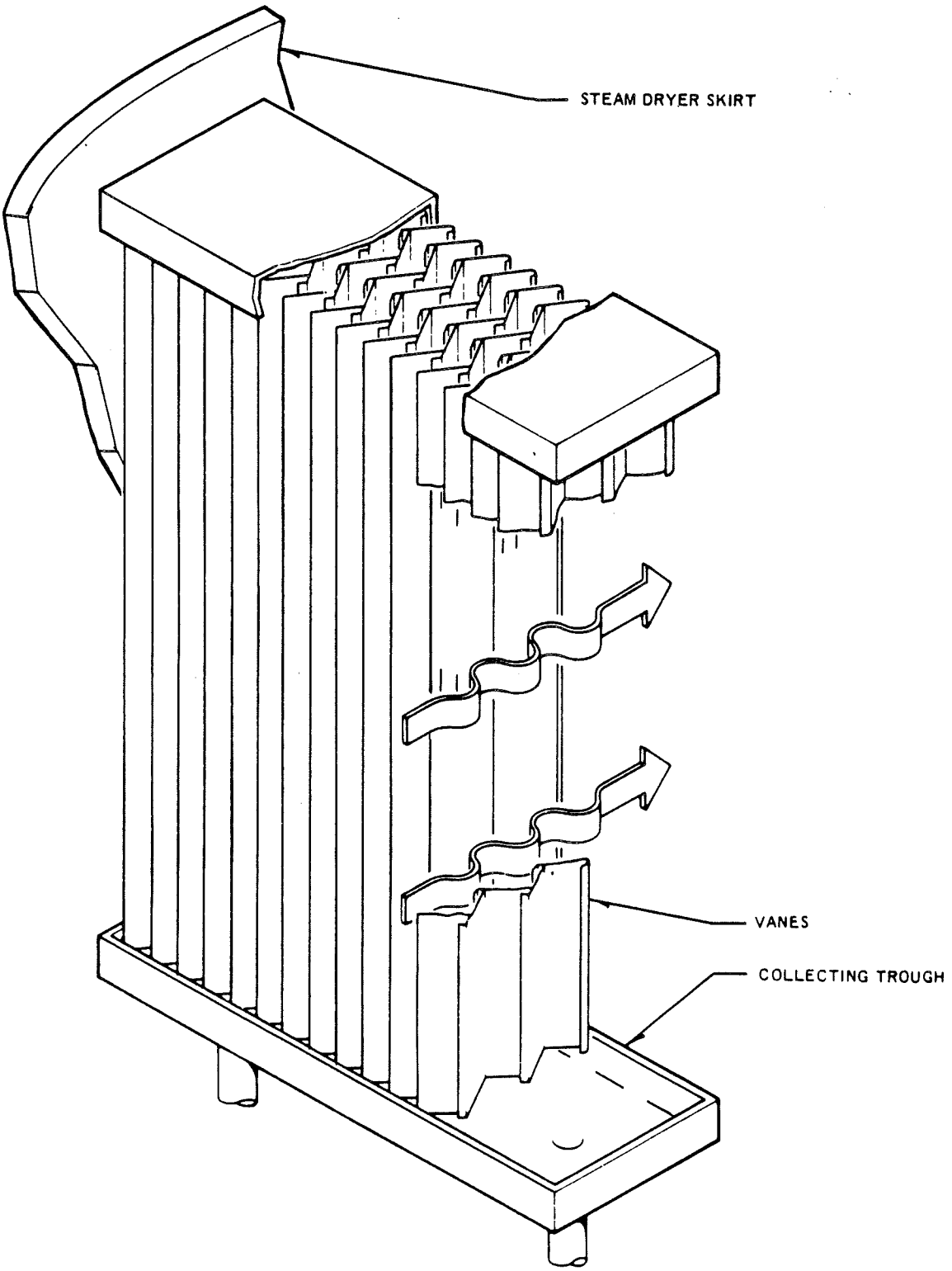

Fermi 2
UPDATED FINAL SAFETY ANALYSIS REPORT

FIGURE 4.1-4

STEAM DRYER

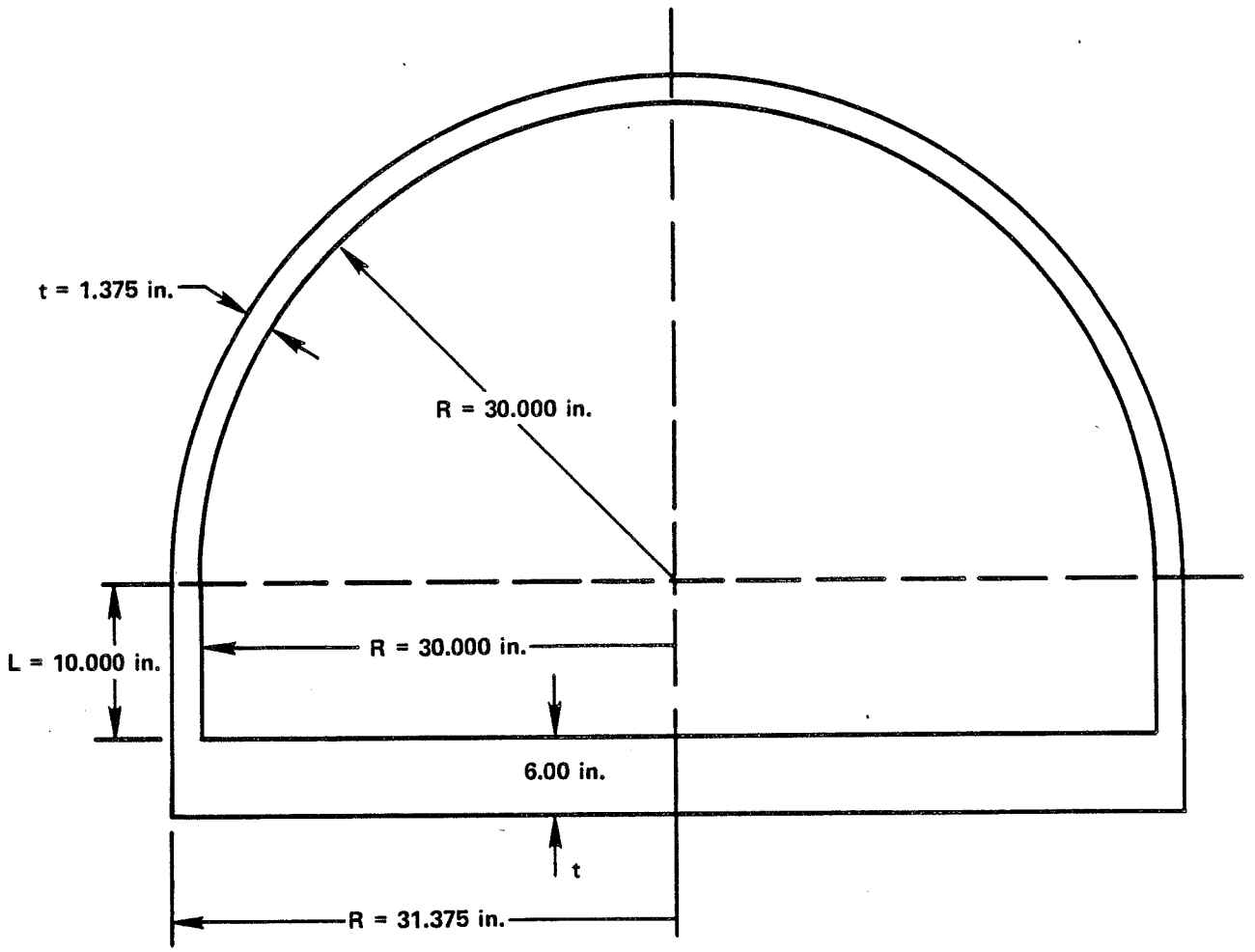

MATERIAL	SA 533 Gr. B LOW ALLOY STEEL
YOUNG'S MODULUS	29 X 10^6 psi
POISSON'S RATIO	0.3
COEFFICIENT OF THERMAL EXPANSION	6.6 X 10^{-6} $(^oF)^{-1}$

Fermi 2
UPDATED FINAL SAFETY ANALYSIS REPORT

FIGURE 4.1-5

PRESSURE VESSEL ANALYSIS

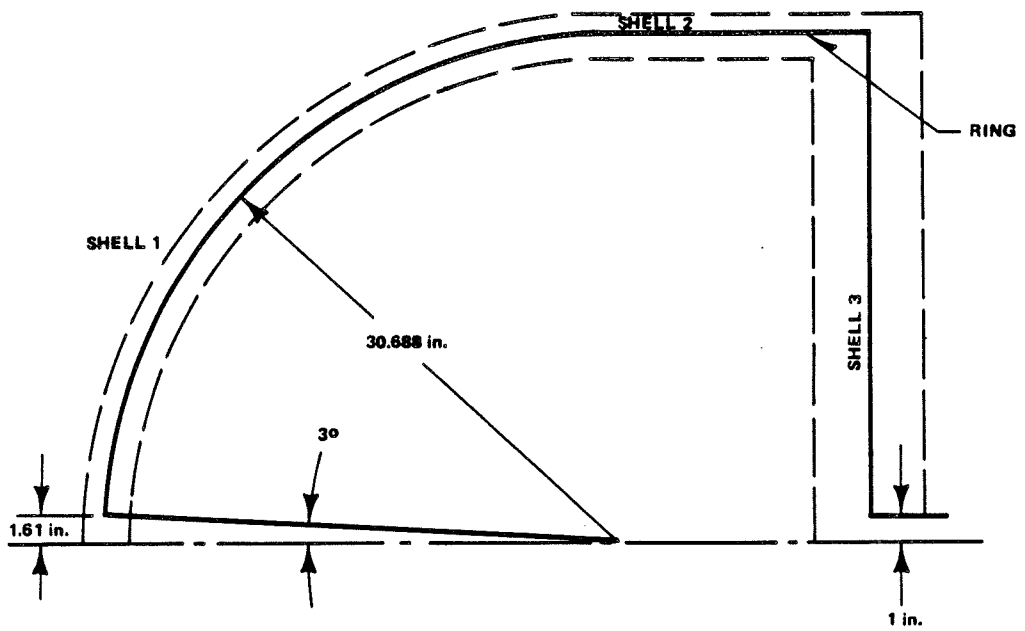

Fermi 2
UPDATED FINAL SAFETY ANALYSIS REPORT

FIGURE 4.1-6

MULTISHELL MODEL

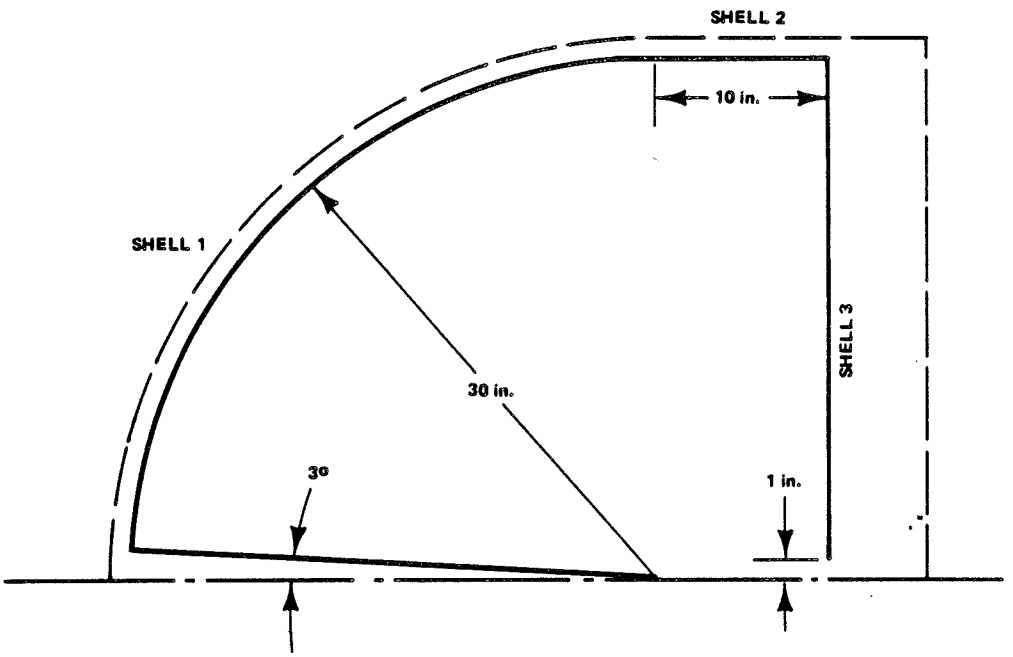

Fermi 2
UPDATED FINAL SAFETY ANALYSIS REPORT

FIGURE 4.1-7

OMP MODEL

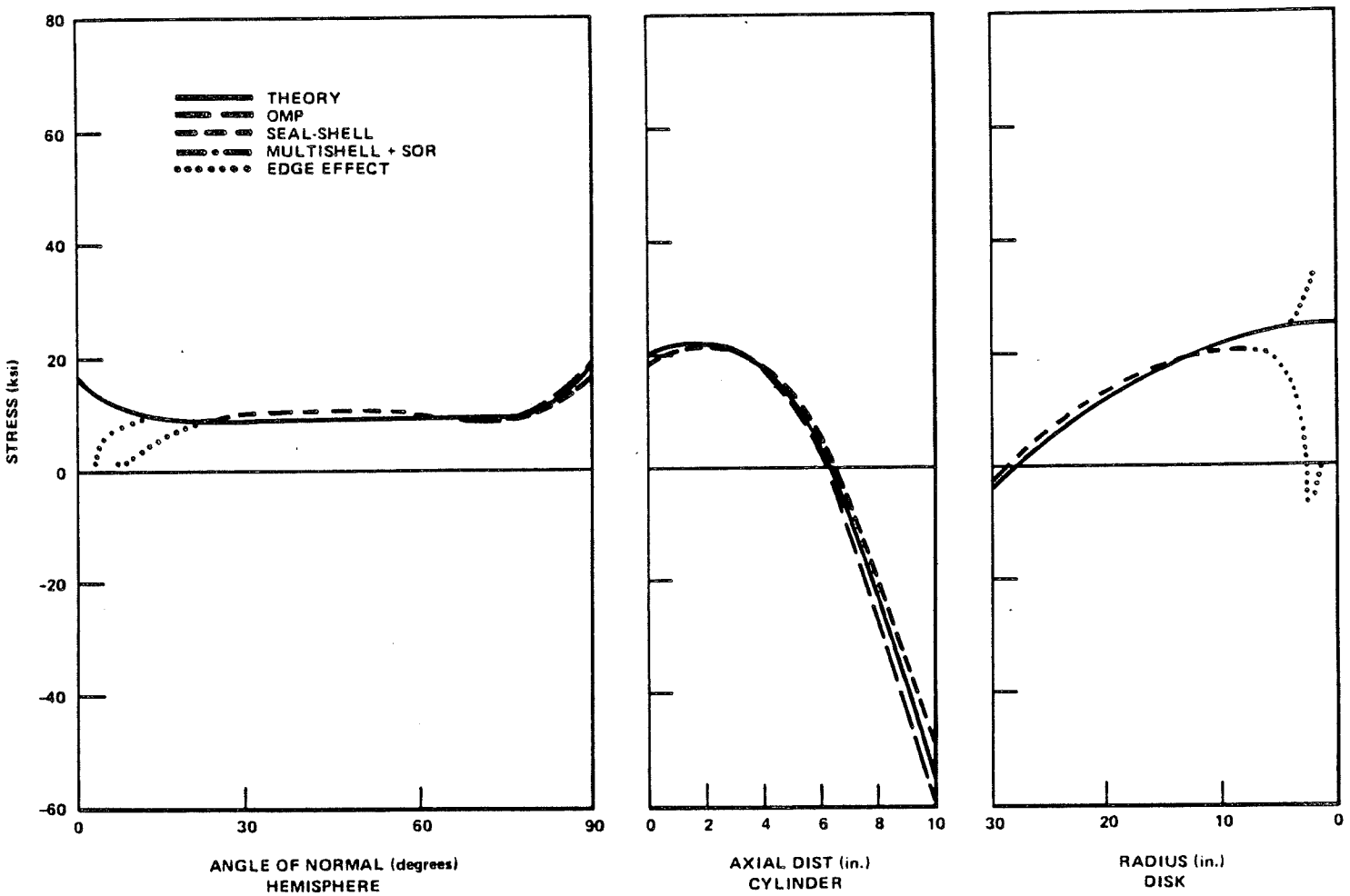

Fermi 2
UPDATED FINAL SAFETY ANALYSIS REPORT

FIGURE 4.1-8

950 PSI INTERNAL PRESSURE AXIAL STRESS
OUTER SURFACE

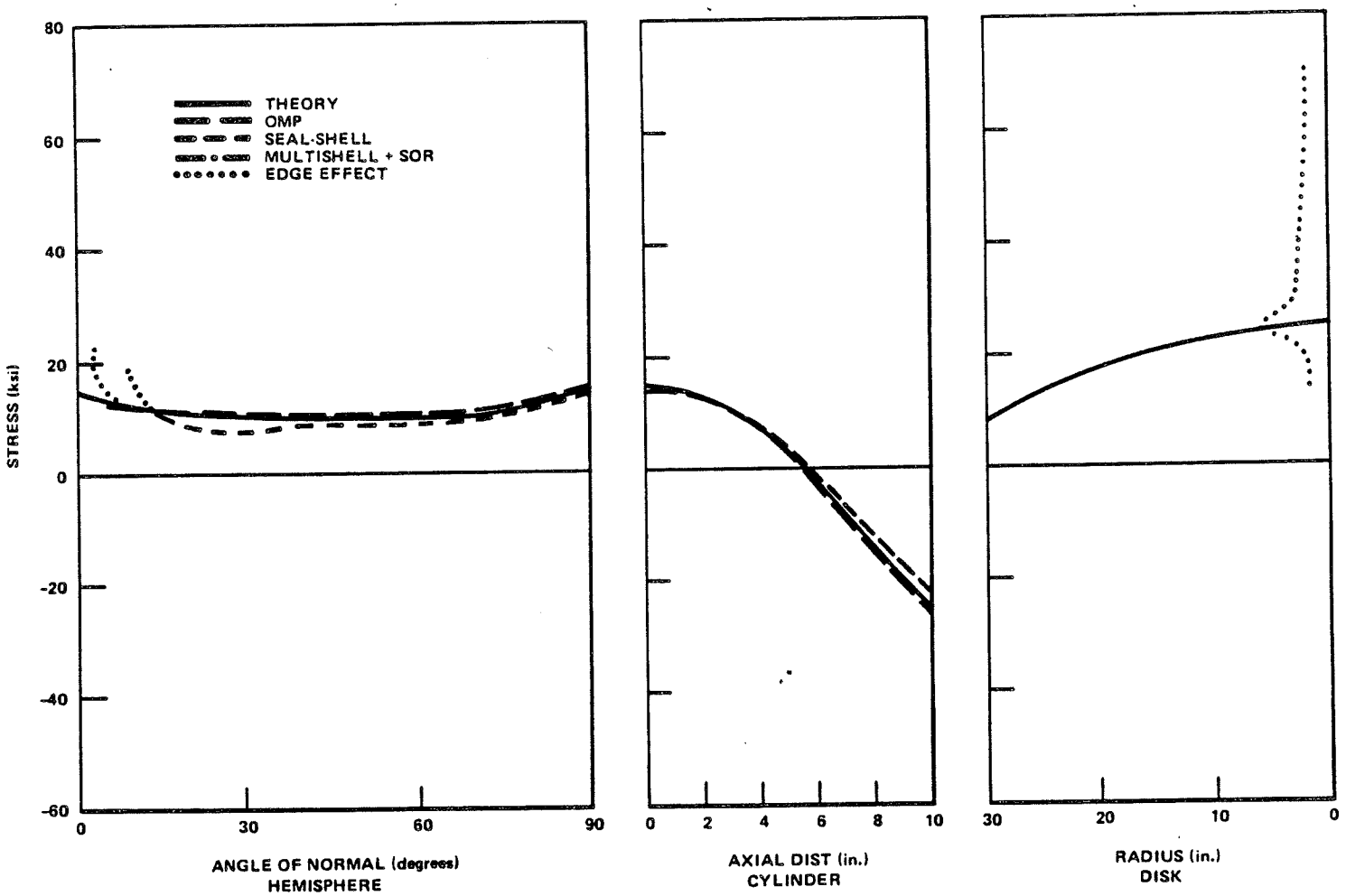

Fermi 2
UPDATED FINAL SAFETY ANALYSIS REPORT

FIGURE 4.1-9

950 PSI INTERNAL PRESSURE HOOP STRESS
OUTER SURFACE

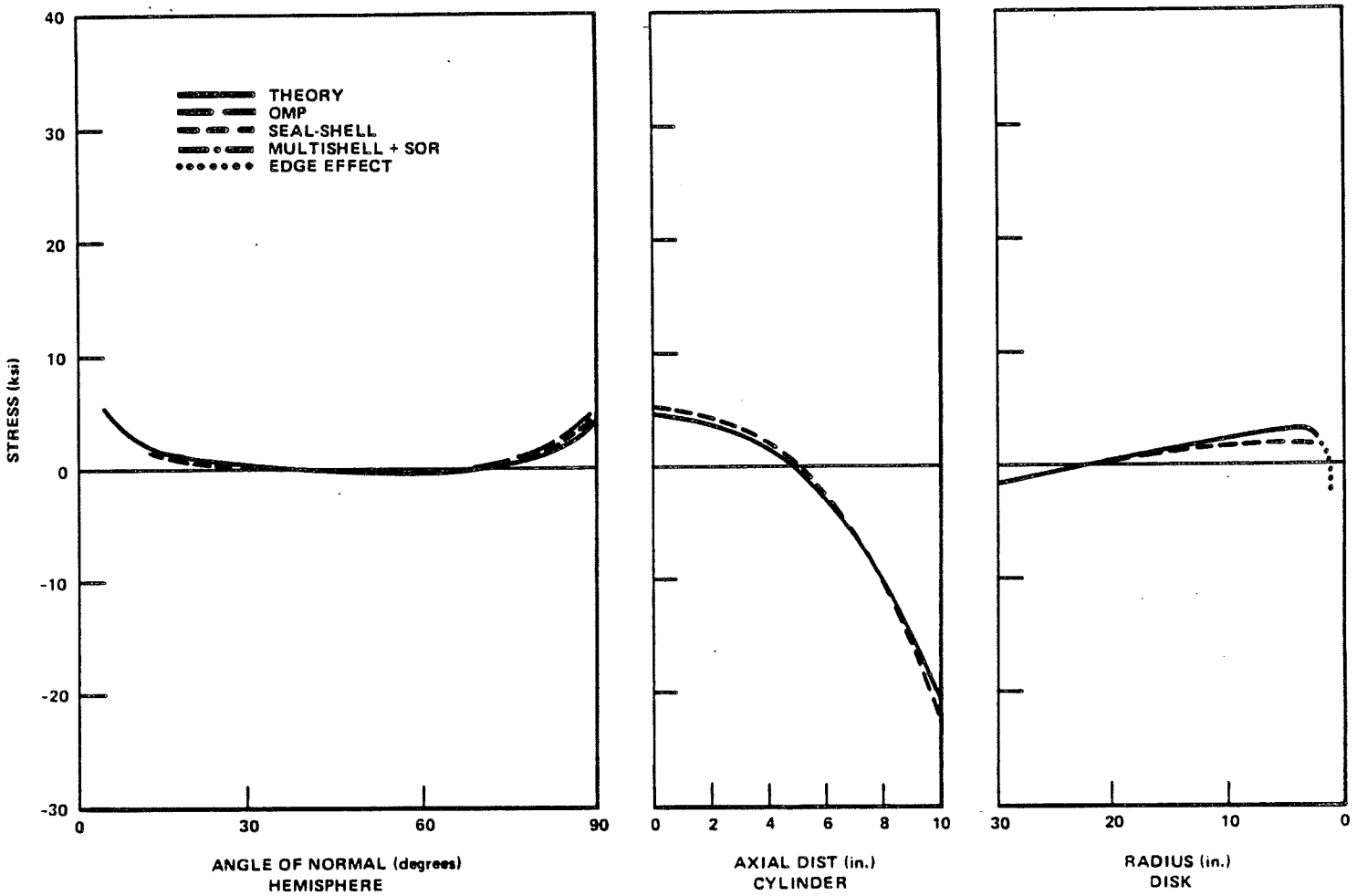

Fermi 2
UPDATED FINAL SAFETY ANALYSIS REPORT

FIGURE 4.1-10

AXIAL TEMPERATURE GRADIENT AXIAL STRESS
OUTER SURFACE

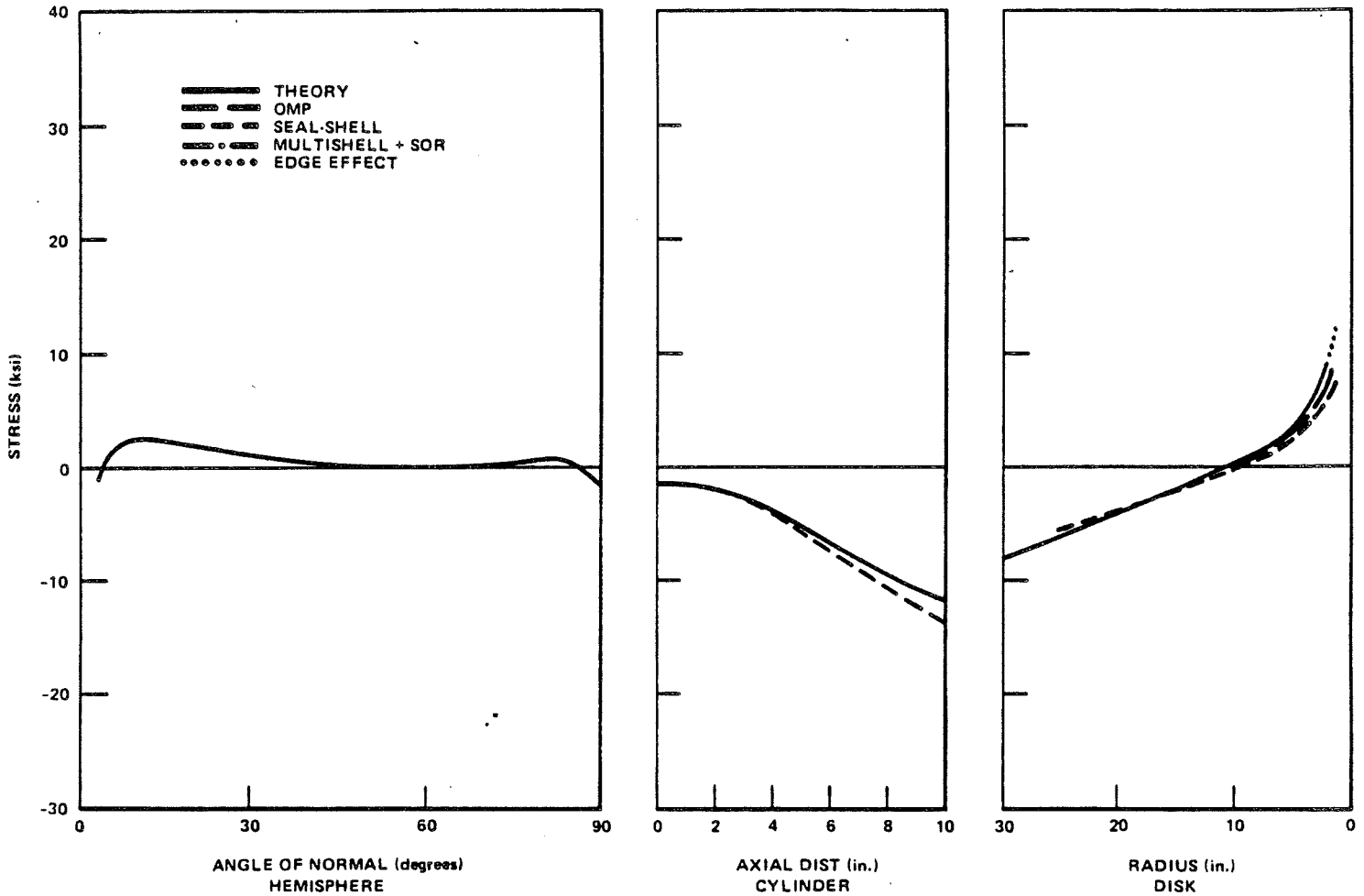

Fermi 2
UPDATED FINAL SAFETY ANALYSIS REPORT

FIGURE 4.1-11

AXIAL TEMPERATURE GRADIENT HOOP STRESS
OUTER SURFACE

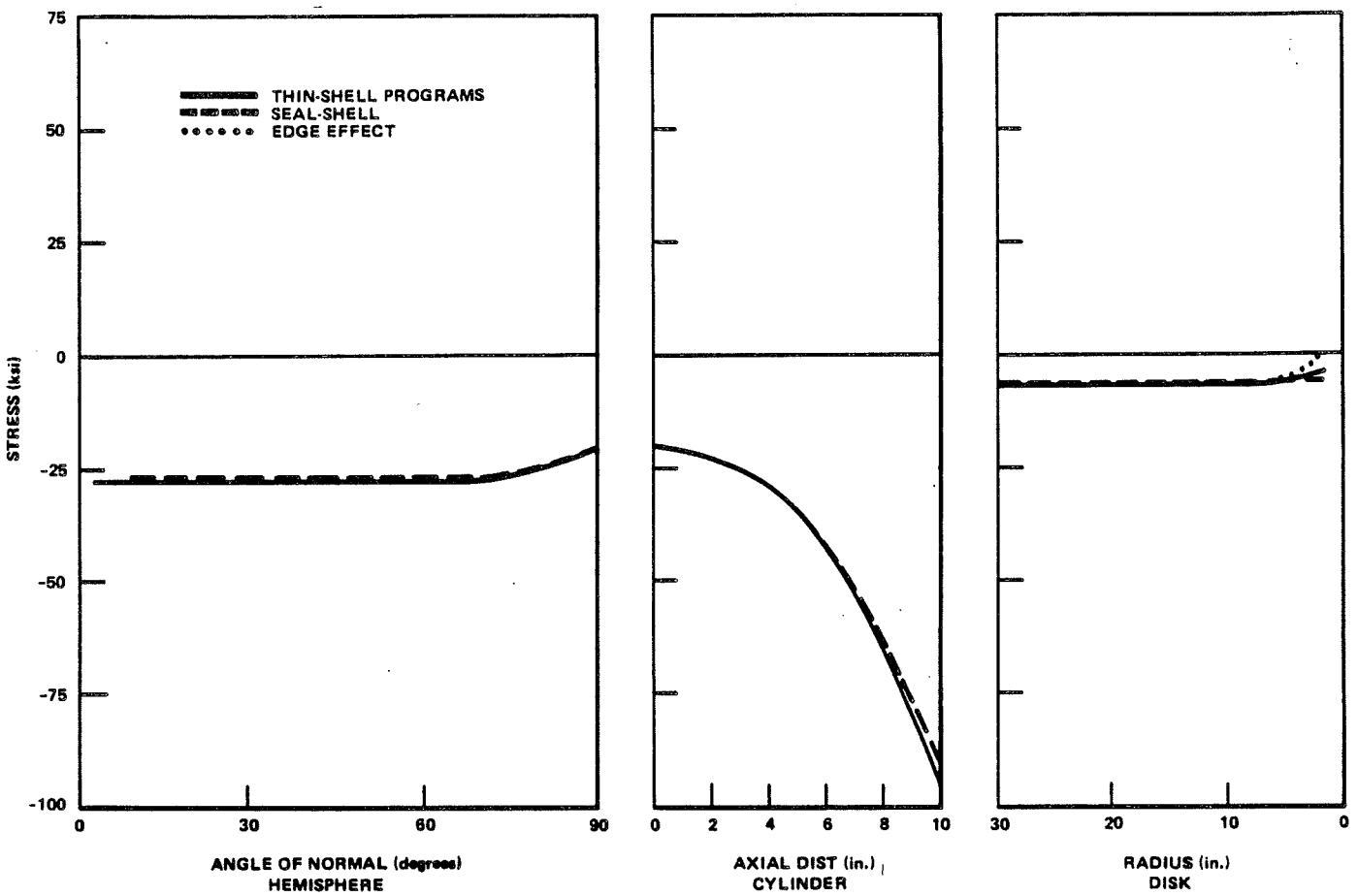

Fermi 2
UPDATED FINAL SAFETY ANALYSIS REPORT

FIGURE 4.1-12

LINEAR RADIAL TEMPERATURE GRADIENT
AXIAL STRESS – OUTER SURFACE

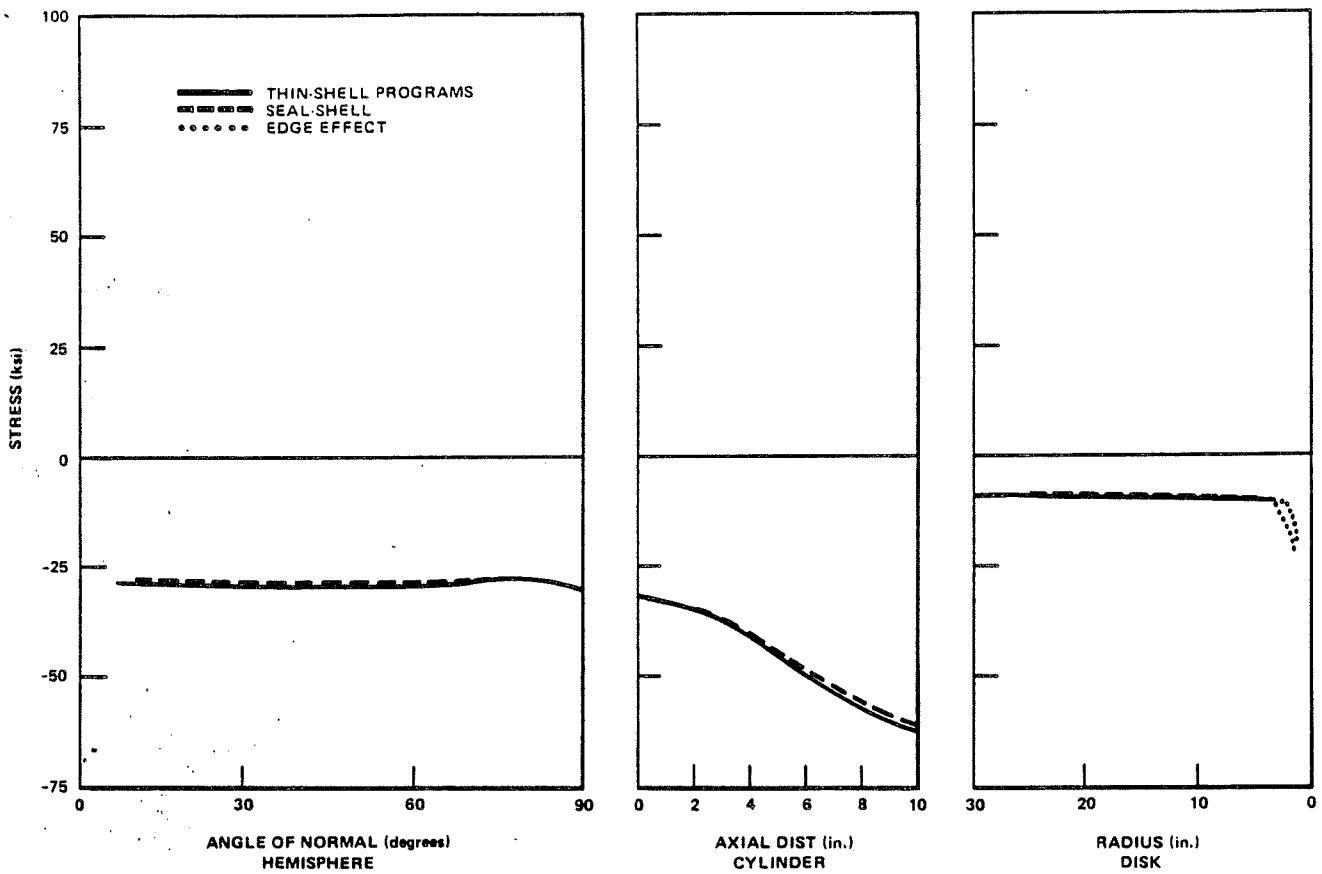

Fermi 2
UPDATED FINAL SAFETY ANALYSIS REPORT

FIGURE 4.1-13

LINEAR RADIAL TEMPERATURE GRADIENT HOOP STRESS – OUTER SURFACE

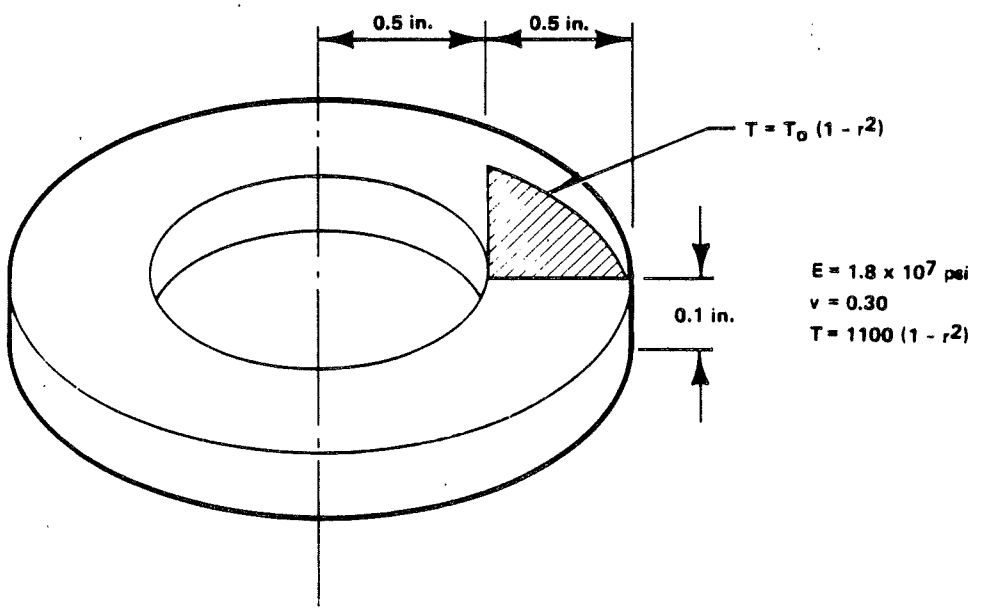

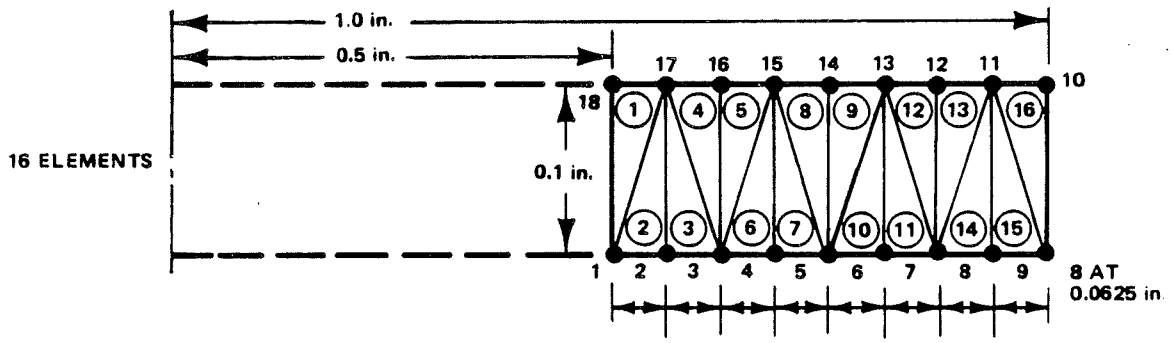

● DENOTES NODE POINTS

◯ DENOTES ELEMENT NUMBER

Fermi 2
UPDATED FINAL SAFETY ANALYSIS REPORT

FIGURE 4.1-14

ASME COMPUTER PROGRAM
VERIFICATION PROBLEM 19 AND
FINITE ELEMENT MODEL

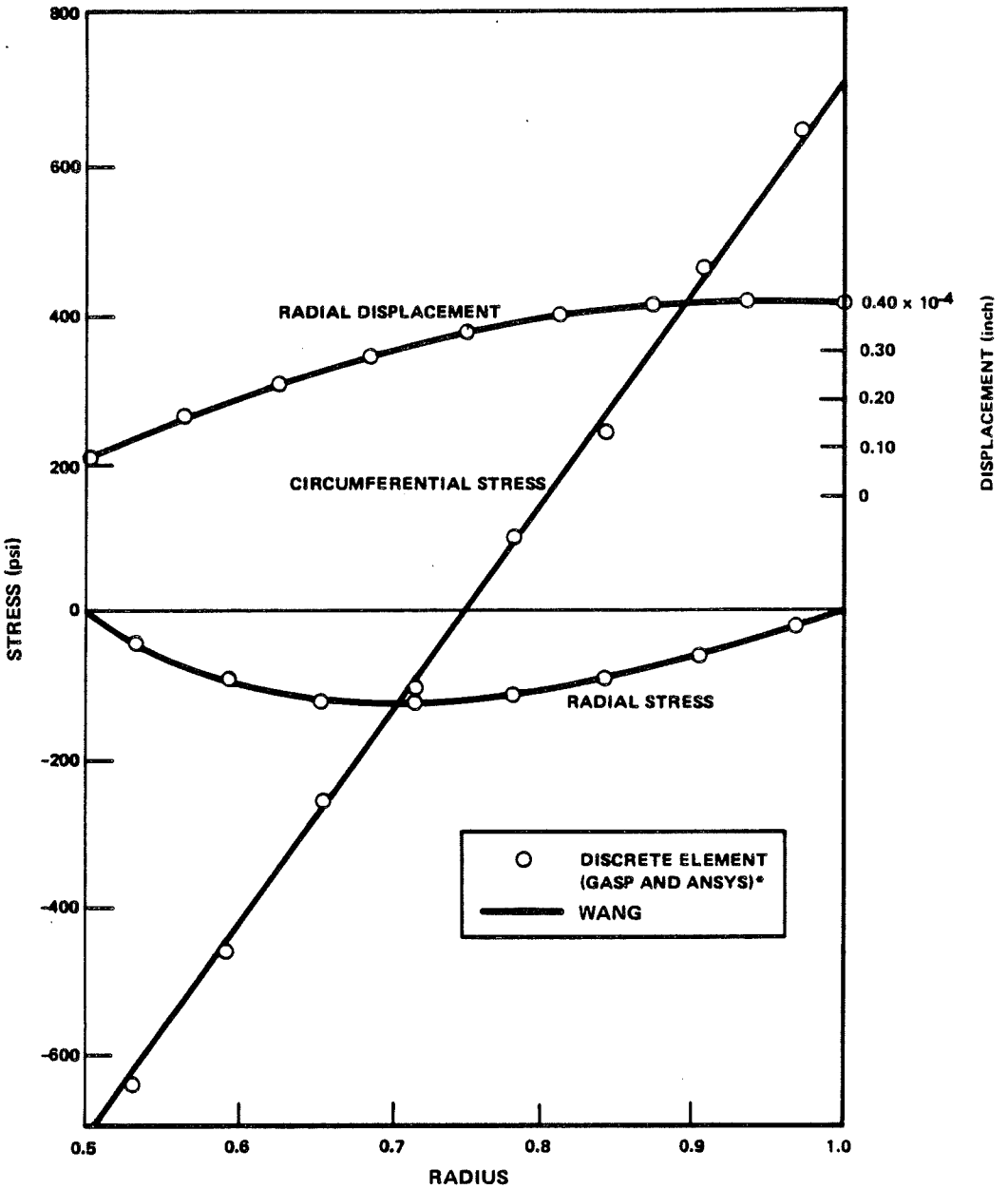

** ALL STRESS VALUES ARE AVERAGES OF STRESSES IN TWO NEIGHBORING TRIANGULAR ELEMENTS.
** CLOSED FORM SOLUTION FROM REFERENCE 3.

Fermi 2
UPDATED FINAL SAFETY ANALYSIS REPORT

FIGURE 4.1-15

COMPARISON OF ANALYTICAL RESULTS FOR PROBLEM 19

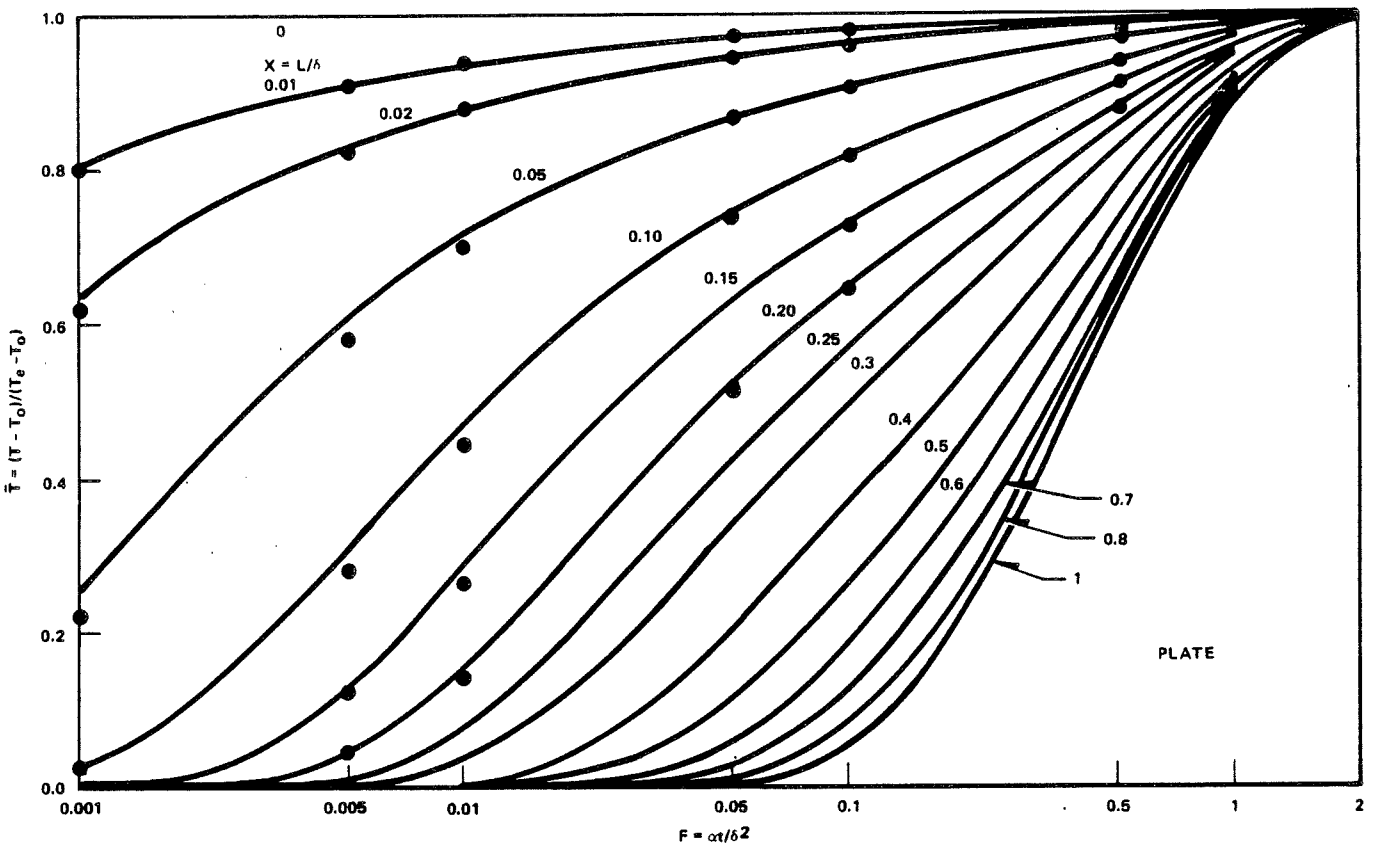

Fermi 2
UPDATED FINAL SAFETY ANALYSIS REPORT

FIGURE 4.1-16

TEMPERATURE RESPONSE OF PLATE THROUGH THICKNESS

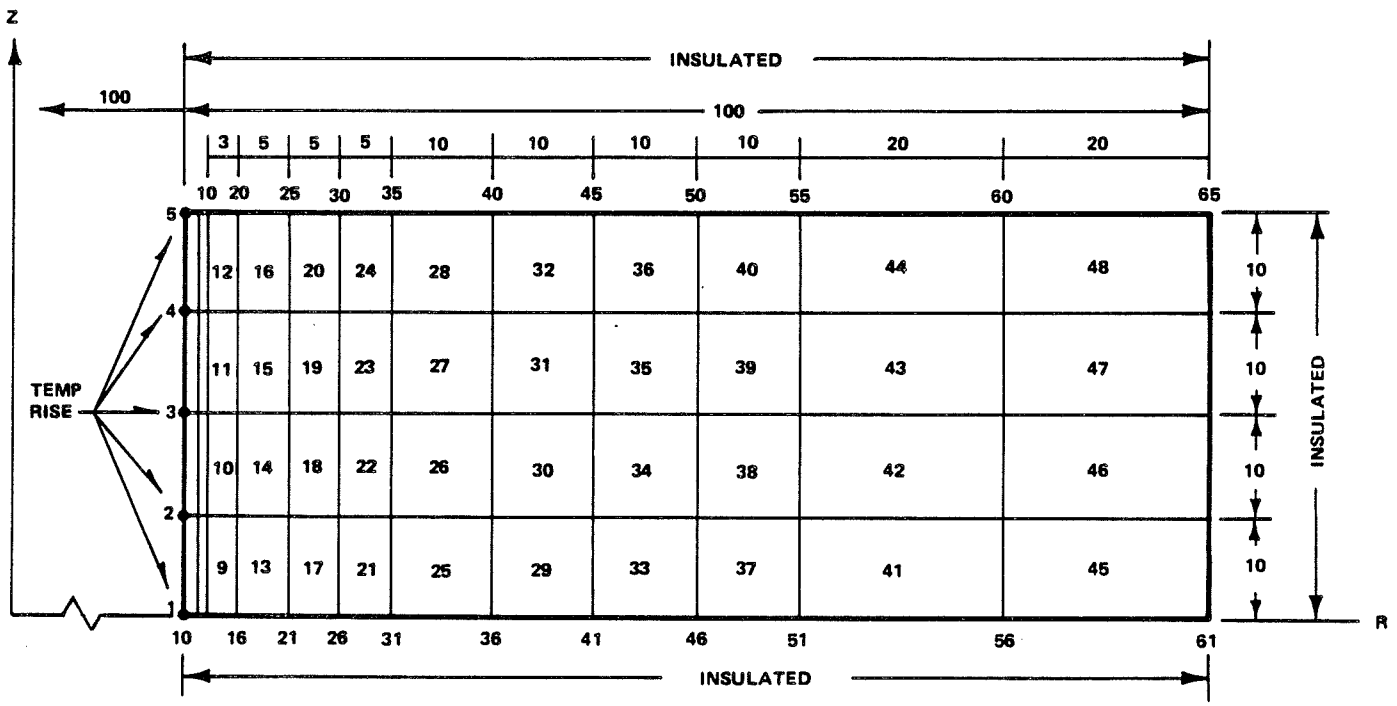

Fermi 2
UPDATED FINAL SAFETY ANALYSIS REPORT

FIGURE 4.1-17

FINITE ELEMENT MESH

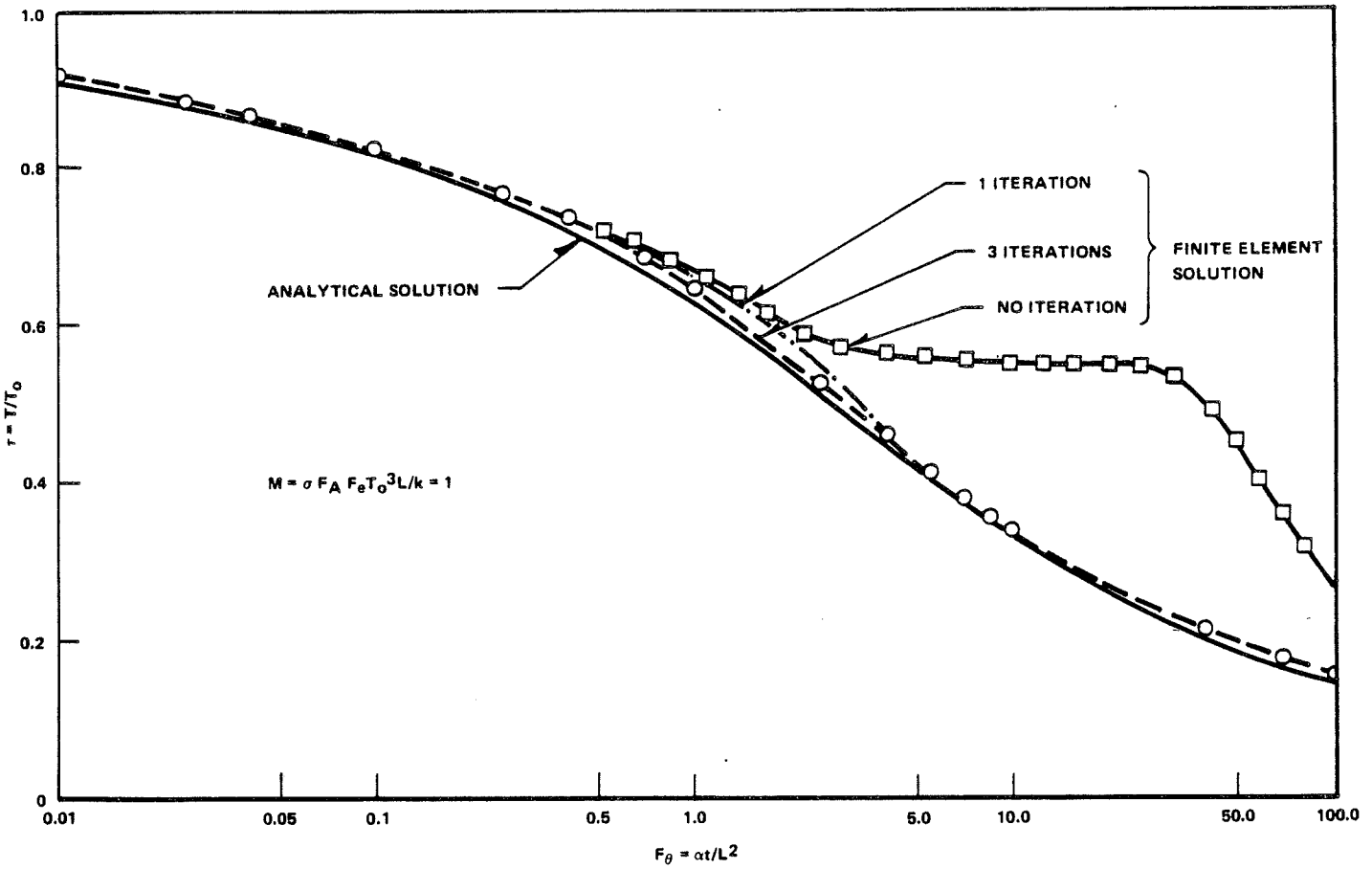

Fermi 2
UPDATED FINAL SAFETY ANALYSIS REPORT

FIGURE 4.1-18

TEMPERATURE RESPONSE OF A PLATE SUBJECTED TO RADIATION

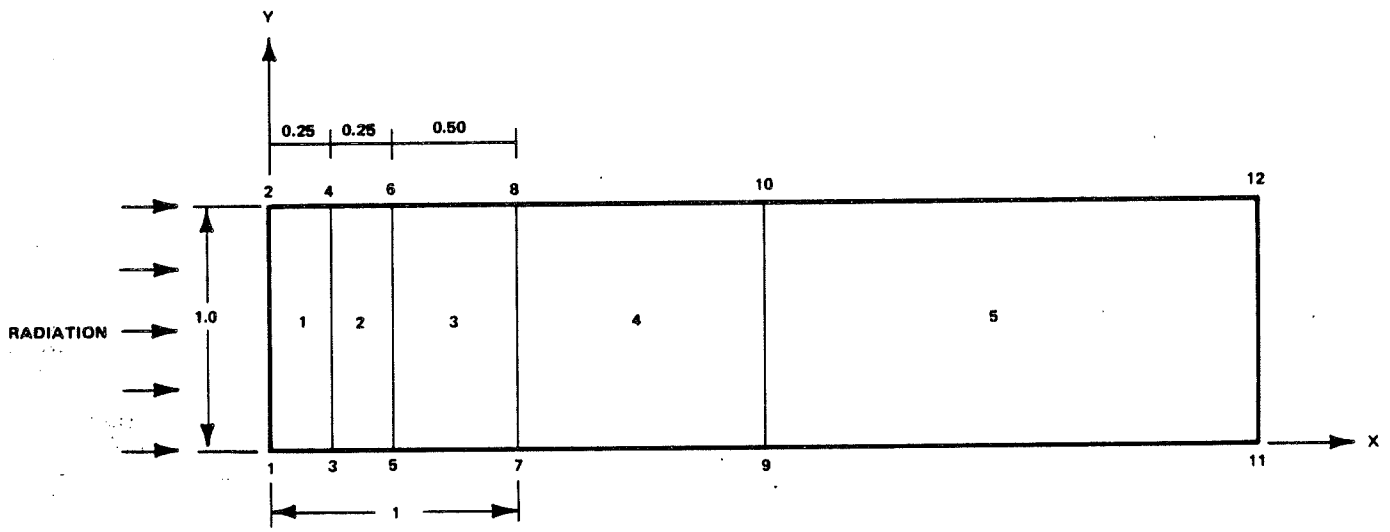

Fermi 2
UPDATED FINAL SAFETY ANALYSIS REPORT

FIGURE 4.1-19

FINITE ELEMENT MESH LAYOUT

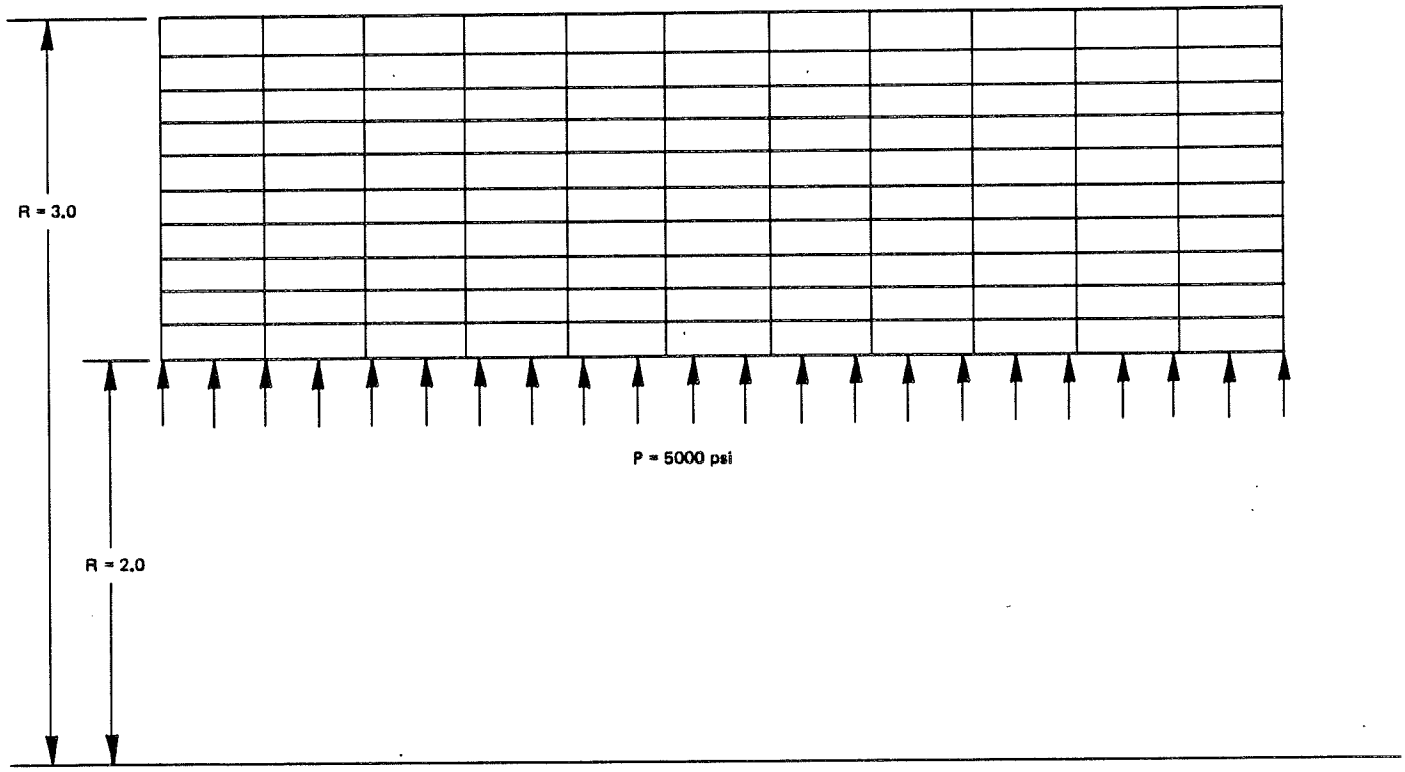

Fermi 2
UPDATED FINAL SAFETY ANALYSIS REPORT

FIGURE 4.1-20

ANALYTICAL MODEL – CASE A

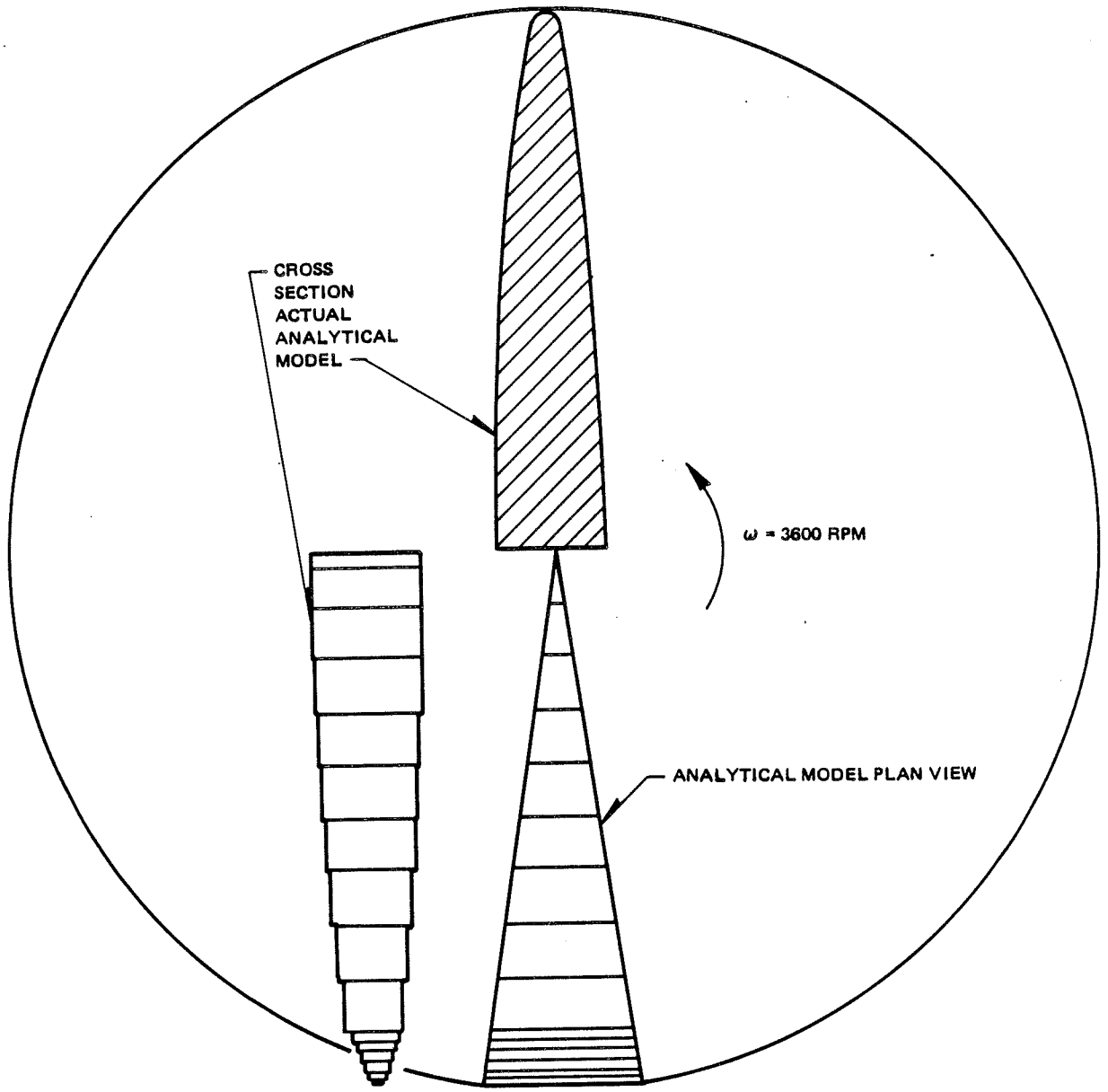

Fermi 2
UPDATED FINAL SAFETY ANALYSIS REPORT

FIGURE 4.1-21

ANALYTICAL MODEL – CASE B

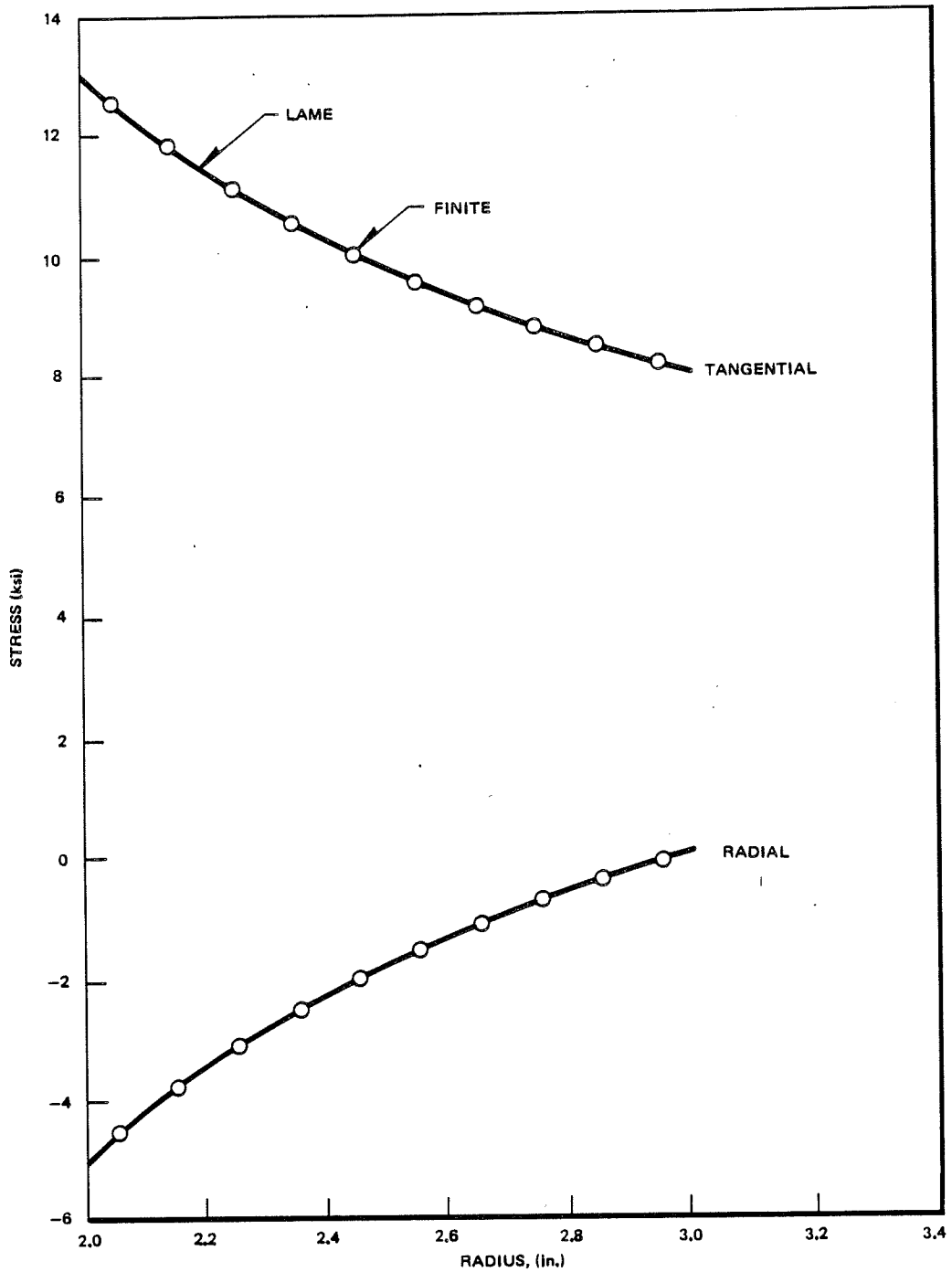

Fermi 2
UPDATED FINAL SAFETY ANALYSIS REPORT

FIGURE 4.1-22

COMPARISON OF STRESSES – CASE A

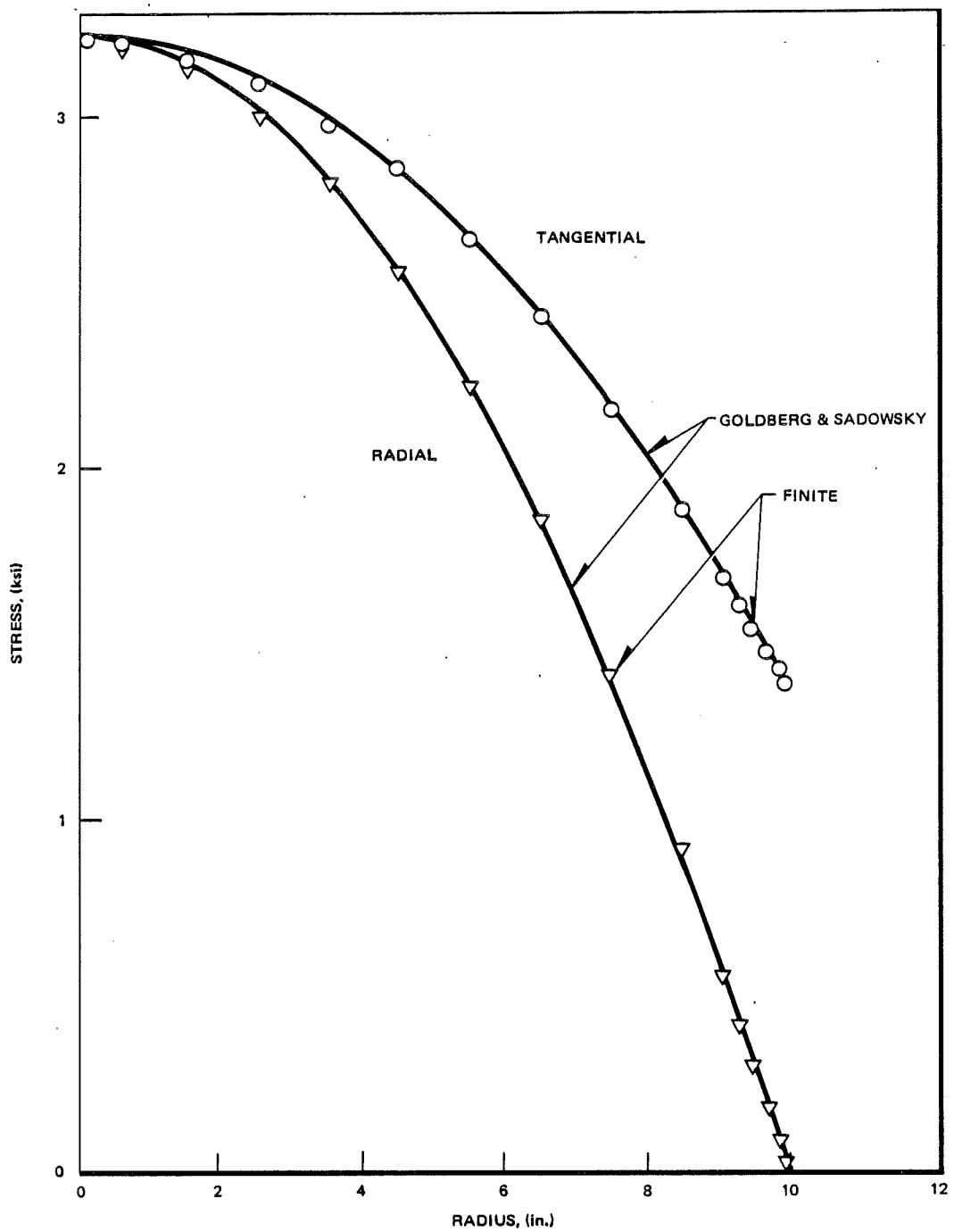

Fermi 2
UPDATED FINAL SAFETY ANALYSIS REPORT

FIGURE 4.1-23

COMPARISON OF STRESSES – CASE B

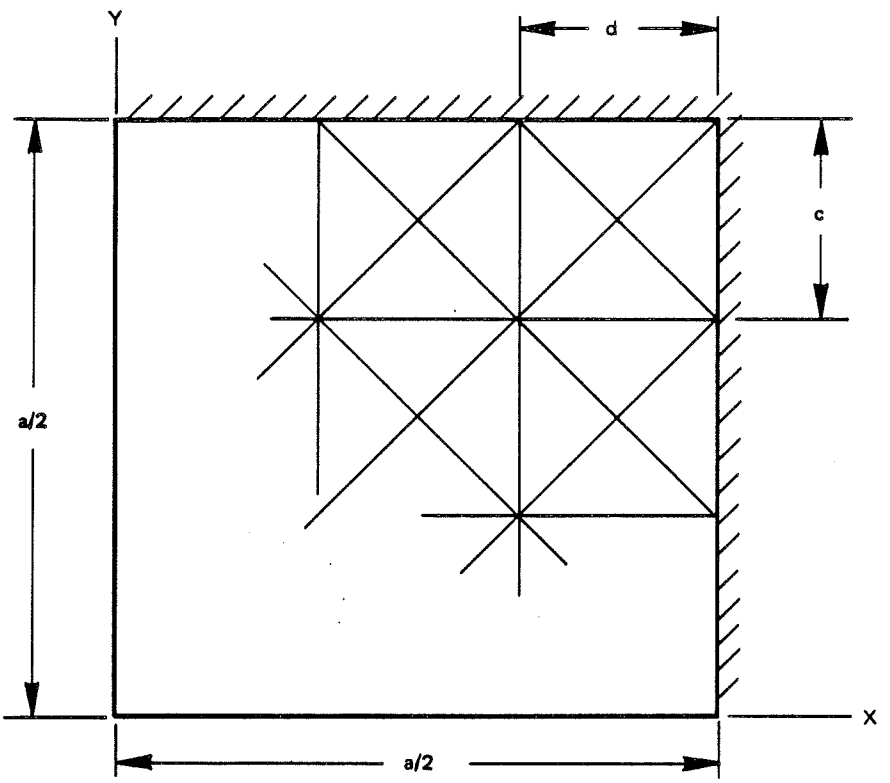

Fermi 2
UPDATED FINAL SAFETY ANALYSIS REPORT

FIGURE 4.1-24

CLAMPED SQUARE PLATE QUARTER PANEL

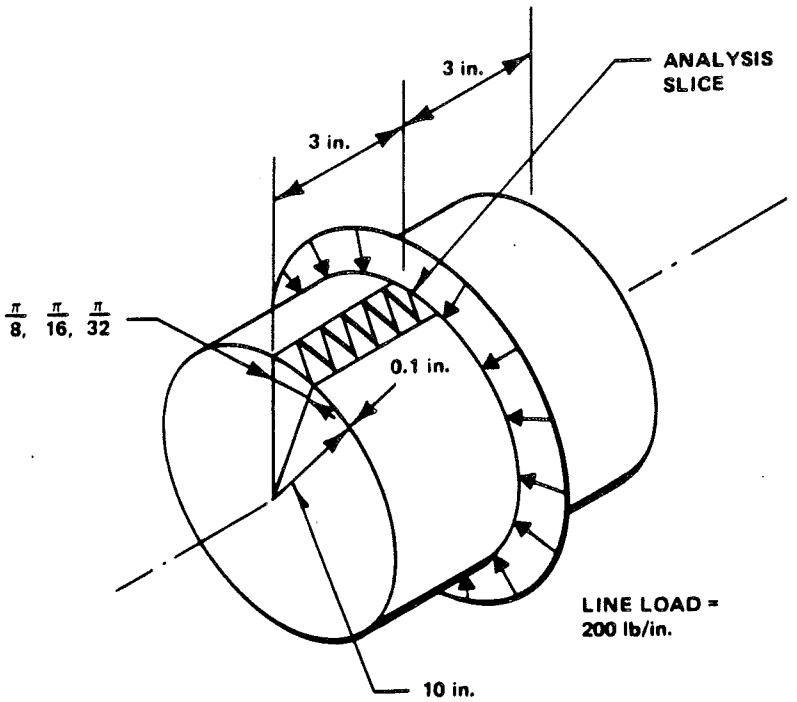

Fermi 2
UPDATED FINAL SAFETY ANALYSIS REPORT

FIGURE 4.1-25

LINE LOADED CYLINDER

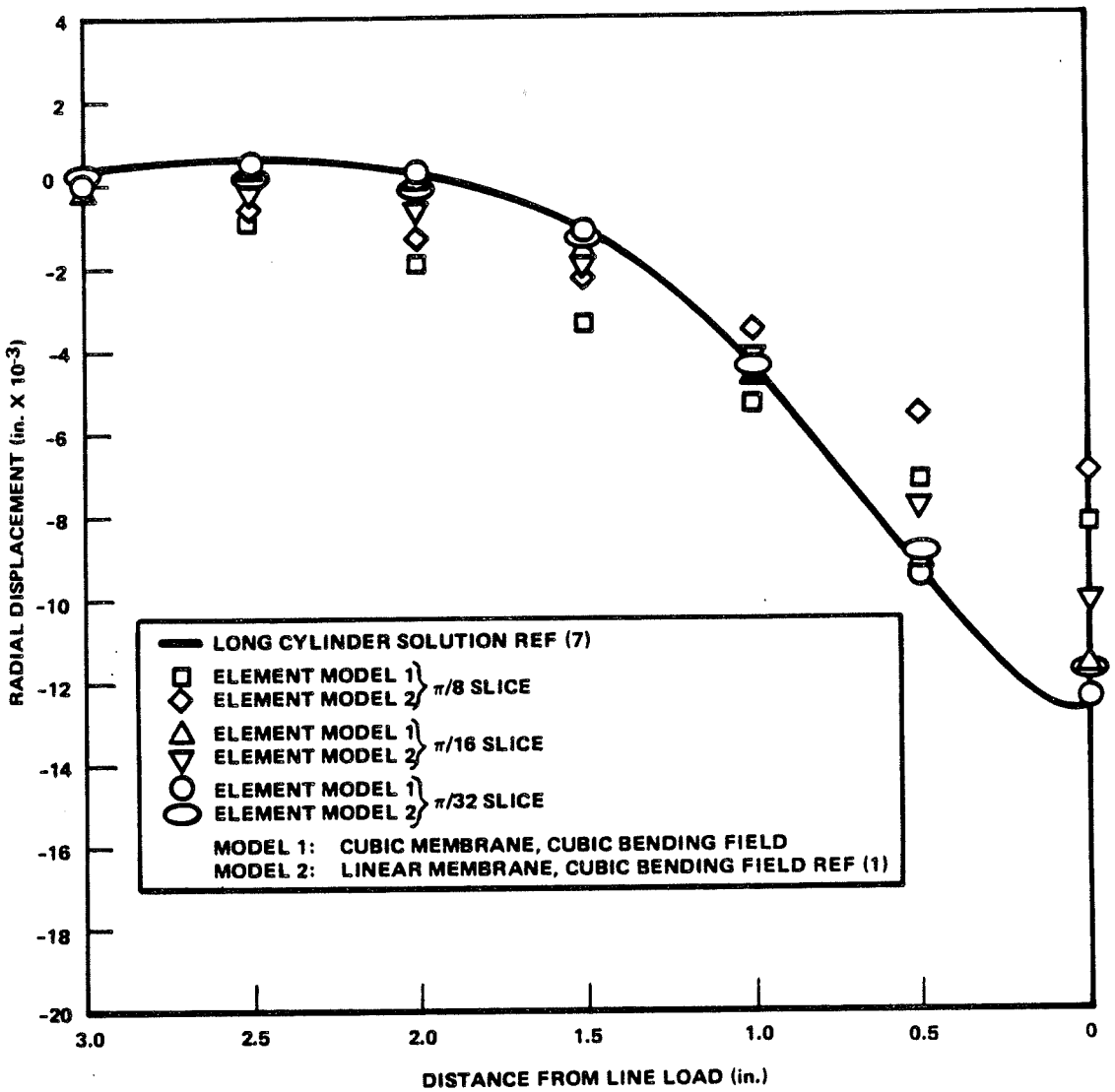

Fermi 2
UPDATED FINAL SAFETY ANALYSIS REPORT

FIGURE 4.1-26

RADIAL DISPLACEMENT FOR LINE LOADED CYLINDER

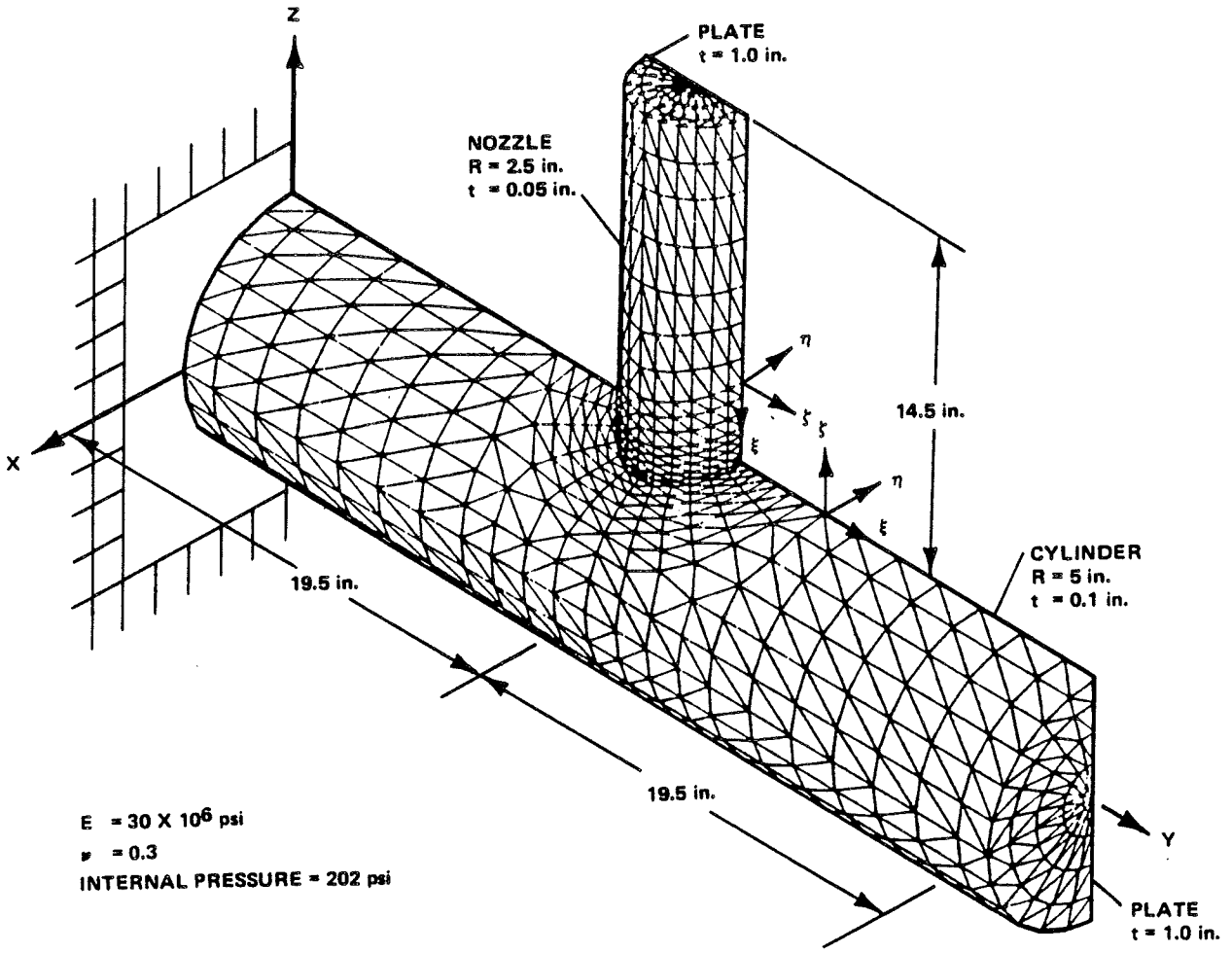

Fermi 2
UPDATED FINAL SAFETY ANALYSIS REPORT

FIGURE 4.1-27

NOZZLE TO CYLINDER INTERSECTION

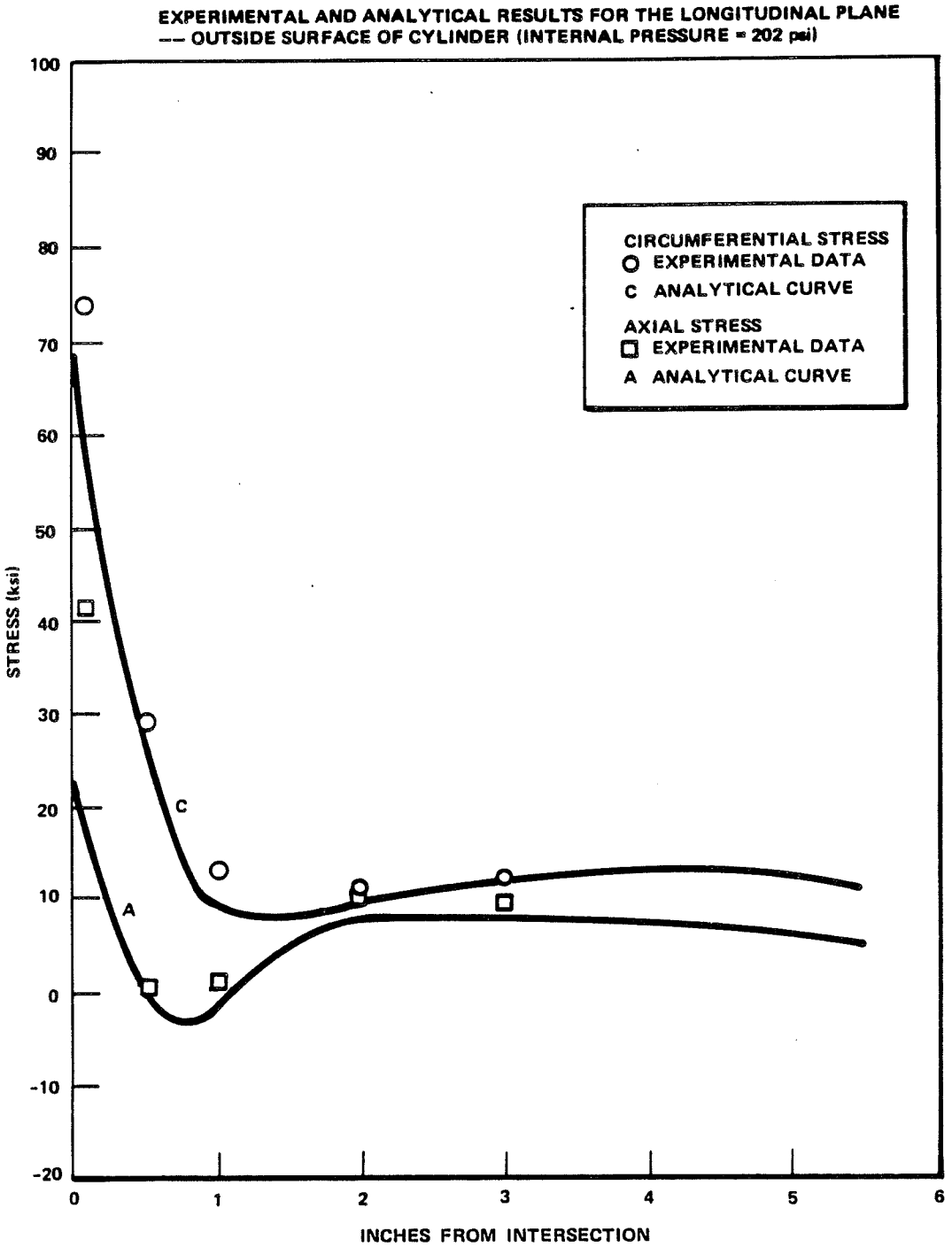

Fermi 2
UPDATED FINAL SAFETY ANALYSIS REPORT

FIGURE 4.1-28

CYLINDER STRESSES

EXPERIMENTAL AND ANALYTICAL RESULTS FOR THE LONGITUDINAL PLANE
— OUTSIDE SURFACE OF NOZZLE (INTERNAL PRESSURE = 202 psi)

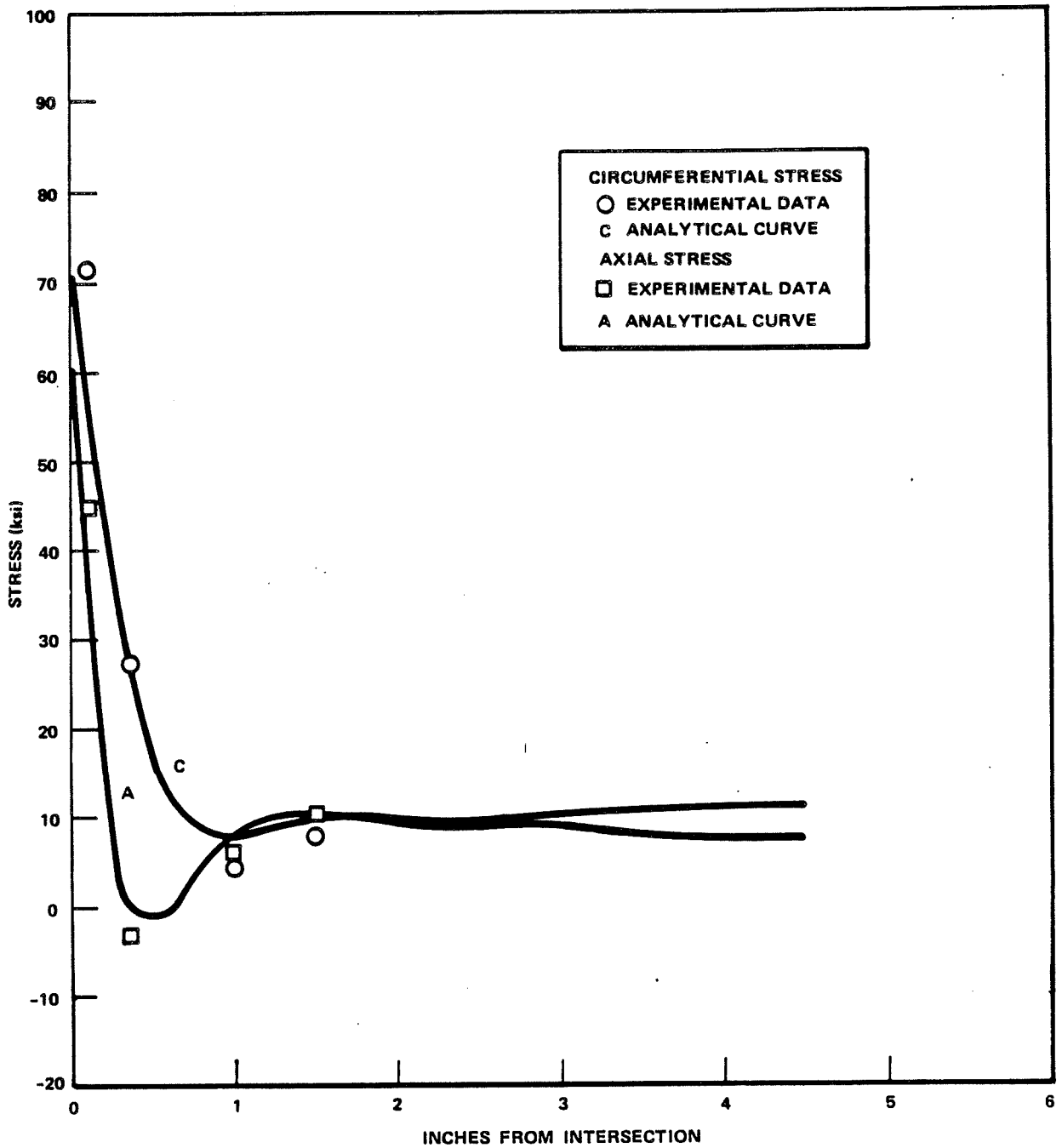

Fermi 2
UPDATED FINAL SAFETY ANALYSIS REPORT

FIGURE 4.1-29

NOZZLE STRESSES

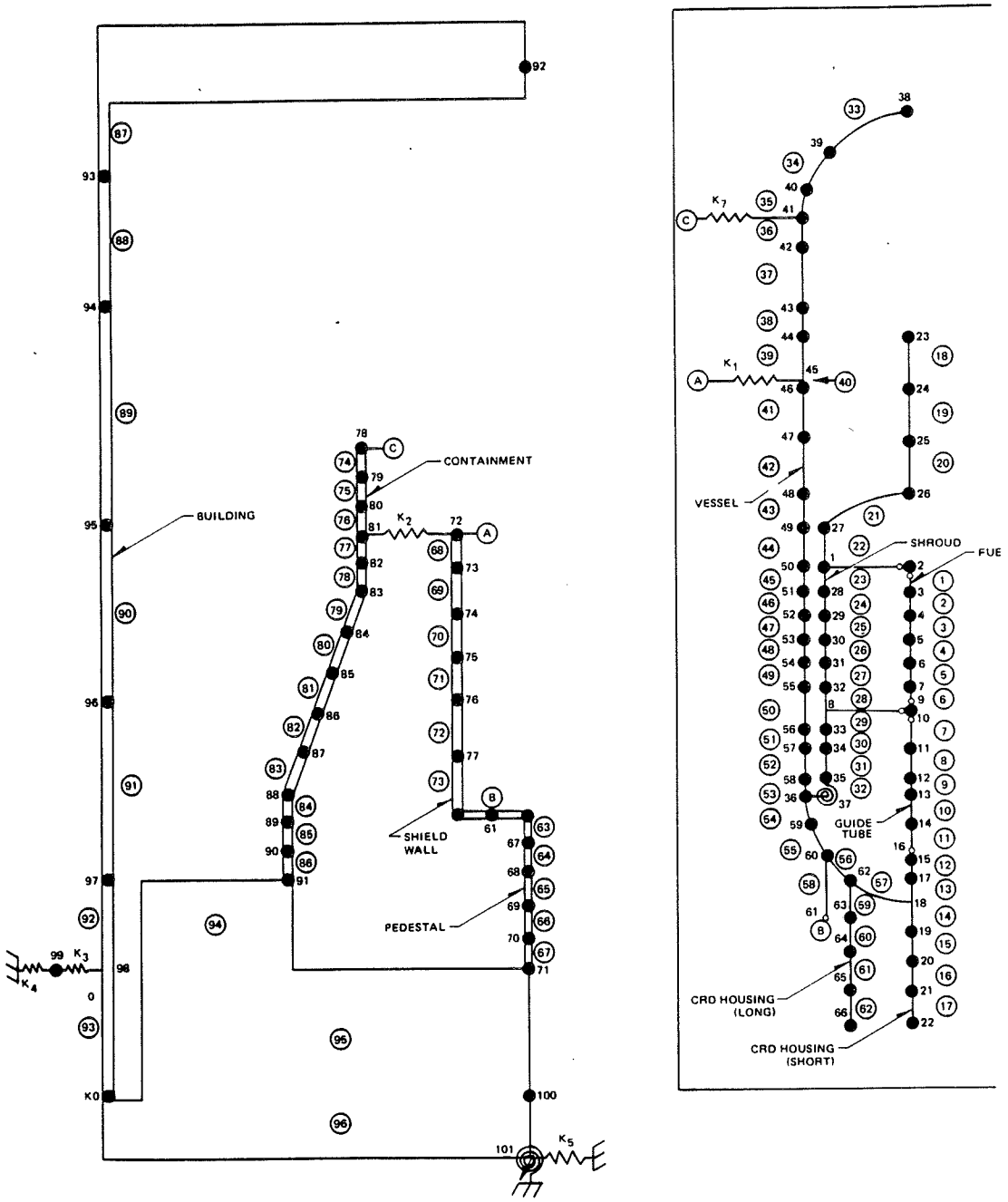

Fermi 2

UPDATED FINAL SAFETY ANALYSIS REPORT

FIGURE 4.1-30

LUMPED MASS MODEL

4.2 FUEL SYSTEM DESIGN

Fermi 2 is a BWR 4 with a 251 in. pressure vessel and 764 fuel assemblies loaded on a C lattice. The subsection numbers in Section 4.2 generally correspond to the subsection numbers of Appendix A of GESTAR II (Reference 1). Any additional information or differences are given for the applicable subsection.

4.2.1 Design Bases

Information in fuel system design bases is provided in Reference 1, Subsection A.4.2.1.

4.2.2 Description and Design Drawings

Information on fuel system design bases is provided in Reference 1, Subsection A.4.2.2, except for the reactivity control assembly description, which is described below.

4.2.2.1 Reactivity Control Assembly

4.2.2.1.1 Control Rods

The control rods perform the dual function of power shaping and reactivity control (See Figures 4.5-8 through 4.5-10). Power distribution in the core is controlled during operation of the reactor by manipulating selected patterns of control rods. Control rod displacement tends to counterbalance steam void effects at the top of the core and results in significant power flattening. See Subsection 4.5.2.1.2 for a description of the control rods.

4.2.3 Design Evaluations

Information on fuel system evaluation for compliance with the design bases is provided in Reference 1, Subsection A.4.2.3.

4.2.4 Testing, Inspection and Surveillance Plans

Information on testing, inspection and surveillance is provided in Reference 1, Subsection A.4.2.4. Fuel assembly surveillance plans are further described below.

Fermi 2 has a pre-established Fuel Reliability Action Plan for detection, analysis, reporting and taking corrective action whenever fuel failures occur. Detection is based primarily on sampling radioactivity in the off-gas system. At the end of a fuel cycle, fuel inspection and reconstitution using proven vendor techniques will be performed as needed to provide a basis for accomplishing the discharge of all failed fuel rods in accordance with a zero-defect goal. A zero-defect goal implies that no detected failed fuel rods will be re-inserted into the core after a refueling outage.

Proven inspection techniques used include the following:

a. Leak-detection tests such as sipping

b. Visual inspection with various aids such as binoculars, borescope, periscope, and/or underwater TV with a photographic record of observations

c. Nondestructive testing of selected fuel rods by ultrasonic test and/or eddy current test techniques

d. Dimensional measurements of selected fuel rods.

Such inspections may also be performed on fuel where there is no indication of fuel failure to obtain additional data on fuel performance. This fuel may either be from discharged bundles or from bundles scheduled for re-irradiation.

Unexpected conditions or abnormalities that may arise, such as distortions, cladding perforation, or surface disturbances, will be analyzed. Resolution of specific technical questions indicated by site examinations may require examination of selected fuel rods in radioactive material laboratory facilities.

Fermi 2 participated in a vendor's lead fuel test assembly program to obtain fuel performance data for an improved fuel design. This program took place with the insertion of full-length lead bundles during the second refueling outage. Performance inspection of this program is complete and only four lead fuel test assemblies were used. They are currently discharged. Additional lead fuel test programs may be instituted as the need requires.

4.2 FUEL SYSTEM DESIGN

REFERENCES

1. General Electric Co. “General Electric Standard Application for Reactor Fuel, GESTAR-II,” NEDE-24011-P-A, (Latest Approved Revision as identified in the COLR).

4.3 NUCLEAR DESIGN

Most of the information in Section 4.3 is provided in the licensing topical report GESTAR II (Reference 1). The design bases and licensing requirements are independent of enrichment.

4.3.1 Design Bases

The design bases are those that are required for the plant to operate, meeting all safety requirements. Safety design bases fall into two categories: (1) the reactivity basis, which prevents an uncontrolled positive reactivity excursion, and (2) the overpower basis, which prevent the core from operating beyond the fuel integrity limits.

4.3.1.1 Reactivity Basis

The nuclear design shall meet the following basis: The core shall be capable of being made subcritical at any time or at any core condition with the highest worth control rod fully withdrawn.

4.3.1.2 Overpower Bases

The Technical Specification limits on minimum critical power ratio (MCPR), maximum linear heat generation rate (MLHGR), and the maximum average planar linear heat generation rate (MAPLHGR) are determined such that the fuel will not exceed required licensing limits during abnormal operational occurrences or accidents.

4.3.2 Description

The BWR core design consists of a light-water moderated reactor, fueled with slightly enriched uranium-dioxide. The use of water as a moderator produces a neutron energy spectrum in which fissions are caused principally by thermal neutrons. At normal operating conditions, the moderator boils, producing a spatially variable distribution of steam voids in the core. The BWR design provides a system for which reactivity is reduced by an increase in the steam void content in the moderator. This void feedback effect is one of the inherent safety features of the BWR system. Any system input which increases reactor power, either in a local or gross sense, produces additional steam voids which reduce reactivity and thereby reduce the power.

4.3.2.1 Nuclear Design Description

The initial fuel loading is composed of three distinct bundle types, each with a unique rod-by-rod enrichment distribution. The bottom and top of each fuel rod in two of these bundle types consists of 6 inches of natural uranium. The third bundle type contains only natural uranium fuel rods. The three unique bundle types are distributed in the initial core based on the principle of minimizing radial power peaking and maximizing core reactivity for the end-of-cycle state. This same strategy is carried into the reload core. A diagram of the cycle-specific reference pattern loading is shown in the cycle-specific supplemental reload licensing report.

The peripheral core zone of the initial core is composed of bundles containing only natural uranium fuel rods. The interior of the core is divided into two zones: an inner zone which comprises about 50 percent of the core area, and an outer zone, a ring, which comprises about 35 percent of the core area. The outer zone consists entirely of the high enrichment bundles. The inner zone is an array of high and medium enrichment bundles arranged in a checkerboard fashion.

Beginning with Cycle 2, the core is loaded with a Control Cell Core (CCC) configuration. The CCC uses a strategy in which control rod movement to offset reactivity changes during power operation is limited to a fixed group of control rods. Each of these rods and its four surrounding fuel bundles comprise a control cell. Low-reactivity bundles are placed in control cells so that control rod motion occurs adjacent to low power fuel. The control cells are located in octant symmetric positions in the core and are separated from each other by a four-bundle cell. All other control rods are normally completely withdrawn from the core while at power.

The reference loading pattern is the basis for all fuel licensing. It is designed with the intent that it will represent, as closely as possible, the actual core loading pattern; however, there will be occurrences where the number and/or types of bundles in the reference design and the actual core loading do not agree exactly.

Any differences between the reference loading pattern and the actual loading pattern are evaluated as described in Reference 1, Section 3.4.

4.3.2.2 Power Distribution

The core power distribution is a function of fuel bundle design, core loading, control rod pattern, core exposure distributions and core coolant flow rate. The thermal performance parameters, MAPLHGR, MLHGR, and MCPR, defined in Table 4.3-1, limit unacceptable core power distributions.

4.3.2.2.1 Power Distribution Calculations

Core power distributions are calculated based on the reference loading pattern shown in the cycle-specific Supplemental Reload Licensing Report. These calculations confirm that the limits established by the thermal performance parameters are not violated. Appropriate design allowances are included at the design stage to ensure that these limits are met. A full range of calculated power distributions along with the resultant exposure shapes and corresponding control rod patterns are also shown in Reference 2.

4.3.2.2.2 Power Distribution Measurements

The techniques for measurement of the power distribution within the reactor core, together with instrumentation correlations and operating limits, are discussed in Reference 3.

4.3.2.2.3 Power Distribution Accuracy

The accuracy of the calculated power distributions is discussed in References 4 and 5.

4.3.2.2.4 Power Distribution Anomalies

Stringent inspection procedures are utilized to ensure the correct arrangement of the core following fuel loading. A fuel loading error (a mislocated or a misoriented fuel bundle in the core) would be a very improbable event, but calculations have been performed to determine the effects of such events on CPR. The inherent design characteristics of the BWR are well suited to limit gross power tilting. The stabilizing nature of the large moderator void coefficient effectively reduces the effect of perturbations on the power distribution. In addition, the in-core instrumentation system, together with the on-line computer, provides the operator with prompt information on the power distribution so that he can readily use control rods or other means to limit the undesirable effects of power tilting. Because of these design characteristics, it is not necessary to allocate a specific margin in the peaking factor to account for power tilt. If, for some reason, the power distribution could not be maintained within normal limits using control rods and flow, then the total core power would have to be reduced.

4.3.2.3 Reactivity Coefficients

Reactivity coefficients, the differential changes in reactivity produced by differential changes in core conditions, are useful in calculating stability and evaluating the response of the core to external disturbances. The base initial condition of the system and the postulated initiating event determine which of the several defined coefficients are significant in evaluating the response of the reactor. The coefficients of interest, relative to BWR systems, are discussed here individually.

There are two primary reactivity coefficients that characterize the dynamic behavior of BWRs; these are the Doppler reactivity coefficient and the moderator void reactivity coefficient. Also associated with the BWR is a power reactivity coefficient and a temperature coefficient. The power coefficient is a combination of the Doppler and void reactivity coefficients in the power operating range, and the temperature coefficient is merely a combination of the Doppler and moderator temperature coefficients. Power and temperature coefficients are not specifically calculated for reload cores. The Doppler and void coefficients are unique for each core, however their values are not typically reported to the customer by the fuel vendor.

4.3.2.3.1 Doppler Reactivity Coefficient

The Doppler coefficient is of prime importance in reactor safety. The Doppler coefficient is a measure of the reactivity change associated with an increase in the absorption of resonance-energy neutrons caused by a change in the temperature of the material in question. The Doppler reactivity coefficient provides instantaneous negative reactivity feedback to any rise in fuel temperature, on either a gross or local basis. The magnitude of the Doppler coefficient is inherent in the fuel design and does not vary significantly among BWR designs. For most structural and moderator materials, resonance absorption is not significant, but in U-238 and Pu-240 an increase in temperature produces a comparatively large increase in the effective absorption cross-section. The resulting parasitic absorption of neutrons causes a significant loss in reactivity. In BWR fuel, in which approximately 96 percent of the uranium

in UO_2 is U-238, the Doppler coefficient provides an immediate negative reactivity response that opposes increased fuel fission rate changes.

Although the reactivity change caused by the Doppler Effect is small compared to other power-related reactivity changes during normal operation, it becomes very important during postulated rapid power excursions in which large fuel temperature changes occur. The most severe power excursions are those associated with rod drop accidents. A local Doppler feedback associated with a 3000°F to 5000°F temperature rise is available for terminating the initial excursion. The Doppler coefficient is determined using the theory and methods described in Reference 6.

4.3.2.3.2 Moderator Void Coefficient

The moderator void coefficient should be large enough to prevent power oscillation due to spatial xenon changes yet small enough that pressurization transients do not unduly limit plant operation. In addition, the void coefficient in a BWR has the ability to flatten the radial power distribution and to provide ease of reactor control due to the void feedback mechanism. The overall void coefficient is always negative over the complete operating range since the BWR design is undermoderated.

A detailed discussion of the methods used to calculate void reactivity coefficients, their accuracy and their application to plant transient analyses is presented in Reference 6.

4.3.2.4 Control Requirements

The General Electric BWR control rod system is designed to provide adequate control of the maximum excess reactivity anticipated during the plant operation. The shutdown capability is evaluated assuming a cold, xenon-free core.

4.3.2.4.1 Shutdown Reactivity

The core must be capable of being made subcritical, with margin, in the most reactive condition throughout the operating cycle with the most reactive control rod fully withdrawn and all other rods fully inserted. The shutdown margin is determined by using the BWR simulator code (Section 3.3 of Reference 1) to calculate the core multiplication at selected exposure points with the strongest rod fully withdrawn. The shutdown margin is calculated based on the carryover of the minimum expected exposure at the end of the previous cycle. The core is assumed to be in the cold, xenon-free condition in order to ensure that the calculated values are conservative. Further discussion of the uncertainty of these calculations is given in References 7 and 8.

As exposure accumulates and burnable poison depletes in the lower exposure fuel bundles, an increase in core reactivity may occur. The nature of this increase depends on specifics of fuel loading and control state.

The cold k_{eff} is calculated with the strongest control rod out at various exposures through the cycle. A value R is defined as the difference between the strongest rod out k_{eff} at beginning of cycle (BOC) and the maximum calculated strongest rod out k_{eff} at any exposure point. The strongest rod out k_{eff} at any exposure point in the cycle is equal to or less than:

$$k_{eff} = k_{eff}\,(\text{Strongest rod withdrawn})_{BOC} + R$$

where

R is always greater than or equal to 0.

The cycle-specific calculated values of k_{eff} with the strongest rod withdrawn at BOC and R are reported in cycle-specific supplemental reload licensing report. For completeness, the uncontrolled k_{eff} and fully controlled k_{eff} values are also reported.

4.3.2.4.2 Reactivity Variations

The excess reactivity designed into the core is controlled by the control rod system supplemented by gadolinia-uranium fuel rods. Control rods are used during the cycle partly to compensate for burnup and partly to control the power distribution.

4.3.2.4.3 Standby Liquid Control System

The Standby Liquid Control System (SLCS) is designed to provide the capability of bringing the reactor, at any time in a cycle, from a full power and minimum control rod inventory (which is defined to be at the peak of the xenon transient) to a subcritical condition with the reactor in the most reactive xenon-free state. The requirements of this system are dependent primarily on the reactor power level and on the reactivity effects of voids and temperature between full power and cold, xenon-free condition. The cycle-specific shutdown capability of the SLCS is given in cycle-specific supplemental reload licensing report.

4.3.2.5 Control Rod Patterns and Reactivity Worths

Control rod patterns are chosen to achieve an exposure distribution approaching the target end-of-cycle exposure shape and a power distribution meeting the thermal limits. Control rod patterns will be altered as necessary to meet these criteria.

4.3.2.6 Criticality of Reactor During Refueling

The core is subcritical at all times.

4.3.2.7 Stability

4.3.2.7.1 Xenon Transients

Boiling water reactors do not have instability problems due to xenon. This has been demonstrated by (1) never having observed xenon instabilities in operating BWRs, (2) special tests which have been conducted on operating BWRs in an attempt to force the reactor into xenon instability, and (3) calculations. All of these indicators have proven that xenon transients are highly damped in a BWR due to the large negative power coefficient (Reference 9).

4.3.2.7.2 Thermal Hydraulic Stability

Information on thermal hydraulic stability is provided in Reference 1, Subsection A.4.3.2.7.2, and is also covered in Subsection 4.4.4.6. Cycle-specific thermal hydraulic stability is covered in cycle-specific supplemental reload licensing report.

4.3.2.8 Vessel Irradiations

4.3.2.8.1 Historical Information

Neutron vessel fluence calculations used for determining the lead factor (the ratio of the surveillance capsule flux to the peak vessel inside surface flux) were carried out using a two-dimensional, discrete ordinate, Sn transport code with general anisotropic scattering. This code was a widely used discrete ordinates code which solved a wide variety of radiation transport problems. Slab, cylinder, and spherical geometries are allowed with various boundary conditions. The fluence calculations incorporate, as an initial starting point, a distributed fission neutron source distribution prepared from core physics data. Anisotropic scattering is considered for all regions. The cross sections are represented by third order Legendre polynomial expansions.

4.3.2.8.2 Extended Power and Measurement Uncertainty Recapture/Thermal Power Optimization Uprate Analysis

An RPV fluence evaluation was performed by GE in support of a planned Fermi 2 extended power uprate (EPU) to 120% of original licensed thermal power. Detailed flux calculations were performed for a representative pre-EPU cycle at the Current Licensed Thermal Power (CLTP) level of 3430 MWt and for an EPU core that was to be representative of future cycles at the target power level of 3952 MWt. The NRC approved GE fluence methodology was used for these flux calculations. In addition, fluence distributions at the Effective-Full-Power-Years (EFPY) of interest were evaluated based on calculated CLTP and anticipated EPU flux distributions, in conjunction with the cycle-dependent energy generation data.

The peak fluence for the RPV inner surface, that was used for developing the P-T curves, was 9.68e17 n/cm2 for 32-EFPY, and 7.13e17 n/cm2 for 24-EFPY. The peak fluence for the girth weld location was calculated based on its elevation between the lower and lower intermediate shell plates, and is also provided in Reference 12. This fluence value was applied to this girth weld and all plates and welds in the lower shell.

The 32-EFPY fluence used in developing the P-T curves detailed in UFSAR Section 5.2.4 is conservatively based upon operation at 3430 MWt for 12.04 EFPY and 3952 MWt for 19.96 EFPY. The 24-EFPY fluence used in developing the P-T curves is conservatively based upon operation at 3430 MWT for 12.04-EFPY, and 3952 MWt for 11.96-EFPY.

The N16 water level instrumentation (WLI) nozzle(s), which are within the beltline region, were also considered in this evaluation. Fluence was determined for the specific location of these nozzles. The peak fluence for the WLI nozzles, that was used for determination of the P-T curves, was 1.74e17 n/cm2 for 32-EFPY, and 1.30e17 n/cm2 for 24-EFPY. The fluence for the N16 WLI nozzles were developed considering implementation of a planned

Measurement Uncertainty Recapture/Thermal Power Optimization (MUR/TPO) uprate, (3486 MWt) but did not include EPU.

The fluence determined for the WLI nozzles is based upon operation at 3293 MWt for 3.4-EFPY, 3430 MWt for 16.38-EFPY, and 3486 MWt for 12.22-EFPY. TPO is expected to be implemented in Cycle 17, or after RF16.

While WLI nozzles were evaluated using MUR/TPO power levels, all other vessel components have been conservatively evaluated considering both EPU and MUR/TPO, where EPU bounds MUR/TPO. The basis for all fluence values is contained in References 12 and 14. Delay of implementation of the extended power uprate increased the conservatism for the beltline Pressure/Temperature curves included in the Pressure and Temperature Limits Report (PTLR) as discussed in Section 5.2.4 of the UFSAR.

The current NRC approved GE methodology for neutron flux calculations is documented in Reference 13. GE's methodology adheres to the guidance contained in Regulatory Guide 1.190 for neutron flux evaluation.

4.3.3 Analytical Methods

Information on the analytical methods is provided in Section 3.3 of Reference 1, and in Reference 13.

4.3.4 Changes

Information on changes relative to the design is provided in Reference 1, Subsection A.4.3.4.

4.3 NUCLEAR DESIGN REFERENCES

1. General Electric Co. "General Electric Standard Application for Reactor Fuel, GESTAR-II," NEDE-24011-P-A, (Latest Approved Revision as identified in the COLR).
2. General Electric Co., "BWR/4 and BWR/5 Fuel Design," NEDE-20944-P, October 1976.
3. General Electric Co., J.F. Carew, "Process Computer Performance Evaluation Accuracy," NEDO-20340, June 1974.
4. General Electric Co., C.L. Martin, "Lattice Physics Methods Verification," NEDO-20939-A, January 1977.
5. General Electric Co., "Steady-State Nuclear Methods," NEDE-30130-P-A (PROPRIETARY) and NEDO-30130-A, April 1985.
6. General Electric Co., R.C. Stirn, "Generation of Void and Doppler Reactivity Feedback for Application to BWR Design," NEDO-20964, December 1975.
7. General Electric Co., G.R. Parkos, "BWR Simulator Methods Verification," NEDO-20946-A, January 1977.
8. General Electric Co., "BWR/4,5,6 Standard Safety Analysis Report, Revision 2," Chapter 4, June 1977.
9. General Electric Co., R.L. Crowther, "Xenon Considerations in Design of Boiling Water Reactors," APED-5640, June 1968.
10. General Electric Co., "Implementation of Regulatory Guide 1.99, Revision 2, for the Fermi 2 Nuclear Power Plant," SASR 90-73, DRF 137-0010, Revision 1, Janaury 1991.
11. General Electric Co. BWR Technology Materials Monitoring & Structural Analysis Services, "Fermi 2 Power Uprate Fracture Toughness Evaluation", letter from T. A. Craine to T. C. Lee, dated July 9, 1991.
12. DTE Energy Fermi-2 Energy Center Neutron Flux Evaluation, Revision 1, GE-NE-0000-0031-6254-R1, dated February 2005.
13. General Electric Co., “Licensing Topical Report, General Electric Methodology for Reactor Pressure Vessel Fast Neutron Flux Evaluations,” NEDC-32983P-A, Rev. 1, dated December 2001 (GEH Proprietary).
14. General Electric Hitachi, “Fluence Estimate for Water Level Instrumentation (N16) at Fermi 2, Rev. 1,0000-0137-3831-R1, June 3, 2013 (GEH Proprietary).

TABLE 4.3-1 DEFINITION OF FUEL DESIGN LIMITS

Maximum Linear Heat Generation Rate (MLHGR)

The MLHGR is the maximum linear heat generation rate expressed in kW/ft for the fuel rod with the highest surface heat flux at a given nodal plane in the bundle. The MLHGR operating limit is fuel rod type dependent. The MLHGR can be monitored to assure that all mechanical design requirements will be met.

Maximum Average Planar Linear Heat Generation Rate (MAPLHGR)

The MAPLHGR is the maximum average linear heat generation rate (expressed in kW/ft) in any plane of a fuel bundle allowed by the plant Technical Specifications for that fuel type. This parameter is obtained by averaging the linear heat generation rate over each fuel rod in the plane, and its limiting value is selected such that:

(a) the peak clad temperature during the design basis loss-of-coolant accident will not exceed 2200°F in the plane of interest, and

(b) all fuel design limits specified in Reference 1, Section 2 will be met if the MLHGR is not monitored for that purpose.

Minimum Critical Power Ratio (MCPR)

The critical power ratio is defined as the ratio of the critical power (bundle power at which some point within the assembly experiences onset of boiling transition) to the operating bundle power. The critical power is determined at the same mass flux, inlet temperature, and pressure that exists at the specified reactor condition. Thermal margin is stated in terms of the minimum value of the critical power ratio, MCPR, which corresponds to the most limiting fuel assembly in the core.

Operating Limit MCPR

The MCPR operating limit is the minimum CPR allowed by the plant Technical Specifications for a given bundle type. The minimum CPR is a function of several parameters, the most important of which are bundle power, bundle flow, and bundle R-factor. The R-factor is dependent upon the local power distribution and details of the bundle mechanical design. The limiting value of CPR is selected for each bundle type such that, during the most limiting event of moderate frequency, the calculated CPR in that bundle is not less than the safety limit CPR. The MCPR operating limit is attained when the bundle power, R-factor, flow and other relevant parameters combine to yield the Technical Specification value.

TABLE 4.3-2 FLUENCE DETERMINATION FOR THE PEAK LOCATION IN THE FERMI 2 VESSEL

HISTORICAL DATA (Reference 10)

Time at Power

EOC1 - 2.92 years at 42.8% CF	1.25 EFPY
Design - 40 years at 80% CF	32 EFPY

Lead Factor

Peak Location ID	1.05*

Dosimeter Flux

Measured Value	4.9×10^{8} n/cm^2-sec
Upper Bound	6.1×10^{8} n/cm^2-sec

Dosimeter Fluence

Measured Value	1.9×10^{16} n/cm^2
Upper Bound	2.4×10^{16} n/cm^2

Peak Vessel ID 32 EFPY Fluence

Nominal Prediction	5.8×10^{17} n/cm^2
Upper Bound	7.3×10^{17} n/cm^2

* Value adjusted from 0.94 to 1.05 (Reference 12)

EPU Fluence Analysis Data (Reference 12)

Calculated Peak Fast Flux at the RPV Inside Surface

Parameter	Elevation (Inches above BAF)	Azimuth (°)	Flux (n/cm^2-s)
RPV ID peak flux (>1.0 MeV) – 3952 MWt	85.1	64.0	1.01E9
RPV ID peak flux (>1.0 MeV) – 3430 MWt	101.6	26.5	8.73E8

Calculated Fast Flux and Lead Factor at Surveillance Capsule Location

Capsule No.	Azimuth (°)	Flux (n/cm^2-s)	Lead Factor
1,2, and 3 – 3952 MWt	30,120, and 300	1.06E9	1.05
1,2, and 3 – 3430 MWt	30,120, and 300	9.11E8	1.04

TABLE 4.3-2 FLUENCE DETERMINATION FOR THE PEAK LOCATION IN THE FERMI 2 VESSEL

Calculated Peak Flux at Shroud Inside Surface (Reference 12)

Parameter	Elevation (Inches above BAF)	Azimuth (°)	Flux (n/cm^2-s)
Shroud ID peak flux (>1.0 MeV) – 3952 MWt	78.4	65.5	2.78E12
Shroud ID peak flux (>1.0 MeV) – 3430 MWt	109.5	24.5	2.37E12

Neutron Flux at Top Guide and Core Plate

Parameter	Flux (n/cm^2-s)
Top Guide bounding flux (>1.0 MeV) – 3952 MWt	1.06E13
Top Guide bounding flux (>1.0 MeV) – 3430 MWt	5.81E12
Core Plate bounding flux (>1.0MeV) – 3952 MWt	7.74E11
Core Plate bounding Flux (>1.0Mev) – 3430 MWt	6.32E11

Calculated Neutron Fluence Values

Parameters	32-EFPY Fluence (n/cm^2)	24-EFPY Fluence (n/cm^2)
RPV ID peak fluence(>1.0MeV)	9.68E17	7.13E17
Shroud ID peak fluence >1.0MeV)	2.65E21	1.94E21
Top guide bounding fluence (>1.0Mev)	8.87E21	6.20E21
Core plate bounding fluence (>1.0 MeV)	7.28E20	5.32E20
Girth weld (elevation 28.3125 inches above BAF) peak fluence (>1.0 MeV)	6.23E17	4.66E17
(N16) Water Level Instrumentation Nozzles Peak fluence (>1.0 MeV)*	1.74E17	1.30E17

* Values determined per Reference 14

4.4. THERMAL-HYDRAULIC DESIGN

Most of the information in Section 4.4 is provided in the licensing topical report GESTAR II (Reference 1).

4.4.1. Design Basis

4.4.1.1. Safety Design Bases

Thermal-hydraulic design of the core shall establish the thermal-hydraulic safety limits for use in evaluating the safety margin relating the consequences of fuel cladding failure to public safety.

4.4.1.2. Requirements for Steady-State Conditions

For purposes of maintaining adequate fuel performance margin during normal steady-state operation, the MCPR must not be less than the required MCPR operating limit, the LHGR must be maintained below the required LHGR limit (MLHGR), and the APLHGR must be maintained below the required APLHGR limit (MAPLHGR). The steady-state MCPR, MLHGR, and MAPLHGR limits are determined by analysis of the most severe moderate frequency anticipated operational occurrences (AOOs) to accommodate uncertainties and provide reasonable assurance that no fuel damage results during moderate frequency AOOs at any time in life.

4.4.1.3. Requirements for Anticipated Operational Occurrences (AOOs)

The MCPR, MLHGR, and MAPLHGR limits are established such that no safety limit is expected to be exceeded during the most severe moderate frequency AOO event. The cycle-specific MCPR, MLHGR, and MAPLHGR limits are provided in the Core Operating Limits Report (COLR) and corresponding licensing basis in the cycle-specific supplemental reload licensing report.

4.4.1.4. Summary of Design Bases

In summary, the steady-state operating limits have been established to ensure that the design bases are satisfied for the most severe moderate frequency AOO. Demonstration that the steady-state MCPR, MLHGR, and MAPLHGR limits are not exceeded is sufficient to conclude that the design bases are satisfied.

4.4.2. Description of Thermal-Hydraulic Design of the Reactor Core

4.4.2.1. Summary Comparison

An evaluation of plant performance from a thermal and hydraulic standpoint is provided in Subsection 4.4.3.

A tabulation of thermal and hydraulic parameters of the core is given in Table 4.4-1 along with a comparison of Fermi 2 to others of similar design. Any changes for reload cores are provided in the cycle-specific supplemental reload licensing report.

4.4.2.2. Critical Power Ratio

A description of the critical power ratio and model used to calculate this ratio is provided in Subsection 4.4.4.1. Criteria used to calculate the critical power safety limit are given in Subsection 1.1.5 of Reference 1.

4.4.2.3. Average Planar Linear Heat Generation Rate (APLHGR)

Models used to calculate the APLHGR limit are given in Reference 1, Subsection 4.2.2, as pertaining to the fuel mechanical design limits and as pertaining to 10 CFR 50, Appendix K, limits provided in the Technical Specifications.

4.4.2.4. Void Fraction Distribution

The core average and maximum exit void fractions in the core at rated power conditions are calculated on a cycle-specific basis.

4.4.2.5. Core Coolant Flow Distribution and Orificing Pattern

The flow distribution to the fuel assemblies and bypass flow paths is calculated on the assumption that the pressure drop across all fuel assemblies and bypass flow paths is the same. This assumption has been confirmed by measuring the flow distribution in boiling water reactors (References 2 through 4). The components of bundle pressure drop considered are friction, local, elevation, and acceleration (Subsections 4.4.2.6.1 through 4.4.2.6.4, respectively). Pressure drop measurements made in operating reactors confirm that the total measured core pressure drop and calculated core pressure drop are in good agreement. There is reasonable assurance, therefore, that the calculated flow distribution throughout the core is in close agreement with the actual flow distribution of an operating reactor.

An iteration is performed on flow through each flow path (fuel assemblies and bypass flow paths), which equates the total differential pressure (plenum to plenum) across each path and matches the sum of the flows through each path to the total core flow. The total core flow less the control rod cooling flow enters the lower plenum. A fraction of this passes through various bypass flow paths. The remainder passes through the orifice in the fuel support plate (experiencing a pressure loss) where some of the flow exits through the fit-up between the fuel support and the lower tieplate and through the lower tieplate holes into the bypass flow region. All initial and reload core fuel bundles have lower tieplate holes. The majority of the flow continues through the lower tieplate (experiencing a pressure loss) where some flow exits through the flow path defined by the fuel channel and lower tieplate into the bypass region. This bypass flow is lower for those fuel assemblies with finger springs. The bypass flow paths considered in the analysis and typical values of the fraction of bypass flow through each flow path are given in Reference 5.

Within the fuel assembly, heat balances on the active coolant are performed nodally. Fluid properties are expressed as the bundle average at the particular node of interest and are based on 1967 International Standard Steam-Water Properties. In evaluating fluid properties a constant pressure model is used.

The relative radial and axial power distributions are used with the bundle flow to determine the axial coolant property distribution, which gives sufficient information to calculate the pressure drop components within each fuel assembly type. When the equal pressure drop criterion described above is satisfied, the flow distributions are established.

4.4.2.6. Core Pressure Drop and Hydraulic Loads

The components of bundle pressure drop considered are friction, local, elevation, and acceleration pressure drops. Pressure drop measurements made in operating reactors confirm that the total measured core pressure drop and calculated core pressure drop are in good agreement.

4.4.2.6.1. Friction Pressure Drop

Friction pressure drop is calculated with a basic model as follows:

$$\Delta P_f = \frac{w^2}{2g_c\rho_\ell}\frac{fL}{D_H A_{ch}^2}\phi_{TPF}^2 \qquad (4.4\text{-}1)$$

where

ΔP_f = friction pressure drop, psi

w = mass flow rate

g_c = acceleration of gravity

ρ_ℓ = average nodal liquid density

D_H = channel hydraulic diameter

A_{ch} = channel flow area

L = incremental length

f = friction factor

ϕ_{TPF}^2 = two-phase friction multiplier

The formulation for the two-phase multiplier is similar to that presented in References 6 and 7 and is based on data that is taken from prototypical BWR fuel bundles.

4.4.2.6.2. Local Pressure Drop

The local pressure drop is defined as the irreversible pressure loss associated with an area change, such as the orifice, lower tieplate, and spacers of a fuel assembly.

The general local pressure drop model is similar to the friction pressure drop and is

$$\Delta P_L = \frac{w^2}{2g_c\rho_\ell}\frac{K}{A^2}\phi_{TPL}^2 \qquad (4.4\text{-}2)$$

where

ΔP_L = local pressure drop, psi

K = local pressure drop loss coefficient

A = reference area for local loss coefficient

ϕ^2_{TPL} = two-phase local multiplier

and w, g, and ρ_ℓ are defined in Equation 4.4-1. The formulation for the two-phase multiplier is similar to that reported in Reference 7. For advanced spacer designs, a quality modifier has been incorporated in the two-phase multiplier to better fit the data. Empirical constants were added to fit the results to data taken for the specific designs of the BWR fuel assembly. These data were obtained from tests performed in single-phase water to calibrate the orifice, the lower tieplate, and the holes in the lower tieplate, in both single- and two-phase flow to derive the best fit design values for the spacer and upper tieplate pressure drop. The range of test variables was specified to include the range of interest for BWRs. New test data are obtained whenever there is a significant design change to ensure the most applicable methods are used.

4.4.2.6.3. Elevation Pressure Drop

The elevation pressure drop is based on the relation:

$$\Delta P_E = \bar{\rho}\Delta L; \qquad (4.4\text{-}3)$$

$$\bar{\rho} = \rho_f(1-\alpha) + \rho_g\alpha$$

where

ΔP_E = elevation pressure drop, psi

ΔL = incremental length

$\bar{\rho}$ = average water density

α = nodal average void fraction

ρ_f, ρ_g = saturated water and vapor density, respectively

The void fraction model used is an extension of the Zuber-Findlay model (Reference 8), and uses an empirically fit constant to predict a large block of steam void fraction data. Checks against new data are made on a continuing basis to ensure the best models are used over the full range of interest of Boiling Water Reactors.

4.4.2.6.4. Acceleration Pressure Drop

A reversible pressure change occurs when an area change is encountered, and an irreversible loss occurs when the fluid is accelerated through the boiling process. The basic formulation for the reversible pressure change resulting from a flow area change in the case of single-phase flow is given by:

$$\Delta P_{ACC} = (1-\sigma_A^2)\frac{W^2}{2g_c\rho_\ell A_2^2} \qquad (4.4\text{-}4)$$

$$\sigma_A = \frac{A_2}{A_1} = \frac{\text{final flow area}}{\text{initial flow area}}$$

where

ΔP_{ACC} = acceleration pressure drop

A_2 = final flow area

A_1 = initial flow area

In the case of two-phase flow, the liquid density is replaced by a density ratio so that the reversible pressure change is given by:

$$\Delta P_{ACC} = (1 - \sigma_A^2)\frac{W^2 \rho_H}{2 g_c \rho_{KE}^2 A_2^2} \quad (4.4\text{-}5)$$

where:

$\frac{1}{\rho_H} = \frac{x}{\rho_g} + \frac{(1-x)}{\rho_\ell}$, homogeneous density

$\frac{1}{\rho_{KE}^2} = \frac{x^3}{\rho_g^2 \alpha^2} + \frac{(1-x)^3}{\rho_\ell^2 (1-\alpha)^2}$, kinetic energy density

where:

α = void fraction at A_2

x = steam quality at A_2

and other terms are as previously defined. The basic formulation for the acceleration pressure change due to density change is:

$$\Delta P_{acc} = \frac{w^2}{g A_{ch}^2}\left[\left(\frac{1}{\rho_{M_{OUT}}}\right) - \left(\frac{1}{\rho_{M_{IN}}}\right)\right] \quad (4.4\text{-}6)$$

where

$$\frac{1}{\rho_{M_{OUT}}} = \frac{x_{OUT}^2}{\rho_g \alpha_{OUT}} + \frac{(1-x_{OUT})^2}{\rho_\ell (1-\alpha_{OUT})}$$

$$\frac{1}{\rho_{M_{IN}}} = \frac{x_{IN}^2}{\rho_g \alpha_{IN}} + \frac{(1-x_{IN})^2}{\rho_\ell (1-\alpha_{IN})}$$

and is evaluated at the inlet and outlet of each axial node. Other terms are as previously defined. The total acceleration pressure drop in Boiling Water Reactors is on the order of a few percent of the total pressure drop.

4.4.2.7. Correlation and Physical Data

General Electric Company has obtained substantial amounts of physical data in support of the pressure drop and thermal-hydraulic loads discussed in Subsection 4.4.2.6. Correlations have been developed to fit these data to the formulations discussed.

4.4.2.7.1. Pressure Drop Correlations

General Electric Company has taken significant amounts of friction pressure drop data in multi-rod geometries representative of BWR plant fuel bundles and correlated both the friction factor and two-phase multipliers on a best fit basis using the pressure drop formulations reported in Subsections 4.4.2.6.1 and 4.4.2.6.3. Tests are performed in single-phase water to calibrate the orifice and the lower tieplate, and in both single- and two-phase flow to arrive at best-fit design values for spacer and upper tieplate pressure drop. The range of test variables is specified to include the range of interest to BWRs. New data are taken whenever there is a significant design change to ensure the most applicable methods are in use at all times.

Applicability of the single-phase and two-phase hydraulic models discussed in Subsections 4.4.2.6.1 and 4.4.2.6.3 was confirmed by prototype flow tests. The typical range of the test data is summarized in Table 4.4-2.

4.4.2.7.2. Void Fraction Correlation

The void fraction correlation includes effects of pressure, flow direction, mass velocity, quality, and subcooled boiling.

4.4.2.7.3. Heat Transfer Correlation

The Jens-Lottes (Reference 9) heat transfer correlation is used in fuel design to determine the cladding-to-coolant heat transfer coefficients for nucleate boiling.

4.4.2.8. Thermal Effects of Anticipated Operational Occurrences

The evaluation of the core's capability to withstand the thermal effects resulting from anticipated operational occurrences (AOOs) is covered in Chapter 15 (Accident Analysis) and the cycle-specific reload analysis.

4.4.2.9. Uncertainties in Estimates

Uncertainties in thermal-hydraulic parameters are considered in the statistical analysis which is performed to establish the fuel cladding integrity safety limit documented in Subsection 4.4.4.1.1. The uncertainties considered and their input values for the analysis are shown in Table 4.4-3.

4.4.2.10. Flux Tilt Considerations

For flux tilt considerations, refer to Subsection 4.3.2.2.

4.4.3. Description of the Thermal and Hydraulic Design of the Reactor Coolant System

4.4.3.1. Plant Configuration Data

4.4.3.1.1. Reactor Coolant System Configuration

The reactor coolant system is described in Section 5.1 and shown in isometric perspective in Figure 5.5-1. The piping sizes, fittings, and valves are listed in Table 5.5-1.

4.4.3.1.2. Reactor Coolant System Thermal-Hydraulic Data

The steady-state distribution of temperature, pressure, and flow rate for each flow path in the reactor coolant system is shown in Figure 5.1-1a and 5.1-1b.

4.4.3.1.3. Reactor Coolant System Geometric Data

Volumes of regions and components within the reactor vessel are shown in Figure 5.1-2.

Table 4.4-4 provides the flow path length, height, liquid level, minimum elevations, and minimum flow areas for each major flow path volume within the reactor vessel and for the recirculation loops of the reactor coolant systems.

Table 4.4-5 provides the lengths and sizes of all safety injection lines to the reactor coolant system.

4.4.3.2. Operating Restrictions on Pumps

Expected recirculation pump performance curves are shown in Figures 4.4-1 and 4.4-2. These curves are valid for all conditions with a normal operating range varying from approximately 20 percent to 115 percent of rated pump flow.

The pump characteristics, including considerations of net positive suction head (NPSH) requirements, are the same for the conditions of a two-pump and one-pump operation as described in Subsection 5.5.1. Subsection 4.4.3.3 gives the operating limits imposed on the recirculation pumps by cavitation, pump loads, bearing design flow starvation, and pump speed.

4.4.3.3. Power-Flow Operating Map

4.4.3.3.1. Limits for Normal Operation

A BWR must operate with certain restrictions because of pump NPSH, overall plant control characteristics, and core thermal power limits. A typical power-flow map for the power range of operation is shown in Figure 4.4-3. The nuclear system equipment, nuclear instrumentation, and the reactor protection system (RPS), in conjunction with operating procedures, maintain operations within the area of this map for normal operating conditions. The boundaries on this map are as follows:

a. Natural circulation line, A: The power-versus-flow operating state of the reactor moves along this line for the normal control rod withdrawal sequence in the absence of recirculation pump operation.

b. Recirculation pump minimum speed line, B: The minimum speed of the recirculation pumps is 20 percent as established by the mechanical stops.

Startup operations of the plant are normally carried out with the recirculation pumps operating at approximately 30 percent speed. The power-versus-flow operating state for the reactor follows the 30 percent speed line for the normal control rod withdrawal sequence.

c. APRM rod block line and APRM scram lines: The APRM rod block line represents a power level above which rod blocks will be encountered if the control rods are manipulated. This line is defined by the equation: Power = 0.62w + 57.4 percent, with a maximum of 110 percent, where w is the loop recirculation flow as a percentage of the loop recirculation flow which produces a rated core flow of 100 million lb/hr at 100 percent of rated thermal power. The APRM scram line represents a power level above which a reactor scram will occur. This line is defined by the equation: Power = 0.62w + 63.1 percent, with a maximum of 115.5 percent. The APRM rod block line is intentionally kept below the APRM scram line to prevent rod withdrawal before it causes a reactor scram.

d. Cavitation protection line: This line (minimum power line) results from the recirculation pump and jet pump NPSH requirements. The recirculation pumps are automatically switched to 30 percent speed when the feedwater flow drops below a preset value.

e. Maximum extended load line limit (MELLL) and increased core flow (ICF) lines: The MELLL line is above the 100 percent rod line and represents a region hereafter referred to as the MELLL region (References 9a, 9b, and 9c). The MELLL region allows rated power operation down to 83 percent of rated core flow. Below 83 percent of rated core flow, the boundary of the analyzed operating region is defined by an analytical approximation of the rod line which passes through the rated power and 83 percent core flow point.

The ICF region allows rated power operation with core flows up to 105 percent of rated. Below 100% power, 105% core flow is held constant at 105% until power is 3430 MWth. Then the ICF boundary is expanded to allow for constant pump speed operation corresponding to 105 percent core flow at 3430 MWth. This expands the allowable operating map to 114 percent rated core flow at 36.0 percent rated power at which the expected recirculation pump cavitation region is encountered.

4.4.3.3.2. Performance Characteristics

Other performance characteristics shown on the power/flow operating map are

a. Recirculation pump constant speed line, C or D: These lines show the change in flow associated with power changes while maintaining constant recirculation pump speed

b. Constant rod lines: These lines show the change in power associated with flow changes while maintaining constant control rod position (for example, 50 percent rod density pattern line).

4.4.3.3.3. Regions of the Power/Flow Map

For normal operating conditions, the nuclear system equipment, nuclear instrumentation, and the RPS, in conjunction with operating procedures, maintain operation outside the exclusion areas of the power/flow map. The main regions of the power/flow map are discussed below to clarify operational capabilities.

a. Region I: This is the transition region between natural circulation operation and 20 percent pump speed operation. Steady-state conditions cannot exist in this area because the recirculation pumps cannot be operated below 20 percent speed. Normal startup is along the 30 percent pump speed line near this region

b. Region II: This region (including the increased core flow or ICF region) represents the normal operating zone of the power/flow map where power changes can be made, either by control rod movement or by core flow changes, achieved by changing recirculation pump drive speed. (The Technical Specifications contain limitations on operating in certain areas of Region II)

c. Region III: This is the low power area of the map where cavitation can be expected in the recirculation pumps and in the jet pumps. Operation within this region is precluded by system interlocks that set the recircula-tion pumps to 30 percent speed whenever feedwater flow is less than a preset value (typically 20 percent of rated flow).

4.4.3.4. Temperature-Power Operating Map (PWR)

Not applicable.

4.4.3.5. Load-Following Characteristics

The following simple description of BWR operation with recirculation flow control summarizes the principal modes of normal power range operation. Assuming the plant to be initially hot with the reactor critical, full power operation can be approached following the sequence shown as Points 1 to 6 in Figure 4.4-3. The first part of the sequence (1 to 3) is achieved with control rod withdrawal and manual, individual recirculation pump control. Individual pump startup procedures are provided that achieve 30 percent of full pump speed in each loop. Power, steam flow, and feedwater flow are increased as control rods are manually withdrawn until the feedwater flow has reached approximately 20 percent. An interlock prevents low-power/high-recirculation flow combinations that create recirculation pump and jet pump cavitation problems.

Reactor power increases as the operating state moves from Point 2 to Point 3 due to the inherent flow control characteristics of the BWR. Once the feedwater interlock is cleared, the operator can manually increase recirculation flow in each loop until the operating state reaches Point 3, the lower limit of the flow control range. At Point 3, the operator can switch to simultaneous recirculation pump control. Thermal output can then be increased by either control rod withdrawal or recirculation flow increase. For example, the operator can increase power in the ways indicated by Points 3a or 5c. With a slight rod withdrawal and an increase of recirculation flow to 90 percent rated flow, Point 3a can be achieved. If, however, it is

desired to maintain the lowest recirculation flow, power can be increased by withdrawing control rods until Point 5c is reached. The recirculation system individual loop controllers are limited, and these limits established the operating state (refer to Section 7.7). The operating map is shown in Figure 4.4-3 with the designated flow control range expected.

The curve labeled "MELLL line" represents a typical steady-state power flow characteristic for a fixed rod pattern. It is slightly affected by xenon, core leakage flow assumptions, and reactor vessel pressure variations. However, for this example, these effects have been neglected.

Normal power range operation is along or below the MELLL and ICF line. If load-following response is desired in either direction, plant operation near 90 percent power provides most capability. If maximum load-pickup capability is desired, the nuclear system can be operated near Point 5c, with fast load response available all the way up to Point 6a, rated power.

The large negative operating reactivity and power coefficients that are inherent in the BWR provide important advantages as follows:

a. Good load following with well-damped behavior and little undershoot or overshoot in the heat transfer response

b. Load following with recirculation flow control

c. Strong damping of spatial power disturbances.

Design of the single-cycle BWR plant includes the ability to follow load demand over a reasonable range. This load-following capability is accomplished, under operator control, by variation of reactor recirculation flow. The reactor power level can be controlled by flow over approximately 35 percent power when on the 100% rod line.

To increase reactor power, it is necessary to increase the recirculation flow rate, which sweeps some of the voids from the moderator, causing an increase in core reactivity. As the reactor power increases, more steam is formed and the reactor stabilizes at a new power level with the transient excess reactivity balanced by the new void formation. No control rods are moved to accomplish this power level change. Conversely, when a power reduction is required, it is necessary only to reduce the recirculation flow rate. When this is done, more voids in the moderator automatically decrease the reactor power level to be commensurate with the new recirculation flow rate. Again, no control rods are moved to accomplish the power reduction.

Varying the recirculation flow rate (flow control) is more advantageous, relative to load following, than using control rod positioning. Flow variations perturb the reactor uniformly in the horizontal planes and ensure a flatter power distribution and reduced transient allowances. As flow is varied, the power and void distributions remain approximately constant at the steady-state end points for a wide range of flow variations. After adjusting the power distribution by positioning the control rods at a reduced power and flow, the operator can then bring the reactor to rated conditions by increasing flow, with the assurance that the power distribution will remain approximately constant. Section 7.7 describes how recirculation flow is varied.

4.4.3.6. Thermal and Hydraulic Characteristics Summary Table

The thermal-hydraulic characteristics are provided in Table 4.4-1 for the core and tables of Section 5.5 for other portions of the reactor coolant system.

4.4.4. Evaluation

The thermal-hydraulic design of the reactor core and reactor coolant system is based upon an objective of no fuel damage during normal operation or during anticipated operational occurrences. This design objective is demonstrated by analysis as described in the following sections.

4.4.4.1. Critical Power

The objective for normal operation and AOOs is to maintain nucleate boiling and thus avoid a transition to film boiling. Operating limits are specified to maintain adequate margin to the onset of the boiling transition. The figure of merit utilized for plant operation is the critical power ratio. This is defined as the ratio of the critical power (bundle power at which some point within the assembly experiences onset of boiling transition) to the operating bundle power. The critical power is determined at the same mass flux, inlet temperature, and pressure which exists at the specified reactor condition. Thermal margin is stated in terms of the minimum value of the critical power ratio, MCPR, which corresponds to the most limiting fuel assembly in the core. To ensure that adequate margin is maintained, a design requirement based on a statistical analysis was selected as follows:

> Moderate frequency AOOs caused by a single operator error or equipment malfunction shall be limited such that, considering uncertainties in manufacturing and monitoring the core operating state, more than 99.9 percent of the fuel rods would be expected to avoid boiling transition (Reference 10).

Both the transient (safety) and normal operating thermal limits in terms of MCPR are derived from this basis. A discussion of these limits follows.

4.4.4.1.1. Fuel Cladding Integrity Safety Limit

The generation of the Minimum Critical Power Ratio (MCPR) limit requires a statistical analysis of the core near the limiting MCPR condition. The statistical analysis is used to determine the MCPR corresponding to the transient design requirement given in Reference 1. The MCPR fuel cladding integrity safety limit applies not only for core wide AOOs, but is also applied to the localized rod withdrawal error AOO.

4.4.4.1.1.1. Statistical Model

The statistical analysis utilizes a model of the BWR core which simulates the plant process variables and the 3D-Monicore PANACEA core modeling function. This code produces a critical power ratio (CPR) map of the core based on inputs of power distribution, flow, and heat balance information. Details of the procedure are documented in Appendix IV of Reference 10 and Section 4 of Reference 38. Random Monte Carlo selections of all operating parameters based on the uncertainty ranges of manufacturing tolerances,

uncertainties in measurement of core operating parameters, calculational uncertainties, and statistical uncertainty associated with the critical power correlations (References 11 through 13) are imposed upon the analytical representation of the core and the resulting bundle critical power ratios are calculated. Applications of critical power correlation uncertainties to critical power ratio calculations are presented in References 10, 14, 15, 38, 39 and 40.

The minimum allowable critical power ratio is set to correspond to the criterion that 99.9 percent of the rods are expected to avoid boiling transition by interpolation among the means of the distributions formed by all the trials.

4.4.4.1.1.2. Bounding BWR Statistical Analysis

Statistical analyses are performed for each operating cycle that provides the fuel cladding integrity safety limit MCPR. The analyses are performed for the specific core loading and the specific bundle design to be used in the given cycle. Core radial power distributions are selected to reasonably bound the number of bundles at or near thermal limits. The assumed local fuel pin power distribution is based on the specific bundle design. The analyses are performed for multiple exposure points throughout the cycle. Typically the most limiting value is applied over the entire cycle, but exposure-dependent values are technically correct and may be applied if necessary.

Uncertainties used in the analyses are listed in Table 4.4-3, including the uncertainty associated with the appropriate critical power correlation. The critical power correlation uncertainty used in the Safety Limit MCPR determination is that uncertainty associated with the operating regions that can be obtained during normal operation or during Anticipated Operational Occurrences (AOO).

The results of the analyses show that at least 99.9 percent of the fuel rods in the core are expected to avoid boiling transition if the MCPR is equal to or greater than the applicable value listed in Tech Spec 2.1.1.2. Therefore, based on the results of the statistical analysis, the fuel cladding integrity safety limit is an MCPR equal to the values presented in Tech Spec 2.1.1.2.

4.4.4.1.2. MCPR Operating Limit Calculational Procedure

A plant-unique MCPR operating limit is established to provide adequate assurance that the cycle specific fuel cladding integrity safety limit for that plant is not exceeded for any moderate frequency AOO. This operating requirement is obtained by addition of the maximum ΔCPR value for the most limiting AOO (including any imposed adjustment factors) from conditions postulated to occur at the plant to the cycle specific fuel cladding integrity safety limit.

4.4.4.1.2.1. Calculational Procedure for AOO Pressurization Events

Core-wide rapid pressurization events (turbine trip w/o bypass, load rejection w/o bypass, feedwater controller failure) are analyzed using TRACG which has been approved for application to AOO transients. TRACG uses a multi-dimensional two-fluid model and a three-dimensional kinetics model consistent with the GEMINI method. The application of TRACG is described in References 48 and 49. The set of methods used (GENESIS,

GEMINI or TRACG) will be identified in the supplemental reload licensing report; however, application of a different approved method set may be used subsequently for the same cycle.

4.4.4.1.2.2. Calculational Procedure for AOO Slow Events

The slower core-wide anticipated operational occurrence, loss of feedwater heating, is analyzed using either the steady-state 3-D BWR Simulator Code (Reference 18 for GENESIS methods or Reference 21 for GEMINI methods), or the REDY transient model (References 23 through 25) as described in Reference 26. Inadvertent HPCI startup is not analyzed when its enthalpy is bounded by that of the loss of feedwater heating event (Reference 37). When necessary, it is analyzed using the REDY transient model.

4.4.4.1.2.3. Rod Withdrawal Error Calculational Procedure

The reactor core behavior during the rod withdrawal error transient is calculated by doing a series of steady-state three-dimensional coupled nuclear-thermal-hydraulic calculations using the 3-D BWR Simulator (Reference 18 for GENESIS methods or Reference 21 for GEMINI methods).

4.4.4.1.2.4. Event Descriptions

Descriptions of the limiting AOO events are given in Chapter 15 for the cycle-specific reload analysis. The AOO descriptions given are used as a basis for the typical analyses performed. Some plant-unique analyses will differ in certain aspects from the typical calculational procedure. These differences arise because of utility-selected margin improvement options.

4.4.4.1.2.5. MCPR Operating Limit Calculation

The operating limit MCPR for rapid AOOs is calculated by using the TASC computer program (Reference 28). Cycle-dependent plant initial conditions for the MCPR operating limit analysis and the resulting parameters are given in the cycle-specific supplemental reload licensing report.

4.4.4.1.2.6. MCPR Uncertainty Considerations

The deterministic ΔCPR value which results from ODYN/TASC or TRACG evaluations (for all rapid pressurization AOOs) must be adjusted such that a 95/95 ΔCPR/ICPR licensing basis is calculated (i.e., 95 percent probability with 95 percent confidence that the safety limit will not be violated). The NRC Safety Evaluation Report which describes these requirements and procedures is given in Reference 29.

Fermi 2 has the choice of operating under either Option A or Option B.

Option A Operating under Option A with the GENESIS set of methods, an NRC-imposed factor of 1.044 is applied to the MCPR for each event to account for code uncertainties. With the GEMINI set of methods, the MCPR for each event is determined using statistically evaluated scram times. Plants that do not demonstrate compliance with the statistically evaluated scram times must operate using a higher limit that does not take credit for these scram times. The

higher limit will also be referred to as Option A. Details are provided in Reference 29.

Option B Under Option B, the ΔCPR/ICPR ratio for the pressurization events is evaluated on either a plant-unique or generic statistical basis per the methodology and procedures of References 29 and 30 for GENESIS, and Reference 31 for GEMINI. The generic basis utilizes adjustment factors which are dependent on plant and event type. Reference 29 summarizes these factors for the GENESIS set of methods. For the GEMINI set of methods, the adjustment factors and their application are described in Reference 31. Since both the GENESIS and GEMINI adjustment factors take credit for conservatism in the scram speed assumed for the transient analyses, each plant operating under Option B must demonstrate that its actual scram speeds are within the distribution assumed in the derivation of the adjustment factors. This conformance procedure is described in Reference 29.

The cycle-specific adjusted MCPR values for all rapid pressurization events are given in the cycle-specific supplemental reload licensing report.

If the ΔCPR is calculated by TRACG (References 48 and 49), the ΔCPR and the OLMCPR are calculated such that less than 0.1% of the fuel rods will be subject to boiling transition during the transient.

4.4.4.1.2.7. Low Flow and Low Power Effects on MCPR

The operating limit MCPR must be increased for low flow because, in the BWR, power increases as core flow increases, which results in a corresponding lower MCPR. If the MCPR at a reduced flow condition were at the 100 percent power and flow MCPR operating limit, a sufficiently large inadvertent flow increase could cause the MCPR to decrease below the fuel cladding integrity safety limit MCPR.

The plant is licensed for the average power range monitor (APRM), rod block monitor (RBM), Technical Specification improvement program (ARTS), and has both power and flow dependent limits imposed on the operating limit MCPR (OLMCPR) (References 9a and 9b). The flow dependent OLMCPR, $MCPR_f$, is defined as a function of the core flow rate. The plant specific $MCPR_f$ is shown in the Core Operating Limits Report (COLR). The power dependent OLMCPR, $MCPR_p$, is determined from the product of the OLMCPR at 100 percent power [OLMCPR (100)] with a power dependent term, k_p. For power between 25 percent rated and 29.5 percent rated (bypass for turbine stop valve and control valve fast closure scram signal) there are two values for $MCPR_p$, one for core flows > 50 percent rated and the other for core flows ≤ 50 percent rated, as shown in COLR. Once the power exceeds 29.5 percent, the $MCPR_p$ is determined from a single curve of k_p which must be multiplied by [OLMCPR (100)] to produce the reduced power OLMCPR, $MCPR_p$. The OLMCPR to be used is the most limiting value of either $MCPR_p$ or $MCPR_f$.

4.4.4.1.2.8. End-of-Cycle Coastdown Considerations

AOO analyses are performed at the full power, end-of-cycle (EOC), all-rods-out condition. Once an individual plant reaches this condition, it may shutdown for refueling or it may be

placed in a coastdown mode of operation. In this type of operation the control rods are held in the all-rods-out position and the plant is allowed to coastdown to a lower percent of rated power while maintaining rated increased core flow. The power profile during this period is assumed to be a linear function with respect to exposure. It is expected that the actual profile will be a slow, exponential curve. An analysis to the linear approximation, however, will be conservative, since it overpredicts the power level for any given exposure.

In Reference 32, evaluations were made at 90 percent, 80 percent, and 70 percent power level points on the linear curve. The results show that the pressure and MCPR from the limiting pressurization AOO exhibit a larger margin for each of these points than the EOC full power, full flow case. MLHGR limits for the full power, rated increased core flow case are conservative for the coastdown period, since the power will be decreasing and rated increased core flow will be maintained. Therefore, it can be concluded that the coastdown operation beyond full power operation is conservatively bounded by the analysis at the EOC conditions. In Reference 33, this conclusion is confirmed for coastdown operation down to 40 percent power and is shown to hold for analyses performed with ODYN.

4.4.4.2. Core Hydraulics

Core hydraulics models and correlations are discussed in Subsection 4.4.2.

4.4.4.3. Influence of Power Distributions

The influence of power distributions on the thermal-hydraulic design is discussed in Reference 10.

4.4.4.4. Core Thermal Response

The thermal response of the core for accidents and expected AOO conditions is given in Chapter 15 and cycle specific reload analysis.

4.4.4.5. Analytical Methods

The analytical methods, thermodynamic data, and hydrodynamic data used in determining the thermal and hydraulic characteristics of the core are documented in Subsection 4.4.4.1.2.

4.4.4.6. Thermal-Hydraulic Stability Analysis

4.4.4.6.1. Introduction

There are many definitions of stability, but for feedback processes and control systems it can be defined as follows: A system is stable if, following a disturbance, the transient settles to a steady, noncyclic state.

A system may also be acceptably safe even if it oscillates, provided that any limit cycle of the oscillations is less than a prescribed magnitude. Instability, then, is either a continual departure from a final steady-state value or a greater-than-prescribed limit cycle about the final steady-state value.

The mechanism for instability can be explained in terms of frequency response. Consider a sinusoidal input to a feedback control system which, for the moment, has the feedback disconnected. If there were no time lags or delays between input and output, the output would be in phase with the input. Connecting the output to subtract from the input (negative feedback or 180° out-of-phase connection) would result in stable closed-loop operation. However, natural laws can cause phase shift between output and input, and should the phase shift reach 180° the feedback signal would reinforce the input signal rather than subtract from it. If the feedback signal were equal to or larger than the input signal (loop gain equal to one or greater), the input signal could be disconnected and the system would continue to oscillate. If the feedback signal were less than the input signal (loop gains less than one), the oscillations would die out.

It is possible for an unstable process to be stabilized by adding a control system. In general, however, it is preferable that a process with inherent feedback be designed to be stable by itself before it is combined with other processes and control systems. The design of the BWR is based on the premise that individual system components are stable under expected operating conditions.

4.4.4.6.2. Description

Three types of stability considered in the design of BWRs are

a. Reactor core (reactivity) stability

b. Channel hydrodynamic stability

c. Total system stability.

Reactivity feedback instability of the reactor core could drive the reactor into power oscillations. Hydrodynamic channel instability could impede heat transfer to the moderator and drive the reactor into power oscillations. The total system stability considers control system dynamics combined with basic process dynamics. A stable system is analytically demonstrated if no inherent limit cycle or divergent oscillation develops within the system as a result of calculated step disturbances of any critical variable, such as steam flow, pressure, neutron flux, and recirculation flow.

The criteria to be considered are stated in terms of two compatible parameters. The first parameter is the decay ratio x_2/x_o, designated as the ratio of the magnitude of the second overshoot to the first overshoot resulting from a step perturbation. A plot of the decay ratio is a graphic representation of the physical responsiveness of the system which is readily evaluated in a time-domain analysis. The second parameter is the damping coefficient ζ_n, the definition of which corresponds to the pole pair closest to the j_ω axis in the s-plane for the system closed-loop transfer function. This parameter also applies to the frequency domain interpretation. The damping coefficient is related to the decay ratio as shown in Figure 4.4-4.

4.4.4.6.3. Stability Criteria

General Design Criterion 12 of 10 CFR 50, Appendix A, states that the reactor core and associated coolant, control, and protection systems shall be designed to assure power oscillations which can result in conditions exceeding specified acceptable fuel design limits are not possible or can be reliably and readily detected and suppressed.

The assurance that the total plant is stable, is demonstrated analytically when the decay ratio, x_2/x_o, is less than 1.0, or equivalently, when the damping coefficient, ζ_n, is greater than zero for each type of stability discussed. It is necessary to differentiate between stability related limit cycles and small, acceptable cyclic behavior that is always present, even in the most stable reactors. Acceptable cyclic behavior is caused by physical nonlinearities (deadband and striction) in real control systems and is not representative of inherent hydrodynamic or reactivity instabilities in the reactor. The ultimate performance limit criteria for the three types of dynamic performance are summarized below in terms of decay ratio and damping coefficient

a. Channel hydrodynamic stability: x_2/x_o less than 1, ζ_n greater than 0

b. Reactor core (reactivity) stability: x_2/x_o less than 1, ζ_n greater than 0

c. Total system stability: x_2/x_o less than 1, ζ_n greater than 0

To assure stable operation, these criteria should be satisfied for all attainable conditions of the reactor that may be encountered in the course of plant operation. For stability purposes, the most severe condition to which these criteria will be applied corresponds to the highest attainable rod-line intersection with natural circulation flow.

Under certain operating conditions, power oscillations induced by thermal-hydraulic instability have been observed in other BWR facilities. If power and flow oscillations become large enough, the MCPR Safety Limit could be challenged. Fermi 2 has implemented the BWROG Long Term Stability Solution Option III. An Oscillation Power Range Monitor (OPRM) Upscale Function is incorporated into each APRM channel to reliably and readily detect power oscillation which could result from thermal-hydraulic instability in the operating ranges where such instability has been determined to be credible. The OPRM Upscale Function generates a trip signal to RPS upon detection of power oscillations, which causes an automatic scram to suppress the oscillation while it is still small. This automatic detection and suppression methodology provides protection against violation of the MCPR Safety Limit for power oscillations. The OPRM Upscale Function is described in References 34 – 37.

4.4.4.6.4. Conclusion

Stability-based MCPR Operating Limits are calculated for each operating cycle. These calculated values validate the selected OPRM setpoints for a given core configuration. Thus, the core design, combined with hardware, software, and selected system setpoints for detection and suppression of thermal-hydraulic power oscillations conform to the requirements of General Design Criterion 12 of 10 CFR 20, Appendix A.

4.4.5. Testing and Verification

The testing and verification techniques used to ensure that the planned thermal and hydraulic design characteristics of the core have been provided, and will remain within required limits throughout core lifetime, are discussed in Chapter 14. A summary follows.

a. Preoperational testing: Tests are performed during the preoperational test program to confirm that construction is complete and that all process and safety equipment is operational. Baseline data are taken to assist in the evaluation of

subsequent tests. Heat balance instrumentation, jet pump flow, and core temperature instrumentation are calibrated, and set-points are verified

b. Initial startup: Core performance (for example, peaking factors and LHGR) is evaluated periodically when the reactor is operating at greater than 25 percent power to verify the core expected and actual performance margins and to ensure that the reactor is operating within allowable limits.

4.4.6. Instrumentation Requirements

4.4.6.1. Operating Parameters

The reactor vessel instrumentation monitors the key reactor vessel operating parameters during planned operations. This ensures sufficient control of the parameters. The following reactor vessel sensors are discussed in Subsections 7.6.1.2 and 7.6.1.13:

a. Reactor vessel temperature

b. Reactor vessel water level

c. Reactor vessel coolant flow rates and differential pressures

d. Reactor vessel internal pressure

e. Neutron monitoring system.

4.4.6.2. Loose Parts Monitoring System

System has been abandoned.

4.4 THERMAL-HYDRAULIC DESIGN

REFERENCES

1. General Electric Co. "General Electric Standard Application for Reactor Fuel, GESTAR-II," NEDE-24011-P-A, (Latest Approved Revision as identified in the COLR).
2. General Electric Co., "Core Flow Distribution in a Modern Boiling Water Reactor as Measured in Monticello," NEDO-10299A, October 1976.
3. H. T. Kim and H. S. Smith, "Core Flow Distribution in a General Electric Boiling Water Reactor as Measured in Quad Cities Unit 1," NEDO-10722A, August 1976.
4. General Electric Co., "Brunswick Steam Electric Plant Unit 1 Safety Analysis Report for Plant Modifications to Eliminate Significant In-Core Vibrations," NEDO-21215, March 1976.
5. General Electric Co., "Supplemental Information for Plant Modification to Eliminate Significant In-Core Vibration," NEDE-21156 (PROPRIETARY), February 1976.
6. R. C. Martinelli and D. E. Nelson, "Prediction of Pressure Drops During Forced Convection Boiling of Water," ASME Trans., 70, 695-702, 1948.
7. C. J. Baroozy, "A Systematic Correlation for Two-Phase Pressure Drop," Heat Transfer Conference (Los Angeles), AICLE, Preprint No. 37, 1966.
8. N. Zuber and J. A. Findlay, "Average Volumetric Concentration in Two-Phase Flow Systems," Transactions of the ASME Journal of Heat Transfer, November 1965.
9. W. H. Jens and P. A. Lottes, "Analysis of Heat Transfer, Burnout, Pressure Drop and Density Data for High Pressure Water," USAEC Report-4627, 1972.
10. 9a. GE Nuclear Energy, Maximum Extended Operating Domain Analysis for Detroit Edison Company Enrico Fermi Energy Center Unit 2, NEDC-31843P, July 1990.
11. 9b. Letter from NRC to Detroit Edison, "Amendment No. 69 to Facility Operating License No. NPF-43: TAC No. 77676," May 15, 1991.
12. 9c. GE Nuclear Energy, Maximum Extended Load Line Limit and Feedwater Heater Out-of-Service Analysis for Enrico Fermi Energy Center Unit 2, NEDC-31515, Revision 1, August 1989.
13. General Electric Co., "General Electric BWR Thermal Analysis Basis (GETAB): Data, Correlation and Design Application," NEDE-10958-PA and NEDO-10958-A, January 1977.
14. Letter from J. S. Charnley (GE) to C. O. Thomas (NRC), "Amendment 15 to General Electric Licensing Topical Report NEDE-24011-P-A," January 23, 1986.
15. Letter from J. S. Charnley (GE) to C. O. Thomas (NRC), "Amendment 14 to General Electric Licensing Topical Report NEDE-24011-P-A," October 2, 1985.

REFERENCES

16. Letter from J. S. Charnley (GE) to M. W. Hodges (NRC), "Changes to the U. S. Supplement of GESTAR (Pertaining to Proposed Amendment 18 of GESTAR)," August, 1987.
17. Letter from J. S. Charnley (GE) to M. W. Hodges (NRC), "Application of GESTAR-II Amendment 15," March 22, 1988.
18. Letter from J. S. Charnley (GE) to M. W. Hodges (NRC), "Application of GEXL to GE8x8NB Fuel," April 13, 1988.
19. General Electric Co., "Qualification of the One-Dimensional Core Transient Model for BWR's," NEDO-24154, Vol. 1 and 2; October 1978.
20. General Electric Co., "Qualification of the One-Dimensional Core Transient Model for BWR's," NEDO-24154-P, Vol. 3; October 1978.
21. J. A. Wooley, "Three Dimensional BWR Core Simulator," NEDO-20953A, January 1977.
22. Letter from J. F. Quirk (GE) to P. S. Check (NRC), "ODYN Improvements," September 25, 1981.
23. Letter from H. C. Pfefferlen (GE) to D. G. Eisenhut (NRC), "Correction of ODYN Errors," June 8, 1982.
24. General Electric Co., "Steady-State Nuclear Methods," NEDE-30130-P-A and NEDO-30130-A, April 1985.
25. Letter from J. S. Charnley (GE) to C. O Thomas (NRC), "Amendment 11 to GE LTR NEDE-24011-P-A," February 27, 1985.
26. R. B. Linford, "Analytical Methods of Plant Transient Evaluations for the General Electric Boiling Water Reactor," NEDO-10802, February 1973.
27. R. B. Linford, "Analytical Methods of Plant Transient Evaluations for the GE BWR Amendment No. 1," NEDO-10802-01, June 1975.
28. R. B. Linford, "Analytical Methods of Plant Transient Evaluations for the GE BWR Amendment No. 2," NEDO-10802-02, June 1975.
29. Letter from R. E. Engel (GE) to T. A. Ippolito (NRC), "Change in GE Methods for Analysis of Cold Water Injection Transients," September 30, 1980.
30. General Electric Co., "Analytical Model for Loss-of-Coolant Analyses in Accordance with 10CFR50 Appendix K," NEDE-20566-P and NEDO-20566, January 1976.
31. Letter from K. W. Cook (GE) to F. Schroeder and D. G. Eisenhut (NRC), "Implementation of a Revised Procedure for Calculating Hot Channel Transient ΔCPR, July 20, 1979.

4.4 THERMAL-HYDRAULIC DESIGN

REFERENCES

32. Letter from R. C. Tedesco (NRC) to G. G. Sherwood (GE), "Acceptance for Referencing General Electric Licensing Topical Report NEDO-24154/NEDE-24154P," February 4, 1981.
33. Letter from R. H. Buchholz (GE) to P. S. Check (NRC), "ODYN Adjustment Methods for Determination of Operating Limits," January 19, 1981.
34. Letter from J. S. Charnley (GE) to C. O. Thomas (NRC), "Supplementary Information Regarding Amendment 11 to GE Licensing Topical Report NEDE-20411-P-A," October 9, 1985.
35. Letter from R. A. Bolger (Commonwealth Edison Co.) to B. C. Rusche (USNRC), "QC-2 Proposed Amendment to Facility License No. DPR-30," Docket No. 50-265.
36. Letter from R. E. Engel (GE) to T. A. Ippolito (NRC), "End of Cycle Coastdown Analyzed with ODYN/TASC," September 1, 1981.
37. Licensing Topical Report NEDC-32410P-A, “Nuclear Measurement Analysis and Control Power Range Neutron Monitor (NUMAC-PRNM) Retrofit Plus Option III Stability Trip Function” October 1995, and NEDC-32410P-A Supplement 1, November 1997.
38. NRC Generic Letter 94-02, “Long-Term Solutions and Upgrade of Interim Operating Recommendations for Thermal-Hydraulic Instabilities in Boiling Water Reactors”, July 1994.
39. Licensing Topical Report NEDO-32465-A, “Reactor Stability Detect and Suppress Solutions Licensing Basis Methodology for Reload Applications”, August 1996.
40. NEDO-31960-A and NEDO-31960-A Supplement 1, “BWR Owner’s Group Long-Term Stability Solutions Licensing Methodology” November 1995.
41. NEDC-32601P-A, “Methodology and Uncertainties for Safety Limit MCPR Evaluations”, August 1999.
42. NEDC-32694P-A, “Power Distribution Uncertainties for Safety Limit MCPR Evaluation”, August 1999.
43. NEDC-32505P-A, Revision 1, ”R-Factor Calculation Method for GE11, GE12, and GE13 Fuel”, July 1999.
44. NEDC-32868P, Revision 1, “GE14 Compliance With Amendment 22 of NEDE-24011-P-A (GESTAR-II)”, September 2000.
45. NEDE-31917P, “GE11 Compliance with Amendment 22 of NEDE-24011-P-A (GESTAR-II)”, April 1991.
46. Letter from William T. O’Connor to USNRC, NRC-04-0074, “Proposed License Amendment Request to Revise Technical Specification 2.1, Safety Limit Minimum Critical Power Ratio”, dated October 7, 2004.

4.4 THERMAL-HYDRAULIC DESIGN

REFERENCES

47. Global Nuclear Fuel, Supplemental Reload Licensing Report for Fermi 2 (Latest approved edition as identified in COLR)

48. TRACG Application for Anticipated Operational Occurrences (AOO) Transient Analyses, NEDE-32906P-A, Revision 3, September 2006.

49. Migration to TRACG04 / PANAC11 from TRACG02 / PANAC10 for TRACG AOO and ATWS Overpressure Transients, NEDE-32906P Supplement 3-A, Rev. 1, April 2010.

TABLE 4.4-1 THERMAL AND HYDRAULIC DESIGN CHARACTERISTICS OF THE INITIAL REACTOR CORE

General Operating Conditions	(201-444)	(218-560)	Fermi 2 (251-764)
Reference design thermal output, MWt	1931	2436	3293
Power level for engineered safety features, MWt	2028	2558	3430
Steam flow rate, at 420°F final feedwater temperature, millions lb/hr	8.303	10.5	14.159
Core coolant flow rate, millions lb/hr	61.5	77.0	100
Feedwater flow rate, millions lb/hr	8.284	10.4	14.127
System pressure, nominal in steam dome, psia	1020	1020	1020
System pressure, nominal core design, psia	1,035	1035	1035
Coolant saturation temperature at core design pressure, °F	549	548.8	549
Average power density, kW/liter	49.2	49.2	48.7
Maximum linear heat generation rate, kW/ft	13.4	13.4	13.4
Average linear heat generation rate, kW/ft	5.4	5.4	5.3
Core total heat transfer area, ft^2	43,511	54,879	74,871
Maximum heat flux, Btu/hr-ft^2	361,600	361,600	361,600
Average heat flux, Btu/hr-ft^2	145,000	145,060	143,700

TABLE 4.4-1 THERMAL AND HYDRAULIC DESIGN CHARACTERISTICS OF THE INITIAL REACTOR CORE

General Operating Conditions	(201-444)	(218-560)	Fermi 2 (251-764)
Design operating minimum critical power ratio	1.24	1.22	1.24
Core inlet enthalpy at 420°F FFWT[a], Btu/lb	527.1	526.9	526.1
Core inlet temperature, at 420°F FFWT[a], °F	532	532	532
Core maximum exit voids within assemblies, percent	76.2	76.0	77.1
Core average void fraction, active coolant	0.412	0.422	0.418
Maximum fuel temperature,°F	3435	3435	3435
Active coolant flow area per assembly, $in.^2$ (BOL)	15.824	15.824	15.824
Core average inlet velocity, ft/sec	6.72	6.65	6.34
Maximum inlet velocity, ft/sec	8.28	7.1	7.78
Total core pressure drop, psi	23.71	23.89	21.25
Core support plate pressure drop, psi	19.28	19.46	16.83
Average orifice pressure drop			
Central region, psi	5.93	8.0	5.12
Peripheral region, psi	15.93	16.52	13.95
Maximum channel pressure loading, psi	12.39	12.86	10.88

[a] Final feedwater temperature.

TABLE 4.4-2 TYPICAL RANGE OF TEST DATA

Measured Parameter	Test Conditions
Adiabatic tests	
Spacer single-phase loss coefficient	$Re^{a} = 0.5 \times 10^{5}$ to 3.5×10^{5}
Lower tie plate and orifice single-phase loss coefficient	T = 100 to 500°F
Upper tie plate single-phase friction factor	
Spacer two-phase loss coefficient	P = 800 to 1400 psia
Two-phase friction multiplier	$G = 0.5 \times 10^{6}$ to 1.5×10^{6} lb/hr-ft^2 X = 0 to 40 percent
Diabatic tests	
Heated bundle pressure drop	P = 800 to 1400 psia $G = 0.5 \times 10^{6}$ to 1.5×10^{6} lb/hr-ft^2

[a] Reynolds Number.

TABLE 4.4-3 UNCERTAINTIES USED IN STATISTICAL ANALYSIS

Quality	Standard Deviation (% of Point)	Comment
Feedwater Flow	1.8	This is the largest component of total reactor power uncertainty.
Feedwater Temperature	0.8	These are the other significant parameters in core power determination.
Reactor Pressure	0.7	
Core Inlet Temperature	0.2	Affected quality annular flow length and boiling length.
Core Total Flow	2.5[a]	Flow is not measured directly, but is calculated from jet pump ΔP. The listed uncertainty in total core flow corresponds to 11.2 percent standard deviation in each individual jet pump flow. Conservative estimates of the uncertainties of flow through all the bypass flow path yielded an overall bypass flow uncertainty of 0.6 percent. This uncertainty, combined with the 2.0 percent core flow measurement uncertainty, yields a total uncertainty of 2.1 percent; hence, the contribution of the bypass flow uncertainty has already been conservatively included in the 2.5 percent core flow uncertainty used for the GETAB statistical analysis.
Channel Flow Area	2.0	This accounts for manufacturing and service induced variations in the free flow area within the channel.
Friction Factor Multiplier	6.0	Accounts for uncertainty in the correlation representing two-phase pressure losses.
Channel Friction Factor Multiplier	5.0	Represents variation in the pressure loss characteristics of individual channels. Pressure loss variations affect the core flow distribution, influencing the mass flux.
TIP Readings Random Uncertainty	1.20[b]	
R Factor	2.0	This is a function of the uncertainty in local fuel rod power.

[a] This uncertainty is 6.0 percent for single recirculation pump.

[b] This value is for two recirculation pumps operational. For single recirculation pump, this uncertainty is 2.85 percent.

TABLE 4.4-4 REACTOR COOLANT SYSTEM GEOMETRIC DATA

	Flow Path Length (in.)	Height and Liquid Level (in.)	Elevation of Bottom of Each Volume[a] (in.)	Minimum Flow Area ($ft.^2$)
A. Lower plenum	216.5	216.5 216.5	-161.5	92.5
B. Core	163.0	163.0 163.0	55.0	152.0
C. Upper plenum and separators	185.0	185.0 185.0	217.5	45.0
D Dome (above normal water level)	299.5	299.5 0	402.5	352.0
E. Downcomer area	311.0	311.0 311.0	-30.0	118.0
F. Recirculation loops and jet pumps (one loop)	97.0 ft	492.0 492.0	-472.5	0.538

[a] Reference point is recirculation outlet nozzle centerline.

TABLE 4.4-5 LINE LENGTHS AND SIZES OF SAFETY INJECTION LINES[a]

RHR Pumps

Pump A:
20-in. diameter/40-ft length joins
24-in. diameter/170-ft length
24-in. diameter/170-ft length joins
24-in. diameter/30-ft length
24-in. diameter/30-ft length joins
12-in. diameter/30-ft length

Pump B:
Same as Pump A

Pump C: 20-in. diameter/60-ft length joins
24-in. diameter/170-ft length
24-in. diameter/170-ft length joins
24-in. diameter/30-ft length
24-in. diameter/30-ft length joins
12-in. diameter/30-ft length

Pump D:
Same as Pump C

HPCI Pumps Discharge

10-in. pipe diameter increases to 14-in. pipe diameter
Length: 2 ft, 10 in.
Other: 14-in. pipe diameter/170-ft length
12-in. pipe diameter/32-ft length

LPCI Pump Discharge

Pumps A and B:
28-in. pipe diameter/40-ft length
22-in. pipe diameter/30-ft length
12-in. pipe diameter/15-ft length

Core Spray

Pumps A and C:
12-in pipe diameter/132-ft length
14-in. pipe diameter/150-ft length

Pumps B and D:
12-in pipe diameter/127-ft length
14-in pipe diameter/182-ft length

[a] These piping dimensions are for information only. The piping dimensions are shown on the applicable Piping Isometrics. The associated pressure drops are determined in the applicable Hydraulic Calculations.

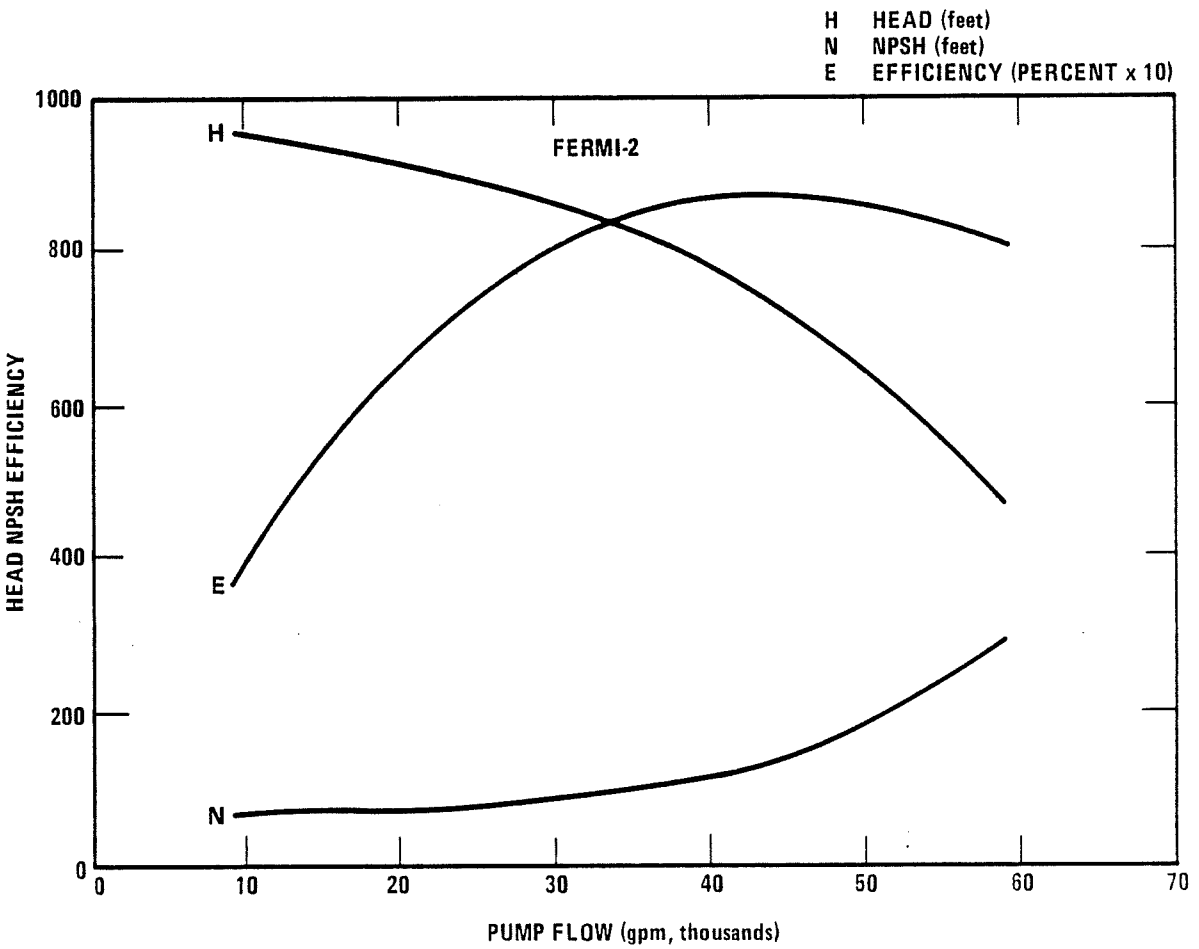

Fermi 2
UPDATED FINAL SAFETY ANALYSIS REPORT

FIGURE 4.4-1

VARIABLE SPEED PUMP PERFORMANCE (RECIRCULATION PUMP)

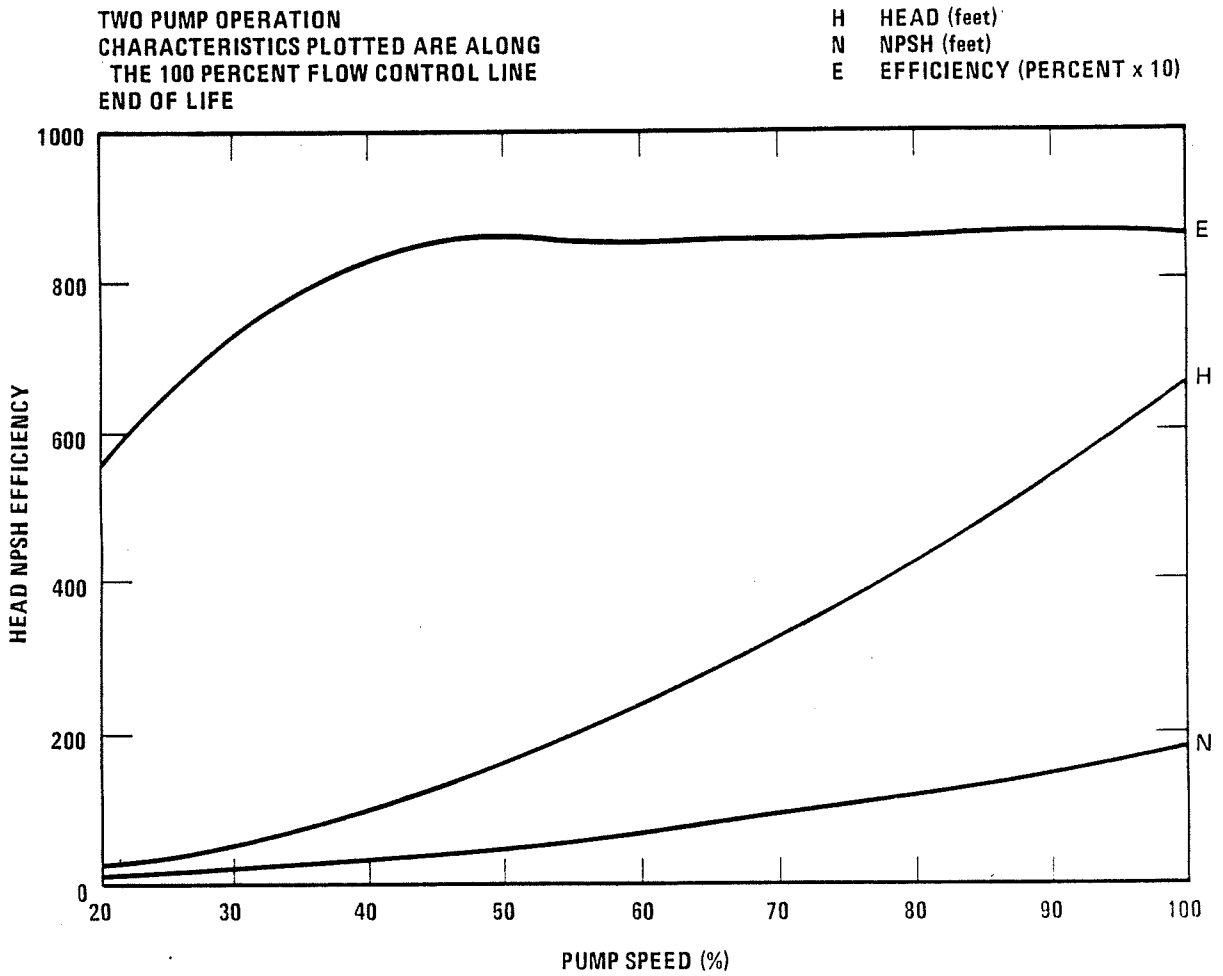

Fermi 2
UPDATED FINAL SAFETY ANALYSIS REPORT

FIGURE 4.4-2

EXPECTED PUMP PERFORMANCE (RECIRCULATION PUMP)

FERMI-2 POWER/FLOW MAP

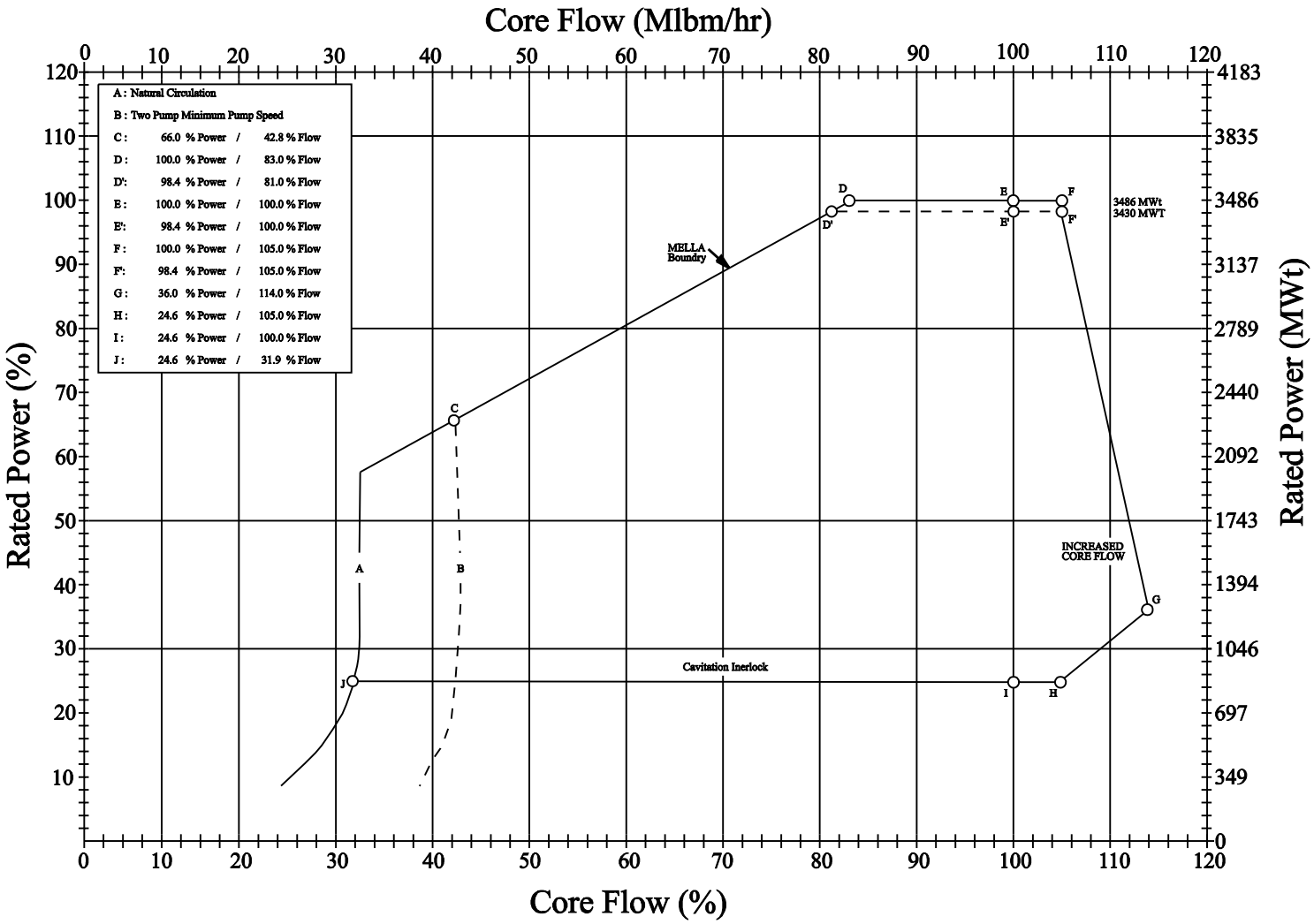

Fermi 2

UPDATED FINAL SAFETY ANALYSIS REPORT

FIGURE 4.4-3

TYPICAL POWER / FLOW OPERATING MAP

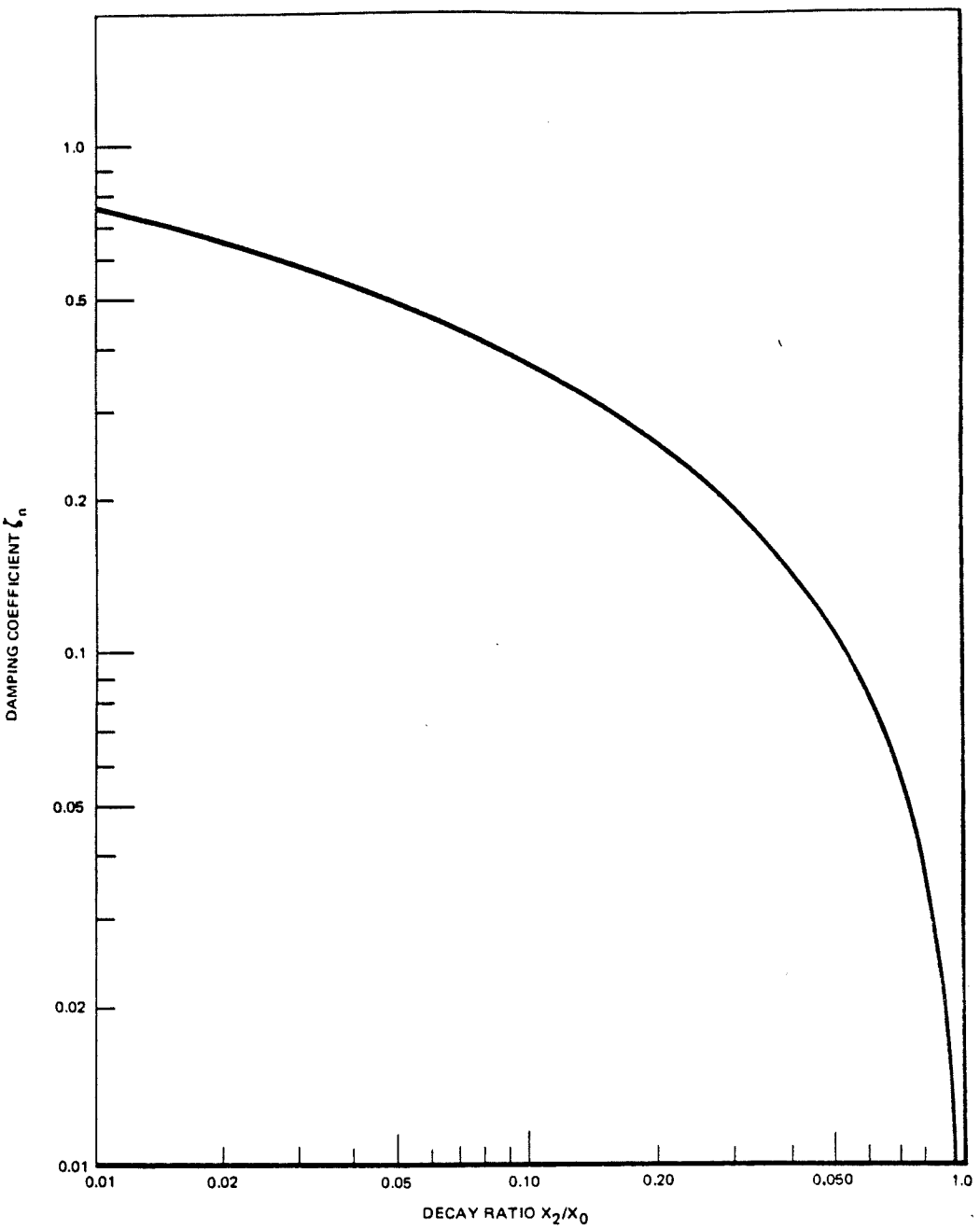

Fermi 2
UPDATED FINAL SAFETY ANALYSIS REPORT

FIGURE 4.4-4

DAMPING COEFFICIENT VERSUS DECAY RATIO (SECOND ORDER SYSTEMS)

4.5 REACTOR MECHANICAL DESIGN

4.5.1 Reactor Core Support Structures and Internals Mechanical Design

4.5.1.1 Design Bases

4.5.1.1.1 General Design Bases

4.5.1.1.1.1 Safety Design Bases

The reactor core support structures and internals meet the following safety design bases:

a. They are arranged to provide a floodable volume in which the core can be adequately cooled in the event of a breach in the nuclear system process barrier external to the reactor pressure vessel (RPV)

b. Deformation is limited to ensure that the control rods and core standby cooling systems can perform their safety functions

c. Mechanical design of applicable structures ensures that safety design bases items a. and b. are satisfied so that the safe shutdown of the plant and removal of decay heat are not impaired.

4.5.1.1.1.2 Power Generation Design Bases

The reactor core support structures and internals shall be designed in accordance with the following power generation design bases.

a. They provide the proper coolant distribution during all anticipated normal operating conditions to allow power operation of the core without fuel damage

b. They are arranged to facilitate refueling operations

c. They are designed to facilitate inspection.

4.5.1.1.2 Specific Design Characteristics

4.5.1.1.2.1 Design Loading Combinations

The design loading combinations of the RPV internals are covered in Subsection 4.5.1.3.1.1.

4.5.1.1.2.2 Stress, Deformation, and Fatigue Limits for Reactor Internals (Except Core Support Structures)

The stress, deformation, and fatigue criteria listed in Tables 4.5-1 through 4.5-4 are used or the criteria shall be based on the criteria established in applicable codes and standards for similar equipment, by manufacturers' standards, or by empirical methods based on field experience and testing. For the quantity SF_{min} (minimum safety factor) appearing in those tables, the following listed values shall be used.

Design Condition	SF_{min}
Normal	2.25
Upset	2.25
Emergency	1.5
Fault	1.125

4.5.1.1.2.3 Stress, Deformation, and Fatigue Limits for Core Support Structures

The stress, deformation, and fatigue criteria presented in Tables 4.5-5, 4.5-6, and 4.5-7 are used. These criteria are supplemented, where applicable, by the criteria for the reactor internals in the previous paragraph, but in no case shall the criteria presented in these tables be exceeded for core support structures.

4.5.1.1.2.4 Fuel Assembly Restraints

The fuel assembly structural design shall demonstrate sufficient dimensional stability and sufficient fuel rod support to maintain core geometry, thus avoiding fuel damage for both planned operation and abnormal operational transients.

4.5.1.1.2.5 Material Selection

The material used for fabricating most of the reactor core support and reactor internal structures is solution heat treated, unstabilized type 304 austenitic stainless steel conforming to ASTM specifications. Weld procedures and welders are qualified in accordance with the intent of Section IX of the ASME Boiler and Pressure Vessel (B&PV) Code. Further controls for stainless steel welding are covered in Subsection 5.2.5.

All the materials of construction exposed to the reactor coolant are resistant to stress corrosion in the BWR coolant. Conservative corrosion allowances are provided for all exposed surfaces of carbon or low-alloy steels.

Contaminants in the reactor coolant are controlled to very low limits by the reactor water-quality specifications. No detrimental effects occur on any of the materials from allowable contaminant levels in the high-purity reactor coolant. Radiolytic products in a BWR have no adverse effects on the construction materials.

4.5.1.1.2.6 Radiation Effects

Where feasible, the design is such that irradiation effects on the material properties are minimized. Where irradiation effects cannot be minimized, the design of the RPV internals either has provisions for replaceable components, or the design is shown to satisfy a set of stress and fatigue design limits that have been arrived at considering the effect of irradiation damage on the fracture toughness, ductility, and tensile properties of the materials.

4.5.1.1.2.7 Shock Loads

The components are designed so as to accommodate the loadings discussed in Section 3.9.

4.5.1.2 Description

The core support structures and RPV internals (excluding fuel, control rods, and in-core nuclear instrumentation) include the following components.

a. Core support structures
    1. Shroud
    2. Shroud support
    3. Core support and hold-down bolts
    4. Top guide (including wedges, bolts, and keepers)
    5. Fuel support pieces
    6. Control rod guide tubes.

b. Reactor pressure vessel internals
    1. Jet pump assemblies and instrumentation
    2. Shroud head and steam separator assembly (including shroud head bolts)
    3. Steam dryers
    4. Feedwater spargers
    5. Deleted
    6. Differential pressure and liquid control line
    7. In-core flux monitor guide tubes and stabilizers
    8. Surveillance sample holders
    9. Core spray lines and spargers.

The overall arrangement of the structures within the RPV is shown in Figure 4.1-1.

A general assembly drawing of the important reactor components is shown in Figure 4.5-1.

The floodable inner volume of the RPV can be seen in Figure 4.5-2. It is the volume inside the core shroud up to the level of the jet pump suction inlet.

The core support structure is used to form partitions within the RPV, to sustain pressure differentials across the partitions, to direct the flow of the coolant water, and to locate laterally and support the fuel assemblies, control rod guide tubes, and steam separators. Figure 4.5-2 shows the RPV internal flow paths.

4.5.1.2.1 Shroud

The core shroud is a stainless steel cylindrical assembly that provides a partition to separate the upward flow of coolant through the core from the downward recirculation flow. This partition separates the core region from the downcomer annulus, thus providing a floodable region following a recirculation line break.

The volume enclosed by the shroud is characterized by three regions. The upper shroud surrounds the core discharge plenum, which is bounded by the shroud head on top and the top guide below. The central portion of the shroud surrounds the active fuel and forms the longest section of the shroud. This section is bounded at the bottom by the core support. The lower shroud, surrounding part of the lower plenum, is welded to the RPV shroud support (Section 5.4).

4.5.1.2.2 Shroud Head and Steam Separator Assembly

The shroud head and steam separator assembly is bolted to the top of the upper shroud to form the top of the core discharge plenum. This plenum provides a mixing chamber for the steam/water mixture before it enters the steam separators. Individual stainless steel axial flow steam separators, shown in Figure 4.l-3, are attached to the top of standpipes that are welded into the shroud head. The steam separators have no moving parts. In each separator, the steam/water mixture rising through the standpipe passes vanes that impart a spin to establish a vortex separating the water from the steam. The separated water flows from the lower portion of the steam separator into the downcomer annulus.

4.5.1.2.3 Core Support Plate

The core support plate consists of a circular stainless steel plate with bored holes stiffened with a rim and beam structure. The plate provides lateral support and guidance for the control rod guide tubes, in-core flux monitor guide tubes, and peripheral fuel supports. The last item is also supported vertically by the core support plate.

The entire assembly is bolted to a support ledge between the central and lower portions of the core shroud. Alignment pins that engage slots and bear against the shroud are used to correctly position the assembly before it is secured.

The flow holes in the core support plate were plugged, and two holes for each fuel bundle were drilled in the lower tie plate. This modification reduces the channel box wear from flow-induced instrument tube vibrations caused by flow through the bypass holes in the lower core support plate. The above fixes are similar to that provided for Peach Bottom 2. A detailed discussion of the channel box wear problem and the solution is provided in Reference 1.

4.5.1.2.4 Top Guide

The top guide is formed by a series of stainless steel beams joined at right angles to form square openings, with the beams fastened to a peripheral rim. Each large opening provides lateral support and guidance for four fuel assemblies or, in the case of peripheral fuel, one or two fuel assemblies. Notches are provided in the bottom of the beam intersections to anchor the in-core flux monitors and startup neutron sources (all neutron sources were removed from the core during the first refueling outage).

4.5.1.2.5 Fuel Support

The fuel supports, shown in Figure 4.5-3, are of two basic types: namely, peripheral supports and four-lobed orificed fuel supports. The peripheral fuel support is located at the outer edge

of the active core and is not adjacent to control rods. Each peripheral fuel support supports one fuel assembly and contains a single orifice assembly designed to ensure proper coolant flow to the fuel peripheral assembly. Each four-lobed orificed fuel support supports four fuel assemblies and is provided with orifice plates to ensure proper coolant flow distribution to each rod-controlled fuel assembly. The four-lobed orificed fuel supports rest in the top of the control rod guide tubes which are supported laterally by the core support. The control rods pass through slots in the center of the four-lobed orificed fuel support. A control rod and the four adjacent fuel assemblies represent a core cell (Subsection 4.1.2.1.4).

4.5.1.2.6 Control Rod Guide Tubes

The control rod guide tubes, located inside the RPV, extend from the top of the control rod drive (CRD) housing up through holes in the core support plate. Each tube is designed as the guide for a control rod and as the vertical support for a four-lobed orificed fuel support piece and the four fuel assemblies surrounding the control rod. The bottom of the guide tube is supported by the CRD housing (Section 5.4), which in turn transmits the weight of the guide tube, fuel support, and fuel assemblies to the RPV bottom head. A thermal sleeve is inserted into the CRD housing from below and is rotated to lock the control rod guide tube in place. A key is inserted into a locking slot in the bottom of the CRD housing to hold the thermal sleeve in position.

4.5.1.2.7 Jet Pump Assemblies

The jet pump assemblies are located in two semicircular groups in the downcomer annulus between the core shroud and the RPV wall. The design and performance of the jet pump are covered in detail in References 2 and 3. Each stainless steel jet pump consists of driving nozzles, suction inlet, throat or mixing section, and diffuser (Figure 4.5-4). The driving nozzle, suction inlet, and throat are joined together as a removable unit, and the diffuser is permanently installed. High-pressure water from the recirculation pumps (Subsection 5.5.l) is supplied to each pair of jet pumps through a riser pipe welded to the recirculation inlet nozzle thermal sleeve. A riser brace consists of cantilever beams extending from pads on the RPV wall.

The nozzle entry section is connected to the riser by a metal-to-metal, spherical-to-conical seal joint. Firm contact is maintained by a hold-down clamp. The throat section is supported laterally by a bracket attached to the riser. There is a slip-fit joint between the throat and diffuser. The diffuser is a gradual conical section changing to a straight cylindrical section at the lower end.

Evaluations performed by GE have shown that jet pump riser beam failures have resulted from intergranular stress corrosion cracking (IGSCC). Comparison of the failed BWR 3 beam with the BWR 4-6 beam structural design (i.e., the Fermi 2 design) has identified that the BWR 4-6 beam operates at a peak stress 14 percent lower than that of the BWR 3 design at the current joint preload. Because the time to crack initiation and subsequent failure increases with a decrease in stress, a reduction in preload was evaluated. The results of this evaluation, together with flow tests performed on prototypical components, have demonstrated the operational acceptability of a preload reduction to 25,000 lb. From relationships developed from field experience and laboratory stress corrosion tests, the

minimum time to crack initiation for the Fermi 2 jet pump beam is estimated to increase by a factor of 4 with respect to the BWR 3 jet pump beam. In summary, Edison

a. Reduced the preload on all jet pump beams from 30,000 to 25,000 lb

b. Plans to inspect the jet pump beams during plant outages at a frequency to be determined from the surveillance of lead operating plants of this design.

By taking the above actions, the likelihood of beams developing cracks during the projected life of the plant is remote, and the likelihood of the cracks leading to beam failure before detection is extremely remote. However, if replacement beams that do not require periodic ultrasonic inspections are developed, Edison's position will be reevaluated.

In 1993, a jet pump hold-down beam failure occurred at a BWR-6. While previous failures occurred in the middle section of the beam, the recent failure occurred in the transition to the arms at the ends of the beam, with the cause of the failure identified as IGSCC. The most significant new findings resulting from this failure were that while the material and stress conditions were about the same at the beam middle and end sections, fracture mechanics evaluations indicated that crack growth to failure could occur in the beam ends in less than one 18-month operating cycle.

As a result of this failure, Edison elected to replace all jet pump hold down beams during the fourth refueling outage with replacement hold-down beam bolt assemblies. The new replacement beams received high temperature anneal (HTA) heat treatment during manufacturing and are less susceptible to IGSCC than the beams that were originally installed. Prior to and following installation in the RPV, the beam/bolt assemblies were inspected utilizing the latest inspection technology. The beams were preloaded to 25,000 lbs, consistent with the previous installation, and will be subjected to inservice inspection. The recommended inservice inspection interval provided in IE Bulletin 80-07 and NUREG/CR-3052 is once every 10 years. Subsequent UT and alternative inspections will be performed during future refueling outages based on industry experiences and the recommendations provided in NUREG/CR-3052.

If a crack is detected in a jet pump hold-down beam, that beam will be replaced by one of a suitable material and design before the return to power operation.

4.5.1.2.8 Steam Dryers

The steam dryers remove moisture from the wet steam leaving the steam separators. The extracted moisture flows down the dryer vanes to the collecting troughs, then flows through tubes into the downcomer annulus (Figure 4.l-4). A skirt extends from the bottom of the dryer vane housing to the steam separator standpipe, below the water level. This skirt forms a seal between the wet steam plenum and the dry steam flowing from the top of the dryers to the steam outlet nozzles.

4.5.1.2.9 Feedwater Spargers

The feedwater spargers are perforated stainless steel headers located in the mixing plenum above the downcomer annulus (Figure 4.l-l). A separate sparger is fitted to each feedwater nozzle and is shaped to conform to the curve of the RPV wall. Feedwater flow enters the center of the spargers and is discharged radially inward to mix the cooler feedwater with the

downcomer flow from the steam separators before it contacts the RPV wall. The feedwater also serves to condense the steam in the region above the downcomer annulus and to subcool the water flowing to the jet pumps and recirculation pumps.

4.5.1.2.10 Core Spray Lines

The core spray lines are the means for directing flow to the core spray nozzles that distribute coolant so that peak fuel cladding temperatures of 2200°F are not exceeded during accident conditions.

Two core spray lines enter the RPV through the two core spray nozzles (Figure 4.1-1 and Section 6.3). The lines divide immediately inside the RPV. The two halves are routed to opposite sides of the RPV and are supported by clamps attached to the RPV wall. The lines are then routed downward into the downcomer annulus and pass through the upper shroud immediately below the flange. The flow divides again as it enters the center of the semicircular sparger, which is routed halfway around the inside of the upper shroud. The ends of the two spargers are supported by brackets designed to accommodate thermal expansion. The line routing and supports are designed to accommodate differential movement between the shroud and RPV. The other core spray line is identical except that it enters the opposite side of the RPV, and the spargers are at a slightly different elevation inside the shroud. The correct spray distribution pattern is provided by a combination of distribution nozzles pointed radially inward and downward from the spargers (Section 6.3).

4.5.1.2.11 Differential Pressure and Liquid Control Line

The differential pressure and liquid control line (Figure 4.l-l) serves a dual function within the RPV: to provide a path for the injection of the liquid control solution into the coolant stream (discussed in Subsection 4.5.2.4) and to sense the differential pressure across the core support plate (Section 5.4). This line enters the RPV at a point below the core shroud as two concentric pipes. In the lower plenum, the two pipes separate. The inner pipe terminates near the lower shroud with a perforated length below the core support plate. It is used to sense the pressure below the core support plate during normal operation and to inject liquid control solution if required. This location facilitates good mixing and dispersion. The inner pipe also reduces thermal shock to the RPV nozzle should the standby liquid control system (SLCS) be actuated. The outer pipe terminates immediately above the core support plate and senses the pressure in the region outside the fuel assemblies.

4.5.1.2.12 In-Core Flux Monitor Guide Tubes

The in-core flux monitor guide tubes provide a means of positioning fixed detectors in the core as well as providing a path for calibration monitors (traversing in-core probe or TIP system), and extend from the top of the in-core flux monitor housing (Section 5.4) in the lower plenum to the top of the core support plate. The power range detectors for the power range monitoring units and the dry tubes for the source range monitor and intermediate range monitor (SRM/IRM) detectors are inserted through the guide tubes. A latticework of clamps, tie bars, and spacers gives lateral support and rigidity to the guide tubes. The bolts and clamps are welded in place, after assembly, to prevent loosening during reactor operation.

4.5.1.2.13 Surveillance Sample Holders

The surveillance sample holders are welded baskets containing impact and tensile specimen capsules (Subsection 5.2.4.4). The baskets hang from the brackets that are attached to the inside wall of the RPV and extend to mid-height of the active core. The radial positions are chosen to expose the specimens to the same environment and maximum neutron fluxes experienced by the RPV itself while avoiding jet pump removal interference or damage.

4.5.1.2.14 Neutron Startup Source

The source assembly is comprised of two basic components: a source holder and a gamma source. The source holder is hollow, cylindrical, stainless steel sheathed, and spring loaded. It seals a beryllium tube from reactor water. The gamma source is a stainless-steel-sheathed assembly that houses neutron-irradiated antimony. In the neutron irradiation, some of the antimony is converted to ^{122}Sb, some to ^{124}Sb, and some remains unconverted. ^{122}Sb and ^{124}Sb emit gamma radiation.

Prior to startup, the gamma sources are inserted in the source holders. Neutrons are emitted from the beryllium as gamma radiation is absorbed. The gammas from the ^{124}Sb contribute almost all the generation of neutrons, as the half-life of ^{124}Sb is 60 days while the half-life of ^{122}Sb is 2.8 days. Most of the ^{122}Sb has decayed away during the postirradiation testing and shipment.

All sources assemblies were removed from the core during the first refueling outage.

4.5.1.3 Safety Evaluation

4.5.1.3.1 Evaluation Methods

To determine that the safety design bases are satisfied, responses of the RPV internals to loads imposed during normal, upset, emergency, and faulted conditions are examined. The effects on the ability to insert control rods, cool the core, and flood the inner volume of the RPV are determined.

4.5.1.3.1.1 Input for Safety Evaluation

The operating conditions that provide the basis for the design of the reactor internals to sustain normal, upset, emergency, and faulted conditions as well as combinations of design loadings that are accounted for in design of the core support structure are covered in Table 4.5-8.

In addition, each combination of operating loads is categorized with respect to either normal, upset, emergency, or faulted conditions as well as the associated design stress intensity or deformation limits.

The bases for the proposed design stress and deformation criteria are also specified in Chapter 3.

4.5.1.3.1.2 Events To Be Evaluated

Examination of the spectrum of conditions for which the safety design basis must be satisfied reveals three significant events.

a. Recirculation line break (LOCA) - The accident results in pressure differentials, within the RPV, that may exceed normal loads

b. Steam line break accident - This is a break in one main steam line between the RPV and the flow restrictor. The accident results in significant pressure differentials across some of the structures within the reactor

c. Earthquake - It subjects the core support structures and reactor internals to significant forces as a result of ground motion.

For other conditions existing during normal operation, abnormal operational transients, and accidents, the loads affecting the core support structures and reactor internals are less severe than these three postulated events.

4.5.1.3.2 Recirculation Line and Steam Line Break

4.5.1.3.2.1 Accident Definition

Both a recirculation line break (the largest liquid break) and an inside steam line break (the largest steam break) are considered in determining the design-basis accident (DBA) for the reactor internals. The recirculation line break is the same as the design-basis LOCA described in Section 6.3. A sudden, complete circumferential break is assumed to occur in one recirculation loop.

The analysis of the steam line break assumes a sudden, complete circumferential break of one main steam line between the RPV and the main steam line restrictor. This is not the same accident described in Section 15.6, which has greater potential radiological effects. A steam line break upstream of the flow restrictors produces a larger blowdown area and thus a faster depressurization rate than a break downstream of the restrictors. The larger blowdown area results in greater pressure differentials across the reactor assembly internal structures.

The steam line break accident produces higher pressure differentials across the reactor internal structures than does the recirculation line break. This results from the higher reactor depressurization rate associated with the steam line break. The depressurization rate is proportional to the mass flow rate and the excess of fluid escape enthalpy above saturated water enthalpy, h_f. Mass flow rate is inversely proportional to escape enthalpy, h_e, and therefore the depressurization rate is approximately proportional to $[1 - (h_f/h_e)]$. Consequently, depressurization rate decreases as $[1 - (h_f/h_e)]$ decreases; that is, the depressurization rate is less for mixture flow than for steam flow. Therefore, the steam line break is the DBA for internal pressure differentials.

4.5.1.3.2.2 Effects of Initial Reactor Power and Core Flow

For purposes of illustration, the maximum internal pressure loads can be considered to be composed of two parts: steady-state and transient pressure differentials. For a given plant,

the core flow and power are the two major factors that influence the reactor internal pressure differentials. The core flow essentially affects only the steady-state part. For a fixed power, the greater the core flow, the larger the steady-state pressure differential. The core power affects both the steady-state and the transient parts. As the power is decreased there is less voiding in the core and consequently the steady-state core pressure differential is less. However, less voiding in the core also means that less steam is generated in the RPV and thus the depressurization rate and the transient part of the maximum pressure load are increased. Figure 4.4-3 is a power-flow map that defines the permissible operating conditions of the reactor (Subsection 4.4.3.3 discusses the boundaries on this map). From this range of operating conditions, it is necessary to determine the combination of core power and flow that results in the maximum internal pressure loads.

Consider the historical study where the power is 3430 MWt and the core flow is at 105 percent of rated conditions (the maximum point on the operating map). Since a decrease in power results in higher transient pressure differentials, a more severe initial condition might be the condition of 754.6 MWt, 116 percent flow. In going from 3430 MWt, 105 percent flow to 754.6 MWt, 116 percent flow condition, the steady-state pressure differential has a net decrease. There is an increase due to the slight increase in flow and a decrease due to the decrease in power (lower core pressure drop). The transient pressure differential increases due to the decrease in power. However, the maximum pressure load (steady-state plus transient) has a net increase for the low power condition. If the power is decreased below 754.6 MWt, the core flow must also be reduced. Analysis has shown that the decrease in flow and power reduces the steady-state part of the maximum pressure load more than the corresponding increase in the transient part. Hence, the maximum pressure loads (steady-state plus transient) are less if the core flow is reduced from its maximum value. Therefore, the maximum internal pressure loads occur following an inside steam line break from an initial condition in which the reactor is at the minimum power associated with the maximum core flow (754.6 MWt, 116 percent flow).

Table 4.5-9 lists the maximum pressure loads occurring across the reactor internals during the accident for two cases in the study. Case 1 is for an initial condition of (3694 MWt) and 105 percent core flow. Case 2 is for the maximum pressure loads that occur from the initial condition of (771 MWt), 116 percent flow. Comparison of Cases 1 and 2 illustrates the generalized statements made above concerning the relationship between the maximum internal pressure loads and core power and flow.

Realistically, if an inside steam line break were to occur, the maximum internal pressure loads would probably be closer to Case 1. This is because the plant will probably be operating at or near full power. Also, the Case 2 condition, although possible, is rather abnormal in that rated core flow is neither required nor desirable at such a reduced power condition.

4.5.1.3.2.3 Break Size Spectrum Analysis

It has been determined that the maximum internal pressure loads occur from an initial condition in which the reactor is at the minimum power associated with the maximum core flow. It has also been concluded that these maximum loads occur for an inside steam line break, the largest possible steam break. The initial reactor condition chosen for this break

analysis is the worst case condition determined above (22 percent steam flow, 116 percent recirculation flow).

4.5.1.3.2.4 Conclusions

It is concluded from the above study, that the maximum pressure loads acting on the reactor internal components result from an inside steam line break occurring while the reactor is at 22 percent power associated with the 116 percent core flow (Table 4.5-9, Case 2).

It has also been pointed out that, although possible, it is not probable that the reactor would be operating at the rather abnormal condition of minimum power and maximum core flow. More realistically, the reactor would be at or near a full-power condition and thus the expected maximum pressure loads acting on the internal components would be as listed under Case 1 in Table 4.5-9.

4.5.1.3.2.5 Response of Structures Within the Reactor Pressure Vessel to Pressure Differences

The maximum differential pressures are used in combination with other structural loads to determine the total loading on the various structures within the reactor. The structures are then evaluated to assess the extent of deformation and buckling instability, if any. Of particular interest are the responses of the guide tubes and the metal channels around the fuel bundles, and the potential leakage around the jet pump joints.

Guide Tube

The guide tube is evaluated for buckling instability caused by externally applied pressure. Two primary modes of failure have been analyzed and are described in Subsection 4.5.2.1.3. For a guide tube with minimum wall thickness (t = 0.144 in.) and maximum allowed ovality, the pressure which causes yield stress is 93 psi compared to the design pressure of 37.5 psi. The design pressure is greater than the 21.1 psi maximum pressure differential the guide tube experiences, including accident conditions.

The stress the guide tube could experience has been calculated to be 6200 psi due to external pressure (30 psi - Reference 5), a 1.2g earthquake (include deadweight loading) and lateral loading due to coolant flow, while yield stress at 575°F is 17,450 psi. It is concluded that the guide tube does not fail under the assumed conditions. Additional guide tube analyses are given in References 6 and 7.

Fuel Channel

The fuel channel load resulting from an internally applied pressure is evaluated utilizing a fixed-beam analytical model under a uniform load. Tests to verify the applicability of the analytical model indicate that the model is conservative. A roller, at the top of some of the control rods, guides the blade as it is inserted. If the gap between channels is less than the diameter of the roller, the roller deflects the channel walls as it makes its way into the core. The friction force is a small percentage of the total force available to the CRDs for overcoming such friction, and it is concluded that the main steam line break accident does not impede the insertability of the control rod.

Marathon C and Ultra-HD Control Rods without rollers have been designed to take reactor clearances into account. Evaluations of the roller-less control rods have concluded that there is no interference or fit issues related to this design.

Loads Assessment of Fuel Assembly Components

General Electric has prepared the licensing topical report NEDE-21175-3-P, "BWR Fuel Assembly Evaluation of Combined SSE and LOCA Loadings," dated July 1982, on behalf of the Licensing Review Group (LRG), to incorporate a detailed discussion of the fuel liftoff model and a bounding analysis applicable to Fermi 2 for combined faulted loads (safe-shutdown earthquake and LOCA annulus ρ) and transmitted this report to the NRC in a letter dated July 27, 1982, from J. F. Quirk of GE to Mr. Hal Bernard of the NRC. Subsection 3.9.1.5 provides additional information on the structural evaluation of Fermi 2 fuel assemblies under safe-shutdown earthquake (SSE) and LOCA loads. See Subsection 4.2.3 for further information.

Jet Pump Joints

Jet pump joints have been analyzed to evaluate the potential leakage from within the floodable inner volume of the RPV during the recirculation line break and subsequent low-pressure coolant injection (LPCI) reflooding. Because the jet pump diffuser is welded to the shroud support, the only remaining source of leakage from the lower plenum to the downcomer annulus is the jet pump throat-to-diffuser joint. These joints for all jet pumps leak no more than a total of 225 gpm.

The LPCI capacity is sized to accommodate 600 gpm leakage at these locations plus an additional 200 gpm to accommodate accepted internal flaws associated with the core baffle access hole cover and RS-1 jet pump riser. It is concluded that the RPV structures retain sufficient integrity during the recirculation line break accident to allow reflooding of the inner volume of the RPV and in sufficient time to prevent significant increases in cladding temperature.

4.5.1.3.3 Earthquake

The seismic loads acting on the structures within the RPV are based on a dynamic analysis of a model similar to that shown in Figure 4.5-7. Seismic analysis is performed by coupling this lumped mass model of the RPV and internals with the building model to determine the system natural frequencies and mode shapes. The relevant displacement, acceleration, and load response are then determined by the modal superposition time history method.

4.5.1.3.4 Conclusions

Response analyses of the reactor structures show that deformations are sufficiently limited to allow both adequate control rod insertion and proper operation of the emergency core cooling system (ECCS). Sufficient integrity of the structures is retained during accident conditions to allow successful reflooding of the RPV inner volume. The analyses considered various loading combinations, including loads imposed by external forces. Thus, safety design bases listed in Subsection 4.5.1.1.1.1 are satisfied.

4.5.1.4 Design Loading Categories

Refer to Table 4.5-8 and Section 3.9.

4.5.1.5 Design-Basis Criteria

The reactor core support structures and internals meet the safety requirements and power generation requirements in Subsection 4.5.1.1. This is accomplished without exceeding the design-basis conditions for normal, upset, emergency, and faulted conditions described in Table 4.5-8. The internals' and core support structures' design stress and deformation criteria are specified in Chapter 3.

4.5.2 Reactivity Control System

The reactivity control system consists of the control rods, the CRDs, the supplementary reactivity control, and the SLCS. Because of the nature of this material, each item is discussed in this subsection on a system basis.

4.5.2.1 Control Rods

4.5.2.1.1 Design Bases

4.5.2.1.1.1 General Design Bases

Safety Design Bases

The safety design bases are as follows.

a. The control rods shall have sufficient mechanical strength to prevent displacement of their reactivity control material

b. The control rods shall have sufficient strength and be designed to prevent deformation that could inhibit their motion

c. Each control rod shall have a device to limit its freefall velocity sufficiently to avoid damage to the nuclear system process barrier by the rapid reactivity increase resulting from a free-fall of one control rod from its fully inserted position to the position where the drive was withdrawn.

Power Generation Design Basis

The reactivity control mechanical design shall include reactivity control devices (control rods and gadolinia burnable poison) that contain and position the material that controls the excess reactivity in the core. Control rods should have the capability of being removed or replaced, as required.

4.5.2.1.1.2 Specific Design Characteristics

Control Rod Clearances

The basis of the mechanical design of the control rod blade clearances is that there will be no interference that restricts the passage of the control rod blade. A clearance study that generically applied to BWR 4 and BWR 5 C-lattice plants with 0.100 channels was issued in October 1975 (reference G.E. 767E667, Revision 0).

Mechanical Insertion Requirements

Mechanical insertion requirements during normal operation are selected to provide adequate operability and load-following capability, and to be able to control the reactivity addition resulting from burnout of peak shutdown xenon at 100 percent power.

Scram insertion requirements are chosen to provide sufficient shutdown margin to meet all safety criteria for plant operational transients described in Chapter 15.

Material Selection

The selection of materials for use in the control rod design is based on their in-reactor properties. The irradiated properties of type 304 austenitic stainless steel (which comprises the major portion of the assembly), type 304S "Rad Resist" stainless steel, boron carbide (B_4C) powder, hafnium metal, Inconel X750, and PH13-8Mo are well known and are taken into account in establishing the mechanical design of the control rod components.

Radiation Effects

The radiation effects on B_4C powder include the release of gaseous products, and the B_4C cladding is designed to sustain the resulting internal pressure buildup. The corrosion rate and the physical properties (density, modulus of elasticity, dimensional aspects) of austenitic stainless steel, Inconel-X, and hafnium are essentially unaffected by the irradiation experienced in the BWR reactor core. The effects on the mechanical properties, such as yield strength, ultimate tensile strength, elongation, and ductility on the high purity type 304S rad resist stainless steel cladding also are well known and are considered in mechanical design.

Positioning Requirements

Rod positioning increments (notch lengths) are selected to provide adequate power-shaping capability. The combination of rod speed and notch length must also meet the limiting reactivity addition rate criteria.

4.5.2.1.2 Description

The control rods perform the dual function of power shaping and reactivity control (see Figure 4.5-8). Power distribution in the core is controlled during operation of the reactor by manipulating selected patterns of control rods. Control rod displacement tends to counterbalance steam void effects at the top of the core and results in significant power flattening.

All the control rods consist of a cruciform array of stainless steel tubes filled with boron carbide powder or hafnium metal. Original, Duralife-140, and Duralife-215 control rods are surrounded by a stainless steel sheath. Marathon C and Ultra-HD control rods have absorber tubes that are edge welded to form the cruciform shape.

The control rod assemblies shall be full length. The Marathon C control rods are 9.84 inches in total span. The Ultra-HD control rods are 9.81 inches in total span. All other control rods are 9.88 inches in total span. Control rods are separated uniformly throughout the core on a 12 inch pitch. Each control rod is surrounded by four fuel assemblies. The absorber material used in the original equipment control rods (the control rods originally supplied with the plant) is the boron carbide powder only. Newer General Electric designs employ hafnium metal as an additional absorber to extend the service life of the control rods. The thicker sheath material used in the Duralife-140 and Duralife-215 models has allowed the removal of the stiffener rods in the original design without a loss of limiting mechanical load capability. The Duralife-140 model has an increased number of B_4C absorber tubes in each wing. In addition, the length of the B_4C absorber rods in the Duralife-140 and Duralife-215 has been reduced to accommodate a six inch hafnium plate (tip) at the top. The Duralife-215 model, in addition to the six inch tip employed by the Duralife-140, has a reduced number of B_4C absorber rods in each wing to accommodate 3 hafnium rods. The Marathon C model has replaced the absorber tubes and sheath arrangement with an array of square tubes. The Ultra-HD model replaced the Marathon C tube geometry with more cylindrical tubes that have increased wall thickness for improved strength.

For original control rods, Duralife 140 and Duralife 215 models, the main structural member of a control rod is made of Type-304 stainless steel and consists of a top handle, a bottom casting with a velocity limiter and control rod drive coupling, a vertical cruciform center post, and four U-shaped absorber tube sheaths. The top handle, bottom casting, and center post are welded into a single skeletal structure. The U-shaped sheaths are fusion welded to the center post, handle, and castings on the newer designs to form a rigid housing to contain the absorber material. On the original equipment control rods resistance (spot) welding was employed. The fusion weld fabrication eliminates the overlap area between the sheath and the handle, tie rod and velocity limiter. By eliminating the overlap, the potential for crevice corrosion cracking in adverse water chemistry conditions is eliminated. Analyses and tests have shown that the fusion welded control rod is equal to or better than the spot welded control rod under all loading conditions. The bail handle on the newer control rods was extended (as an option) to minimize the use of blade guides during refueling outages. Rollers at the top and bottom of the control rod guide the control rod as it is inserted and withdrawn from the core. The control rods are cooled by the core bypass flow. The U-shaped sheaths are perforated to allow coolant to circulate freely about the absorber tubes. In addition, coolant grooves are included in the hafnium absorber plate at the top of the newer control rods. Operating experience has shown that control rods constructed as described above are not susceptible to dimensional distortions.

For the original control rod and Duralife 140 and Duralife 215 models, the boron carbide (B_4C) powder in the absorber tubes is compacted to about 70 percent of its theoretical density. The boron carbide contains a minimum of 76.5 percent by weight natural boron; the boron-10 (B-10) minimum content of the boron is 18 percent by weight. The absorber tubes in the originally supplied control rods are made of Type-304 stainless steel. The absorber tubes in the newer control rods are a high purity Type 304S "Rad Resist" stainless steel. The high purity stainless steel has an improved resistance to intergrannular stress corrosion cracking (IGSCC).

Each absorber tube of the originally supplied control rods, the Duralife 140 and Duralife 215 models is 0.188 inch in outside diameter. The originally supplied control rods and the Duralife 140 model have a 0.025-inch wall thickness. The Duralife 215 has a reduced wall thickness of 0.020 inch. Absorber tubes are sealed by a plug welded into each end. The boron carbide is longitudinally separated into individual compartments by stainless steel balls at approximately 16 inch intervals. The steel balls are held in place by a slight crimp of the tube. Should boron carbide tend to compact further in service, the steel balls will distribute the resulting voids over the length of the absorber tube.

For Marathon C blades, each square absorber tube has an internal cylinder with 0.204 inside diameter with a nominal 0.021 inch wall thickness. These tubes are loaded with either B_4C powder or hafnium. B_4C powder is compacted to 70 percent of its theoretical density and is contained in capsules which are then loaded into the absorber tubes. The space between the capsules and the wall of the absorber tubes allows the B_4C to swell before contact is made with the absorber tubes, providing improved resistance to stress corrosion. These capsules are designed to securely contain the B_4C powder while allowing helium released from B_4C to migrate through the absorber tube. Empty capsules may be used in the absorber tubes to provide a plenum for helium released from other capsules within the absorber tubes. After the capsules are installed inside the absorber tubes the ends of the tube are seal welded. The square absorber tubes are welded lengthwise to form the four wings of the cruciform control rod blade.

Ultra-HD absorber tubes are loaded with either B_4C capsules or hafnium. B_4C capsules in Ultra-HD control rods are similar to B_4C capsules in the Marathon C control rods. However, the dimensions of the Ultra-HD B_4C capsule are sized such that clearance exists between the capsule and absorber tube, even at 100% local depletion. This, combined with a thicker capsule wall, results in slightly less B_4C powder mass in each capsule. The condition of clearance between capsule and absorber tube at 100% local depletion provides a significant structural advantage for the Ultra-HD designs over the Marathon C design, as no strain is induced in the absorber tube due to swelling of the B_4C capsule. Empty capsules may be used in the absorber tubes to provide a plenum for helium released from other capsules within the absorber tubes. After the capsules are installed inside the absorber tubes the ends of the tube are seal welded. The absorber tubes are welded lengthwise to form the four wings of the cruciform control rod blade.

The Duralife 140 and Duralife 215 models have a slight increase in cold reactivity worth due to the increased volume of boron carbide. The increase is small but in the conservative direction for increased shutdown margin. The Marathon C and Ultra-HD control rods have matched reactivity worth to the original control rods. Because the increase is small, no changes in lattice physics calculations or 3D-Monicore computer constants are required and no accident analyses are affected.

The nuclear operational lifetime of the control rods is determined by the burnup of ^{10}B from neutron absorption and local B_4C loss from B_4C swelling. The nuclear lifetime limit is reached when there is a 10 percent loss in relative control worth of any quarter axial section of the blade. The mechanical lifetime limit for control rods due to B_4C swelling is bounded by the nuclear operational lifetime limit. The mechanical lifetime limit for GE-Hitachi BWR control rods is reached at 40 years of in-core residency time for all blade types.

The structural effect of helium gas buildup in the absorber rod, due to B-10 neutron absorption and radiolysis of small amounts of water vapor in the absorber rod, was evaluated by General Electric using a two-dimensional finite element computer model of the absorber tubing and end plug. The helium gas pressure was calculated using an empirical correlation for the helium release fraction from the B_4C matrix as a function of percent B-10 depletion, which varies from 4 percent to 30 percent.

The control rod velocity limiter (Figures 4.5-8 through 4.5-10) is an integral part of the bottom assembly of each control rod. This engineered safety feature (ESF) system protects against a high reactivity insertion rate by limiting the control rod velocity in the event of a control rod drop accident. It is a one-way device in that the control rod scram velocity is not significantly affected, but the control rod dropout velocity is reduced to a permissible limit.

Three different types of velocity limiters are employed. On the originally supplied control rods and the Duralife 140 model the velocity limiter is in the form of two nearly mated conical elements made from a single casting (Figure 4.5-9). The lower conical element is separated from the upper conical element by four radial spacers 90 degrees apart and is at a 15° angle relative to the upper conical element. The cast velocity limiter employs a single reversed jet. The velocity limiter on the Duralife 215 and Marathon C model has been redesigned to offset the weight of the hafnium absorber. This machined velocity limiter employs an optimized twin reversed jet (Figure 4.5-10). The velocity limiter on Ultra-HD control rods is a cast/fabricated hybrid called the FabriCast. The FabriCast velocity limiter uses a casting for the "vane" of the velocity limited (Figure 4.5-10), which has identical geometry to the "vane" portion of the single piece cast velocity limiter (called "original" in Figure 4.5-10). Because the geometry is the same, the FabriCast velocity limiter has the same drop speed and scram insertion performance as the original single piece cast velocity limiter design. Ultra-HD control rods can be configured with either a FabriCast velocity limiter or the previous cast velocity limiters used on Duralife and Marathon CRBs.

The hydraulic drag forces on a control rod are proportional to approximately the square of the rod velocity and are negligible at normal rod-withdrawal or rod-insertion speeds. However, during the scram stroke the rod reaches high velocity, and the drag forces must be overcome by the drive mechanism.

To limit control rod velocity during dropout but not during scram, the velocity limiter is provided with a streamlined profile in the scram (upward) direction. When a control rod with a cast velocity limiter is scrammed, water flows over the smooth surface of the upper conical element into the annulus between the guide tube and the limiter. For the redesigned velocity limiter, water flows over the conical element into the annulus between the element and the CRD coupling socket and the annulus between the guide tube and the limiter. In the dropout direction, however, for the cast velocity limiter, water is trapped by the lower conical element and discharged through the annulus between the two conical sections. For the machined velocity limiter, the trapped water is discharged in two directions. Because this water is jetted in a partially reversed direction into water flowing upward in the annulus, a severe turbulence is created, thereby slowing the descent of the control rod assembly to less than 5 ft/sec at 70°F (Appendix A of Reference 8).

4.5.2.1.3 Safety Evaluation

4.5.2.1.3.1 Materials Adequacy Throughout Design Lifetime

The adequacy of the materials throughout the design life was evaluated in the mechanical design of the control rods. The primary materials, B_4C powder, hafnium, and high purity Type 304S "Rad Resist" stainless steel, have been found suitable in meeting the demands of the BWR environment.

4.5.2.1.3.2 Dimensional and Tolerance Analysis

Layout studies are done to ensure that, given the worst combination of extreme detail part tolerance ranges at assembly, no interference exists that will restrict the passage of control rods. In addition, preoperational and operational verification is made on each control blade system to show that the acceptable levels of operational performance are met. See Subsections 4.5.2.1.4 and 4.5.2.2.4.

4.5.2.1.3.3 Thermal Analysis of the Tendency To Warp

The various parts of the control rod assembly remain at approximately the same temperature during reactor operation, negating the problem of distortion or warpage. What little differential thermal growth could exist is allowed for in the mechanical design. A minimum axial gap is maintained between absorber rod tubes and the control rod frame assembly for this purpose. In addition, dissimilar metals are avoided to further this end.

4.5.2.1.3.4 Forces for Expulsion

An analysis has been performed that evaluates the maximum pressure forces which could tend to eject a control rod from the core. The results of this analysis are given in Subsection 4.5.2.2.3.1. In summary if the collet were to remain open, which is unlikely, calculations indicate that the steady-state control rod withdrawal velocity would be 2 fps for a pressure-under line break, the limiting case for rod withdrawal.

4.5.2.1.3.5 Functional Failure of Critical Components

The consequences of a functional failure of critical components have been evaluated, and the results are covered in Subsection 4.5.2.2.3.1.

4.5.2.1.3.6 Precluding Excessive Rates of Reactivity Addition

In order to preclude excessive rates of reactivity addition, the design is based on analyses that have been performed both on the velocity limiter device and the effect of probable control rod failures (see Subsection 4.5.2.2.3.1).

4.5.2.1.3.7 Effect of Fuel Rod Failure on Control Rod Channel Clearances

The CRD mechanical design ensures a sufficiently rapid insertion of control rods to preclude the occurrence of fuel rod failures that could hinder reactor shutdown by causing significant distortions in channel clearances.

4.5.2.1.3.8 Mechanical Damage

Analysis has been performed for all areas of the control system showing that system mechanical damage does not affect the capability to continuously provide reactivity control.

In addition to the analysis performed on the CRD (Subsections 4.5.2.2.3.1 and 4.5.2.2.3.2), the following discussion summarizes the analysis performed on the control rod guide tube.

The guide tube can be subjected to any or all of the following loads:

a. Inward load due to pressure differential

b. Lateral loads due to flow across the guide tube

c. Dead weight

d. Seismic.

In all cases, analysis was performed considering both a recirculation line break and a steam line break, events that result in the largest hydraulic loadings on a control rod guide tube.

Two primary modes of failure were considered in the guide tube analysis: exceeding allowable stress and excessive elastic deformation. It was found that the allowable stress limit will not be exceeded and that the elastic deformations of the guide tube never are great enough to cause the free movement of the control rod to be jeopardized.

The first mode of failure is evaluated by the addition of all the stresses resulting from the maximum loads for the faulted condition. This results in the maximum theoretical stress value for that condition. Making a linear superposition of all calculated stresses and comparing this value to the allowable limit defined by the ASME B&PV Code yields a factor of safety of approximately three. Using the allowable limit for faulted conditions, the factor of safety is approximately 4.2.

Evaluation of the second mode of failure is based on clearance reduction between the guide tube and the control rod. The minimum allowable clearance is about 0.1 in. This assumes maximum ovality and minimum diameter of the guide tube and the maximum control rod dimension. The analysis showed that if the approximate 6000 psi for the faulted condition were entirely the result of differential pressure, the clearance between the control rod and the guide tube would reduce by a value of approximately 0.01 in. This gives a design margin of 10 between the theoretically calculated maximum displacement and the minimum allowable clearance.

Two types of instability were considered in the analysis of guide tube design. The first was the classic instability associated with vertically loaded columns. The second was the diametral collapse when a circular tube experiences external-to-internal differential pressure.

The limited axially applied load is approximately 77,500 lb resulting in a material compressive stress of 17,450 psi (code allowable stress). Comparing the actual load to the yield stress level gives a design margin greater than 20 to 1. From these values it is concluded that the guide tube is not an unstable column.

When a circular tube experiences external-to-internal differential pressure, two modes of failure are possible, depending on whether the tube is "long" or "short." In the analysis here the guide tube is taken to be an infinitely long tube with the maximum allowable ovality and

minimum wall thickness. The conditions will result in the lowest critical pressure calculation for the guide tube (that is, if the tube were "short," the critical pressure calculation would give a higher number). The critical pressure is approximately 140 psi. However, if the maximum allowable stress is reached at a pressure lower than the critical pressure, then that pressure is limiting. This is the case for a BWR guide tube. The allowable stress of 17,450 psi will be reached at approximately 96 psi. Comparing the maximum possible pressure differential for a steam line break to the limiting pressure of 96 psi gives a design margin greater than 3 to 1. Therefore, the guide tube is not unstable with respect to differential pressure. References 6 and 7 provide a detailed discussion of analyses and design margins for the control rod guide tube.

4.5.2.1.3.9 Evaluation of Control Rod Velocity Limiter

The control rod velocity limiter limits the free-fall velocity of the control rod. This velocity is evaluated by the control rod drop accident analysis described in Subsection 15.4.9.

4.5.2.1.4 Testing and Inspection

The control rod absorber tube tests are examples of the quality control tests performed on the control rods. The absorber tube tests include the following:

a. The ^{10}B fraction of the boron content of each lot of boron carbide is verified

b. Weld integrity of the finished absorber tubes is verified by helium leak testing.

The Surveillance Test Program is described in Subsection 4.5.2.2.4.5 and in the Technical Specifications.

Fermi 2 procedures require replacement of control blades when a 10 percent reduction of rod worth occurs.

4.5.2.1.5 Instrumentation

The instrumentation for both the control rods and CRDs is defined by that given for the reactor manual control system (RMCS). The objective of the RMCS is to provide the operator with the means to make changes in nuclear reactivity so that reactor power level and power distribution can be controlled. The system allows the operator to manipulate control rods.

The design bases and further discussion are covered in Subsection 7.7.1.

4.5.2.2 Control Rod Drive System

4.5.2.2.1 Design Bases

4.5.2.2.1.1 Safety Design Bases

The CRD mechanical system shall meet the following safety design bases:

a. Design shall provide for a control rod insertion sufficiently rapid that no fuel damage results from any abnormal operating transient

b. Design shall include positioning devices, each of which individually supports and positions a control rod

c. Each positioning device shall

1. Prevent its control rod from withdrawing as a result of a single malfunction

2. Be individually operated so that a failure in one positioning device does not affect the operation of any other positioning device

3. Be individually energized when rapid control rod insertion (scram) is signaled so that failure of power sources external to the positioning device does not prevent the positioning devices of other control rods from being inserted

4. Be locked to its control rod to prevent undesirable separation.

d. The CRD mechanisms and that part of the CRD hydraulic system necessary for scram shall be designed to Category I requirements.

4.5.2.2.1.2 Power Generation Design Basis

The CRD system design shall provide for positioning the control rods to control power generation in the core.

4.5.2.2.2 Description

The CRD system controls gross changes in core reactivity and neutron flux shape by incrementally positioning neutron-absorbing control rods within the reactor core in response to manual control signals. It is also required to shutdown the reactor by rapidly inserting withdrawn control rods into the core in response to a manual or automatic signal. The CRD system consists of locking piston, CRD mechanisms, and the CRD hydraulic system (including hydraulic control units, interconnecting piping, instrumentation, and electrical controls).

4.5.2.2.2.1 Control Rod Drive Mechanisms

The CRD mechanism (drive) used for positioning the control rod in the reactor core is a double-acting, mechanically latched, hydraulic cylinder using water as its operating fluid (Figures 4.5-11 through 4.5-14). The individual drives are mounted on the bottom head of the RPV. The drives do not interfere with refueling and are operative even when the head is removed from the RPV. The drives are also readily accessible for inspection and servicing. The bottom location makes maximum use of the water in the reactor as a neutron shield and gives the least possible neutron exposure to the drive components. Using water from the condensate treatment system or condensate storage tank as the operating fluid eliminates the need for special hydraulic fluid. Drives are able to use simple piston seals whose leakage does not contaminate the reactor water and does cool the drive mechanisms and their seals.

The drives are capable of inserting or withdrawing a control rod at a slow, controlled rate, as well as providing rapid insertion when required. A mechanism on the drive locks the control rod in 6-in. increments of stroke over the length of the core.

A coupling spud at the top end of the drive index tube (piston rod) engages and locks into a mating socket at the base of the control rod. The weight of the control rod is sufficient to engage and lock this coupling. Once locked, the drive and rod form an integral unit that must be manually unlocked by specific procedures before the components can be separated.

The drive holds its control rod in distinct latch positions until the hydraulic system actuates movement to a new position. Withdrawal of each rod is limited by the seating of the rod in its guide tube. Withdrawal beyond the full-out limit can be accomplished only if the rod and drive are uncoupled. Withdrawal past the full-out limit is annunciated by an over travel alarm.

The individual rod indicators, grouped in one control panel display, correspond to relative rod locations in the core. A separate, smaller display is located just below the large display on the vertical part of the benchboard. This smaller display presents the positions of the control rod selected for movement and its adjacent rods.

For display purposes, the control rods are considered in groups of four adjacent rods centered around a common core volume. Each group is monitored by four local power range monitor (LPRM) strings (Subsection 7.6.1). Rod groups at the periphery of the core may have less than four rods and less than 4 LPRM strings. The small rod display shows the positions, in digital form, of the rods in the group to which the selected rod belongs. A white light indicates which of the four rods is the one selected for movement.

4.5.2.2.2.2 Control Rod Drive Components

Figure 4.5-12 illustrates the operating principle of a CRD. Figures 4.5-13 and 4.5-14 illustrate the CRD in more detail. The main components of the CRD and their functions are described as follows.

The CRD piston is mounted at the lower end of the index tube. This tube functions as a piston rod. The CRD piston and index tube make up the main moving assembly in the CRD. The CRD piston operates between positive end stops, with a hydraulic cushion provided at the upper end only. The piston has both inside and outside seal rings and operates in an annular space between the fixed piston tube assembly and the drive inner cylinder tube. Because the type of inner seal used is effective in only one direction, the lower sets of seal rings are mounted with one set sealing in each direction.

A pair of nonmetallic bushings prevents metal-to-metal contact between the piston tube assembly and the inner cylinder surface. The outer piston rings are segmented step-cut seals with expander springs holding the segments against the cylinder wall. A pair of split bushings on the outside of the piston prevents piston contact with the inner cylinder wall. The effective piston area for downtravel, or withdrawal, is approximately 1.2 $in.^2$ versus 4.1 $in.^2$ for uptravel, or insertion. This difference in driving area tends to balance the control rod weight and ensures a higher force for insertion than for withdrawal.

The index tube is a long hollow shaft made of either nitrided type 304 or Grade XM-19 stainless steel. Circumferential locking grooves, spaced every 6 in. along the outer surface, transmit the weight of the control rod to the collet assembly.

The collet assembly serves as the index tube locking mechanism. It is located in the upper part of the drive unit. This assembly prevents the index tube from accidentally moving downward. The assembly consists of the collet fingers, a return spring, a guide cap, a collet housing (part of the cylinder, tube, and flange), and the collet piston.

The problem of IGSCC in the collet assembly is discussed in Subsection 4.5.2.2.4.5.

Locking is accomplished by fingers mounted on the collet piston at the top of the drive cylinder. In the locked or latched position, the fingers engage a locking groove in the index tube.

The collet piston is normally held in the latched position by a force of approximately 150 lb supplied by a spring. Metal piston rings are used to seal the collet piston from RPV pressure. The collet assembly will not unlatch until the collet fingers are unloaded by a short, automatically sequenced, drive-in signal. A pressure, approximately 180 psi above RPV pressure, must then be applied to the collet piston to overcome spring force, slide the collet up against the conical surface in the guide cap, and spread the fingers out so they do not engage a locking groove.

A guide cap is fixed in the upper end of the CRD assembly. This member provides the unlocking cam surface for the collet fingers and serves as the upper bushing for the index tube.

If reactor water is used during a scram to supplement accumulator pressure, it is drawn through a filter on the guide cap.

The piston tube is an inner cylinder, or column, extending upward inside the CRD piston and index tube. The piston tube is fixed to the bottom flange of the CRD and remains stationary. Water is brought to the upper side of the CRD piston through this tube. A series of progressively decreasing orifices at the top of the tube form the hydraulic buffer to cushion the CRD piston at the end of its scram stroke.

A stationary piston, called the stop piston, is mounted on the upper end of the piston tube. This piston provides the seal between RPV pressure and the space above the drive piston. It also functions as a positive end stop at the upper limit of control rod travel. A stack of spring washers just below the stop piston helps absorb the final mechanical shock at the end of control rod travel. The stop piston seal rings are similar to the drive piston outer seal rings. A bleed-off passage to the center of the piston tube is located between the two pairs of rings. This arrangement allows seal leakage from the RPV (during a scram) to be bled directly to the discharge line. The lower pair of seals is used only during the cushioning of the CRD piston at the upper end of the stroke.

The center tube of the CRD mechanism forms a well to contain the position indicator probe. This probe is an aluminum extrusion attached to an aluminum housing. Mounted on the extrusion are hermetically sealed, magnetically operated position indicator switches. Each switch is sheathed in a braided glass sleeve, and the entire probe assembly is protected by a thin-walled stainless steel tube. The switches are actuated by a ring magnet located at the bottom of the drive piston.

The drive piston, piston tube, and indicator tube are all of nonmagnetic stainless steel, allowing the individual switches to be operated by the magnet as the piston passes. One switch is located at each position corresponding to an index tube groove, thus allowing indication at each latching point. An additional switch is located at each midpoint between latching points to indicate the intermediate positions during drive motion. Thus, indication is provided for each 3 in. of travel. Duplicate switches are provided for the full-in and full-out positions. One additional switch (an overtravel switch) is located at a position below the normal full-out position. Because the limit of downtravel is normally provided by the control rod itself as it reaches the backseat position of the control rod guide tube, the CRD can pass this position and actuate the overtravel switch only if it is uncoupled from its control rod. A convenient means is thus provided to verify that the drive and control rod are coupled after installation of a drive or at any time during plant operation.

A flange and cylinder assembly is made up of a heavy flange welded to the CRD cylinder. A sealing surface on the upper face of this flange forms the seal to the drive housing flange. The seals contain reactor pressure and the two hydraulic control pressures. Teflon-coated, stainless steel rings are used for these seals. The CRD flange contains the integral ball, or two-way, check (ball-shuttle) valve. This valve directs either the RPV pressure or the CRD system driving pressure, whichever is higher, to the underside of the CRD piston. Reactor pressure vessel pressure is admitted to this valve from the annular space between the drive and drive housing through passages in the flange.

Water used to operate the collet piston passes between the outer tube and the cylinder tube. The inside of the cylinder tube is honed to provide the surface required for the drive piston seals.

Both the cylinder tube and outer tube are welded to the CRD flange. The upper ends of these tubes have a sliding fit to allow for differential expansion.

The upper end of the index tube is threaded to receive a coupling spud. The coupling (Figure 4.5-11) accommodates a small amount of angular misalignment between the CRD and the control rod. Six spring fingers allow the coupling spud to enter the mating socket on the control rod. A plug then enters the spud and prevents uncoupling.

Two means of uncoupling are provided. With the RPV head removed, the lock plug can be raised against the spring force of approximately 50 lb by a rod extending up through the center of the control rod to an unlocking handle located above the control rod velocity limiter. The control rod, with the lock plug raised, can then be lifted from the CRD.

The lock plug can also be pushed up from below, if it is desired to uncouple a drive without removing the RPV head for access. In this case, the central portion of the drive mechanism is pushed up against the uncoupling rod assembly, which raises the lock plug and allows the coupling spud to disengage the socket as the drive piston and index tube are driven down.

The control rod is heavy enough to force the spud fingers to enter its socket and push the lock plug up, allowing the spud to enter the socket completely and the plug to snap back into place. Therefore, the CRD can be coupled to the control rod using only the weight of the control rod. However, with the lock plug in place, a force in excess of 50,000 lb is required to pull the coupling apart.

Materials of Construction

Factors that determine the choice of construction materials are discussed in the following paragraphs.

The index tube must withstand the locking and unlocking action of the collet fingers. A compatible bearing combination must be provided that is able to withstand moderate misalignment forces. The reactor environment limits the choice of materials suitable for corrosion resistance. The column and tensile loads can be satisfied by either an annealed 300 series or Grade XM-19 stainless steel. The wear and bearing requirements are provided by hard facing the completed tube. To obtain suitable corrosion resistance, a carefully controlled process of surface preparation is employed.

The coupling spud is made of Inconel-750 that is aged for maximum physical strength and the required corrosion resistance. Because misalignment tends to cause chafing in the semispherical contact area, the part is protected by a thin chromium plating (electrolyzed). This plating also prevents galling of the threads attaching the coupling spud to the index tube.

Inconel-750 is used for the collet fingers, which must function as leaf springs when cammed open to the unlocked position. Colmonoy-6 hard facing provides a long-wearing surface, adequate for design life, to the area contacting the index tube and unlocking cam surface of the guide cap.

Graphitar-14 is selected for seals and bushings on the CRD piston and stop piston. The material is inert and has a low friction coefficient when water-lubricated. Because some loss of strength is experienced at higher temperatures, the drive is supplied with cooling water to hold temperatures below 250°F. The Graphitar is relatively soft, which is advantageous when an occasional particle of foreign matter reaches a seal. The resulting scratches in the seal reduce sealing efficiency until worn smooth, but the CRD design can tolerate considerable water leakage past the seals into the RPV.

An alternate material approved for use in the seals and bushings in Graphitar-3030, due to its higher strength and superior wear resistance characteristics.

All CRD components exposed to RPV water are made of AISI 300 series stainless steel except the following.

a. Seals and bushings on the CRD piston and stop piston are either Graphitar-14 or Graphitar-3030

b. All springs and members requiring spring action (collet fingers, coupling spud, and spring washers) are made of Inconel-750

c. The ball check valve is a Haynes Stellite cobalt-base alloy

d. Elastomeric O-ring seals are ethylene propylene

e. Collet piston rings are Haynes-25 alloy

f. Certain wear surfaces are hard-faced with Colmonoy-6

g. Nitriding by a proprietary new hard facing process and chromium plating is used in certain areas where resistance to abrasion is necessary

h. The CRD piston head is made of ARMCO 17-4Ph.

i. An alternate material acceptable for the index and piston tube is nitrided Grade XM-19SS.

j. An equivalent piston tube assembly contains an anti-rotation pin made of nickel-chromium-iron wire per GE spec B14H19.

Pressure-containing portions of the CRDs are designed and fabricated in accordance with requirements of Section III of the ASME B&PV Code.

4.5.2.2.2.3 Control Rod Drive Hydraulic System

The CRD hydraulic system supplies and controls the pressure and flow to and from the drives through hydraulic control units (HCUs). The water discharged from the CRDs during a scram flows through the HCUs to the scram discharge volume (SDV). The water discharged from a CRD during a normal control rod positioning operation flows through the HCU and the exhaust header, and is dispersed into the RPV via the HCUs of other nonmoving drives.

The CRD hydraulic system also supplies water for the reactor vessel instrumentation reference leg backfill system.

The CRD hydraulic system design is shown in Figure 4.5-15. The hydraulic requirements, identified by the function they perform, are as follows:

a. Normal accumulator hydraulic charging pressure is required. Flow to the accumulators is required only during scram reset or system startup

b. Drive pressure of approximately 250 psi above RPV pressure is required. A flow rate of approximately 4 gpm to insert a control rod and 2 gpm to withdraw a control rod is required

c. Cooling water to the CRDs is required at approximately 6 to 30 psi above RPV pressure and at a flow rate of approximately 0.3 gpm times the number of drive units. Cooling water can be interrupted for short periods without damaging the drive

d. The SDV is sized to receive and contain all the water discharged by the CRDs during a scram. A minimum volume of 3.34 gal per CRD is required.

The CRD hydraulic systems provide the required functions with the pumps, filter, valves, instrumentation, and piping shown in Figure 4.5-15 (Sheets 1 and 2) and described in the following paragraphs.

Duplicate components are included, where necessary, to ensure continuous system operation if an inservice component requires maintenance.

One supply pump pressurizes the system with water from the condensate treatment system or condensate storage tank. One spare pump is provided for standby. A discharge check valve prevents backflow through the nonoperating pump. A portion of the pump discharge flow is diverted through a minimum flow bypass line to the condensate storage tank. This flow is controlled by an orifice and is sufficient to prevent immediate pump damage if the pump discharge is inadvertently closed.

The primary source of water for the CRD system is the condensate treatment system. There are two pump suction filters installed in parallel for each CRD pump. The CRD pump operation has been demonstrated for many years at this level of filtration. The drive water filters have cleanable elements. One drive water filter is operated at a time. There are Y-strainers downstream of the drive water filters that protect the CRD hydraulic system in the event of filter-element failure. A sampling of the CRD system water is continuously delivered to the reactor water-sampling station for monitoring. Necessary corrective actions would be taken if a significant change in CRD system water quality were to result from the failure of a drive water filter. The total pressure drop across the drive-water filters is continuously monitored with an alarm on high pressure differential.

The CRD pump provides water for the reactor vessel instrumentation reference leg backfill system. A small amount of water is injected into two reference legs to prevent the accumulation of noncondensable gases. The backfill lines are tapped to the CRD charging water header.

Provisions have been taken to keep the water in the CRD hydraulic system from freezing. The CRD system is completely contained within the reactor building. This building is well heated and ventilated; it also receives most of the heat loss from the reactor system. It is therefore incredible that the temperature would drop below freezing while the plant is operating. The CRD system water supply is normally taken from the condensate demineralizers via the torus water management system; no portion of this line is outside the building. Backup supply is provided by the condensate storage tank. Subsection 9.2.6 describes the procedure used to keep the tank from freezing. The valve pit from the tank is only partially above grade. Heat sources into this valve pit are sufficient to keep the temperature well above freezing. The lines from the pit to the turbine building are 42 in. or more below grade and, consequently, are not subject to freezing.

Accumulator charging pressure is established by the discharge pressure of the system supply pump. During scram the scram inlet (and outlet) valves open and permit the stored energy in the accumulators to discharge into the CRDs. The resulting pressure decrease in the water header allows the CRD supply pump to increase flow rate substantially into the CRDs via the charging water header. The flow sensing system upstream of the accumulator charging header detects high flow and closes the flow control valve. This action maintains increased flow through the charging water header.

Pressure in the charging header is monitored in the main control room with a pressure indicator and low-pressure alarm.

The failure of a CRD pump or the plugging of a drive water filter would result in a loss of pressure in the CRD charging water header, which directly feeds each hydraulic control unit accumulator. The effect that this can have on the ability to scram the rods is minimized for the following reasons:

a. At reactor pressures greater than 600 psig, the rods can scram with specified insertion times independent of the accumulator pressure

b. If header pressure were lost because of CRD pump failure, the operator could readily restore header pressure by bringing the second pump on line

c. If header pressure were lost because of filter plugging, the parallel filter could be brought into service

d. Accumulator depressurization is prevented by check valve No. 115 (see Figure 4.5-15) to retain accumulator scram capability, especially if reactor pressure is below 600 psig.

Each accumulator is monitored with a pressure switch that activates individual low pressure alarms that have setpoints which are above the limit established in the Technical Specifications. An alarm annunciates for any accumulator at or before the pressure reaches the setpoint value provided in the Technical Specifications. The setpoint value has been conservatively established by the design to assure a margin of accumulator operability sufficient to scram the associated control rod.

By design, control rod scram can be accomplished without the accumulator pressure when the reactor vessel pressure is at or above 600 psig. If the reactor were operating at a pressure of less than 600 psig, a manual scram would be required upon receipt of the first accumulator low pressure alarm that follows a loss of charging water header pressure. This design required manual scram is a very conservative action because the core is designed to be shut down from all operating conditions with the most reactive control rod fully withdrawn. The plant operating procedures call for a manual scram at a reactor pressure limit above the design 600 psig as required by the Technical Specifications in case of a loss of accumulator function. This additional conservatism of the Technical Specifications adds more margin to assure the scram function during plant power operation, startup or refueling when applicable.

The manual scram capability of the accumulators is periodically verified by a pressure drop surveillance to confirm that operators have at least 10 minutes of accumulator scram capability upon loss of control rod drive system hydraulic charging capability.

During normal operation, the flow control valve maintains a constant system flow rate. This flow is used for drive flow, drive cooling, and system stability.

Control rod drive water pressure required in the drive header is maintained by the drive pressure control valve, which is manually adjusted from the main control room. A flow rate of approximately 6 gpm (the sum of the flow rate required to insert and withdraw a control rod) normally passes from the CRD water pressure stage through two solenoid-operated stabilizing valves (arranged in parallel) and then goes into the cooling water line downstream from the drive/cooling-water pressure control valve. The flow through one stabilizing valve equals the drive insert flow; that of the other stabilizing valve equals the CRD withdrawal flow. When a CRD is operated, the required flow is diverted to that CRD while closing the appropriate stabilizing valve. Thus, flow through the CRD pressure control valve is always constant.

Flow indicators in the CRD water header and in the line downstream from the stabilizing valves allow the flow rate through the stabilizing valves to be adjusted when necessary. Differential pressure between the RPV and the CRD pressure stage is indicated in the main control room.

The cooling water header is located downstream from the drive/ cooling water pressure control valve. The cooling water pressure control valve is manually adjusted from the main control room to produce the required cooling water pressure. The flow through the flow

control valve is virtually constant. Therefore, once adjusted, the drive/cooling water pressure control valve can maintain its required pressure independent of reactor pressure. Changes in setting of the pressure control valves are required only to adjust for changes in the cooling requirements of the CRDs, as their seal characteristics change with time.

Failure of the drive/cooling water pressure control valve in the full-open or full-closed position would cause some perturbation in CRD system operation, but it does not present a safety problem or affect the scram capability of the CRD system. If the pressure control valve (PCV) were to fail to a full-open position, the cooling water pressure would increase and the drive water pressure would decrease. The resulting cooling water pressure increase could cause control rods to drift inward. The existence of rod drifts would be alarmed to the control room operator for appropriate action. The resulting drop in drive water pressure would make normal control rod notch movements impossible, but would not affect the ability of the scram function. Conversely, if the PCV were to fail to a full-closed position, the cooling water pressure would decrease while the drive water pressure would increase. The reduction in cooling water pressure (and flow) would eventually lead to high CRD temperature being alarmed in the control room. In the limiting case, the resulting increase in drive water pressure would reach the shutoff pressure of the supply pump (1600 psig). The occurrence of this condition during withdrawal of a drive at zero reactor pressure will result in a drive pressure increase from 260 psig to no more than 1600 psig. Calculations indicated that the drive would accelerate from 3 in./sec to approximately 6 in./sec. The rod movement would stop as soon as the driving signal is removed. In both of the cases described above, the manually operated bypass PCV, in conjunction with isolation valves upstream and downstream of the primary PCV, would enable the operators to take corrective action.

A flow indicator in the main control room monitors cooling water flow. A differential pressure indicator in the main control room indicates the difference between RPV pressure and CRD cooling water pressure. Although the CRDs can function without cooling water, seal life is shortened by long-term exposure to reactor temperatures. The temperature of each CRD is recorded in the relay room, and excessive temperatures are annunciated by a control room alarm.

Exhaust water from a moving drive is dispersed to the RPV via the HCUs of nonmoving drives.

In order to eliminate the problem of cracking of the CRD return line (CRDRL), the CRDRL was removed and the CRDRL nozzles were capped. The modification meets the requirements of NRC (Reference 13), on the subject of CRDRL removal as follows:

a. Equalizing valves between the cooling water header and the normal drive movement exhaust water header have been incorporated

b. Exhaust water headers have been changed to stainless steel

c. The flow stabilizer loop is stainless steel and is routed directly to the cooling water header.

All modifications were constructed and inspected consistent with the applicable sections of the ASME B&PV Code.

Figure 4.5-15 shows the CRD hydraulic system with the return line eliminated. The reactor water makeup capability of the CRD system with this modification is 135 gpm at 1110 psig reactor vessel pressure (before the modification, the makeup capability was 170 gpm).

The SDV consists of header piping, which connects to each HCU and drains into an instrument volume. The header piping is sized to receive and contain all the water discharged by the CRDs during a scram, independent of the instrument volume. Each of the two sets of headers has a directly connected scram discharge instrument volume attached to the low point of the header piping. Thus, the large-diameter pipe of the instrument volume serves as a vertical extension of the SDV (although no credit is taken for it in determining scram discharge volume requirements).

During normal plant operation, the SDV is empty and vented to atmosphere through its open vent and drain valve. When a scram occurs, upon a signal from the safety circuit, these vent and drain valves are closed to conserve reactor water. Lights in the main control room indicate the position of these valves. Redundant vent and drain valves are provided to ensure against loss of reactor coolant from the SDV following a scram.

During a scram, the SDV partly fills with water discharged from above the drive pistons. While scrammed, the CRD seal leakage from the reactor continues to flow into the SDV until the discharge volume pressure equals the RPV pressure. A check valve in each HCU prevents reverse flow from the scram discharge header volume to the CRD. When the scram signals are cleared from the reactor protection system (RPS), the SDV signal is overridden with a keylock override switch, and the scram discharge volume is drained and returned to atmospheric pressure.

Remote manual switches in the pilot valve solenoid circuits allow the discharge volume vent and drain valves to be tested without disturbing the RPS. Closing the SDV valves allows the outlet scram valve seats to be leak tested by timing the accumulation of leakage inside the scram discharge volume.

Four liquid level switches and two level transmitters connected to each instrument volume monitor the volume for abnormal water level. They provide redundant and diverse inputs to the RPS scram function and provide inputs for control room annunciation and control rod withdrawal block functions (see Figure 4.5-15).

Each level transmitter provides input to actuate a trip unit. Three different level setpoints are used. At the lowest level, a level switch actuates to indicate that the volume is not completely empty during postscram draining or to indicate that the volume starts to fill through leakage accumulation at other times during reactor operation. At the second level, one level switch produces a rod withdrawal block to prevent further withdrawal of any control rod when leakage accumulates to approximately half the capacity of the instrument volume. The remaining two switches and two transmitter-actuated trip units are interconnected with the trip channels of the RPS and initiate a reactor scram should water accumulation fill the instrument volume.

Modifications of the SDV instrumentation and vent and drain valves were made to meet the criteria stated in the NRC's Generic Safety Evaluation Report BWR Scram Discharge System, dated December 1, 1980.

The design deficiencies in the SDV that were identified in the Safety Evaluation Report (SER) were

a. Inadequate hydraulic coupling between the SDV headers and the instrument volume

b. Complex vent and drain piping connections to the SDV

c. Failure mechanisms for the instrument volume level instrumentation

d. Failure of the control air system resulting in the potential inability to scram.

Items a. and d. were not applicable to Fermi 2 because adequate coupling is ensured by the integral coupling of the 12-in. instrument volume to the 8-in. SDV header.

Criteria of the BWR Owners subgroup were used in the design for items b. and c. The vent and drain valves are redundant and routed as dedicated lines. The instrumentation was upgraded on each instrument volume.

The instrumentation connections are made to the instrument volume and not to the drain line. Each instrument volume has one alarm, one rod block, and four scram level instruments. The two new scram level instruments are diverse.

Hydraulic Control Units

Each HCU furnishes pressurized water, on signal, to a CRD unit. The CRD then positions its control rod as required. Operation of the electrical system that supplies scram and normal control rod positioning signals to the HCU is described in Subsections 7.2.1 and 7.7.1.

The basic components in each HCU are manual, pneumatic, and electrical valves; an accumulator; related piping; electrical connections; filters; and instrumentation (Figures 4.5-15 and 4.5-16). The components and their functions are described in the following paragraphs.

The insert CRD valve is solenoid operated and opens on an insert signal. The valve supplies drive water to the bottom side of the main CRD piston.

The insert exhaust valve also opens by solenoid on an insert signal. The valve discharges water from above the CRD piston to the exhaust water header.

The withdraw CRD valve is solenoid operated and opens on a withdraw signal. The valve supplies drive water to the top of the drive piston.

The solenoid-operated withdraw exhaust valve opens on a withdraw signal and discharges water from below the main CRD piston to the exhaust header. The withdraw exhaust valve also serves as the settle valve. The valve opens following any normal CRD insert, the valve stays open a little longer on a withdrawal. This allows the control rod and its CRD to settle back into the nearest latch position.

The speed control valves regulate the control rod insertion and withdrawal rates during normal operation. They are manually adjustable flow-control valves used to regulate the water flow to and from the volume beneath the main drive piston. A correctly adjusted valve does not require readjustment except to compensate for changes in CRD seal leakage.

The scram pilot valves are operated from the RPS trip system. Two scram pilot valves control both the scram inlet valve and the scram exhaust valve by depressurizing the scram

air header. The scram pilot valves are identical, three-way, solenoid-operated, normally energized valves. Upon a loss of electrical signal to the pilot valves, such as the loss of external ac power, the inlet ports close and the exhaust ports open on both pilot valves. The pilot valves (Figure 4.5-15) are arranged so that the trip system signal must be removed from both valves before air pressure can be discharged from the scram valve operators. This prevents the inadvertent scram of a single CRD in the event of a failure of one of the solenoid pilot valves.

The scram exhaust valve opens slightly before the scram inlet valve, exhausting water from above the CRD piston. The exhaust valve opens faster than the inlet valve because of a larger spring in the valve operator. Otherwise the valves are similar.

The scram inlet valve opens to supply pressurized water to the bottom of the CRD piston. This quick-opening globe valve is operated by an internal spring and system pressure. It is closed by air pressure applied to the top of its diaphragm operator. A position-indicator switch on this valve energizes a light in the main control room as soon as both of the valves start to open.

The scram accumulator stores sufficient energy to fully insert a control rod at lower RPV pressures. At higher RPV pressures, the accumulator pressure is assisted or replaced by RPV pressure.

The accumulator is a hydraulic cylinder with a free-floating piston. The piston separates the water on top from the nitrogen below. A check valve in the accumulator charging line prevents loss of water pressure in the event supply pressure is lost.

During normal plant operation, the accumulator piston is seated at the bottom of its cylinder. Loss of nitrogen decreases the nitrogen pressure, and this actuates a pressure switch that sounds an alarm in the main control room.

To ensure that the accumulator is always able to produce a scram, it is continuously monitored for water leakage. A float-type level switch actuates an alarm if water leaks past the piston barrier and collects in the accumulator instrumentation block.

4.5.2.2.2.4 Control Rod Drive System Operation

The CRD system performs rod insertion, rod withdrawal, and scram. These operational functions are described in the following paragraphs.

Rod insertion is initiated by a signal from the operator to the insert valve solenoids. This signal causes both insert valves to open. The insert CRD valve applies differential drive pressure of approximately 90 psi under the CRD piston. The insert exhaust valve allows water from above the CRD piston to discharge to the exhaust header.

As illustrated in Figure 4.5-12, the locking mechanism is a ratchet-type device and does not interfere with rod insertion. The speed at which the CRD moves is determined by the flow through the insert speed control valve, which is set for approximately 4 gpm for a shim speed (nonscram operation) of 3 in./sec. During normal insertion, the pressure is adjusted by the speed control valve to compensate for CRD pipe length losses.

Rod withdrawal is, by design, more involved than insertion. The collet finger (latch) must be raised to reach the unlocked position (see Figure 4.5-12). The notches in the index tube and

the collet fingers are shaped so that the downward force on the index tube holds the collet fingers in place. The index tube must be lifted before the collet fingers can be released. This is done by opening the CRD insert valves (in the manner described in the preceding paragraph) for approximately 1 sec. The withdraw valves are then opened, applying driving pressure above the drive piston and opening the area below the piston to the exhaust header. As the piston rises, the collet fingers are cammed outward by the guide cap, away from the index tube.

The pressure required to release the latch is set and maintained at a level high enough to overcome the force of the latch return spring plus the force of reactor pressure opposing movement of the collet piston. When this occurs, the index tube is unlatched and free to move in the withdraw direction. Water displaced by the CRD piston flows out through the withdraw speed control valve, which is set to give the control rod a shim speed of 3 in./sec. The entire valving sequence is automatically controlled and is initiated by a single operation of the rod withdraw switch.

During a scram, the scram pilot valves and scram valves are operated as previously described. With the scram valves open, accumulator pressure is admitted under the CRD piston, and the area over the drive piston is vented to the SDV.

The large differential pressure (depending on charging water header pressure and RPV pressure) produces a large upward force on the index tube and control rod. This force gives the rod a high initial acceleration and provides a large margin of force to overcome any possible friction. After the initial acceleration is achieved, the CRD continues at a nearly constant velocity. This characteristic provides a high initial rod insertion rate. As the CRD piston nears the top of its stroke, the piston seals close off the flow passages (buffer orifices) in the piston tube, and the CRD slows.

Prior to a scram signal and assuming the accumulator is normally charged, the inlet scram valve opens and the full water-side pressure is available at the CRD acting on a 4.1-in.^{2} area. As CRD motion begins, this pressure drops to the gas-side pressure less line losses between the accumulator and the CRD. At low RPV pressures, the accumulator completely discharges with a resulting gas-side pressure of approximately 575 psig. At reactor operating pressure, the accumulator only partially discharges, with reactor pressure providing the necessary scram force when reactor pressure exceeds scram accumulator pressure.

The CRD accumulators are required to scram the control rod when the reactor pressure is low. When the reactor pressure is low, the accumulator retains sufficient stored energy to ensure the complete insertion of the control rod in the required time. The accumulator is not required in order to scram the control rod in time when the reactor is close to or at full operating pressure. In this instance, the reactor pressure alone scrams the control rod in the required time. However, the accumulator does provide an additional energy boost to the reactor pressure in providing scram action at RPV pressures less than accumulator pressures.

The CRD system, with accumulators, provides the following scram performances at full-power operation, in terms of elapsed time after deenergization of the scram pilot valve solenoids for the drives to attain the scram strokes listed in the table below. The scram insertion time is an analytical limit that assures the scram reactivity curve used in the transient analyses is met. Some control rods can be slower than the listed scram insertion

times as long as others are faster so that the analytical scram reactivity curve is met. (Reference 12)

Position Inserted From Fully Withdrawn	Scram Insertion Time (sec)
46	0.457
36	1.084
26	1.841
6	3.361

The alternative rod insertion (ARI) feature provides an alternative means for initiating scram if there is a failure in the electrical portion of the RPS during an operational transient that normally requires a reactor scram. The ARI enables the insertion of reactor control rods by depressurizing the scram pilot valve air header through valves that are redundant and diverse from the RPS-initiated backup scram valves.

The redundant reactivity system signal to insert control rods results in energizing the eight ARI solenoid valves. Two ARI valves in series with the backup scram valves also have parallel functioning check valves to vent air from the air supply line in case an ARI valve fails. These two valves and four other ARI valves vent the A and B hydraulic control unit scram valve pilot air headers to the atmosphere in order to depressurize the headers and scram all rods. Two additional valves vent the portion of the scram air header that serves the scram discharge volume drain and vent lines, closing the vent and drain valves and isolating the SDV. (See also Subsection 7.6.1.18.)

4.5.2.2.3 Evaluation of Scram Time

The rod scram function of the CRD system provides the negative reactivity insertion required by the safety design basis (c.1) in Subsection 4.5.2.2.1.1. The scram time shown in the description is adequate as shown by the transient analyses of Section 15.1. Sufficient driving force is available to overcome the retarding force during a scram. The control rod weighs 154 lb in water and 183 lb in air. The index tube weighs 62 lb in water and 71 in air. Other moving parts weigh about 5 lb so the wet drive line weight is about 225 lb.

At the start of motion, assuming the accumulator is normally charged, the CRD pump will be supplying charging water at a pressure greater than RPV pressure at the inlet scram valve. This supplies a large differential to assist opening of the valve and exists until drive motion starts. Pressure at the CRD immediately drops to reactor pressure due to losses in the piping and valves, and reactor pressure is applied through the ball check valve in the CRD. This pressure is actually slightly less than reactor pressure caused by flow losses as the water comes down the annulus between the CRD and thermal sleeve. The pressure is applied to the 4.1-in.^{2} under piston area. The area above the piston, 1.25 in.^{2}, is vented to the SDV, and initially drops to atmospheric pressure. As soon as drive motion starts, line losses in the discharge line raise the pressure over the piston to about 180 psi. The balance of the over-piston area (4.1 minus 1.25 in.^{2}) is exposed to reactor pressure. Available force, assuming a stuck rod, reduces simply to 1.25 x 1000 or 1250 lb throughout the stroke after accumulator energy is expended. Since the available force is constant at 1250 lb from the beginning of

motion to the end of the strokes, no plot of the force developed by the CRD mechanism versus stroke for a scram with the accumulator and RPV at nominal pressure is necessary.

4.5.2.2.3.1 Analysis of Malfunction Relating to Rod Withdrawal

There are no known single malfunctions that cause the unplanned withdrawal of even a single control rod. However, if multiple malfunctions are postulated, studies show that an unplanned rod withdrawal can occur at withdrawal speeds that vary with the combination of malfunctions postulated. In all cases the subsequent withdrawal speeds are less than that assumed in the control rod drop accident analysis as discussed in Subsection 15.4.9. Therefore, the physical and radiological consequences of such rod withdrawals are less than those analyzed in the control rod drop accident.

Drive Housing Fails at Attachment Weld

The bottom head of the RPV has a penetration for each CRD location. A CRD housing is raised into position inside each penetration and fastened by welding. The CRD is raised into the CRD housing and bolted to a flange at the bottom of the housing. The housing material is seamless, type 304 stainless steel pipe with a minimum tensile strength of 75,000 psi. The basic failure considered here is a complete circumferential crack through the housing wall at an elevation just below the J-weld.

Static loads on the housing wall include the weight of the CRD and the control rod, the weight of the housing below the J-weld, and the reactor pressure acting on the 6-in.-diameter cross-sectional area of the housing and the CRD. Dynamic loading results from the reaction force during CRD operation.

If the housing were to fail as described, the following sequence of events is foreseen. The housing would separate from the RPV. The control rod, CRD, and housing would be blown downward against the support structure by reactor pressure acting on the cross-sectional area of the housing and the CRD. The downward motion of the CRD and associated parts would be determined by the gap between the bottom of the CRD and the support structure and by the deflection of the support structure under load. In the current design, maximum deflection is approximately 3 in. If the collet were to remain latched, no further control rod ejection would occur (Reference 9); the housing would not drop far enough to clear the RPV penetration. Reactor water would leak at a rate of approximately 180 gpm through the 0.03-in. diametral clearance between the housing and the RPV penetration.

If the basic housing failure were to occur while the control rod is being withdrawn (this is a small fraction of the total CRD operating time), and if the collet were to stay unlatched, the following sequence of events is foreseen: the housing would separate from the RPV and the drive and housing would be blown downward against the CRD housing support. Calculations indicate that the steady-state rod withdrawal velocity would be 0.3 fps. During withdrawal, pressure under the collet piston would be approximately 250 psi greater than the pressure over it. Therefore, the collet would be held in the unlatched position until driving pressure was removed from the pressure-over port.

Rupture of Hydraulic Line(s) to Control Rod Drive Housing Flange

There are three types of possible rupture of hydraulic lines to the CRD housing flange:

a. Pressure-under line break

b. Pressure-over line break

c. Coincident breakage of both of these lines.

For the case of a pressure-under line break, a partial or complete circumferential opening is postulated at or near the point where the line enters the housing flange. Failure is more likely to occur after another basic failure wherein the CRD housing or housing flange separates from the RPV. Failure of the housing, however, does not necessarily lead directly to failure of the hydraulic lines.

If the pressure-under line were to fail and if the collet were latched, no control rod withdrawal would occur. There would be no pressure differential across the collet piston and therefore no tendency to unlatch the collet. Consequently, the associated control rod could not be inserted or withdrawn.

The ball check valve is designed to seal off a broken pressure-under line by using reactor pressure to shift the check ball to its upper seat. If the ball check valve were prevented from seating, reactor water would leak to the atmosphere. Because of the broken line, cooling water could not be supplied to the CRD involved. Loss of cooling water would cause no immediate damage to the CRD. However, prolonged exposure of the CRD to temperatures at or near reactor temperature could lead to deterioration of material in the seals. High temperature would be indicated to the operator by the thermocouple in the position-indicator probe. A second indication would be high cooling water flow.

If the basic line failure were to occur while the control rod is being withdrawn, the hydraulic force would not be sufficient to hold the collet open, and spring force normally would cause the collet to latch and stop rod withdrawal. However, if the collet were to remain open, calculations indicate that the steady-state control rod withdrawal velocity would be 2 fps.

The case of the pressure-over line break considers the complete breakage of the line at or near the point where it enters the housing flange. If the line were to break, pressure over the CRD piston would drop from reactor pressure to atmospheric pressure. Any significant reactor pressure (approximately 600 psig or greater) would act on the bottom of the CRD piston and fully insert the CRD. Insertion would occur regardless of the operational mode at the time of the failure. After full insertion, reactor water would leak past the stop piston seals, the contracting seals on the drive piston, and the collet piston seals. This leakage would exhaust to the atmosphere through the broken pressure-over line. The leakage rate at 1000 psi reactor pressure is estimated to be 4 gpm nominal but not more than 80 gpm, based on experimental measurements. If the reactor were hot, drive temperature would increase. This situation would be indicated to the reactor operator by the drift alarm, by the fully inserted drive, by a high drive temperature (indicated and printed out on a recorder in the relay room), and by operation of the drywell sump pump.

For the simultaneous breakage of the pressure-over and pressure-under lines, pressures above and below the CRD piston would drop to zero, and the ball check valve would close the broken pressure-under line. Reactor water would flow from the annulus outside the CRD, through the RPV ports, and to the space below the drive piston. As in the case of pressure-over line breakage, the CRD would then insert (if the reactor were above 600 psi) at a speed dependent on reactor pressure. Full insertion would occur regardless of the operational mode

at the time of failure. Reactor water would leak past the CRD seals and out the broken pressure-over line to the atmosphere, as described previously. Control rod drive temperature would increase. Indication in the main control room would include the drift alarm, the fully inserted CRD, the high CRD temperature printed out on a recorder in the relay room, and operation of the drywell sump pump.

For the evaluation of CRD hydraulic line failures outside the containment, see Subsection 3.6.2.2.6.

All Control Rod Drive Flange Bolts Fail in Tension

Each CRD is bolted to a flange at the bottom of a CRD housing. The flange is welded to the CRD housing. Bolts are made of AISI-4140 steel, with a minimum tensile strength of 125,000 psi. Each bolt has an allowable load capacity of approximately 15,700 lb. Capacity of the eight bolts is approximately 125,800 lb. As a result of the reactor design pressure of l250 psig, the major load on all eight bolts is approximately 45,000 lb.

If a progressive or simultaneous failure of all bolts were to occur, the CRD would separate from the housing. The control rod and the CRD would be blown downward against the support structure. Impact velocity and support structure loading would be slightly less than that for CRD housing failure, because reactor pressure would act on the CRD cross-sectional area only and the housing would remain attached to the RPV. The CRD would be isolated from the cooling-water supply. Reactor water would flow downward past the velocity limiter piston, through the large CRD filter, and into the annular space between the thermal sleeve and the CRD. For worst-case leakage calculations, the large filter is assumed to be deformed or swept out of the way so it would offer no significant flow restriction. At a point near the top of the annulus, where pressure would have dropped to 350 psi, the water would flash to steam and cause choke-flow conditions. Steam would flow down the annulus and out the space between the housing and the CRD flanges to the atmosphere. Steam formation would limit the leakage rate to approximately 840 gpm.

If the collet were latched, control rod ejection would be limited to the distance the CRD can drop before coming to rest on the support structure. There would be no tendency for the collet to unlatch, because pressure below the collet piston would drop to zero. Pressure forces, in fact, exert l435 lb to hold the collet in the latched position.

If the bolts failed during control rod withdrawal, pressure below the collet piston would drop to zero. The collet, with l650 lb return force, would latch and stop rod withdrawal.

Weld Joining Flange to Housing Fails in Tension

The failure considered is a crack in or near the weld that joins the flange to the housing. This crack extends through the wall and completely around the housing. The flange material is forged, type 304 stainless steel, with a minimum tensile strength of 75,000 psi. The housing material is seamless, type 304 stainless steel pipe, with a minimum tensile strength of 75,000 psi. The conventional, full-penetration weld of type 308 stainless steel has a minimum tensile strength approximately the same as that of the parent metal. The design pressure and temperature are l250 psig and 575°F. Reactor pressure acting on the cross-sectional area of the CRD; the weight of the control rod, CRD, and flange; and the dynamic reaction force during CRD operation result in a maximum tensile stress at the weld of approximately 6000 psi.

If the basic flange-to-housing joint failure occurred, the flange and the attached CRD would be blown downward against the support structure. The support structure loading would be slightly less than that for CRD housing failure, because reactor pressure would act only on the CRD cross-sectional area. Lack of differential pressure across the collet piston would cause the collet to remain latched and limit control rod motion to approximately 3 in. Downward CRD movement would be small; therefore, most of the CRD would remain inside the housing. The pressure-under and pressure-over lines are flexible enough to withstand the small displacement and remain attached to the flange. Reactor water would follow the same leakage path described above for the flange-bolt failure, except that exit to the atmosphere would be through the gap between the lower end of the housing and the top of the flange. Water would flash to steam in the annulus surrounding the CRD. The leakage rate would be approximately 840 gpm.

If the basic failure were to occur during control rod withdrawal (a small fraction of the total operating time) and if the collet were held unlatched, the flange would separate from the housing. The CRD and flange would be blown downward against the support structure. The calculated steady-state rod withdrawal velocity would be 0.13 fps. Because pressure-under and pressure-over lines remain intact, driving water pressure would continue to the CRD, and the normal exhaust line restriction would exist. The pressure below the velocity limiter piston would drop below normal as a result of leakage from the gap between the housing and the flange. This differential pressure across the velocity limiter piston would result in a net downward force of approximately 70 lb. Leakage out of the housing would greatly reduce the pressure in the annulus surrounding the CRD. Thus, the net downward force on the CRD piston would be less than normal. The overall effect of these events would be to reduce rod withdrawal to approximately one-half normal speed. With a 560-psi differential across the collet piston, the collet would remain unlatched; however, it should relatch as soon as the CRD signal is removed.

Housing Wall Ruptures

This failure is a vertical split in the CRD housing wall just below the bottom head of the RPV. The flow area of the hole is considered equivalent to the annular area between the CRD and the thermal sleeve. Thus, flow through this annular area, rather than flow through the hole in the housing, would govern leakage flow. The housing is made of type 304 stainless steel seamless pipe, with a minimum tensile strength of 75,000 psi. The maximum hoop stress of 5530 psi results primarily from the reactor design pressure (1250 psig) acting on the inside of the housing.

If such a rupture were to occur, reactor water would flash to steam and leak through the hole in the housing to the atmosphere at approximately 1030 gpm. Choke-flow conditions would exist, as described above for the flange-bolt failure. However, leakage flow would be greater because flow resistance would be less; that is, the leaking water and steam would not have to flow down the length of the housing to reach the atmosphere. A critical pressure of 350 psi causes the water to flash to steam.

No pressure differential across the collet piston would tend to unlatch the collet; but the CRD would insert as a result of loss of pressure in the CRD housing, causing a pressure drop in the space above the CRD piston.

If this failure occurred during control rod withdrawal, CRD withdrawal would stop, but the collet would remain unlatched. The CRD would be stopped by a reduction of the net downward force on the CRD line. The net force reduction would occur when the leakage flow of 1030 gpm reduces the pressure in the annulus outside the CRD to approximately 540 psig, thereby reducing the pressure acting on top of the CRD piston to the same value. A pressure differential of approximately 710 psi would exist across the collet piston and hold the collet unlatched as long as the operator held the withdraw signal.

Flange Plug Blows Out

To connect the RPV ports with the bottom of the ball check valve, a hole of 3/4-in. diameter is drilled in the CRD flange. The outer end of this hole is sealed with a plug of 0.812-in. diameter and 0.250-in. thickness. A full-penetration, type 308 stainless steel weld holds the plug in place. The postulated failure is a full circumferential crack in this weld and subsequent blowout of the plug.

If the weld was to fail, the plug was to blow out, and the collet remained latched, there would be no control rod motion. There would be no pressure differential across the collet piston acting to unlatch the collet. Reactor water would leak past the velocity limiter piston, down the annulus between the CRD and the thermal sleeve, through the RPV ports and drilled passage, and out the open plug hole to the atmosphere at approximately 320 gpm. Leakage calculations assume only liquid flows from the flange. Actually, hot reactor water would flash to steam, and choke-flow conditions would exist. Thus, the expected leakage rate would be lower than the calculated value. Control rod temperature would increase and initiate an alarm in the control room.

If this failure were to occur during control rod withdrawal and if the collet were to stay unlatched, calculations indicate that control rod withdrawal speed would be approximately 0.24 fps. Leakage from the open plug hole in the flange would cause reactor water to flow downward past the velocity limiter piston. A small differential pressure across the piston would result in an insignificant driving force of approximately 10 lb, tending to increase withdrawal velocity.

A pressure differential of 295 psi across the collet piston would hold the collet unlatched as long as the driving signal was maintained.

Flow resistance of the exhaust path from the CRD would be normal because the ball check valve would be seated at the lower end of its travel by pressure under the CRD piston.

Ball Check Valve Plug Blows Out

As a means of access for machining the ball check valve cavity, a 1.25-in.-diameter hole has been drilled in the flange forging. This hole is sealed with a plug of 1.31-in. diameter and 0.38-in. thickness. A full-penetration weld, utilizing type 308 stainless steel filler, holds the plug in place. The failure postulated is a circumferential crack in this weld leading to a blowout of the plug.

If the plug were to blow out while the drive was latched there would be no control rod motion. No pressure differential would exist across the collet piston to unlatch the collet. As in the previous failure, reactor water would flow past the velocity limiter, down the annulus between the drive and thermal sleeve, through the vessel ports and drilled passage, through the ball check valve cage, and out the open plug hole to the drywell. The leakage

calculations indicate the flow rate would be 350 gpm. This calculation assumes liquid flow, but flashing of the hot reactor water to steam would reduce this rate to a lower value.

Drive temperature would rapidly increase and initiate an alarm in the control room.

If the plug failure were to occur during control rod withdrawal (it would not be possible to unlatch the drive after such a failure), the collet would relatch at the first locking groove. If the collet were to stick, calculations indicate the control rod withdrawal speed would be 11.8 fps. There would be a large retarding force exerted by the velocity limiter because of a 35-psi pressure differential across the velocity limiter piston.

Control Rod Drive Pressure Control Valve Closure (Reactor Pressure, 0 psig)

The pressure to move a CRD is controlled by adjustment of the drive/cooling water pressure control valve. This valve is motor-operated and adjusted to a fixed opening. The normal pressure drop across this valve is 230 psi.

If the flow through the CRD pressure control valve were to be stopped, as by a valve closure or flow blockage, the CRD pressure would increase to the shutoff pressure of the supply pump. The occurrence of this condition during withdrawal of a CRD at zero RPV pressure will result in a CRD pressure increase from 260 psig to no more than 1600 psig. Calculations indicate that the drive would accelerate from 3 in./sec to approximately 6 in./sec. A pressure differential of l670 psi across the collet piston would hold the collet unlatched. Flow would be upward, past the velocity limiter piston, but retarding force would be negligible. Rod movement would stop as soon as the driving signal was removed.

Ball Check Valve Fails To Close Passage to Reactor Pressure Vessel Ports

Should the ball check valve sealing the passage to the RPV ports be dislodged and prevented from reseating following the insert portion of a CRD withdrawal sequence, water below the CRD piston would return to the reactor through the RPV ports and the annulus between the CRD and the housing rather than through the speed control valve. Because the flow resistance of this return path would be lower than normal, the calculated withdrawal speed would be 2 fps. During withdrawal, differential pressure across the collet piston would be approximately 40 psi. Therefore, the collet would tend to latch and would have to stick open before continuous withdrawal at 2 fps could occur. Water would flow upward past the velocity limiter piston, generating a small retarding force of approximately 120 lb.

Hydraulic Control Unit Valve Failures

Various failures of the valves in the HCU can be postulated, but none could produce differential pressures approaching those described in the preceding paragraphs and none alone could produce a high velocity withdrawal. Leakage through either one or both of the scram valves produces a pressure that tends to insert the control rod rather than to withdraw it. If the pressure in the scram discharge volume should exceed reactor pressure following a scram, a check valve in the line to the scram discharge header prevents this pressure from operating the CRD mechanisms.

Collet Fingers Fail To Latch

The failure is presumed to occur when the drive withdraw signal is removed. If the collet fails to latch, the drive continues to withdraw at a fraction of the normal speed. This assumption is made because there is no known means for the collet fingers to become

unlocked without some initiating signal. Because the collet fingers will not cam open under a load, accidental application of a down signal does not unlock them. (The drive must be given a short insert signal to unload the fingers and cam them open before the collet can be driven to the unlock position.) If the drive withdrawal valve fails to close following a rod withdrawal, the collet would remain open and the drive continue to move at a reduced speed.

Withdrawal Speed Control Valve Failure

Normal withdrawal speed is determined by differential pressures in the CRD and is set for a nominal value of 3 in./sec. Withdrawal speed is maintained by the pressure regulating system and is independent of RPV pressure. Tests have shown that accidental opening of the speed control valve to the full-open position produces a velocity of approximately 6 in./sec. The CRD system prevents rod withdrawal and it has been shown above that only multiple failures in a CRD unit and in its control unit could cause an unplanned rod withdrawal.

4.5.2.2.3.2 Scram Reliability

High scram reliability is the result of a number of features of the CRD system. For example

a. An individual accumulator is provided for each control rod drive with sufficient stored energy to scram at lower reactor pressures. The reactor vessel itself, at pressures above 600 psi, will supply the necessary force to insert a drive

b. Each drive mechanism has its own scram and pilot valves so only one drive can be affected if a scram valve fails to open. Two pilot valves are provided for each drive. Both pilot valves must be deenergized to initiate a scram

c. The RPS and the HCUs are designed so that the scram signal and mode of operation override all others

d. The collet assembly and index tube are designed so they will not restrain or prevent control rod insertion during scram

e. The SDV is monitored for accumulated water and will scram the reactor before the volume is reduced to a point that could interfere with a scram.

4.5.2.2.3.3 Control Rod Support and Operation

Each control rod is independently supported and controlled as required by safety design bases.

4.5.2.2.3.4 Common Mode Failures of Reactivity Control Systems

The CRD system and the standby liquid control system (SLCS), which is the backup reactivity control system, do not share any instrumentation or components. Thus, a common mode failure of the reactivity systems would be limited to an accident event that could damage essential equipment in the two independent systems.

A seismic event or the postulated accident environments are not considered potential common mode failures because the essential (scram) portions of the CRD system are designed to Category I standards and to operate as required under the environmental

conditions of the postulated design-basis accident. The SLCS is tested and maintained as a safety-related system.

No common mode power failure is considered credible. The scram function of the CRD system is fail-safe on a loss of power and is designed to override any other function of the CRD system. The SLCS has two independent power supplies to its essential redundant pumps and valves. The power supplies to the SLCS are switched to the onsite standby diesels on a loss of normal power sources.

The design of the SDV incorporates separate instrument volumes for each division of CRDs. Each SDV 8-in. header is integrally coupled to its 12-in. instrument volume. This design is not susceptible to the common mode problem of earlier designs caused by a 2-in. line connecting the SDVs to a single instrument volume.

General Electric completed a reliability analysis of the BWR scram system in 1976. The overall probability of failure was assessed to be 5×10^{-6} per year. The major contributor to this failure probability value was a common mode failure in the electrical trip circuit. The analysis identified design modifications that were made and that reduced the failure probability value to less than 1×10^{-7} per year.

The most recent analysis of CRD system reliability, which takes into account the design changes directed at reducing the potential for common mode failure in the mechanical portion of the CRD system (i.e., changes in the SDV), reaffirms that the CRD unreliability value is still estimated to be less than 1×10^{-7} per year.

NOTE: General Electric defined failure to be noninsertion of the CRDs in the following manner: greater than 50 percent in a checkerboard pattern, greater than 31 percent in a random pattern, or more than 4 in a cluster.

4.5.2.2.4 Inspection and Testing

4.5.2.2.4.1 Development Tests

The development drive (one prototype) testing up to the submittal of the original FSAR included more than 5000 scrams and approximately 100,000 latching cycles. One prototype was exposed to simulated operating conditions for 5000 hr. These tests yielded the following results:

a. The drive easily withstands the forces, pressures, and temperatures imposed

b. Wear, abrasion, and corrosion of the nitrided type 304 stainless steel parts are negligible. Mechanical performance of the nitrided surface is superior to that of materials used in earlier operating reactors

c. The basic scram speed of the CRD has a satisfactory margin above minimum plant requirements at any RPV pressure

d. Usable seal lifetimes in excess of l000 scram cycles can be expected.

4.5.2.2.4.2 Factory Quality Control Tests

Quality control of welding, heat treatment, dimensional tolerances, material verification, and similar factors is maintained throughout the manufacturing process to ensure reliable performance of the mechanical reactivity control components. Some of the quality control tests performed on the CRD mechanisms and HCUs follow.

a. Control rod drive mechanism tests

1. Pressure welds on the CRDs are hydrostatically tested in accordance with ASME codes
2. Electrical components are checked for electrical continuity and resistance to ground
3. Control rod drive parts that cannot be visually inspected for dirt are flushed with filtered water at high velocity. No significant foreign material is permitted in effluent water
4. Seals are tested for leakage to demonstrate correct seal operation
5. Each CRD is tested for shim motion, latching, and control rod position indication
6. Each drive is subjected to cold scram tests at various reactor pressures to verify correct scram performance.

b. Hydraulic-control unit tests

1. Hydraulic systems are hydrostatically tested in accordance with the applicable code
2. Electrical components and systems are tested for electrical continuity and resistance to ground
3. Correct operation of the accumulator pressure and level switches is verified
4. The unit's ability to perform its part of a scram is demonstrated. Correct operation and adjustment of the insert and withdrawal valves are demonstrated.

4.5.2.2.4.3 Operational Tests

After installation, all rods and CRD mechanisms can be tested through their full stroke for operability.

During normal operation, each time a control rod is withdrawn a notch, the operator can observe the in-core monitor indications to verify that the control rod is following the CRD mechanism. All control rods that are partially withdrawn from the core can be tested for rod

following by inserting or withdrawing the rod one notch and returning it to its original position, while the operator observes the in-core monitor indications.

To make a positive test of control rod to CRD coupling integrity, the operator can withdraw a control rod to the end of its travel and then attempt to withdraw the CRD to the overtravel position. Failure of the CRD to overtravel demonstrates rod-to-drive coupling integrity.

Hydraulic supply subsystem pressures can be observed from instrumentation in the main control room. Scram accumulator pressures can be observed on the nitrogen pressure gages.

4.5.2.2.4.4 Acceptance Tests

Criteria for acceptance of the individual CRD mechanisms and the associated control and protection systems were incorporated in specifications and test procedures covering three distinct phases: preinstallation, after installation prior to startup, and during startup testing.

The preinstallation specification defined criteria and acceptable ranges of such characteristics as seal leakage, friction, and scram performance under fixed test conditions, which must be met before the component can be shipped.

The after-installation, prestartup tests included normal and scram motion and were primarily intended to verify that piping, valves, electrical components, and instrumentation were properly installed. The test specifications included criteria and acceptable ranges for CRD speed, time settings, scram valve response times, and control pressures. These tests were intended more to document system condition than to test performance.

During initial preoperational testing, an observer who was in direct communication with the control room observed the operation of each individual control rod and verified that there was no binding or restriction to rod motion and listened for any scraping or binding noises that might signify rod misalignment. In addition, the friction of each CRD was measured as indicated by the differential pressure developed across the CRD piston during notch withdrawal. These differential pressure traces were compared against reference traces to ensure proper operation and the absence of abnormal friction.

As fuel was placed in the reactor, the startup test procedure was followed. The tests in this procedure are intended to determine that the initial operational characteristics meet the limits of the specifications over the range of primary coolant temperatures and pressures from ambient to operating. The initial testing program is described in Chapter 14.

4.5.2.2.4.5 Surveillance Tests

The surveillance requirements for the CRD system are included in the Technical Specifications.

To detect any increased friction of the control rods due to postulated bowing of the fuel channel boxes, Edison has committed to a surveillance program that includes guidelines for channel box rotation to minimize the potential for channel bowing. In addition, after core alterations and before reaching 40 percent power, a CRD friction test is performed for cells exceeding the established guidelines or exceeding exposures equivalent to 30,000 MWd/t. In lieu of friction testing, fuel channel deflection measurements may be used to identify the amount of remaining channel lifetime for channels exceeding the equivalent of 30,000

MWd/t, associated fuel bundle exposure. During each major refueling outage, friction testing is performed by letting the control rod settle under its own weight for two notches. Control rod drive friction is acceptable if the rod settles to the next notch within 10 sec. The control blade is in its most constrained, highest friction location when it is fully inserted. The ability of the blade to settle from this position demonstrates that the CRD friction is less than the weight of the blade (approximately 250 lb).

Fermi 2 has implemented a program that addresses a possible problem with IGSCC in the collet assembly of the CRD mechanism. The program is consistent with GE recommendations. It consists of the following three parts:

a. An augmented surveillance and inspection program

b. Modification of CRD operations to eliminate unnecessary thermal cycling

c. Modification of the CRD water supply to provide high-purity deaerated water to the CRD system during plant operation.

The Fermi 2 program consists of the following corresponding actions:

a. Each rod not fully inserted will be tested to confirm operability by inserting one or more notches in accordance with the frequency specified in the Technical Specifications.

   All CRDs removed from the reactor for maintenance or for access to inservice CRD housing inspections will have a dye penetrant examination made of the outer surface of the collet retainer tube. CRDMs which do not experience any performance problems and are removed for inspection undervessel, or to replace a flange o-ring, for example, will not require a dye penetrant examination. CRDMs that are rebuilt after seeing reactor service will receive a dye penetrant examination of the collet retainer tube. The criteria established by GE in Service Information Letter (SIL) 139 will be used to decide rejection. The term collet retainer tube refers to a portion of the outer tube, and replacement of a rejected collet retainer tube requires a new cylinder, tube, and flange subassembly

b. A CRD with a high-temperature alarm will not be cooled by giving it repeated drive signals.

c. The source of water for the CRD system has been changed to the condensate treatment system effluent with the condensate storage tank as backup. The water source is very pure and of very low oxygen content

   A flowing sample line downstream of the drivewater filter has been installed to provide for conductivity and oxygen grab sample measurement.

The use of high-purity deaerated water effects a significant increase in the time to crack formation. General Electric estimated that the time to crack initiation in current CRD collet retainer tubes may be increased by a factor of 100 with this reduction in dissolved oxygen content.

4.5.2.2.4.6 Instrumentation

The general functional requirements for the CRD are discussed in Subsection 4.5.2.1.5.

4.5.2.3 Supplementary Reactivity Control

4.5.2.3.1 Design Basis

The fuel rods containing supplementary reactivity control shall have sufficient mechanical strength to prevent displacement of their reactivity control material.

4.5.2.3.2 Description

The reactivity control requirements of the initial core load considerably exceed the equilibrium core requirements because all the fuel in the initial core loading is fresh. To meet the reactivity control requirements of the initial core load, or any core load with excess reactivity, gadolinia-urania fuel rods are placed in each enriched fuel assembly. Some assemblies contain more gadolinium than others to improve transverse power flattening. Also, some assemblies contain axially distributed gadolinium to improve axial power flattening. For a detailed discussion of gadolinia fuels, refer to Subsection 4.3.2.

4.5.2.3.3 Safety Evaluation

The description shows that the gadolinia-urania fuel rods meet the design-basis requirements (Subsection 4.3.2).

4.5.2.3.4 Inspection and Testing

The same rigid quality control requirements observed for standard UO_2 fuel are employed in manufacturing gadolinia-urania fuel. Gadolinia-bearing UO_2 fuel pellets of a given enrichment and gadolinia concentration are maintained in separate groups throughout the manufacturing process. The percent enrichment and gadolinia concentration characterizing a pellet group are identified by a stamp on the pellet.

Fuel rods are individually numbered prior to loading of fuel pellets into the fuel rods for three reasons: to identify which pellet group is to be loaded in each fuel rod, to identify which position in the fuel assembly each fuel rod is to be loaded into, and to facilitate total material accountability for a given project. For the initial core, longer upper end plug shanks for gadolinia-bearing rods ensured their correct placement within the fuel assembly. For reload cores, a uniform end plug is used for all rods. Correct placement is ensured by an automated bundle assembly machine.

The following QC inspections are made.

a. Gadolinia concentration in the gadolinia-urania powder blend is verified

b. Sintered pellet UO_2-Gd_2O_3 solid-solution homogeneity across a fuel pellet is verified by examination of metallographic specimens

c. Gadolinia-urania pellet identification is verified

d. Gadolinia-urania fuel rod identification is checked.

All assemblies and rods of a given project are inspected to ensure overall accountability of fuel quantity and placement for the project.

4.5.2.4 Standby Liquid Control System

4.5.2.4.1 Design Bases

The standby liquid control system (SLCS) is a special-event plant capability system and is tested and maintained as a safety-related system. The system is designed with a high degree of reliability and with certain safety features; however, it is not required to meet the safety design-basis requirements of the safety systems. The SLCS process equipment, instrumentation and control essential for injection of the sodium pentaborate solution into the reactor are designed to withstand the safe shutdown earthquake.

The SLCS shall meet the following design bases:

a. Backup capability for reactivity control shall be provided, independent of normal reactivity control provisions in the nuclear reactor, to be able to shut down the reactor if the normal control ever becomes inoperative

b. The backup system shall have the capacity for controlling the reactivity difference between the steady-state rated operating condition of the reactor with voids and the cold shutdown condition, including shutdown margin, to ensure complete shutdown from the most reactive condition at any time in core life

c. The time required for actuation and effectiveness of the backup control shall be consistent with the nuclear reactivity rate of change predicted between rated operating and cold shutdown conditions. A fast scram of the reactor or operational control of fast reactivity transients is not specified to be accomplished by this system

d. Means shall be provided by which the functional performance capability of the backup control system components can be verified periodically under conditions approaching actual use requirements. A substitute solution, rather than the actual neutron absorber solution, can be injected into the reactor to test the operation of all components of the redundant control system

e. The neutron absorber shall be dispersed within the reactor core in sufficient quantity to provide a reasonable margin for leakage or imperfect mixing

f. The system shall be reliable to a degree consistent with its role as a control system; the possibility of unintentional or accidental shutdown of the reactor by this system shall be minimized

g. The system shall have the capability of controlling suppression pool pH following a LOCA in the event of fuel failure.

4.5.2.4.2 Description

The SLCS (Figure 4.5-17) is manually initiated from the main control room to pump a boron neutron absorber solution into the reactor if the operator believes the reactor cannot be shut down or kept shut down with the control rods. However, insertion of control rods is expected to ensure prompt shutdown of the reactor should it be required.

The SLCS is required to shut down the reactor and keep the reactor from going critical again as it cools. In addition, SLC is required to control suppression pool pH following a LOCA in the event of fuel failure.

The SLCS is needed in the improbable event that not enough control rods can be inserted in the reactor core to accomplish shutdown and cooldown in the normal manner.

The storage tank and active portion of the SLCS necessary for the injection of boron have been reclassified to identify that the SLCS was not originally intended, procured, designed, or classified as safety related, but is being maintained and tested as a safety-related system after completion of its preoperational tests.

The boron solution tank, the test water tank, the two positive-displacement pumps, the two explosive valves, and associated local valves and controls are mounted in the reactor building. The liquid is piped into the RPV and discharged near the bottom of the core shroud so it mixes with the cooling water rising through the core (Subsection 4.5.1.2 and Figure 4.5-2).

The boron absorbs thermal neutrons and thereby terminates the nuclear fission chain reaction in the uranium fuel.

The specified neutron absorber solution is enriched sodium pentaborate ($Na_2B_{10}O_{16}{\cdot}10H_2O$) dissolved in demineralized water. An air sparger is provided in the tank for mixing. To prevent system plugging, the tank outlet is raised above the bottom of the tank.

Whenever it is possible to make the reactor critical, the SLCS shall be able to deliver enough sodium pentaborate solution into the reactor (Figure 4.5-18) to ensure reactor shutdown. This is accomplished by placing the required amount of sodium pentaborate in the standby liquid control tank and filling with demineralized water to at least the low-level alarm point.

The saturation temperature of the recommended solution is approximately 40°F. The SLC tank is installed in a room in which the air temperature is to be maintained within the range of 70°F to 100°F. High or low temperature, or high or low liquid level, causes an alarm in the main control room.

The lines and equipment from the storage tank to the explosive valves are insulated.

The SLCS is completely contained within the reactor building. This building is well heated and ventilated; it also receives most of the heat loss from the reactor system. It is therefore incredible for the water in the SLCS to freeze while the plant is operating.

Each positive displacement pump is sized to inject the solution into the reactor in 50 to 125 minutes, independent of the amount of solution in the tank. The pump and system design pressure between the explosive valves and the pump discharge is 1400 psig. The two relief valves are set slightly under 1400 psig. To prevent bypass flow from one pump in case of

relief valve failure in the line from the other pump, a check valve is installed downstream of each relief valve line in the pump discharge pipe.

SLC is manually initiated upon indication of fuel failure following a LOCA to control suppression pool pH in order to prevent iodine re-evolution. The analysis shows that SLC injection and mixing within 6 hours of the beginning of the event will maintain suppression pool pH 7.0 or higher for the 30-day duration of the accident. The amount of sodium pentaborate solution that is required for reactivity control is sufficient for pH control.

The two explosive-actuated injection valves provide assurance of opening when needed and ensure that boron does not leak into the reactor even when the pumps are being tested.

Each explosive valve is closed by a plug in the inlet chamber. The plug is circumscribed with a deep groove so the end readily shears off when pushed with the valve plunger. This opens the inlet hole through the plug. The sheared end is pushed out of the way in the chamber; it is shaped so it does not block the ports after release.

The shearing plunger is actuated by an explosive charge with dual ignition primers inserted in the side chamber of the valve.

Ignition circuit continuity is monitored by a trickle current, and an alarm occurs in the main control room if either circuit opens. Indicator lights show which primary circuit opened.

The SLCS is actuated by a three-position keylocked switch on the main control room console. This ensures that switching from the "off" position is a deliberate act. Switching to either side starts an injection pump, actuates both of the explosive valves, and closes the reactor cleanup system outboard isolation valve to prevent loss or dilution of the boron. This action occurs only if the SLC system is lined up normally. If either SLC pump breaker is racked out, only one pump and explosive actuated injection valve will operate.

A green light in the main control room indicates that power is available to the pump motor contactor and that the contactor is open (pump not running). A red light indicates that the contactor is closed (pump running).

If the pump lights or explosive valve light indicate that the liquid may not be flowing, the operator can immediately turn the switch to the other side, which actuates the alternative pump.

Cross piping and check valves ensure a flow path through either pump and either explosive valve. Placing the local switch in its “off” position will not terminate pump operation if the switch in the main control room has been placed in the “run” position. This prevents the separation of the pump from the main control room. Pump discharge pressure is also indicated in the main control room.

Equipment drains and tank overflow are not piped to the radwaste system but to separate containers (such as 55-gal drums) that can be removed and disposed of independently to prevent any trace of boron from inadvertently reaching the reactor.

Instrumentation consisting of solution temperature indication, solution level, and heater system status is provided locally at the storage tank.

4.5.2.4.3 Safety Evaluation

The SLCS is a suppression pool pH control system and a redundant reactivity control system and is maintained in a standby operational status in the reactor modes 1 and 2. The system is not expected to be needed for safety reasons because of the large number of independent control rods available to shut down the reactor.

However, to ensure the availability of the SLCS, two sets of pumps and explosive valves are provided in parallel redundancy.

The system is designed to bring the reactor from rated power to a cold shutdown at any time in core life. The reactivity compensation provided reduces reactor power from rated to zero level and allows cooling the nuclear system to room temperature, with the control rods remaining withdrawn in the rated power pattern. It includes the reactivity gains that result from complete decay of the rated power xenon inventory. It also includes the positive reactivity effects from eliminating steam voids, changing water density from hot to cold, reducing Doppler effect in uranium, reducing neutron leakage from boiling to cold, and decreasing control rod worth as the moderator cools. The specified minimum final concentration of boron in the reactor core provides a margin of -0.033 Δk for calculational uncertainties and ensures subcriticality.

Fermi 2 meets the requirements of 10CFR50.62, ATWS Rule, by increasing the enrichment of boron-10 to a minimum of 65 atom percent. The current design of the SLC system is sufficient to handle the increased enrichment of sodium pentaborate solution because the enriched boron solution is chemically similar to the current solution. Using an enriched solution will not change any of the key SLC system process parameters, i.e., flow rate, discharge pressure, required NPSH, etc.

The specified minimum average concentration of natural boron in the reactor to provide the specified shutdown margin, after operation of the SLCS, is 720 ppm. This value is increased by 25 percent to 900 ppm to allow for imperfect mixing and leakage. Thus, calculation of the minimum quantity of sodium pentaborate to be injected into the reactor is based on 900 ppm average concentration in the reactor coolant, including recirculation loops and the RHR system in the shutdown cooling mode, at 70°F and reactor water Level 8.

Cooldown of the nuclear system requires a minimum of several hours to remove the thermal energy stored in the reactor cooling water and associated equipment. The controlled limit for the RPV cooldown is 100°F per hour, and normal operating temperature is approximately 550°F. Use of the main condenser and various shutdown cooling systems requires 10 to 24 hr to lower the RPV to room temperature (70°F). This is the condition of maximum reactivity and, therefore, the condition that requires the maximum concentration of boron.

The injection rate is limited to a range of 8 to 20 ppm/minute change in boron concentration in reactor water, based on the weight of water in the reactor and recirculation loops at normal water level and 70°F. The lower rate ensures that the boron is injected into the reactor in approximately 2 hr. This resulting reactivity insertion is considerably quicker than that covered by the cooldown. However, power cyclic oscillations from uneven mixing of boron in the core at high delivery rates is not a concern because of the steady boron concentration buildup observed in mixing tests, as documented in NEDC-30921.

The SLCS equipment essential for injection of neutron absorber solution into the reactor is designed to withstand the safe shutdown earthquake and is tested and maintained as safety-related equipment.

The SLCS is required to be operable in the event of a station power failure. Therefore, the pumps, valves, and controls are powered from the standby ac power supply. The pumps and valves are powered and controlled from separate buses and circuits.

The SLCS and pumps have sufficient pressure margin, up to the system relief valve setting of approximately 1400 psig, to ensure solution injection into the reactor above the normal pressure in the bottom of the reactor. The nuclear system relief and safety valves begin to relieve pressure above approximately 1100 psig. Therefore, the SLCS positive displacement pumps cannot overpressurize the nuclear system.

Only one of the two standby liquid control pumps and/or explosive actuated injection valves is needed for system operation. If one pump and/or injection valve is found to be inoperable, there is no immediate threat to shutdown capability, and reactor operation and/or rod movement can continue during repairs. The time during which one redundant component upstream of the explosive valves may be out of operation should be consistent with the following: the probability of failure of both the control rod shutdown capability and the alternative component in the SLCS; and the fact that nuclear system cooldown takes several hours while liquid control solution injection takes approximately 2 hr. Since this probability is small, considerable time is available for repairing and restoring the SLCS to an operable condition while reactor operation continues. Assurance that the system will still fulfill its function during repairs is obtained by maintaining the operable status of the redundant pump/valve combination.

Standard Review Plan (SRP) 4.6 states that the SLCS is reviewed by using SRP 9.3.5 to determine its adequacy to perform its function of reactivity control. The following summarizes the comparison of the Fermi 2 SLCS with the acceptance criteria listed in SRP 9.3.5:

a. The system is housed in the reactor building and therefore meets General Design Criterion (GDC) 2 for withstanding natural phenomena

b. The system is located in a missile-free area on the fourth floor of the reactor building. The system piping is studied for pipe whip and jet impingement effects both inside and outside primary containment. These studies show conformance with GDC 4

c. The SLCS meets the requirements for high functional reliability and inservice testability. However, the system design criteria do not specify a single-failure criterion for tanks and piping, but dual pumps and dual explosive valves are incorporated. The reliability criteria are further discussed elsewhere in this section and in Subsection 4.5.2.2.3.4

d. The SLCS is independent of other control systems and is capable of maintaining the core subcritical under cold conditions. Therefore, GDC 26 and GDC 27 are met

e. The classification of system components is given in Table 3.2-1.

f. The location of the SLCS renders it immune to the effects of flooding and tornado missiles. The system meets the criteria for breaks in piping systems outside the drywell.

A discussion in Subsection 4.5.2.2.3.4 addresses the vulnerability of the CRD system and SLCS to common mode failures. The two systems do not share any instrumentation or components. The probability of a common mode failure in the SLCS is dominated by the failure of an operator to actuate the system in a timely manner. The probability of this type of operator error is estimated to be in the range of 1×10^{-1} to 1×10^{-3} per demand, depending on the time required for system activation.

The amount of sodium pentaborate solution that is required for reactivity control is sufficient for pH control. SLC injection and mixing within 6 hours of the beginning of the event will maintain suppression pool pH 7.0 or higher for the 30-day duration of the accident.

4.5.2.4.4 Inspection and Testing

An operational test is performed on the SLCS on an 18-month frequency to:

a. Demonstrate that the pump relief valve setpoint is $\leq$ 1400 psig, and

b. Verify that the relief valve does not actuate during recirculation to the test tank.

Operational testing of the SLCS is performed in at least two parts to avoid inadvertently injecting boron into the reactor.

With the valves to and from the storage tank closed and the three valves to and from the test tank opened, demineralized water in the test tank can be recirculated by locally starting either pump.

The injection portion of the system can be functionally tested by valving the pump suction lines to the test tank and actuating the system from the main control room. Each pump loop and its injection valve are tested. System operation is indicated in the main control room.

After functional tests, the injection valve shear plugs and explosive charges must be replaced and all the valves returned to their normal positions as indicated.

After closing a local locked-open valve to the reactor, leakage through the injection valves can be determined by opening valves at a test connection in the line between the containment isolation check valves. Position indicator lights in the main control room indicate that the local valve is closed for tests or open and ready for operation. Leakage from the reactor through the first check valve can be detected by opening the same test connection when the reactor is pressurized.

The test tank contains demineralized water for approximately 3 minutes of pump operation. Demineralized water from the makeup system or the condensate storage system is available for refilling or flushing the system.

Should the boron solution ever be injected into the reactor, either intentionally or inadvertently, after it is made certain that the normal reactivity controls will keep the reactor subcritical, the boron is removed from the reactor coolant system by flushing for gross dilution followed by operating the reactor water cleanup (RWCU) system (Subsection 5.5.8).

There is practically no effect on reactor operations when the boron concentration has been reduced below approximately 50 ppm.

The concentration of the sodium pentaborate in the solution tank is determined periodically by chemical analysis.

4.5.2.4.5 Instrumentation

The instrumentation and control system for the SLCS is designed to allow the injection of liquid poison into the reactor. The discussion of the SLCS instrumentation is included in Subsection 7.4.1.

4.5.3 Control Rod Drive Housing Supports

4.5.3.1 Safety Objective

The CRD housing supports prevent any significant nuclear transient in the event a drive housing breaks or separates from the bottom of the RPV.

4.5.3.2 Safety Design Bases

The CRD housing supports shall meet the following safety design bases:

a. Following a postulated CRD housing failure, control rod downward motion shall be limited so that any resulting nuclear transient could not be sufficient to cause fuel damage

b. The clearance between the CRD housings and the supports shall be sufficient to prevent vertical contact stresses caused by thermal expansion during plant operation.

4.5.3.3 Description

The CRD housing supports are shown in Figure 4.5-19. Horizontal beams are installed immediately below the bottom head of the RPV, between the rows of CRD housings. The beams are bolted to brackets welded to the steel form liner of the drive room in the reactor support pedestal.

Hanger rods, approximately 10 ft long and 1-3/4 in. in diameter, are supported from the beams on stacks of disk springs. These springs compress approximately 2 in. under the design load.

The support bars are bolted between the bottom ends of the hanger rods. The spring pivots at the top, and the beveled, loose-fitting ends on the support bars prevent substantial bending movement in the hanger rods if the support bars are overloaded.

Individual grids rest on the support bars between adjacent beams. Because a single-piece grid would be difficult to handle in the limited work space and because it is necessary that CRDs, position indicators, and in-core instrumentation components be accessible for inspection and maintenance, each grid is designed for in-place assembly or disassembly. Each grid assembly is made up of two grid plates, a clamp, and a bolt. The top part of the clamp guides

the grid to its correct position directly below the respective CRD housing that it would support in the postulated accident.

When the support bars and grids are installed, a gap of approximately 1 in. at room temperature (approximately 70°F) is provided between the grid and the bottom contact surface of the CRD flange.

During system heatup, this gap is reduced by a net downward expansion of the housings with respect to the supports. In the hot operating condition, the gap is approximately 1/4 in.

In the postulated CRD housing failure, the CRD housing supports are loaded when the lower contact surface of the CRD flange contacts the grid. The resulting load is then carried by two grid plates, two support bars, four hanger rods, their disk springs, and two adjacent beams.

The American Institute of Steel Construction (AISC) Manual of Steel Construction, "Specification for the Design, Fabrication and Erection of Structural Steel for Buildings," was used as a guide in designing the CRD housing support system. However, to provide a structure that absorbs as much energy as practical without yielding, the allowable tension and bending stresses used were 90 percent of yield and the shear stress used was 60 percent of yield. These design stresses are 1.5 times the AISC allowable stresses (60 percent and 40 percent of yield, respectively).

For purposes of mechanical design, the postulated failure resulting in the highest forces is an instantaneous circumferential separation of the CRD housing from the RPV, with an internal pressure of 1250 psig (RPV design pressure) acting on the area of the separated housing. The weight of the separated housing, CRD, and blade, plus the pressure of 1250 psig acting on the area of the separated housing, gives a force of approximately 35,000 lb. This force is multiplied by a factor of three for impact, conservatively assuming that the housing travels through a 1-in. gap before it contacts the supports. The total force (105,000 lb) is then treated as a static load in design.

Selected CRD housing support hanger rods have TIP guide tube supports attached below the support bars.

All CRD housing support subassemblies are fabricated of ASTM-A-36 structural steel, except for the following items:

Item	Material
Grid	ASTM-A-441
Disk springs	Schnorr, Type BS-125-71-8
Hex bolts and nuts	ASTM-A-307
Structure tubing	ASTM-A-46

4.5.3.4 Safety Evaluation

For design purposes, the postulated failure resulting from an instantaneous circumferential separation of the CRD housing from the RPV, with an internal pressure of 1250 psig (RPV design pressure) acting on the area of the separated housing, is the governing design

condition. The vertical force (dead load) of the separated housing, CRD, and blade plus the force of 1250 psig pressure acting on the area of the separated housing multiplied by an impact factor of three gives the design static load on the CRD housing support members. The effect of an earthquake on the design load is not considered in the design because the earthquake load is only 3 percent of the design load.

Downward travel of the CRD housing and its control rod following the postulated housing failure equals the sum of these distances:

a. The compression of the disk springs under dynamic loading

b. The initial gap between the grid and the bottom contact surface of the CRD flange. If the reactor were cold and pressurized, the downward motion of the control rod would be limited to the spring compression (approximately 2 in.) plus a gap of approximately 1 in. If the reactor were hot and pressurized, the gap would be approximately l/4 in. and the spring compression would be slightly less than in the cold condition. In either case, the control rod movement following a housing failure is substantially limited below one drive notch movement (6 in.). Sudden withdrawal of any control rod through a distance of one drive notch at any position in the core does not produce a transient sufficient to damage any radioactive material barrier.

The stress criterion (1.5 times the AISC allowable stresses) is considered desirable for this application and adequate for the "once in a lifetime" loading condition.

The CRD housing supports are in place during power operation and when the nuclear system is pressurized. If a control rod is ejected during shutdown, the reactor remains subcritical because it is designed to remain subcritical with any one control rod fully withdrawn at any time.

At plant operating temperature, a gap of approximately 1/4 in. exists between the CRD housing and the supports. At lower temperatures the gap is greater. Because the supports do not contact any of the CRD housing except during the postulated accident condition, vertical contact stresses are prevented.

4.5.3.5 Inspection and Testing

CRD housing supports are removed for inspection and maintenance of the CRDs. The supports for one control rod can be removed during reactor shutdown, even when the reactor is pressurized, because all control rods are then inserted. When the support structure is reinstalled, it is inspected for correct assembly with particular attention to maintaining the correct gap between the CRD flange lower contact surface and the grid.

4.5 REACTOR MECHANICAL DESIGN

REFERENCES

1. General Electric Company, Peach Bottom Atomic Power Station Units 2 and 3 Safety Analysis Report for Plant Modification to Eliminate Significant Core Vibration, NEDC-20994, filed on Docket 50-277 in September 1975.
2. General Electric Company, Design and Performance of GE BWR Jet Pumps, APED-5460, July 1968.
3. R. H. Moen, Testing of Improved Jet Pumps for the BWR/6 Nuclear System, NEDO-10602, June 1972.
4. Deleted
5. Fermi Response to AEC, "Control Rod Guide Tube Collapse," General Electric Manual 383HA936, August 2, 1973.
6. Letter from C. M. Heidel, Detroit Edison, to A. Giambusso, AEC, EF2-16969, May 9, 1973.
7. Letter from C. M. Heidel Detroit Edison, to A. Giambusso, AEC, EF2-2l952, February 14, 1974.
8. R. G. Stirn et al., Rod Drop Accident Analysis for Large Boiling Water Reactors, NEDO-10527, March 1972.
9. J. E. Benecki, Impact Testing on Collet Assembly for Control Rod Drive Mechanism 7RD Bl44A, APED-555, November 1967.
10. Detroit Edison Company, "Proposed License Amendment - Power Uprate, Power Uprate Safety Analysis," Fermi 2-91-150, September, 1991.
11. GE Nuclear Energy, "Maximum Extended Operating Domain Analysis for Detroit Edison Company, Enrico Fermi Energy Center," NEDC-31843P, July, 1990.
12. Safety Evaluation By The Office Of Nuclear Reactor Regulation Related To Amendment No. 134 To Facility Operating License No. NPF-43, Detroit Edison Company Fermi-2, Docket No. 50-341, October 7, 1999.
13. NRC letter from D. Eisenhut to R.Gridley, GE, January 28, 1980.
14. GE 14 Fuel Design Cycle – Independent Analysis for Fermi Unit 2, GE-NE-0000-0025-3282-00, Table 4-3, November 2004.

TABLE 4.5-1 DEFORMATION LIMIT

(For Reactor Internal Structures Only)

Either One of (Not Both)[a]	General Limit
a. $\frac{DP}{DL}$	$\leq \frac{0.9}{SF_{min}}$
b. $\frac{DP}{DE}$	$\leq \frac{1.0}{SF_{min}}$

where

DP = permissible deformation under stated conditions of normal, upset, emergency, or faulted

DL = analyzed deformation that could cause a system loss of function[b]

DE = experimentally determined deformation that could cause a system loss of function

SF_{min} = minimum safety factor

[a] Equation b. is not used because equation a criteria are met. (Equation b. will not be used unless supporting data are provided to the NRC by GE.)

[b] "Loss of function" can only be defined quite generally until attention is focused on the component of interest. In cases of interest, where deformation limits can affect the function of equipment and components, they will be specifically delineated. From a practical viewpoint, it is convenient to interchange some deformation condition at which function is ensured with the loss of function condition if the required safety margins from the functioning conditions can be achieved. Therefore it is often unnecessary to determine the actual loss of function condition because this interchange procedure produces conservative and safe designs. Examples where deformation limits apply are control rod drive alignment and clearances for proper insertion and core support deformation causing fuel disarrangement or excess leakage of any component.

TABLE 4.5-2 PRIMARY STRESS LIMIT

(For Reactor Internal Structures Only)

Any One of (No More Than One Required)[a]		General Limit
a.	$\frac{PE}{PN}$	$\leq \frac{2.25}{SF_{min}}$
b.	$\frac{LP}{CL}$	$\leq \frac{1.5}{SF_{min}}$
c.	$\frac{PE}{US}$	$\leq \frac{0.75}{SF_{min}}$
d.	$\frac{EP}{US}$	$\leq \frac{0.9}{SF_{min}}$
e.	$\frac{LP}{PL}$	$\leq \frac{0.9}{SF_{min}}$
f.	$\frac{LP}{UF}$	$\leq \frac{0.9}{SF_{min}}$
g.	$\frac{LP}{LE}$	$\leq \frac{1.0}{SF_{min}}$

where

PE = primary stresses evaluated on an elastic basis. The effective membrane stresses are to be averaged through the load-carrying section of interest. The simplest average bending, shear, or torsion stress distribution that will support the external loading will be added to the membrane stresses at the section of interest

PN = permissible primary stress levels under normal or upset conditions under ASME Boiler and Pressure Vessel Code Section III

LP = permissible load under stated conditions of normal, upset, emergency, or faulted

CL = lower bound limit load with yield point equal to $1.5S_m$, where S_m is the tabulated value of allowable stress at temperature of the ASME III Code or its equivalent. The "lower bound limit load" is here defined as that produced from the analysis of an ideally plastic (nonstrain-hardening) material where deformations increase with no further increase in applied load. The lower bound load is one in which the material everywhere satisfies equilibrium and nowhere exceeds the defined material yield strength using either a shear theory or a strain energy of distortion theory to relate multiaxial yield to the uniaxial case

US = conventional ultimate strength at temperature or loading, which would cause a system malfunction, whichever is more limiting

EP = elastic-plastic evaluated nominal primary stress. Strain hardening of the material may be used for the actual monotonic stress-strain curve at the temperature of loading, or any approximation to the actual stress-strain curve that everywhere has a lower stress for the same strain than the

actual monotonic curve may be used. Either the shear or strain energy of distortion flow rule may be used

PL = plastic instability load. The "plastic instability load" is defined here as the load at which any load-bearing section begins to diminish its cross-sectional area at a faster rate than the strain hardening can accommodate the loss in area. This type of analysis requires a true stress-true strain curve or a close approximation based on monotonic loading at the temperature of loading

UF = ultimate load from fracture analyses. For components which involve sharp discontinuities (local theoretical stress concentration < 3) the use of a "fracture mechanics" analysis where applicable, utilizing measurements of plane strain fracture toughness, may be applied to compute fracture loads. Correction for finite plastic zones and thickness effects as well as gross yielding may be necessary. The methods of linear elastic stress analysis may be used in the fracture analysis where its use is clearly conservative or supported by experimental evidence. Examples where "fracture mechanics" may be applied are for fillet welds or end-of-fatigue-life crack propagation

LE = ultimate load or loss of function load as determined from experiment. In using this method, account shall be taken of the dimensional tolerances that may exist between the actual part and the tested part or parts as well as differences that may exist in the ultimate tensile strength of the actual part and the tested parts. The guide to be used in each of these areas is that the experimentally determined load shall use adjusted values to account for material property and dimension variations, each of which has no greater probability than 0.1 of being exceeded in the actual part

---

[a] Equations e., f., and g. are not used because criteria a., b., c., and d. are met. (Equations e., f., and g. will not be used unless supporting data are provided to the NRC by GE.)

TABLE 4.5-3 BUCKLING STABILITY LIMIT

(For Reactor Internal Structures Only)

Any One of (No More Than One Required)[a]		General Limit
a.	$\frac{LP}{PN}$	$\leq \frac{2.25}{SF_{min}}$
b.	$\frac{LP}{SL}$	$\leq \frac{0.9}{SF_{min}}$
c.	$\frac{LP}{SE}$	$\leq \frac{1.0}{SF_{min}}$

where

LP = permissible load under stated conditions of normal, upset, emergency, or faulted

PN = applicable code normal event permissible load

SL = stability analysis load. The ideal buckling analysis is often sensitive to otherwise minor deviations from ideal geometry and boundary conditions. These effects shall be accounted for in the analysis of the buckling stability load. Examples of this are ovality in externally pressurized shells or eccentricity of column members

SE = ultimate buckling collapse load as determined from experiment. In using this method, account shall be taken of the dimensional tolerances that may exist between the actual part and the tested part. The guide to be used in each of these areas is that the experimentally determined load shall be adjusted to account for material property and dimension variations, each of which has no greater probability than 0.1 of being exceeded in the actual part

[a] Equation c. is not used because criteria a. and b. are met. (Equation c. will not be used unless supporting data are provided to the NRC by GE.)

TABLE 4.5-4 FATIGUE LIMIT

(For Reactor Internal Structures Only)

Summation of Fatigue Damage Usage with Design and Operation Loads Following Miner Hypotheses[a]

Any One of (No More Than One Required)	Limit for Normal and Upset Design Conditions
a. Mean fatigue[b,c] cycle usage from analyses	≤ 0.05
b. Mean fatigue[b,c] cycle usage from test	≤ 0.33
c. Design fatigue cycle usage from analysis using the method of Table 4.5-5	≤ 1.0

a. Miner, M. A., "Cumulative Damage in Fatigue," Journal of Applied Mechanics, Vol. 12, ASME, 67, pp. A159-A164, September 1945.

b. Fatigue failure is defined here as a 25 percent area reduction for a load-carrying member which is required to function, or excess leakage, whichever is more limiting.

c. Equations a. and b. are not used because criterion c. is met. (Equations a. and b. will not be used unless supporting data are provided to the NRC by GE.)

TABLE 4.5-5 CORE SUPPORT STRUCTURES: STRESS CATEGORIES AND LIMITS OF STRESS INTENSITY FOR NORMAL AND UPSET CONDITIONS

STRESS CATEGORY	PRIMARY STRESSES		SECONDARY STRESSES	PEAK STRESSES
	MEMBRANE, P_m (NOTES 4, 7 & 8)	BENDING, P_b (NOTES 4, 7 & 8)	MEMBRANE AND BENDING SECONDARY, Q (NOTES 2, 4 & 6)	PEAK, F (NOTES 2, 4 & 6)
NORMAL AND UPSET	P_m S_m ELASTIC ANALYSIS (NOTE 6) OR $.67L_L$ OR LIMIT ANALYSIS (NOTE 10) $.44L_u$ TEST (NOTE 11)	$P_m + P_b$ $1.5S_m$ ELASTIC ANALYSIS (NOTE 6) OR $.67L_L$ OR LIMIT ANALYSIS (NOTE 10) $.44L_u$ TEST (NOTE 11)	$P_m + P_b + Q$ $3S_m$ ELASTIC ANALYSIS (NOTE 1) OR S_L OR PLASTIC ANALYSIS (NOTE 5) FOR CYCLES LESS THAN 1000, USE PEAK (NOTE 12)	$P_m + P_b + Q + F$ ELASTIC FATIGUE (NOTES 3 & 9) S_a $P_m + P_b + Q + F$ S_a ELASTIC-PLASTIC FATIGUE (NOTES 3, 9 & 12)

Note 1: This limitation applies to the range of stress intensity. When the secondary stress is due to a temperature excursion at the point at which the stresses are being analyzed, the value of S_m shall be taken as the average of the S_m values tabulated in Tables I-1.1, I-1.2, and I-1.3 of the ASME Boiler and Pressure Vessel Code Section III (ASME III) for the highest and the lowest temperature of the metal during the transient. When part of the secondary stress is due to mechanical load, the value of S_m shall be taken as the S_m value for the highest temperature of the metal during the transient.

Note 2: The stresses in Category Q are those parts of the total stress that are produced by thermal gradients, structural discontinuities, etc., and do not include primary stresses that may also exist at the same point. It should be noted, however, that a detailed stress analysis frequently gives the combination of primary and secondary stresses directly, and, when appropriate, this calculated value represents the total of $P_m + P_b + Q$, and not Q alone. Similarly, if the stress in Category F is produced by a stress concentration, the quantity F is the additional stress produced by the notch, over and above the nominal stress. For example, if a plate has a nominal stress intensity, $P_m = S$, $P_b = 0$, $Q = 0$, and a notch with a stress concentration K is introduced, then $F = P_m (K - 1)$, and the peak stress intensity equals $P_m + P_m (K - 1) = KP_m$.

TABLE 4.5-5 CORE SUPPORT STRUCTURES: STRESS CATEGORIES AND LIMITS OF STRESS INTENSITY FOR NORMAL AND UPSET CONDITIONS

Note 3: The value of S_a is obtained from the fatigue curves (Figures I-9.1 and I-9.2 of ASME III). The allowable stress intensity for the full range of fluctuation is $2S_a$.

Note 4: The symbols P_m, P_b, Q, and F do not represent single quantities, but rather sets of six quantities representing the six stress components σ_t, σ_l, σ_r, τ_{t1}, τ_{1r}, and τ_{rt}.

Note 5: The quantity S_L denotes the structural action of shakedown load, as defined in Paragraph NB-3213.18 of ASME III, calculated on a plastic basis as applied to a specific location on the structure.

Note 6: The triaxial stresses represent the algebraic sum of the three primary principal stresses ($\sigma_1+\sigma_2+\sigma_3$) for the combination of stress components. Where uniform tension loading is present, triaxial stresses are limited to $4S_m$.

Note 7: For configurations in which compressive stresses occur, the stress limits shall be revised to take into account critical buckling stresses [see Paragraph NB-3211(c) of ASME III]. For external pressure, the permissible "equivalent static" external pressure shall be as specified by the rules of Paragraph NB-3133 of ASME III. Where dynamic pressures are involved, the permissible external pressure shall be limited to 25 percent of the dynamic instability pressure.

Note 8: When loads are transiently applied, consideration should be given to the use of dynamic load amplification and possible change in the modulus of elasticity.

Note 9: In the fatigue data curves, where the number of operating cycles is less than 10, the S_a value should be used for 10 cycles; where the number of operating cycles is more than 10^6, the S_a value should be used for 10 cycles.

Note 10: The quantity L_L is the lower bound limit load with yield point equal to $1.5S_m$, where S_m is the tabulated value of allowable stress at temperature as contained in ASME III. The "lower bound limit load" is here defined as that produced from the analysis of an ideally plastic (nonstrain-hardening) material where deformations increase with no further increase in applied load. The lower bound load is one in which the material everywhere satisfies equilibrium and nowhere exceeds the defined material yield strength, using either a shear theory or a strain energy of distortion theory to relate multiaxial yielding to the uniaxial case.

Note 11: For normal and upset conditions, the limits on primary membrane plus primary bending need not be satisfied in a component if it can be shown from the test of a proto-type or model that the specified loads (dynamic or static equivalent) do not exceed 44 percent of L_u, where L_u is the ultimate load or the maximum load or load combination used in the test. In using this method, account shall be taken of the size effect and dimensional tolerances that may exist between the actual part and the test part or parts as well as the differences that may exist in

TABLE 4.5-5 CORE SUPPORT STRUCTURES: STRESS CATEGORIES AND LIMITS OF STRESS INTENSITY FOR NORMAL AND UPSET CONDITIONS

the ultimate strength or other governing material properties of the actual part and the tested part to ensure that the loads obtained from the test are a conservative representation of the load-carrying capability of the actual component under the postulated loading for normal and upset conditions.

Note 12: The allowable value for the maximum range of this stress intensity is $3S_m$, except for cyclic events that occur less than 1000 times during the design life of the plant. For this exception, in lieu of meeting the $3S_m$ limit, an elastic-plastic fatigue analysis in accordance with ASME III may be performed to demonstrate that the cumulative fatigue usage attributable to the combination of these low events, plus all other cyclic events, does not exceed a fatigue usage value of 1.0.

TABLE 4.5-6 CORE SUPPORT STRUCTURES: STRESS CATEGORIES AND LIMITS OF STRESS INTENSITY FOR EMERGENCY CONDITIONS

STRESS CATEGORY	PRIMARY STRESSES		SECONDARY STRESSES	PEAK STRESSES
	MEMBRANE, P_m (NOTES 1, 2 & 10)	BENDING, P_b (NOTES 1, 2 &10)	MEMBRANE AND BENDING SECONDARY, Q	PEAK, F
EMERGENCY (NOTE 9)	P_m $1.5S_m$ ELASTIC ANALYSIS (NOTE 3) OR L_L LIMIT ANALYSIS (NOTE 4) OR $1.5S_m$ PLASTIC ANALYSIS (NOTE 6) OR $.6L_e$ TEST (NOTE 7) OR S_E STRESS RATIO ANALYSIS (NOTE 8)	$P_m + P_b$ $2.25S_m$ ELASTIC ANALYSIS (NOTE 3) OR L_L LIMIT ANALYSIS (NOTE 4) OR $2.25S_m$ PLASTIC ANALYSIS (NOTES 5 & 6) OR $.5S_u$ (NOTE 5) OR $.6L_e$ TEST (NOTE 7) OR KS_E STRESS RATIO ANALYSIS (NOTE 8)	EVALUATION NOT REQUIRED	EVALUATION NOT REQUIRED

Note 1: The symbols P_m, P_b, Q, and F do not represent single quantities, but rather sets of six quantities representing the six stress components σ_t, σ_l, σ_r, τ_{rl}, τ_{lr}, and τ_{rt}.

Note 2: For configurations in which compressive stresses occur, stress limits shall be revised to take into account critical buckling stresses. For external pressure, the permissible "equivalent static" external pressure shall be taken as 150 percent of that permitted by the rules of Paragraph NB-3133 of the ASME Boiler and Pressure Vessel Code, Section III (ASME III). Where dynamic pressures are involved, the permissible external pressure shall satisfy the preceding requirements or be limited to 50 percent of the dynamic instability pressure.

Note 3: The triaxial stresses represent the algebraic sum of the three primary principal stresses ($\sigma_1+\sigma_2+\sigma_3$) for the combination of stress components. Where uniform tension loading is present, triaxial stresses should be limited to $6S_m$.

Note 4: The quantity L_L is lower bound limit load with yield point equal to $1.5S_m$ (where S_m is the tabulated value of allowable stress at temperature as contained in ASME III). The "lower bound limit load" is here defined as that produced from the analysis of an ideally plastic (nonstrain-hardening) material where

TABLE 4.5-6 CORE SUPPORT STRUCTURES: STRESS CATEGORIES AND LIMITS OF STRESS INTENSITY FOR EMERGENCY CONDITIONS

deformations increase with no further increase in applied load. The lower bound load is one in which the material everywhere satisfies equilibrium and nowhere exceeds the defined material yield strength, using either a shear theory or a strain energy of distortion theory to relate multiaxial yielding to the uniaxial case.

Note 5: The quantity S_u is the ultimate strength at temperature. Multiaxial effects on ultimate strength shall be considered.

Note 6: This plastic analysis uses an elastic-plastic evaluated nominal primary stress. Strain hardening of the material may be used for the actual monotonic stress-strain curve at the temperature of loading, or any approximation to the actual stress-strain curve that everywhere has a lower stress for the same strain than the actual monotonic curve may be used. Either the shear or strain energy of distortion flow rule shall be used to account for multiaxial effects.

Note 7: For emergency conditions, the stress limits need not be satisfied if it can be shown from the test of a prototype or model that the specified loads (dynamic or static equivalent) do not exceed 60 percent of L_e, where L_e is the ultimate load or the maximum load or load combination used in the test. In using this method, account shall be taken of the size effect and dimensional tolerances that may exist between the actual part and the tested part or parts as well as the differences that may exist in the ultimate strength or other governing material properties of the actual part and the tested parts to ensure that the loads obtained from the test are a conservative representation of the load-carrying capability of the actual component under postulated loading for emergency conditions.

Note 8: Stress ratio is a method of plastic analysis that uses the stress ratio combinations (combination of stresses that consider the ratio of the actual stress to the allowable plastic or elastic stress) to compute the maximum load and strain-hardening that the material can carry. The term K is defined as the section factor; $S_e \leq 2S_m$ for primary membrane loading.

Note 9: Where deformation is of concern in a component, the deformation shall be limited to two-thirds of the value given for emergency conditions in the design specification.

Note 10: When loads are transiently applied, consideration should be given to the use of dynamic load amplification and possible change in the modulus of elasticity.

TABLE 4.5-7 CORE SUPPORT STRUCTURES: STRESS CATEGORIES AND LIMITS OF STRESS INTENSITY FOR FAULTED CONDITIONS

STRESS CATEGORIES	PRIMARY STRESSES		SECONDARY STRESSES	PEAK STRESSES
	MEMBRANE, P_m (NOTES 1, 2 & 3)	BENDING, P_b (NOTES 1, 2 & 3)	MEMBRANE AND BENDING SECONDARY, Q	PEAK, F
FAULT (NOTE 7)	P_m $2.4S_m$ ELASTIC ANALYSIS OR $.75S_u$ (NOTE 5) OR $1.33L_L$ LIMIT ANALYSIS (NOTE 4) OR $.67S_u$ PLASTIC ANALYSIS (NOTES 5 & 6) OR $.8L_F$ TEST (NOTE 9) OR S_F STRESS-RATIO ANALYSIS (NOTE 8)	$P_m + P_b$ $3.0S_m$ ELASTIC ANALYSIS OR $1.33L_L$ LIMIT ANALYSIS (NOTE 4) OR $.75S_u$ PLASTIC ANALYSIS (NOTES 5 & 6) OR $.8L_F$ TEST (NOTE 7) OR KS_F STRESS-RATIO ANALYSIS (NOTE 8)	EVALUATION NOT REQUIRED	EVALUATION NOT REQUIRED

Note 1: The symbols P_m, P_b, Q, and F do not represent quantities but rather sets of six quantities representing the six stress components, σ_t, σ_l, σ_r τ_{tl},τ_{lr}, and τ_{rt}.

Note 2: When loads are transiently applied, consideration should be given to the use of dynamic load amplification and possible changes in the modulus of elasticity.

Note 3: For configurations where compressive stresses occur, stress limits take into account critical buckling stresses. For external pressure, the permissible "equivalent static" external pressure shall be taken as 2.5 times that given by rules of paragraph NB-3133 of the ASME Boiler and Pressure Vessel Code Section III (ASME III). Where dynamic pressures are involved, the permissible external pressure shall satisfy the preceding requirements or shall be limited to 75 percent of the dynamic instability pressure.

Note 4: The quantity L_L is the lower bound limit load with yield point equal to $1.5S_m$ (where S_m is the tabulated value of allowable stress at temperature as contained in ASME III). The "lower bound limit load" is here defined as that produced from the analysis of an ideally plastic (nonstrain-hardening) material where deformations increase with no further increase in applied load. The lower

TABLE 4.5-7 CORE SUPPORT STRUCTURES: STRESS CATEGORIES AND LIMITS OF STRESS INTENSITY FOR FAULTED CONDITIONS

bound load is one in which the material everywhere satisfies equilibrium and nowhere exceeds the defined material yield strength, using either a shear theory or a strain energy of distortion theory to relate multiaxial yielding to the uniaxial case.

Note 5: The quantity S_u is the ultimate strength at temperature. Multiaxial effects on ultimate strength shall be considered.

Note 6: This plastic analysis uses an elastic-plastic evaluated nominal primary stress. Strain hardening of the material may be used for the actual monotonic stress-strain curve at the temperature of loading, or any approximation to the actual stress-strain curve that everywhere has a lower stress for the same strain as the actual curve may be used; either the maximum shear stress or the strain energy of distortion flow rule shall be used to account for multiaxial effects.

Note 7: For faulted conditions, the stress limits need not be satisfied if it can be shown from the test of a prototype or model that the specified loads (dynamic or static equivalent) do not exceed 80 percent of L_F, where L_F is the ultimate load or load combination used in the test.

In using this method, account shall be taken of the size effect and dimensional tolerances as well as differences that may exist in the ultimate strength or other governing material properties of the actual part and the tested parts to ensure that the loads obtained from the test are a conservative representation of the load-carrying capability of the actual component under the postulated loading for faulted condition.

Note 8: Stress ratio is a method of plastic analysis that uses the stress ratio combinations (combination of stresses that consider the ratio of the actual stress to the allowable plastic or elastic stress) to compute the maximum load and strain-hardening that the material can carry. The term K is defined as the section factor; S_F is the lesser of $2.4S_m$ or $0.75S_u$ for primary membrane loading.

Note 9: Where deformation is of concern in a component, the deformation shall be limited to 80 percent of the value for faulted conditions in the design specifications.

TABLE 4.5-8 DESIGN LOADING CONDITIONS AND COMBINATIONS

Operating Condition and Stress Limits[a]	Design Loading Conditions and Combinations
Normal and upset	N and A_D or N and U
Emergency	N and R or other conditions which have a 40-year encounter probability from 10^{-1} to 10^{-3}
Faulted	N and A_m and $\overline{R}$ or other conditions which have a 40-year encounter probability from 10^{-3} to 10^{-6}

where

N = normal loads

U = upset loads excluding earthquake

A_D = operating-basis earthquake (OBE), including any associated transients

A_m = safe-shutdown earthquake (SSE), including any associated transients

R = any auxiliary pipe rupture loading, including any associated transients; pipe rupture loadings are not directly considered on piping itself because this is handled by a failure mode analysis

$\overline{R}$ = primary loadings which result from rupture of a main steam line or a recirculation line

[a] The design stress, deformation, and fatigue limits are for RPV and appurtenances - ASME Code Section III.

For core support structures - Refer to Tables 4.5-5, 4.5-6, and 4.5-7.

For reactor internal structures - Refer to Tables 4.5-1 through 4.5-4.

TABLE 4.5-9 PRESSURE DIFFERENTIALS ACROSS REACTOR PRESSURE VESSEL INTERNALS

Reactor Component	Pressure Difference Maximum Occuring During a Steam Line Break (psid)	
	Case 1 (a)	Case 2 (b)
Core plate and guide tube	22.5	25.5
Shroud support ring and lower shroud	45.0	45.0
Upper shroud and shroud head	26.0	26.0
Average channel wall (bottom)	14.0	10.6
Top guide	1.1	1.9

NOTE: For Faulted Conditions using GE14 Fuel see Reference 14.

Case 1 – Reactor initially at 1078 psia, 3694 MWt, 105 x 10^6 lb/hr core flow

Case 2 – Reactor initially at 1020 psia, 771 MWt, 116 x 10^6 lb/hr core flow

a-Data from Power Uprate Analysis (Reference 10)

b-Data from MEOD Analysis (Reference 11)

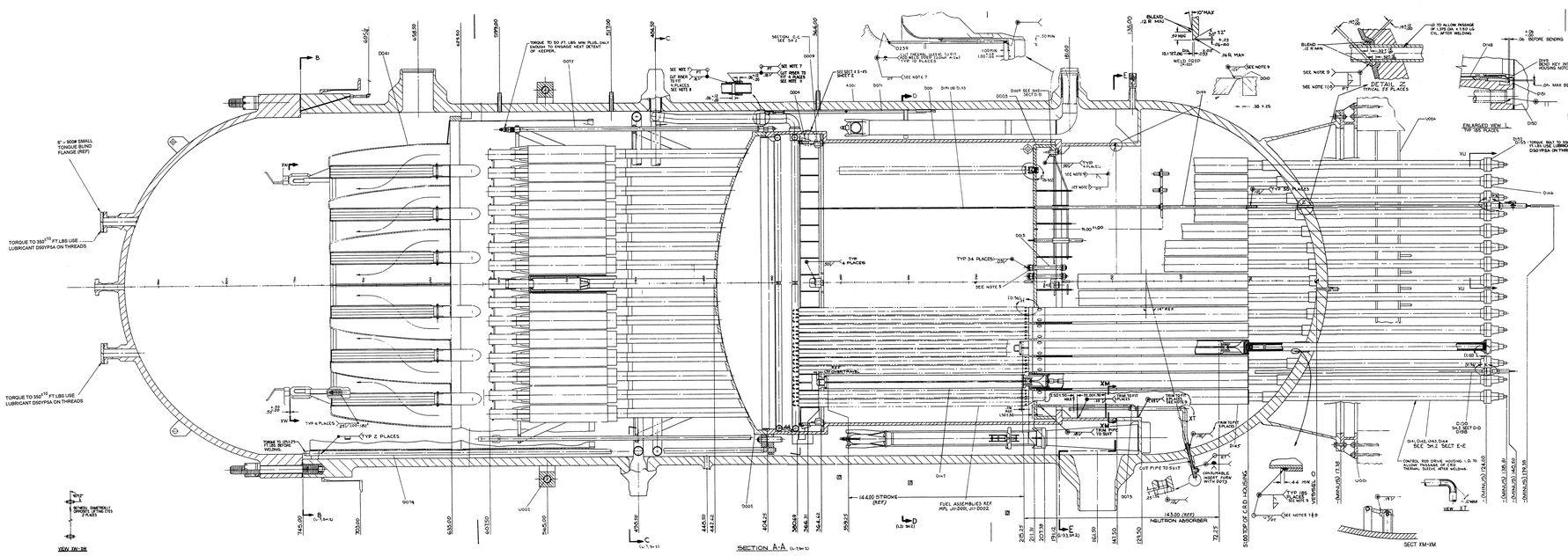

NOTES:

1. FOR REACTOR INSTALLATION AND ASSEMBLY REQUIREMENTS, SEE B11-3010, B11-3020 & B11-3030.
2. ALL FOUR (4) DIGIT PART NUMBERS (E.G. D001) ARE PREFIXED BY B11 (E.G. B11-D001) FOR MPL ITEM NUMBER IDENTIFICATION.
3. ALL ELEVATION DIMENSIONS ARE REFERENCE ONLY.
4. ALL FIELD WELDS ARE AUSTENITIC STAINLESS STEEL TO AUSTENITIC STAINLESS STEEL UNLESS OTHERWISE NOTED.
5. TORQUE CORE SUPPORT STUDS TO 2400 ± 20 FT LBS USE LUBRICANT DSOYPSR ON THREADS, NUT FACES & SPHER SURF OF WASHERS ONLY. DO NOT CONTAMINATE ANY OTHER SURFACES. REMOVE ALL EXCESS LUBRICANTS AFTER TIGHTENING.
6. FINAL ACCESSIBLE SURFACES OF ALL FIELD WELDS, EXCLUDING TACK WELDS, TO BE LIQUID PENETRANT TESTED.
7. ROOT PASS OF WELD TO BE LIQUID PENETRANT TESTED IN ADDITION TO FINAL ACCESSIBLE SURFACE.
8. SURFACE OF h WELD TO BE LIQUID PENETRANT TESTED IN ADDITION TO FINAL ACCESSIBLE SURFACE.
9. THIS WELD IS AUSTENITIC STAINLESS STEEL TO NI-CR-FE.
10. THIS WELD IS NI-CR-FE TO NI-CR-FE.
11. FILLET WELD CALLOUT IS MINIMUM. ACTUAL WELD SHALL EXTEND TO CORNER OF AS-BUILT SHOULDER.
12. TWO PASS MINIMUM SEAL WELD REQUIRED FOR REMAINING THREE SIDES.
13. AT TWO DIAMETERS 90° APART EQUALIZE GAPS AT THE END OF EACH DIAMETER WITHIN ±.015.

Fermi 2
UPDATED FINAL SAFETY ANALYSIS REPORT

FIGURE 4.5-1

GENERAL REACTOR ASSEMBLY DRAWING

REV 10 11/00

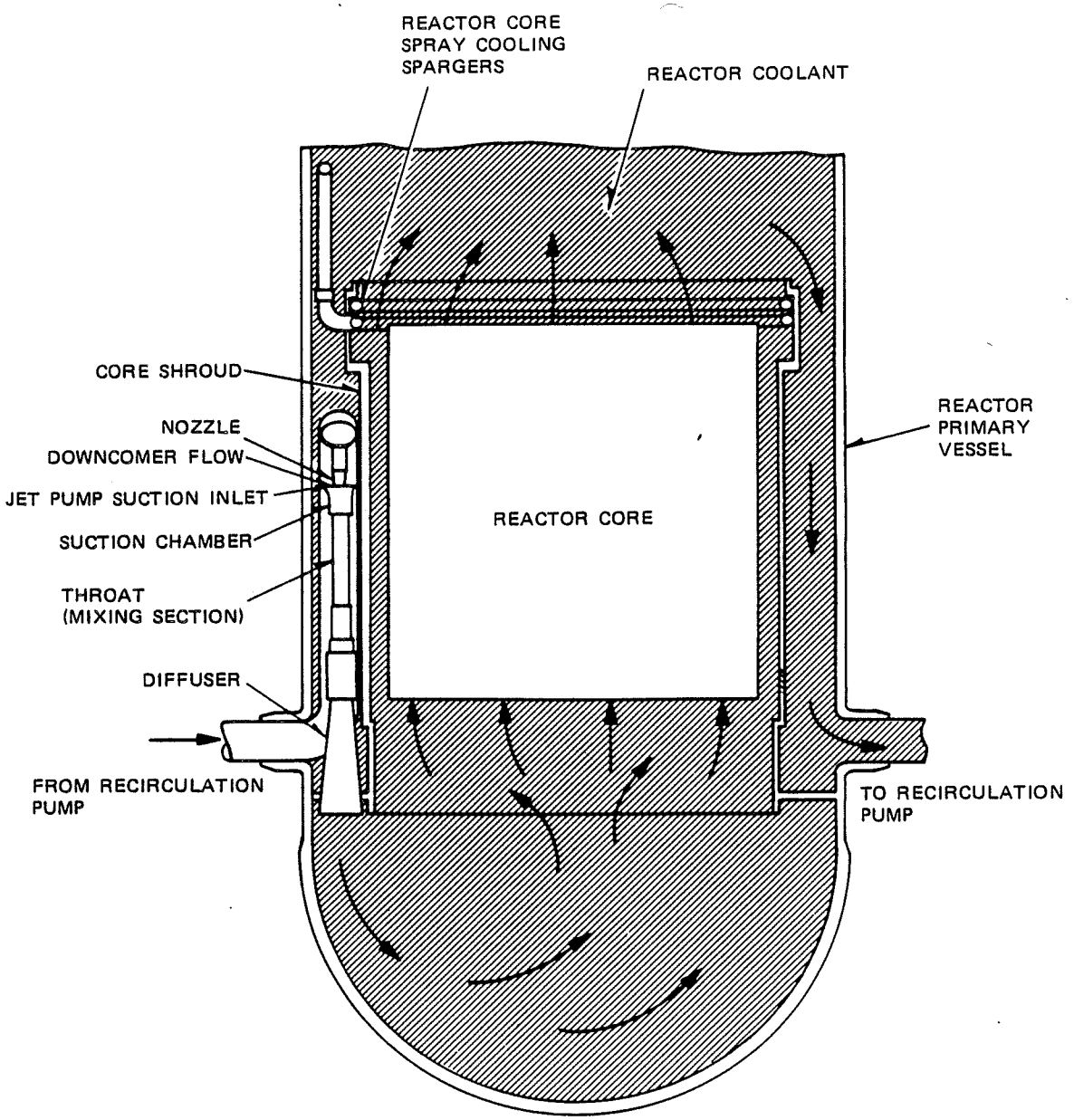

Fermi 2
UPDATED FINAL SAFETY ANALYSIS REPORT

FIGURE 4.5-2

REACTOR INTERNALS FLOW PATHS

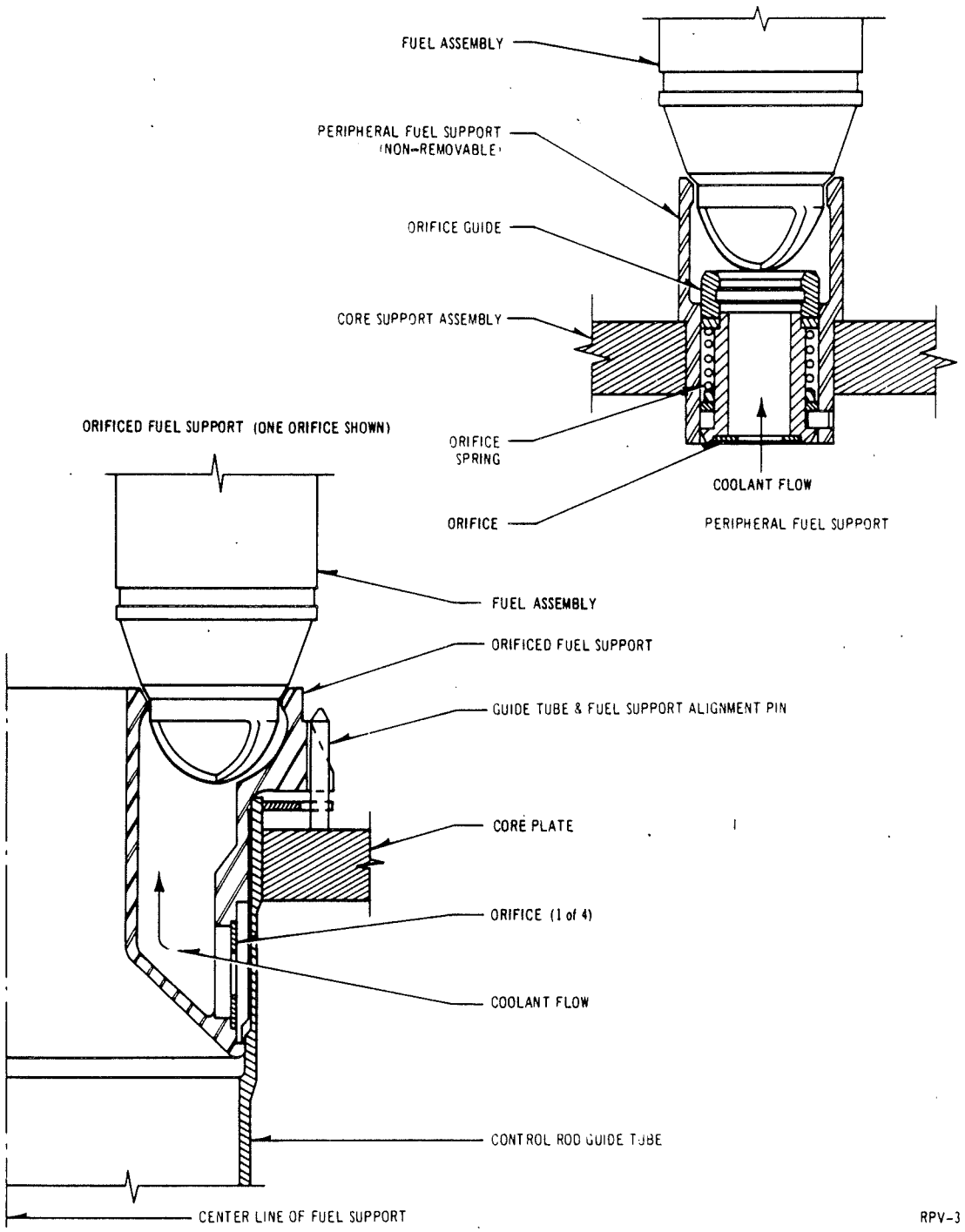

Fermi 2
UPDATED FINAL SAFETY ANALYSIS REPORT

FIGURE 4.5-3

FUEL SUPPORT PIECES

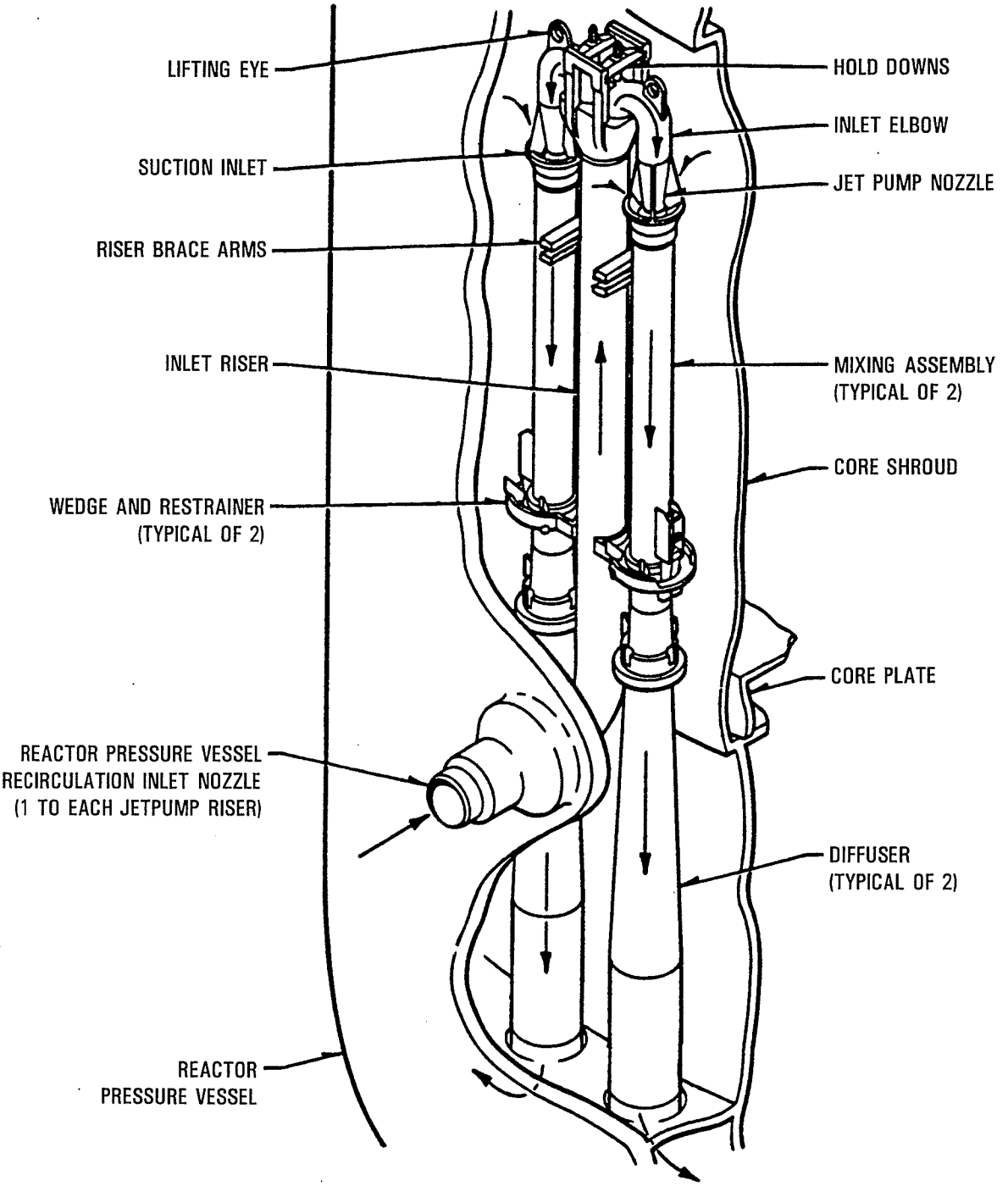

Fermi 2
UPDATED FINAL SAFETY ANALYSIS REPORT

FIGURE 4.5-4

JET PUMP ISOMETRIC

FIGURE 4.5-5 IS INTENTIONALLY DELETED

FIGURE 4.5-6 IS INTENTIONALLY DELETED

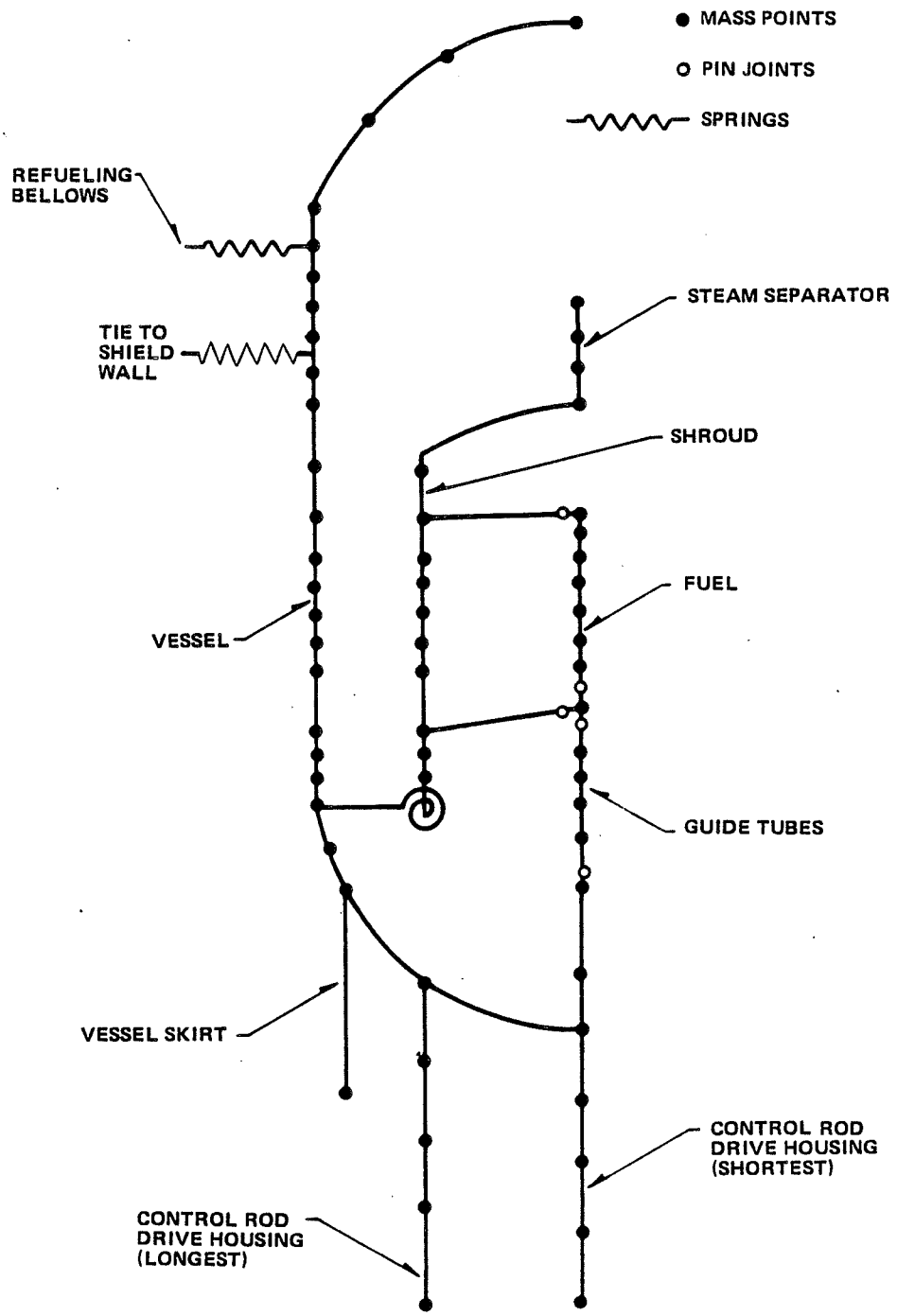

Fermi 2
UPDATED FINAL SAFETY ANALYSIS REPORT

FIGURE 4.5-7

SEISMIC MATHEMATICAL MODEL OF THE REACTOR PRESSURE VESSEL

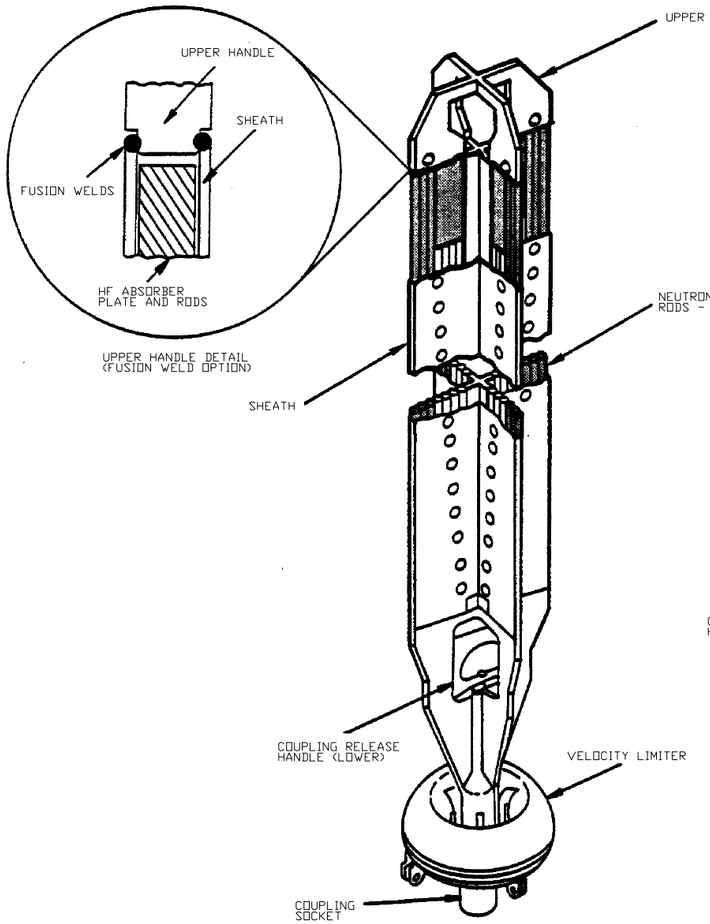

Typical Duralife 215 Control Rod Assembly

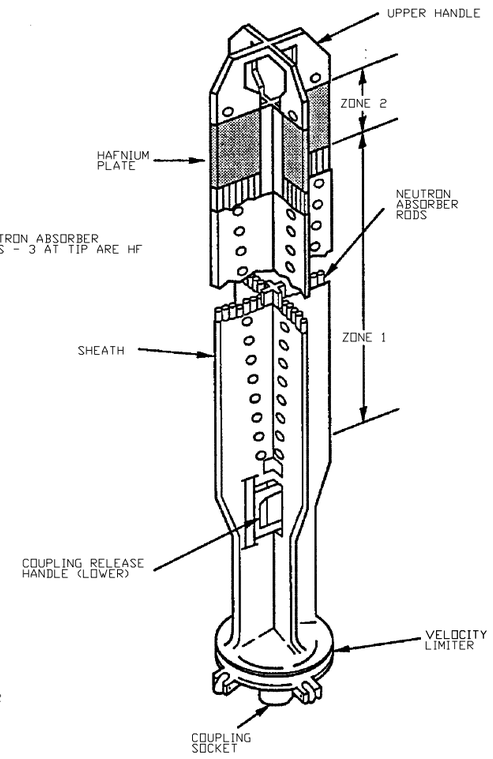

Typical Duralife 140 Control Rod Assembly

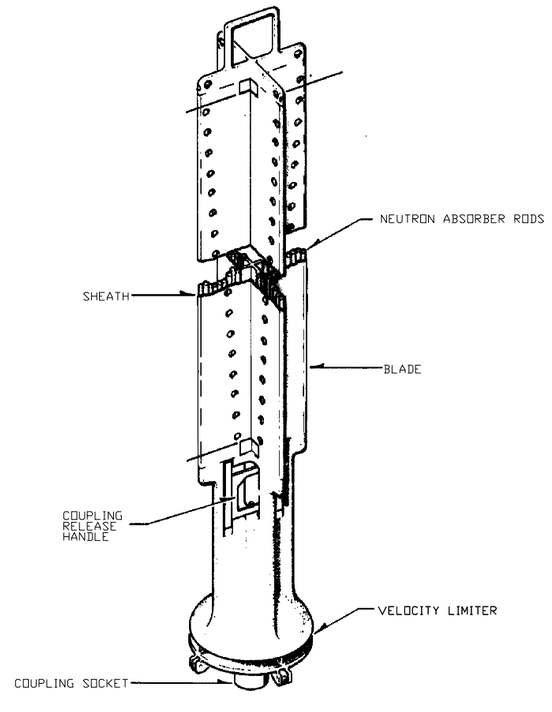

Typical Original Equipment

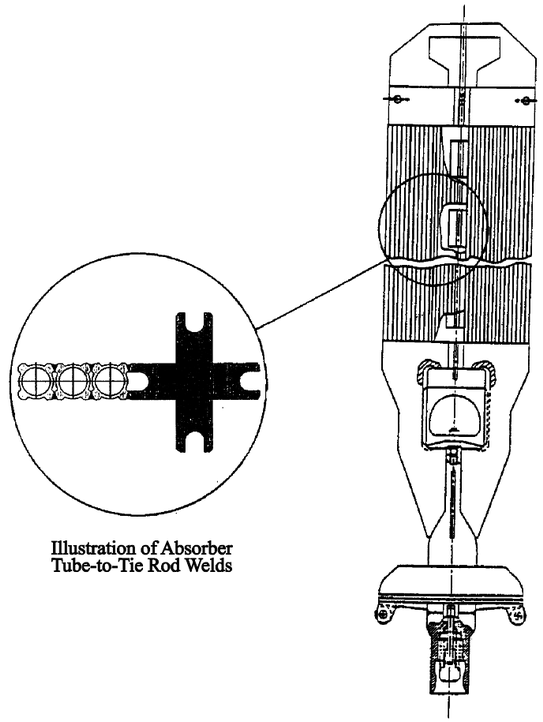

Typical Marathon Control Rod

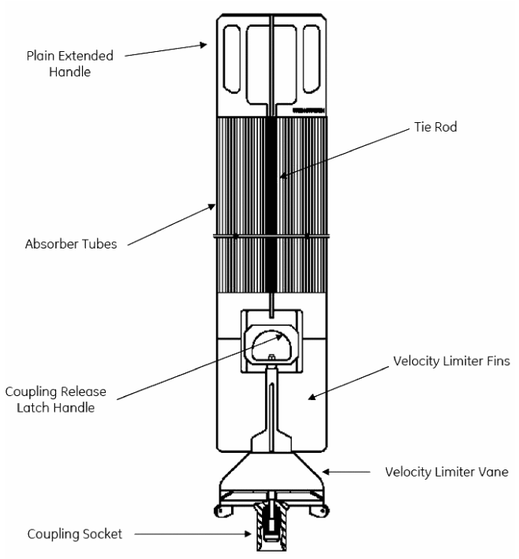

Typical Ultra-HD Control Rod

Fermi 2

UPDATED FINAL SAFETY ANALYSIS REPORT

FIGURE 4.5-8

TYPICAL CONTROL ROD ASSEMBLIES

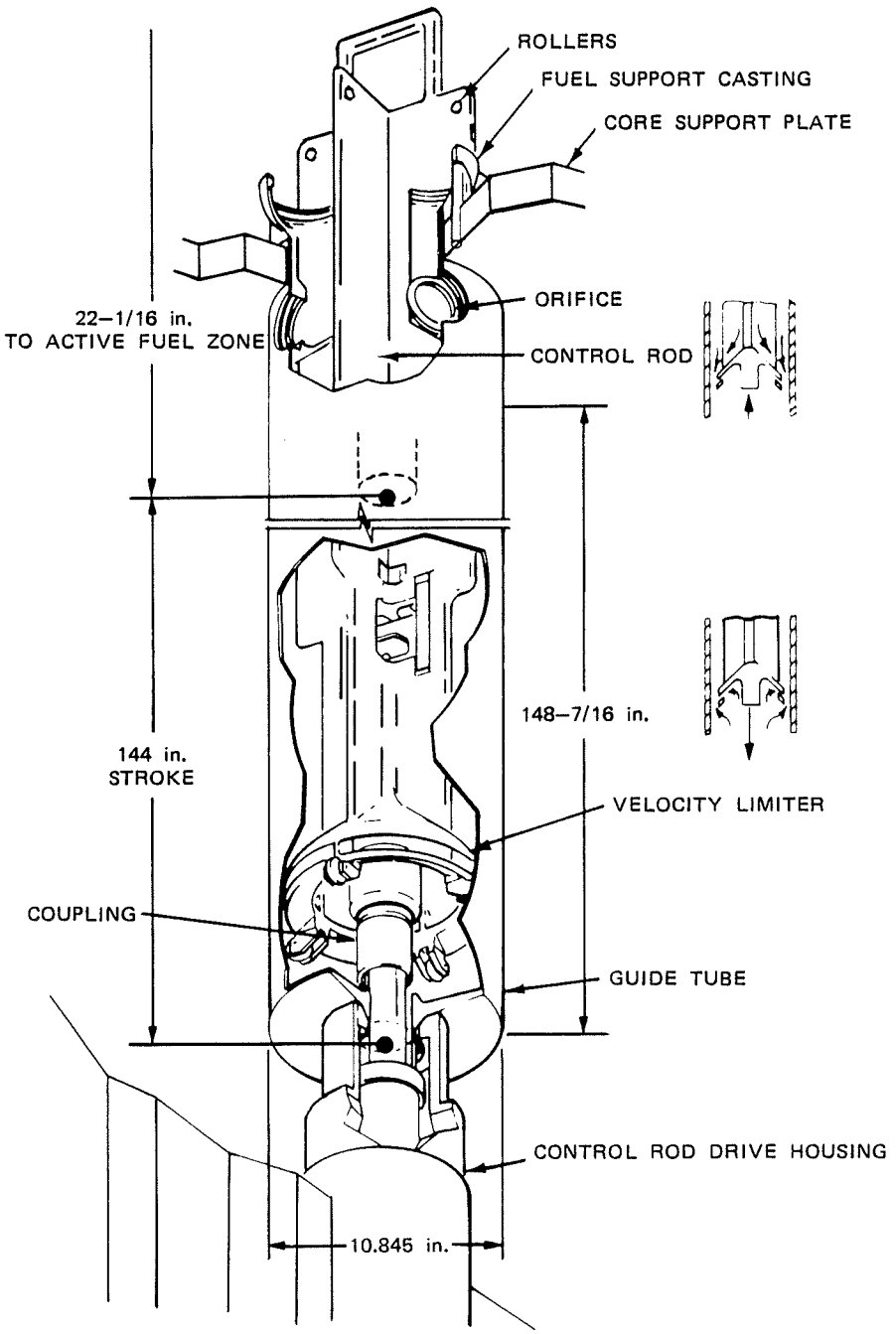

Fermi 2
UPDATED FINAL SAFETY ANALYSIS REPORT

FIGURE 4.5-9

CONTROL ROD VELOCITY LIMITER
DURALIFE 140

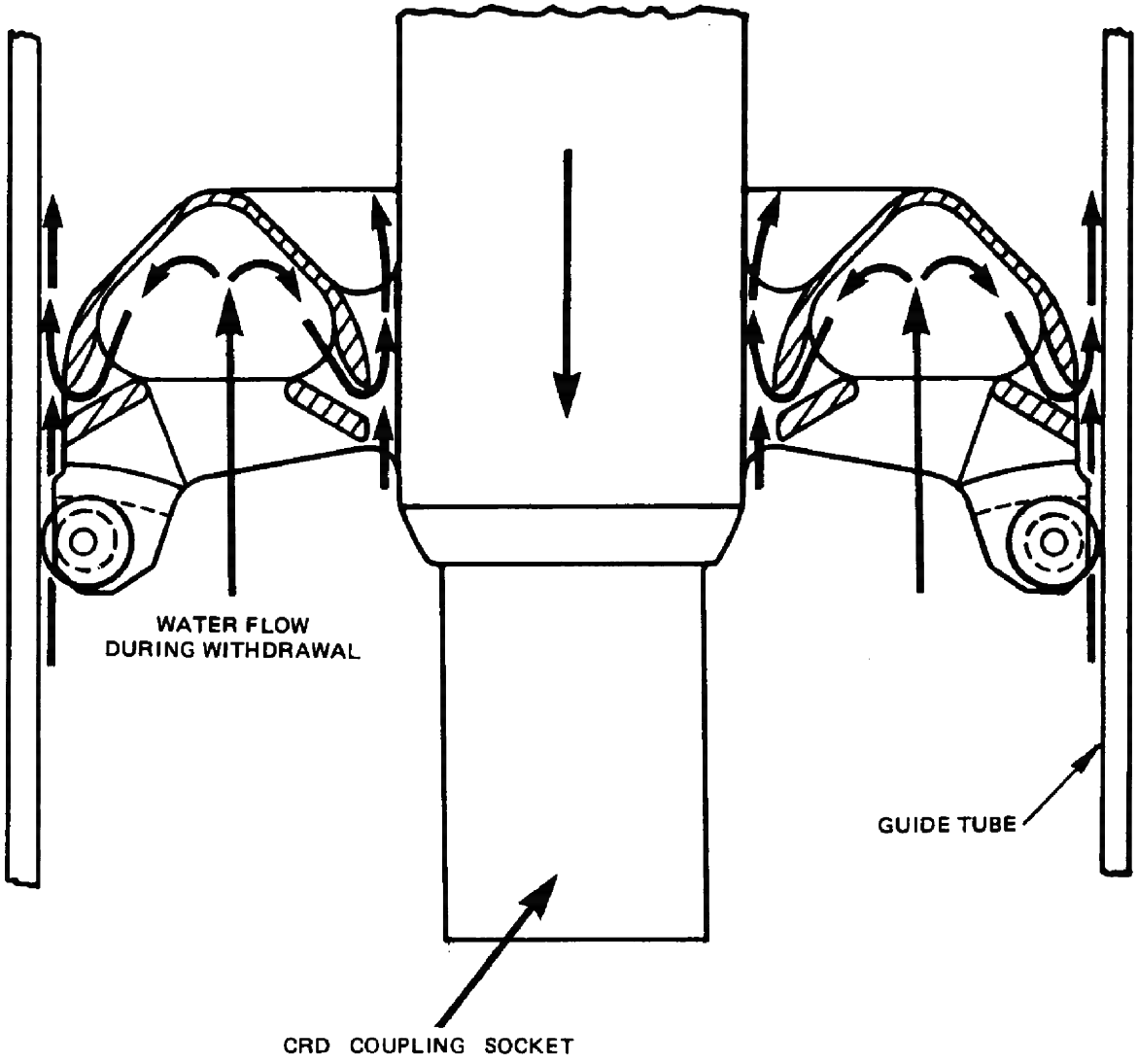

Fermi 2

UPDATED FINAL SAFETY ANALYSIS REPORT

FIGURE 4.5-10

TYPICAL CONTROL ROD
VELOCITY LIMITER OPERATION

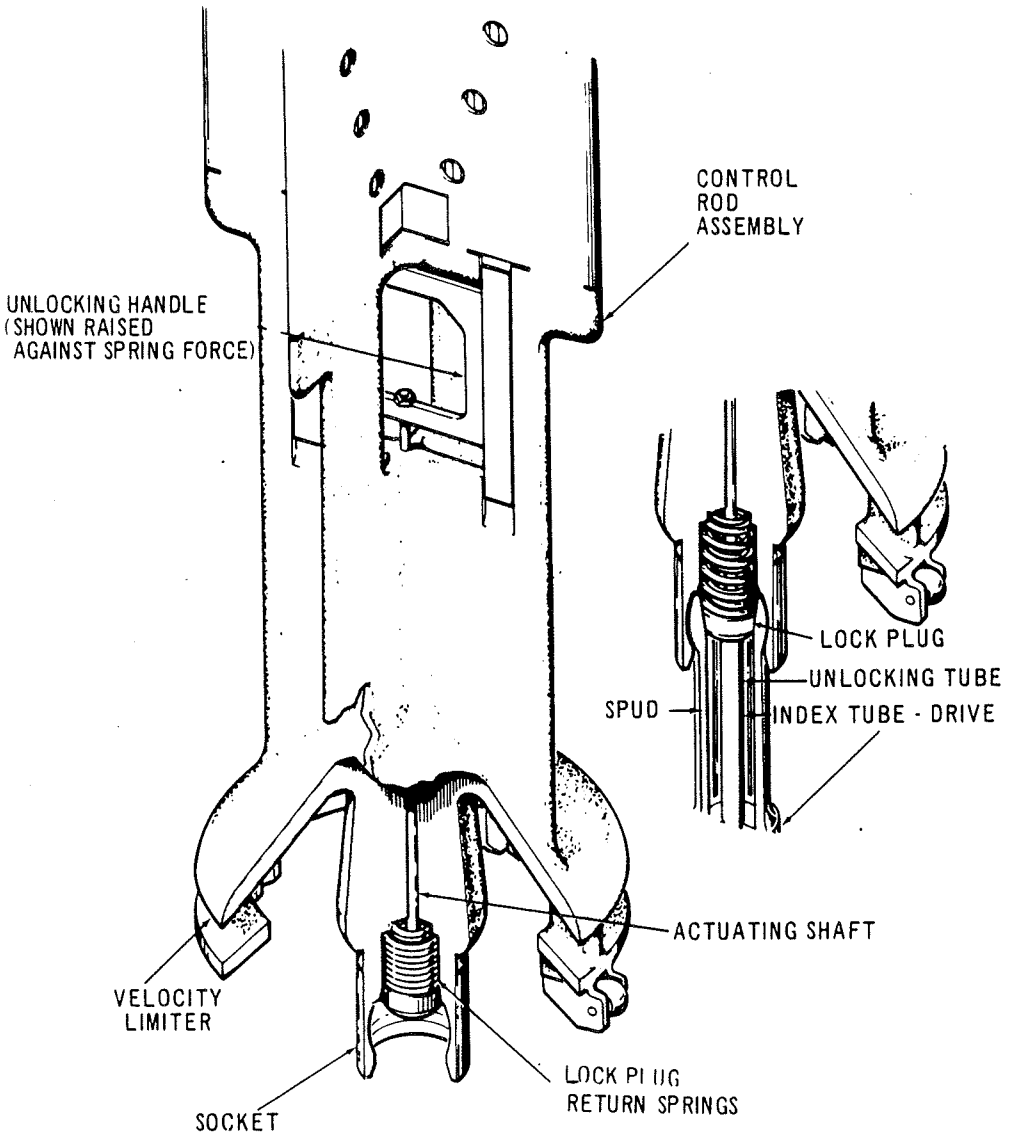

Fermi 2
UPDATED FINAL SAFETY ANALYSIS REPORT

FIGURE 4.5-11

CONTROL ROD AND CONTROL ROD DRIVE COUPLING

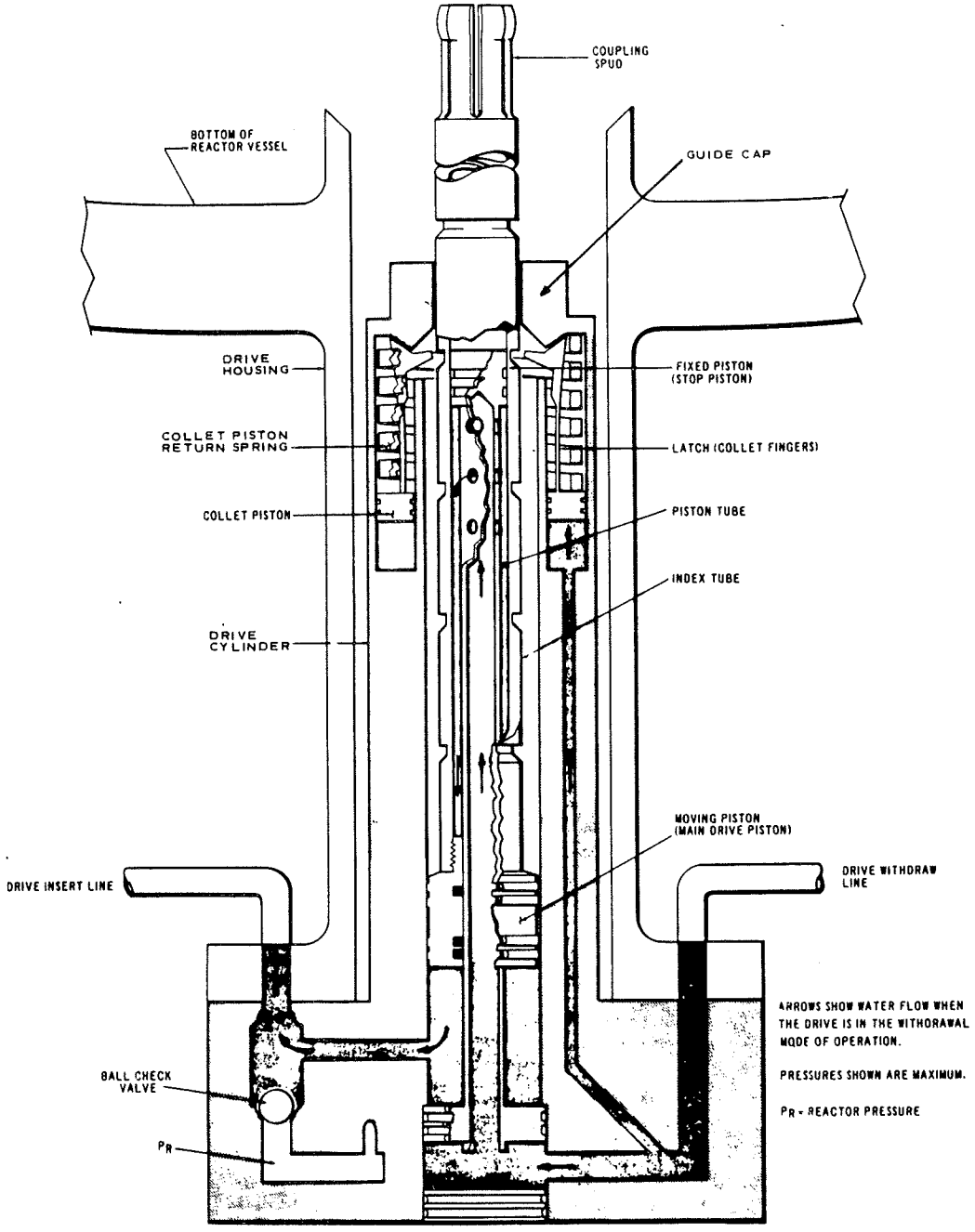

Fermi 2
UPDATED FINAL SAFETY ANALYSIS REPORT

FIGURE 4.5-12

CONTROL ROD DRIVE UNIT

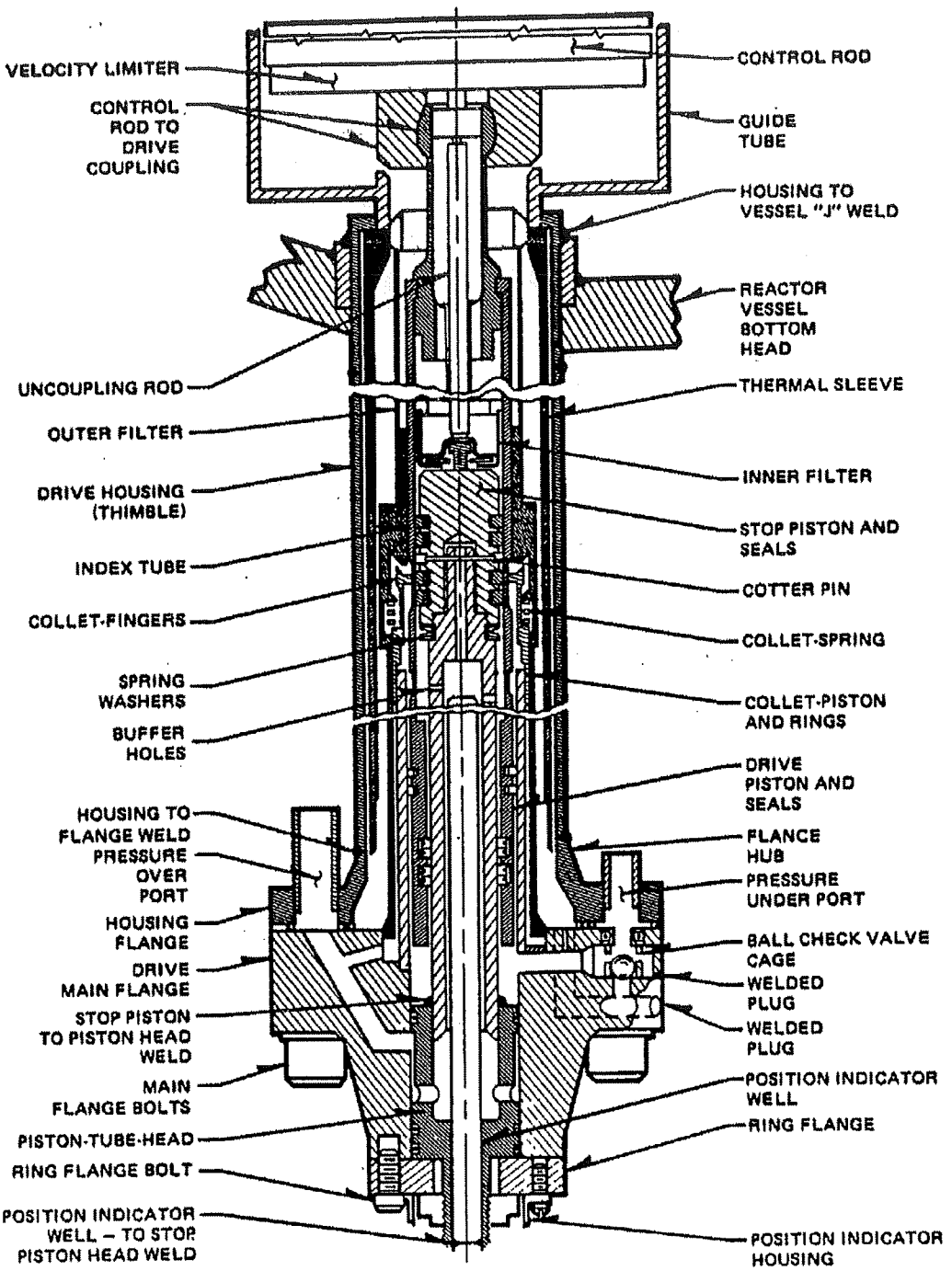

NOTES:

1. THERE ARE EQUIVALENT PISTON TUBE CONFIGURATIONS. EITHER MAYBE INSTALLED. SHOWN IS TYPICAL OF THE ORIGINAL DESIGN
2. WELD LOCATIONS ARE TYPICAL OF THE ORIGINAL PISTON TUBE DESIGN

FERMI 2
UPDATED FINAL SAFETY ANALYSIS REPORT

FIGURE 4.5-13

CONTROL ROD DRIVE UNIT SCHEMATIC

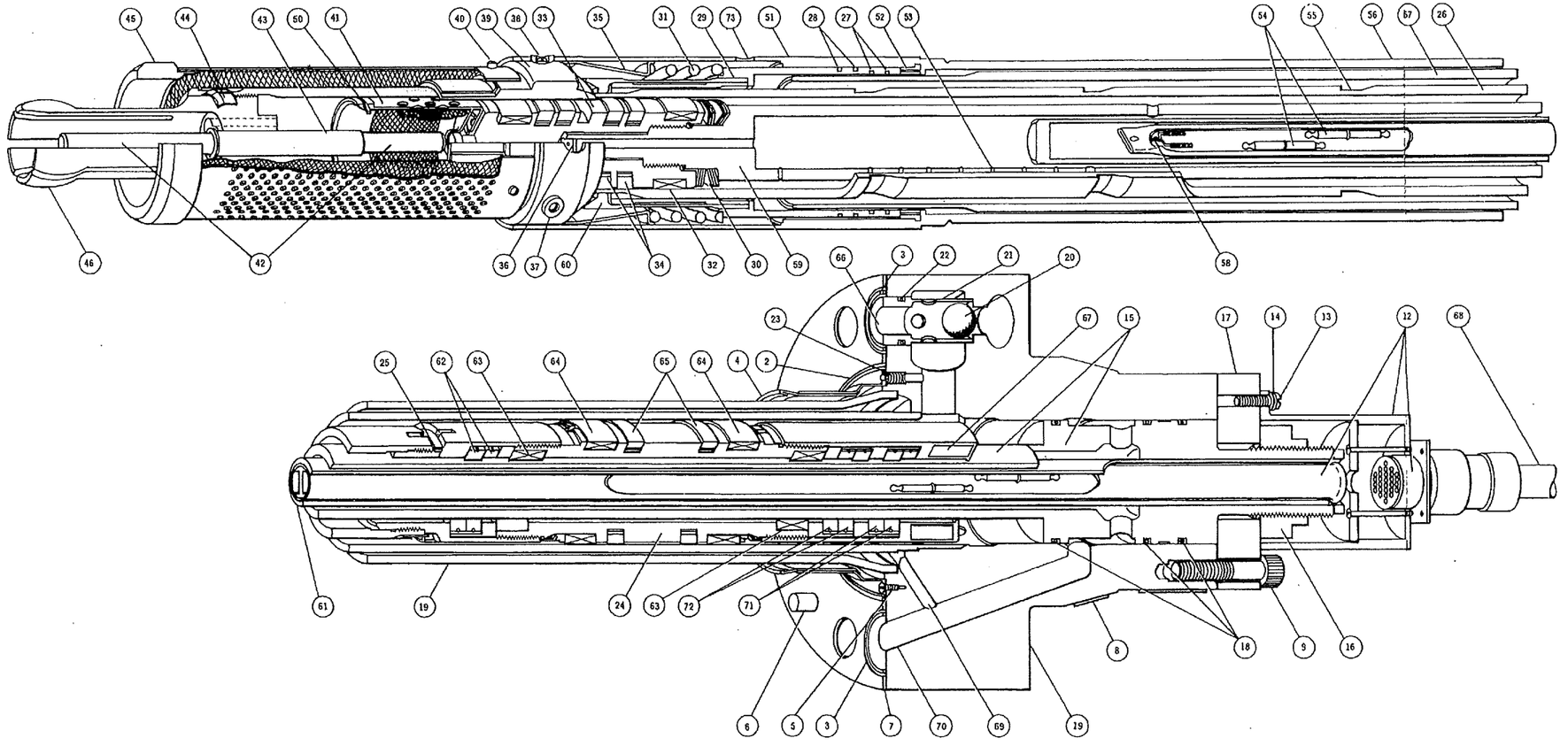

2 – O-RING (CRD FLANGE FACE)
3 – O-RING (INSERT AND WITHDRAW PORTS)
4 – STRAINER
5 – FLAT HEAD SCREW (STRAINER-MOUNTING)
6 – DOWEL ALIGNMENT PIN
7 – O-RING SPACER
8 – NAMEPLATE
9 – SOCKET-HEAD CAP SCREW (RING FLANGE MOUNTING)
12 – POSITION INDICATOR PROBE
13 – FILLISTER-HEAD SCREW (POSITION INDICATOR PROBE MOUNTING)
14 – LOCKWASHER (FOR PART 13)
15 – PISTON TUBE
16 – NUT (PISTON TUBE)
17 – RING FLANGE
18 – O-RING (PISTON TUBE)
19 – CYLINDER, TUBE, AND FLANGE
20 – BALL (CHECK VALVE)
21 – BALL RETAINER
22 – O-RING (BALL RETAINER)
23 – SET SCREW PLUG (COOLING WATER ORIFICE)
24 – DRIVE PISTON
25 – BAND
26 – INDEX TUBE
27 – SEAL RING (COLLET PISTON – INTERNAL)
28 – SEAL RING (COLLET PISTON – EXTERNAL)
29 – COLLET AND PISTON
30 – SPRING WASHERS
31 – COLLET SPRING
32 – SPLIT BUSHING (STOP PISTON)
33 – STOP PISTON
34 – SEAL RING (STOP PISTON)
35 – BARREL
36 – COTTER PIN (STOP PISTON)
37 – PLUG (GUIDE CAP)
38 – FILLISTER-HEAD SCREW (GUIDE CAP PLUG MOUNTING)
39 – GUIDE CAP
40 – DRILLED FILLISTER-HEAD SCREW (OUTER FILTER MOUNTING)
41 – INNER FILTER
42 – ROD
43 – TUBE
44 – BAND
45 – FILTER (OUTER)
46 – SPUD
50 – SEAL RING (INNER FILTER)
51 – COLLET HOUSING (PORTION OF OUTER TUBE)
52 – SPACER (PART OF CYLINDER, TUBE, AND FLANGE)
53 – BUFFER ORIFICES IN PISTON TUBE (TYPICAL)
54 – POSITION INDICATOR SWITCHES
55 – INDEX TUBE NOTCH
56 – OUTER TUBE (PART OF CYLINDER, TUBE, AND FLANGE)
57 – INNER CYLINDER (PART OF CYLINDER, TUBE, AND FLANGE)
58 – THERMOCOUPLE (PART OF POSITION INDICATOR PROBE)
59 – STUD (PORTION OF PISTON TUBE)
60 – COLLET FINGER (PART OF COLLET AND PISTON)
61 – INDICATOR TUBE (PART OF PISTON TUBE)
62 – INNER SEALS (DRIVE PISTON-BUFFER SEALS)
63 – INTERNAL BUSHING (DRIVE PISTON)
64 – EXTERNAL BUSHING (DRIVE PISTON)
65 – OUTER SEALS (DRIVE PISTON)
66 – INSERT PORT (INSERT AND SCRAM INLET/ WITHDRAW OUTLET)
67 – RING MAGNET (PART OF DRIVE PISTON)
68 – CABLE (POSITION INDICATOR)
69 – PORT TO COLLET PISTON (WITHDRAW PRESSURE TO COLLET PISTON)
70 – WITHDRAW PORT (WITHDRAW INLET/ INSERT OUTLET AND SCRAM DISCHARGE)
71 – INNER SEALS (DRIVE PISTON – DRIVE-DOWN SEALS)
72 – INNER SEALS (DRIVE PISTON – DRIVE-UP SEALS)
73 – WATER PORTS IN COLLET HOUSING

NOTES
1. THERE ARE EQUIVALENT PISTON TUBE CONFIGURATIONS. EITHER MAY BE INSTALLED. SHOWN IS THE TYPICAL OF THE ORIGINAL DESIGN.
2. INDICATOR TUBE CONFIGURATION IS TYPICAL OF THE ORIGINAL PISTON TUBE DESIGN.

Fermi 2
UPDATED FINAL SAFETY ANALYSIS REPORT

FIGURE 4.5-14

CONTROL ROD DRIVE UNIT CUTAWAY

HYDRAULIC CONTROL UNIT - TYPICAL FOR C1103D001 THRU 185

REFERENCES

M-2081	DIAGRAM	– CONTROL ROD DRIVE HYDRAULIC SYSTEM (CRD) (PART 1)
M-2082	DIAGRAM	– STAND-BY LIQUID CONTROL SYSTEM (SLC)
M-2084	DIAGRAM	– RESIDUAL HEAT REMOVAL SYSTEM-DIVISION I (RHR)
M-2083	DIAGRAM	– RESIDUAL HEAT REMOVAL SYSTEM-DIVISION II (RHR)
M-2034	DIAGRAM	– CORE SPRAY SYSTEM (CSS)
M-2035	DIAGRAM	– HIGH PRESSURE COOLANT INJECTOR SYSTEM (HPCI)
M-2043	DIAGRAM	– HIGH PRESSURE COOLANT INJECTOR SYSTEM BAROMETRIC CONDENSER
M-2044	DIAGRAM	– REACTOR CORE ISOLATION COOLING SYSTEM (RCIC)
M-2045	DIAGRAM	– REACTOR CORE ISOLATION COOLING SYSTEM BAROMETRIC CONDENSER
M-2046	DIAGRAM	– REACTOR WATER CLEAN-UP (RWCU)
M-2047	DIAGRAM	– REACTOR WATER CLEAN-UP FILTER/DEMINERALIZER (RWCU)
M-2048	DIAGRAM	– FUEL POOL COOLING SYSTEM (FPCI)
M-2049	DIAGRAM	– FUEL POOL COOLING SYSTEM FILTER/DEMINERALIZER
M-5358	DIAGRAM	– REACTOR BUILDING CLOSED COOLING & EMERGENCY COOLING WATER
M-2678	DIAGRAM	– DEMINERALIZED SERVICE WATER RISERS
M-2089	DIAGRAM	– NUCLEAR BOILER SYSTEM
M-2088	DIAGRAM	– RADWASTE PHASE SEPERATORS
M-2006	DIAGRAM	– CONDENSATE STORAGE SYSTEMS
M-2085	DIAGRAM	– STATION AIR SYSTEM
M-2023	DIAGRAM	– FEEDWATER SYSTEM
M-2833	DIAGRAM	– REACTOR RECIRCULATION SYSTEM
M-2090	DIAGRAM	– NUCLEAR BOILER SYSTEM
I-2156-01	DIAGRAM	– REACTOR PROTECTION SYSTEM
I-2110-07	DIAGRAM	– LOGIC, CONTROL ROD DRIVE HYDRAULIC SYSTEM PART 7
M-2015	DIAGRAM	– STATION & CONTROL AIR
M-4100	DIAGRAM	– TORUS WATER MANAGEMENT SYSTEM
M-4615	DIAGRAM	– IAS & NIAS CONTROL AIR
I-2400-04	DIAGRAM	– PLANT PROCESS SAMPLING SYSTEM
M-5449	DIAGRAM	– CRD-PART 2
M-5357	DIAGRAM	– EMERGENCY EQUIP. COOL. WATER (DIV. II)

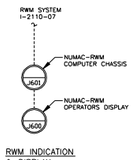

RWM INDICATION & DISPLAY

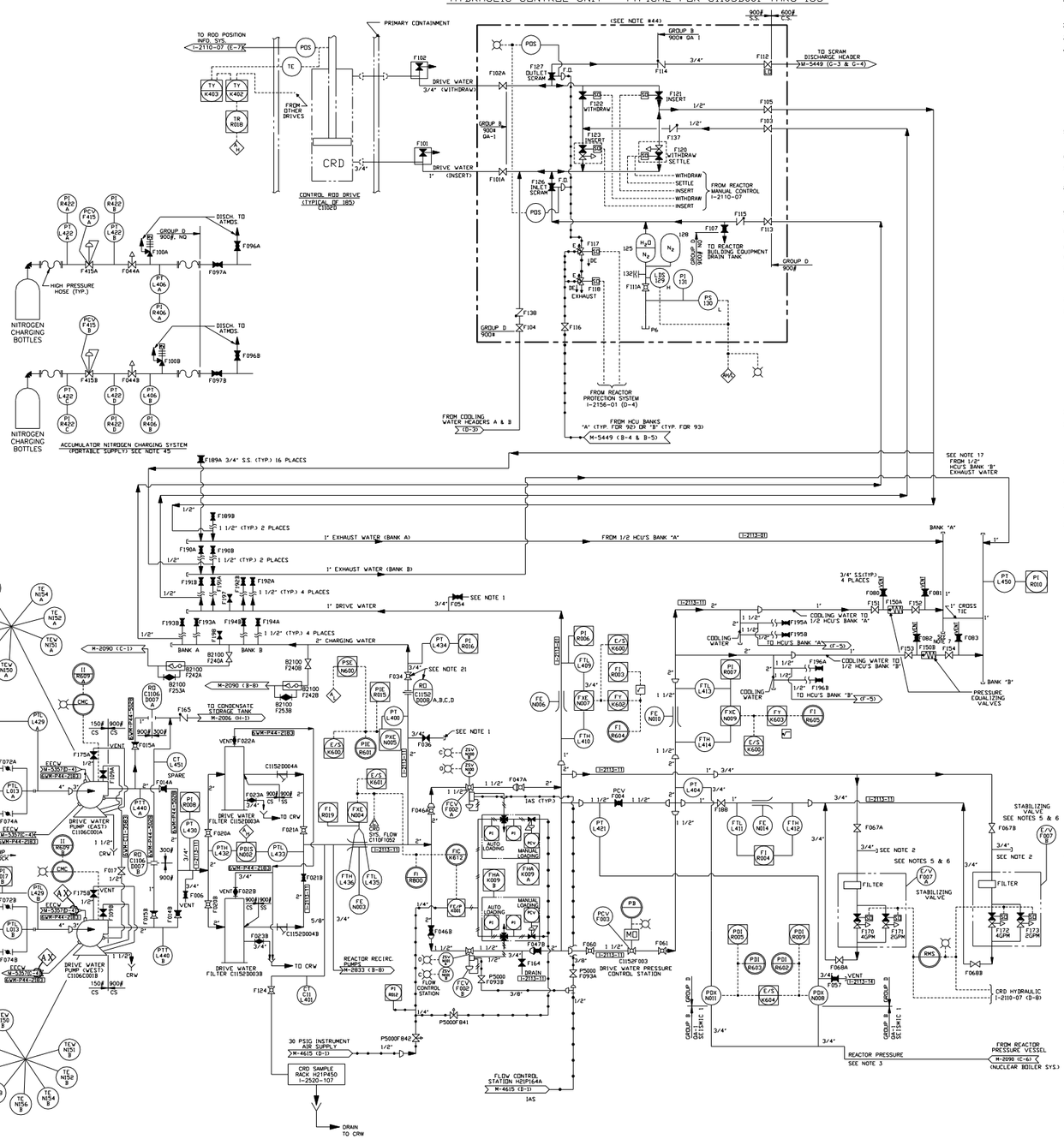

NOTES:

1. AVAILABLE FOR TEMPORARY CONNECTION FOR INSTRUMENT FLUSHING. NO PERMANENT PIPING CONNECTIONS TO BE MADE TO THIS VALVE.
2. PROVIDED FOR FLUSHING.
3. REACTOR PRESSURE SENSING LINE.
4. REFERENCE DOCUMENTS

TITLE	DECO FILE NO.	GE. NO.
A) DESIGN SPECIFICATIONS FOR THE CONTROL ROD DRIVE SYS.	3071 506	

5. VALVE F007A-A (OR F007B-B) CLOSES ON DRIVE INSERT SIGNAL. VALVE F007A-B (OR F007B-A) CLOSES ON DRIVE WITHDRAW SIGNAL, BUT DOES NOT STAY CLOSED DURING SETTING (C-2).
6. STAB. VALVE F007B IS AN ALTERNATE STAB. VALVE F007A (C-2).
7. PROVIDE VENT AND DRAIN VALVES WITH CAP ON DISCHARGE SIDE AT ALL SYS. HIGH AND LOW POINTS RESPECTIVELY.
8. UNLESS OTHERWISE SHOWN; ALL INSTRUMENT PIS NUMBERS ARE PREFIXED C11 ALL VALVE AND EQUIPMENT PIS NUMBERS ARE PREFIXED C1100
9. INSTRUMENT PILOT SOLENOID AND CONTROL AIR PIPING SHALL BE OF A NON CORROSIVE MATERIAL.
10. INDICATING LIGHTS ARE AN INTEGRAL PART OF ALL PB OR CMC TYPE SWITCHES UNLESS OTHERWISE NOTED.
11.
12.
13. PIPE SIZES SHOWN ON THIS DRAWING ARE APPROX. EXCEPT AT POINTS OF CONNECTION WITH G.E. SUPPLIED EQUIPMENT OR PIPING. THE PIPING DESIGNER SHALL CHECK AND ADJUST PIPE SIZE IN ACCORDANCE WITH THE SYSTEM DESIGN SPECIFICATION AND PROCESS DIAGRAM.
14.
15. SOURCE OF CRD SYSTEM WATER SHALL BE NORMALLY FROM CONDENSATE POLISHING DEMIN. SYSTEM. CONDENSATE STORAGE IS AN ALTERNATE SOURCE IF THE TREATMENT SYSTEM IS NOT IN OPERATION.
16. CONTINUOUS FLOW TO REACTOR SAMPLE STATION SHOULD BE APPROX. ONE (1) LITER PER MINUTE AND SHALL BE TWO AND ONE HALF (2 1/2) LITERS PER MINUTE MAX.
17. EXHAUST WATER FLOW FROM ONE MOVING DRIVE IS DISPERSED VIA THE HYDRAULIC CONTROL UNITS OF OTHER NON MOVING DRIVES TO REACTOR PRESSURE VESSEL VIA EXAUST WATER LINES.
18.
19.
20. THESE VALVES MUST BE OPEN FOR DRIVE MOVEMENT.
21. ORIFICES C1152D008A, B, C, AND D ARE CONNECTED IN SERIES AS SHOWN ON DRAWING I-2113-11. THE PRESSURE DROP ACROSS EACH ORIFICE IS 250 PSI AT PUMP RUN OUT CONDITION. VALVE F034 SUPPLEMENTS THE ORIFICES FOR THE REQUIRED PRESSURE DROP.
22. THE SCRAM DISCHARGE VOLUME ARRANGEMENT SHOWN IS FOR REFERENCE ONLY. SEE CRD DESIGN SPEC. FOR REQUIREMENT.
23. PIPING QUALITY CLASS EXTENDS TO CONNECTIONS WITH HCU. HCU DIAGRAM IS SHOWN FOR INFO. ONLY. FOR QUALITY CLASS OF THE HCU, SEE GROUP CLASSIFICATION DIAGRAM.
24. SCRAM DISCHARGE DRAIN MUST BE SUBMURGED DUE TO POTENTIAL RELEASE OF STEAM AND RADIOACTIVE NONCONDENSIBLES.
25. VALVE F159B SHALL BE LOCKED INTO OPEN POSITION TO MAINTAIN ADMINISTRATIVE CONTROL. SEE M-5449.
26. THE C71A-K24A AND K24B RELAYS SHALL BE SET SO THAT THE FD10 AND FD11 VALVES MUST START TO OPEN AT LEAST FIVE (5) SECONDS AFTER THE F180 AND F181 VALVES RESPECTIVELY UPON THE RESET OF A FULL CORE SCRAM. SEE M-5449.
27. THE SCRAM DISCHARGE VOLUME VENT LINE SHALL BE ROUTED VIA A DEDICATED LINE TO THE NON SUBMERGED DISCHARGE. THE VENT SYSTEM PIPING SHOULD NOT CONTAIN SIGNIFICANT FLOW RESTRICTIONS WHICH COULD INHIBIT VENTING OF THE SCRAM DISCHARGE VOLUME TO THE EXTENT OF LIMITING THE SCRAM DISCHARGE VOLUME DRAIN RATE. THE DESIGN OF THE NON SUBMERGED VENT DISCHARGE MUST CONSIDER THE POTENTIAL FOR RELEASE OF RADIOACTIVITY DUE TO THE DISCHARGE OF NON CONDENSIBLES, WATER AND STEAM WHICH MAY OCCUR DURING THE PERIOD AFTER SCRAM PRIOR TO VENT VALVE CLOSURE AND UPON SCRAM RESET WHEN THE VALVES ARE REOPENED WITH THE SCRAM DISCHARGE VOLUME PRESSURIZED.
28. TO PREVENT LOOP SEALS FROM OCCURING IN THE RELATIVELY SMALL DIAMETER LINES OF THE SCRAM DISCHARGE VOLUME (SDV) VENT & DRAIN SYSTEM, A CONTINUOUS DOWNWARD PITCH AWAY FROM THE SCRAM DISCHARGE VOLUME (SVD) VENT AND DRAIN VALVES MUST BE MAINTAINED. THERMAL EXPANSION EFFECTS SHOULD BE ADDRESSED IN THE DESIGN OF THE VENT AND DRAIN SYSTEMS.
29. THE DESIGN OF THE SCRAM DISCHARGE VOLUME (SDV) ASSOCIATED VENT AND DRAIN SYSTEM PIPING AND COMPONENTS MUST CONSIDER THE POTENTIAL PRESSURE, TEMPERATURE, AND TRANSIENT LOADING WHICH MAY RESULT FROM, (A) THE DISCHARGE TO THE SCRAM DISCHARGE VOLUME AND DOWN THE VENT AND DRAIN LINE DURING A FULL SCRAM PRIOR TO VENT AND DRAIN VALVE CLOSURE, (B) THE PRESSURIZATION OF SCRAM DISCHARGE VOLUME TO REACTOR VESSEL PRESSURE FOLLOWING VENT AND DRAIN VALVE CLOSURE, AND (C) DEPRESSURIZATION OF THE SCRAM DISCHARGE VOLUME UPON SCRAM RESET AND OPENING OF THE SCRAM DISCHARGE VOLUME VENT AND DRAIN VALVES.
30. VACUUM BREAKER VALVES (F120A&B) AND VENT VALVES (F010 AND F180) TO BE ON HIGH POINT OF VENT LINE. VACUUM BREAKER VALVES SHALL OPEN ON DIFFERENTIAL PRESSURE SETTING OF NO GREATER THAN FIVE INCHES OF WATER. THE LOCATION OF THE VACUUM BREAKER SHOULD CONSIDER THE POTENTIAL RELEASE OF RADIOACTIVE NONCONDENSIBLES, WATER AND STEAM THAT COULD OCCUR IF THE VACUUM BREAKER VALVES WERE TO FAIL IN AN OPEN POSITION WHEN THE VENT SYSTEM PIPING IS PRESSURIZED. SEE M-5449.
31. INSTRUMENT LOW POINT PIPING TAP SHOULD BE <12 INCHES ABOVE THE SCRAM DISCHARGE INSTRUMENT VOLUME REFERENCE DATUM ELEVATION.
32. THE ELEVATION WITHIN THE SCRAM DISCHARGE INSTRUMENT VOLUME CORRESPONDING TO THE SCRAM INITIATION SET-POINT SHALL BE >10 INCHES BELOW THE LOWEST ELEVATION OF THE HORIZONTAL SCRAM DISCHARGE VOLUME PIPING.
33. SCRAM DISCHARGE VENT AND DRAIN VALVE CONTROL ROOM INDICATORS SHALL INDICATE OPEN WHEN BOTH VALVES OPEN AND SHALL INDICATE CLOSED WHEN EITHER VALVE IS CLOSED.
34. THE PNEUMATIC PIPING FROM THROTTLE VALVE F159B AND SOLENOID VALVES F182, F409A & B TO THE VENT AND DRAIN VALVES F181, F011, F010, F180 SHALL BE ROUTED & SUPPORTED TO MINIMIZE THE POSSIBILITY OF PIPE CRIMP AND ALSO IT SHOULD BE OF ADEQUATE SIZE OR TUBING THICKNESS AND MATERIAL TO MINIMIZE THE CONSEQUENCES OF PIPE CRIMP. INSTALL PER SPEC. 3071-147, NQ, NON-SEISMIC.
35. FOR ADDITIONAL MECHANICAL, PIPING, STRUCTURAL, AND TUBING DETAILS SEE I-2113 DRAWING SERIES.

FOR CONTINUATION OF NOTES SEE DWG. M-5449

Fermi 2

UPDATED FINAL SAFETY ANALYSIS REPORT

FIGURE 4.5-15, SHEET 1

CONTROL ROD DRIVE HYDRAULIC SYSTEM REACTOR BUILDING

DETROIT EDISON COMPANY DRAWING NO. 6M721-2081, REV. AX

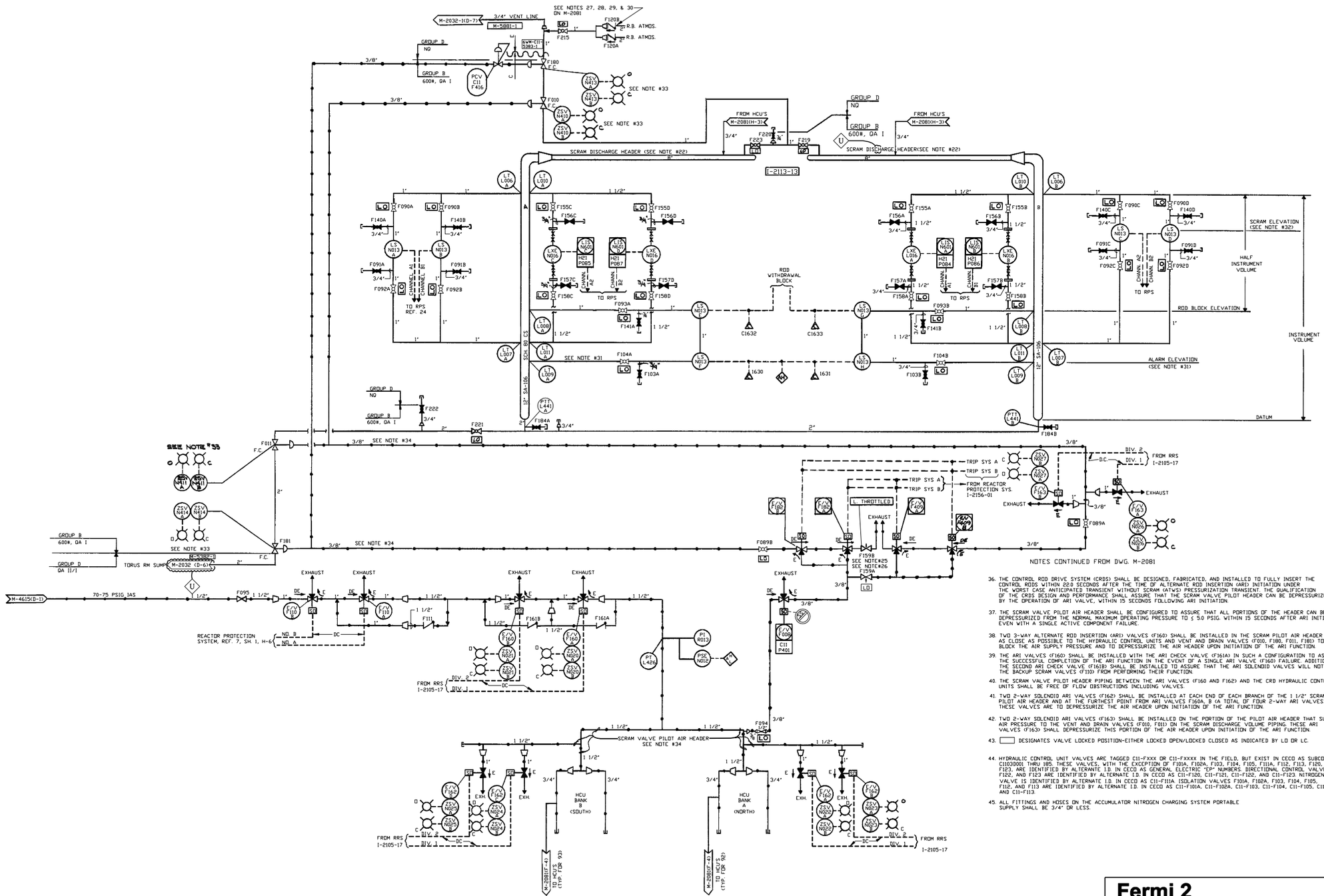

36. THE CONTROL ROD DRIVE SYSTEM (CRDS) SHALL BE DESIGNED, FABRICATED, AND INSTALLED TO FULLY INSERT THE CONTROL RODS WITHIN 22.0 SECONDS AFTER THE TIME OF ALTERNATE ROD INSERTION (ARI) INITIATION UNDER THE WORST CASE ANTICIPATED TRANSIENT WITHOUT SCRAM (ATWS) PRESSURIZATION TRANSIENT. THE QUALIFICATION OF THE CRDS DESIGN AND PERFORMANCE SHALL ASSURE THAT THE SCRAM VALVE PILOT HEADER CAN BE DEPRESSURIZED BY THE OPERATION OF ARI VALVE, WITHIN 15 SECONDS FOLLOWING ARI INITIATION.

37. THE SCRAM VALVE PILOT AIR HEADER SHALL BE CONFIGURED TO ASSURE THAT ALL PORTIONS OF THE HEADER CAN BE DEPRESSURIZED FROM THE NORMAL MAXIMUM OPERATING PRESSURE TO ≤ 5.0 PSIG. WITHIN 15 SECONDS AFTER ARI INITIATION, EVEN WITH A SINGLE ACTIVE COMPONENT FAILURE.

38. TWO 3-WAY ALTERNATE ROD INSERTION (ARI) VALVES (F160) SHALL BE INSTALLED IN THE SCRAM PILOT AIR HEADER AS CLOSE AS POSSIBLE TO THE HYDRAULIC CONTROL UNITS AND VENT AND DRAIN VALVES (F010, F180, F011, F181) TO BLOCK THE AIR SUPPLY PRESSURE AND TO DEPRESSURIZE THE AIR HEADER UPON INITIATION OF THE ARI FUNCTION.

39. THE ARI VALVES (F160) SHALL BE INSTALLED WITH THE ARI CHECK VALVE (F161A) IN SUCH A CONFIGURATION TO ASSURE THE SUCCESSFUL COMPLETION OF THE ARI FUNCTION IN THE EVENT OF A SINGLE ARI VALVE (F160) FAILURE. ADDITIONALLY, THE SECOND ARI CHECK VALVE (F161B) SHALL BE INSTALLED TO ASSURE THAT THE ARI SOLENOID VALVES WILL NOT PREVENT THE BACKUP SCRAM VALVES (F110) FROM PERFORMING THEIR FUNCTION.

40. THE SCRAM VALVE PILOT HEADER PIPING BETWEEN THE ARI VALVES (F160 AND F162) AND THE CRD HYDRAULIC CONTROL UNITS SHALL BE FREE OF FLOW OBSTRUCTIONS INCLUDING VALVES.

41. TWO 2-WAY SOLENOID ARI VALVES (F162) SHALL BE INSTALLED AT EACH END OF EACH BRANCH OF THE 1 1/2" SCRAM VALVE PILOT AIR HEADER AND AT THE FURTHEST POINT FROM ARI VALVES F160A, B (A TOTAL OF FOUR 2-WAY ARI VALVES). THESE VALVES ARE TO DEPRESSURIZE THE AIR HEADER UPON INITIATION OF THE ARI FUNCTION.

42. TWO 2-WAY SOLENOID ARI VALVES (F163) SHALL BE INSTALLED ON THE PORTION OF THE PILOT AIR HEADER THAT SUPPLIES AIR PRESSURE TO THE VENT AND DRAIN VALVES (F010, F011) ON THE SCRAM DISCHARGE VOLUME PIPING. THESE ARI VALVES (F163) SHALL DEPRESSURIZE THIS PORTION OF THE AIR HEADER UPON INITIATION OF THE ARI FUNCTION.

43. ☐ DESIGNATES VALVE LOCKED POSITION-EITHER LOCKED OPEN/LOCKED CLOSED AS INDICATED BY LO OR LC.

44. HYDRAULIC CONTROL UNIT VALVES ARE TAGGED C11-FXXX OR C11-FXXXX IN THE FIELD, BUT EXIST IN CECO AS SUBCOMPONENTS OF C11037001 THRU 185. THESE VALVES, WITH THE EXCEPTION OF F101A, F102A, F103, F104, F105, F111A, F112, F113, F120, F121, F122, AND F123, ARE IDENTIFIED BY ALTERNATE I.D. IN CECO AS GENERAL ELECTRIC "EP" NUMBERS. DIRECTIONAL CONTROL VALVES F120, F121, F122, AND F123 ARE IDENTIFIED BY ALTERNATE I.D. IN CECO AS C11-F120, C11-F121, C11-F122, AND C11-F123. NITROGEN ISOLATION VALVE IS IDENTIFIED BY ALTERNATE I.D. IN CECO AS C11-F111A. ISOLATION VALVES F101A, F102A, F103, F104, F105, F112, AND F113 ARE IDENTIFIED BY ALTERNATE I.D. IN CECO AS C11-F101A, C11-F102A, C11-F103, C11-F104, C11-F105, C11-F112, AND C11-F113.

45. ALL FITTINGS AND HOSES ON THE ACCUMULATOR NITROGEN CHARGING SYSTEM PORTABLE SUPPLY SHALL BE 3/4" OR LESS.

Fermi 2

UPDATED FINAL SAFETY ANALYSIS REPORT

FIGURE 4.5-15, SHEET 2

CONTROL ROD DRIVE HYDRAULIC SYSTEM REACTOR BUILDING

DETROIT EDISON COMPANY DRAWING NO. 6M721-5449, REV. U

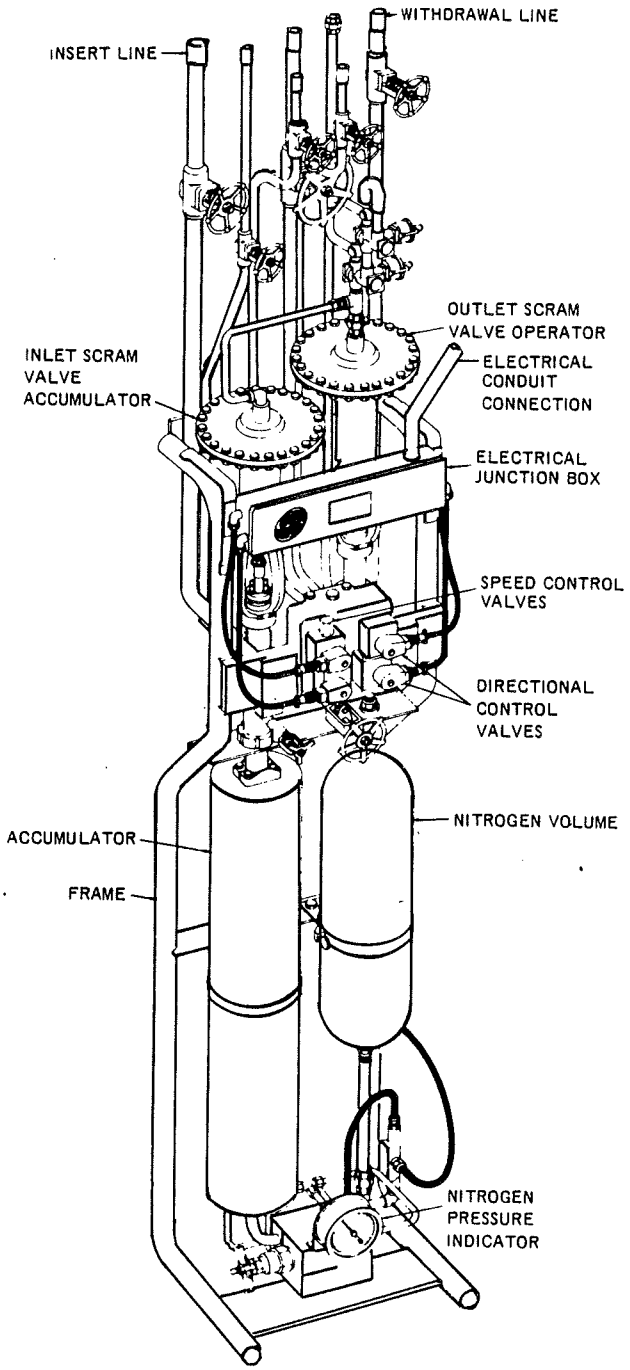

Fermi 2
UPDATED FINAL SAFETY ANALYSIS REPORT

FIGURE 4.5-16

CONTROL ROD DRIVE HYDRAULIC CONTROL UNIT

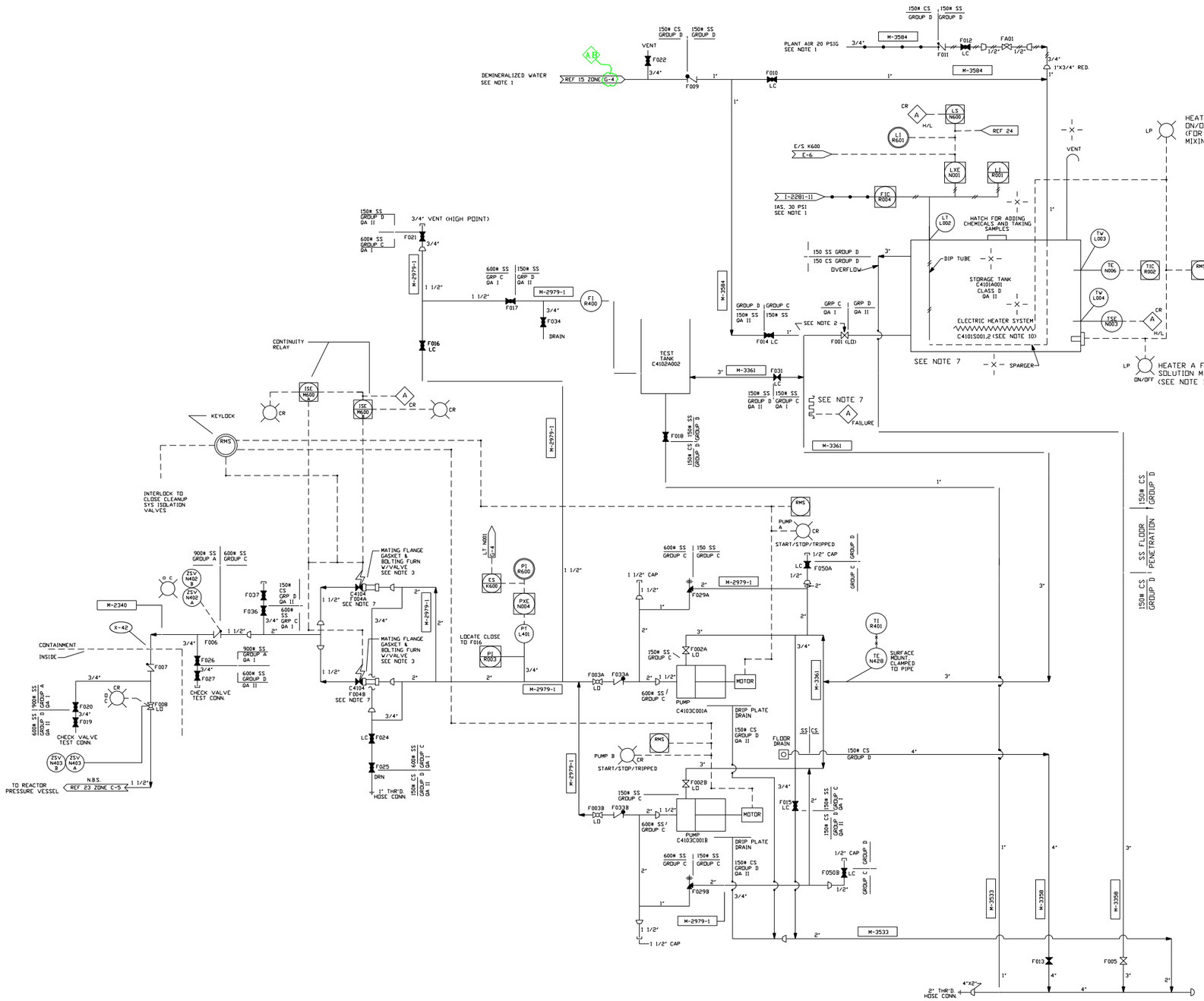

DIAGRAMS

REF. NO.	TITLE	DECO NO.
1	DIAGRAM - CONTROL ROD DRIVE HYDRAULIC SYSTEM (CRD)	M-2081
2	DIAGRAM - STAND-BY LIQUID CONTROL SYSTEM (SLC)	M-2082
3	DIAGRAM - RESIDUAL HEAT REMOVAL SYSTEM DIVISION I (RHR)	M-2084
4	DIAGRAM - RESIDUAL HEAT REMOVAL SYSTEM DIVISION II (RHR)	M-2083
5	DIAGRAM - CORE SPRAY SYSTEM (CSS)	M-2034
6	DIAGRAM HIGH PRESSURE COOLANT INJECTION SYSTEM (HPCI)	M-2035
7	DIAGRAM - HIGH PRESSURE COOLANT INJECTION SYSTEM BAROMETRIC CONDENSER (HPCI)	M-2043
8	DIAGRAM - REACTOR CORE ISOLATION COOLING SYSTEM (RCIC)	M-2044
9	DIAGRAM - REACTOR CORE ISOLATION COOLING SYSTEM BAROMETRIC CONDENSER (RCIC)	M-2045
10	DIAGRAM - REACTOR WATER CLEAN-UP SYSTEM (RWCU)	M-2046
11	DIAGRAM - REACTOR WATER CLEAN-UP FILTER/DEMINERALIZER (RWCU)	M-2047
12	DIAGRAM - FUEL POOL COOLING SYSTEM (FPC)	M-2048
13	DIAGRAM - FUEL POOL COOLING SYSTEM FILTER/DEMINERALIZER (FPC)	M-2049
14	DIAGRAM - REACTOR BLDG CLOSED COOLING & EMERG EQUIP COOLING WATER SYSTEM	M-2027
15	DIAGRAM - DEMINERALIZED SERVICE WATER RISER SYSTEM	M-2678
16	DIAGRAM - NUCLEAR BOILER SYSTEM	M-2089
17	DIAGRAM - REACTOR WATER CLEAN-UP SYSTEM PHASE SEPARATORS (RWCU)	M-2088
18	DIAGRAM - CONDENSATE STORAGE SYSTEM	M-2006
19	DIAGRAM - STATION AIR SYSTEM	M-2085
20	DIAGRAM - FEED WATER SYSTEM	M-2023
21	DIAGRAM - REACTOR RECIRCULATION SYSTEM (RRC)	M-2033
22	DIAGRAM - RESIDUAL HEAT REMOVAL SERVICE WATER SYSTEM	M-2012
23	DIAGRAM - NUCLEAR BOILER SYSTEM	M-2090
24	S/D ERIS SIGNAL POINT #96	I-2174-31
25		
26		
27		
28		

INSTR. & CONTROL

NOTES:
- A. NONE DELETED
- B. NOTE DELETED
- C. NOTE DELETED

REFERENCES:
1. PIPING & INSTRUMENT SYMBOLS GE 197R567 R1-25
2. LEGEND OF SYMBOLS & INSTR IDENT DECO M-2001 FOR PLANT SYSTEM DIAGRAMS

1. THE ELEVATION OF THE DEMINERALIZED WATER AND PLANT AIR SUPPLY LINES SHALL BE ABOVE THE TOP OF THE STORAGE TANK
2. THE ELEVATION OF THE STORAGE TANK SHALL BE ABOVE THE PUMP SUCTION TO ENSURE THAT THE SUCTION LINES ARE ALWAYS FLOODED
3. IN ORDER TO SERVICE THE EXPLOSIVE VALVES AFTER FIRING IT IS NECESSARY TO REMOVE A 6" SPOOL PIECE IMMEDIATELY UPSTREAM OF THE RESPECTIVE VALVE. EACH EXPLOSIVE VALVE IS FURNISHED WITH A MATING SOCKET WELDING TYPE FLANGE FOR SOCKET WELDING TO A 6" SPOOL PIECE.
4. THIS DIAGRAM REPLACES GENERAL ELECTRIC DIAGRAM NO. 729E601AB DECO FILE # R1-3
5. THE PLANT IDENTIFICATION NUMBER FOR THE STANDBY LIQUID CONTROL SYSTEM IS C4100
6. SPECIFIC SYSTEM DESIGN REQUIREMENTS ARE GIVEN IN THE SLC DESIGN SPECIFICATION NUMBER 3071-507
7. PIPING HEAT TRACE FROM STORAGE TANK (C4101A001) TO VALVES F004A AND F004B ABANDONED IN PLACE FOR ENRICHED BORON USE. PIPING LOW TEMPERATURE ALARMS IN THE CONTROL ROOM ARE OPERATIONAL. REFER TO CECO FOR SETPOINTS.
8. QA LEVEL I UNLESS NOTED FOR PIPING ONLY. SEE CECO FOR INSTRUMENTS AND EQUIPMENT CLASSIFICATION.
9. "UNLESS OTHERWISE SHOWN:
   ALL INSTRUMENT PIS NUMBERS ARE PREFIXED C41
   ALL VALVE AND EQUIPMENT PIS NUMBERS ARE PREFIXED C4100"
10. TANK HEATER "A" (C4101S001) IS ABANDONED IN PLACE PER TSR-30753.

LEGEND

1 M----- DWG NO. IDENTIFIES PIPING ISOMETRIC FOR FABRICATION AND ERECTION

Fermi 2

UPDATED FINAL SAFETY ANALYSIS REPORT

FIGURE 4.5-17

STANDBY LIQUID CONTROL SYSTEM P&ID

DETROIT EDISON COMPANY DRAWING NO. 6M721-2082, REV. AB

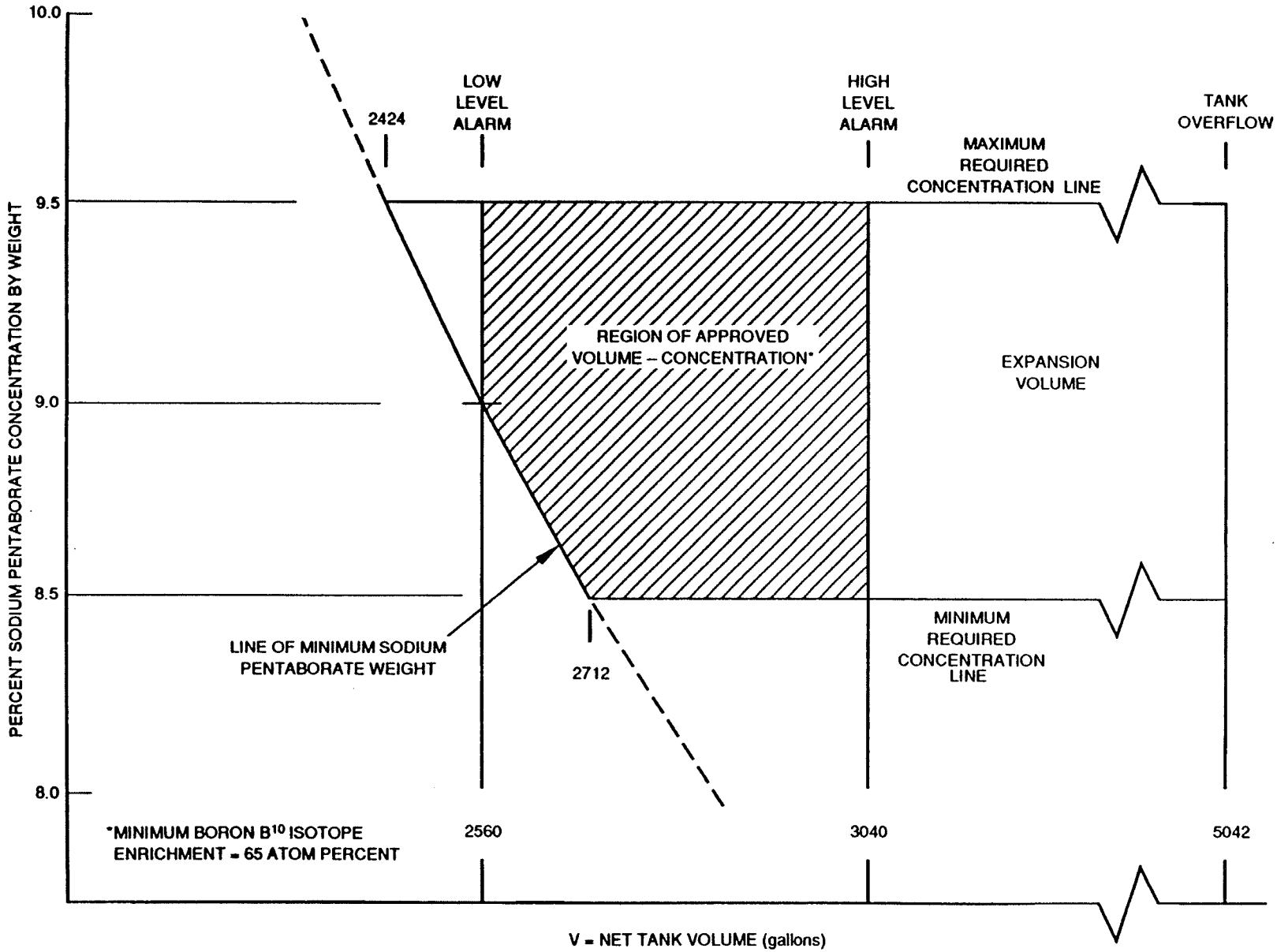

Fermi 2
UPDATED FINAL SAFETY ANALYSIS REPORT

FIGURE 4.5-18

SODIUM PENTABORATE SOLUTION VOLUME CONCENTRATION REQUIREMENTS

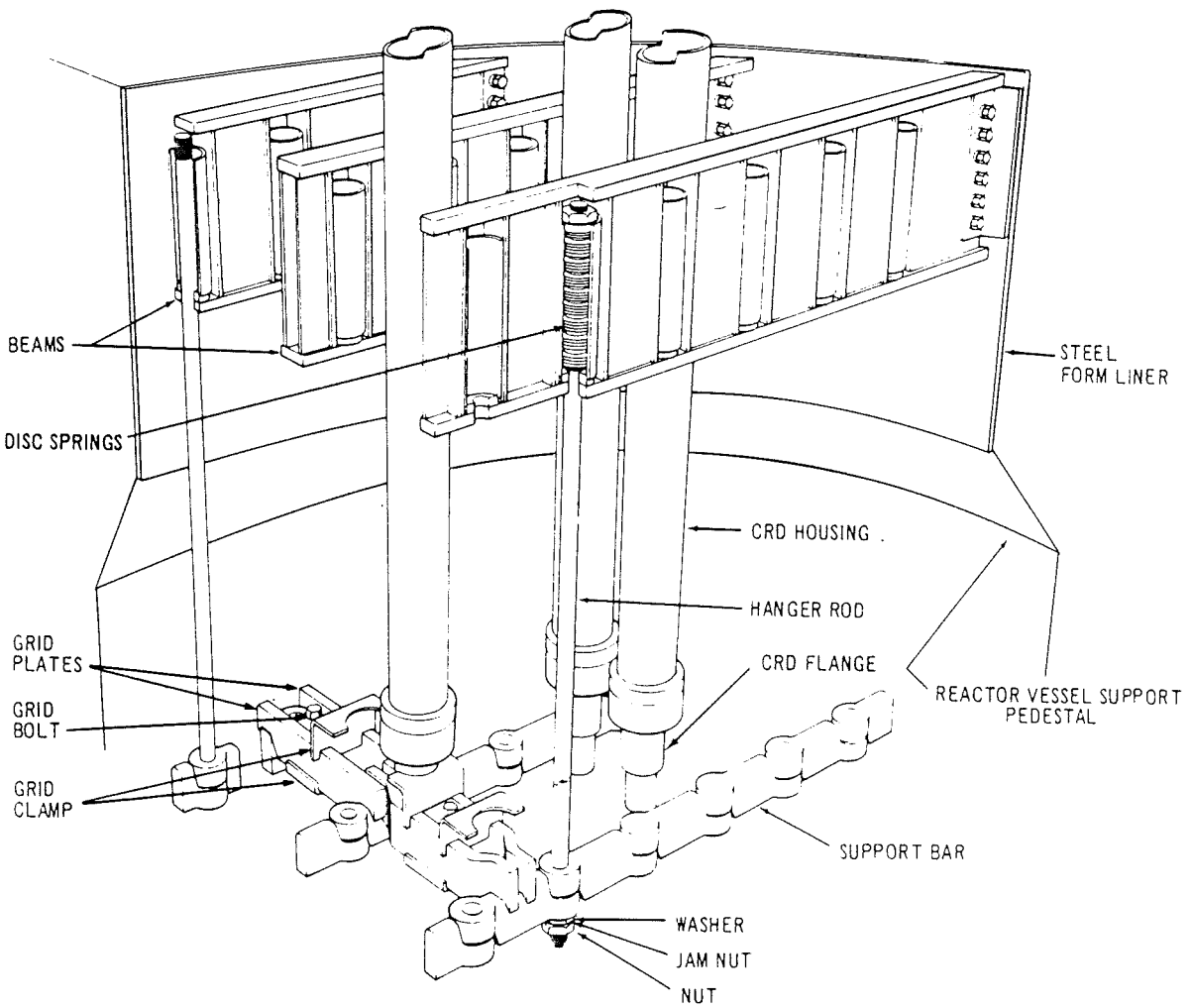

Fermi 2
UPDATED FINAL SAFETY ANALYSIS REPORT

FIGURE 4.5-19

CONTROL ROD DRIVE HOUSING SUPPORT